Development of Novel Unicondylar Knee Implants for Use with Robotic Orthopaedic Tools

Hannah G. Wells, BEng (Hons)

Supervisors: Dr Philip E. Riches

Dr Avril Thomson

Declaration

This thesis is the result of the author's original research. It has been composed by the author and has not been previously submitted for examination which has led to the award of a degree.

Signed:

Date:

Table of Contents

List of Figures

List of Tables

List of Abbreviation

AKSS..... American Knee Society Score

BQ..... One of the final two designs that were manufactured into prototypes

CSV ..... Comma-Separated Values

CT Scan ..... Computed Tomography Scan

FE ..... Finite Element

FEA..... Finite Element Analysis

HSS..... Hospital for Special Surgery

KSS ..... Knee Society Score

MRHA ..... Medicines and Healthcare products Regulatory Agency

OA..... Osteoarthritis

PDS ..... Product Design Specification

PGE_2..... Prostaglandin E2 (also known as dinoprostone)

PMMA ..... Polymethyl methacrylate

PMI ..... Positive Minus and Interesting

T6.2..... One of the final two deigns that were manufactured into prototypes

ROM ..... Range of Movement

TKA ..... Total Knee Arthroplasty

TKR..... Total Knee Replacement (interchangeable with TKA)

TRIZ..... Russian acronym for: Teorya Resheniya Izobretatelskikh Zadatch (теория решения изобретательских задач). – In English it translates to “Theory of Inventive Problem Solving”

UKA..... Unicondylar Knee Arthroplasty

UKR..... Unicondylar Knee Replacement (interchangeable with UKA)

WOMAC.... Western Ontario and MacMaster Universities Osteoarthritis Index

Conference Proceedings

1. "*Primary mechanical stability of unicondylar knee replacement implants*" H.G. Wells, A. Thomson, P.E. Riches. Poster. CAOS (Computer Assisted Orthopaedic Surgery) Milan 2014

2. "*The Effect of Surface Roughness on Bone Cement Adhesion*" H.G. Wells, A. Thomson, P.E. Riches. Oral presentation and poster. CAOS (Computer Assisted Orthopaedic Surgery) Osaka 2016

3. "*The Effect of Surface Roughness on Bone Cement Adhesion*" H.G. Wells, A. Thomson, P.E. Riches. Poster. BORS (The British Orthopaedic Research Society) Glasgow 2016

Acknowledgements

I would like to express my special appreciation to the following people, I don't think I would be able to finish this thesis without their support. Firstly, I would like to thank my supervisors, Philip Riches and Avril Thomson for the opportunity to work with them on this project and for continuous valuable input. Secondly, I would like to show my appreciation for the expertise of the knowledgeable technical support staff at the University of Strathclyde: Jim Docherty, thank you for our wee chats and access to tools throughout my university career; Stephen Murray, John Wilson, and Dale Gibson, thank you for your excellent workshop skills. Thank you to my mentors from the DSA, Zara and Manpreet, for all your assistance developing writing skills. I am also grateful for access to bovine bones provided by Sandyford Abattoir Co. and to John Kelso at the abattoir for obtaining bovine samples. Outside university I relied on the emotional support from my partner, Stephen, and my best friend, Richard. I also got fluffy support from Marvin Rodger and Fiadh Vixen (I wish I had more time to play with Fiadh before her early departure and with Marvin before his sudden departure). Finally, to everyone else who helped me during my time at University; there are too many of you to mention, all your support is greatly valued.

Thank You!

Abstract

Knee arthroplasty surgeries have become an increasingly common procedure in orthopaedics, especially for younger patients. New robotic technology has been introduced into the orthopaedic surgery with good results. The robotic technology is versatile to use and it then opens up the development of potential novel prosthetic designs. This project investigates one type of knee arthroplasty – the unicondylar knee arthroplasty (pseudonyms: unicondylar (or unicompartmental) knee arthroplasty (or replacement) abbreviated to UKA or UKR); and how it can be improved by robotic technology.

The project followed a design process applying a range of methods to generate as many different prosthesis concepts, and then to organise and evaluate the concepts in a systematic manner. The strongest ideas were highlighted and, where possible, were developed into experiments. Some of the experiments were conducted practically in the lab while others were carried out by computer simulations. The project was able to provide constructive insight into novel prosthesis features and provide two prosthesis prototypes fashioned from the concepts. From the final two concepts, the BQ concept was picked due to the overall performance in the experimentation.

Chapter 1

Introduction

As people age they can develop joint problems and for many this can affect their everyday life, particularly with knee joint conditions[1], [2]. While most people are aware of total knee replacements (TKR), medically it is considered the last option. The traditional course of treatment for patients suffering from knee degenerative conditions is to initially go down the route of conservative non-surgical methods. When non-surgical approaches stop being effective for the patient's well-being, surgical interventions are considered, ranging in their invasiveness from arthroscopic surgery[3] to TKR.

TKR involves the removal of cartilage and bone of the distal femoral condyles and proximal tibia plateau (ligaments between the femur and tibia may be removed depending on the TKR model) and replacing it with prosthesis made from metal, polyethylene and/or ceramic. Over the recent years, there have been an increasing interest in unicondylar knee replacement (UKR) for patients with only one side of the knee (one compartment) needs to be replaced. While total knee arthroplasty (TKA) is by far the most common treatment for osteoarthritis (OA), in the time period 1998 to 2005, the increase in the use of unicompartmental

arthroplasty UKA) was more than three times that of TKA[4]. The typical indication for UKA over a TKA is, as mentioned, the patient has isolated deterioration/damage to one compartment of the knee – the tibial-femoral joint. If there are signs of damage or spreading of deterioration to the other compartments then is would be an indication for a TKR (or bi-lateral replacement). It is important to choose the right procedure for the right patient to improve the clinical and survivor statistics. Observing resected tissue from TKR procedures, it has been speculative that between 20 to 60% of patients receiving a TKR could have been potential candidates for a UKR prosthesis instead[5].

The different groups of people interested in UKR will have slightly different justifications for adopting this procedure. Prostheses manufacturers want to sell as many products as they can, so by offering a larger range of knee prosthesis types will attract a larger range of surgeons. UKR is compatible with most TKR and can be "upgraded" for many reasons. Therefore, by offering the full range of knee prosthesis from UKR to revision TKRs, the manufacturer is insuring repeat business. Surgeons and clinicians want to be able to provide all their patients with the best possible option for their individual case. For example, possibly the best option for an elderly patient's knee with arthrosis developed in all the knee compartments would be TKR; whereas a young active patient with healthy ligaments and damage cartilage in only one knee compartment, a TKR is an extreme intervention for this indication and possibly won't have a large range of motion that a UKR could provide[6]–[10]. Finally, patients desire to have quicker recovery time and to regain

full mobility of their knee in the shortest time frame as possible. Compared to TKRs, UKRs are less invasive as the incision is smaller and less tissue (bone and ligaments) is removed thus reducing the patients healing time and any complications[6], [11]–[13]. This improves patient's satisfaction[12], [14], along with patient's health, which is the aim of the medical team.

UKR have fallen in and out of favour over the years; the early results from the 1970's and 1980's were not favourable (problems included loosening of components and technical failures) and therefore, the performance of UKR procedures dropped[11], [15]. The late 1990's brought back the interest of UKR with a mixture of positive long term results from specialist centres and new instrumentation[11], [16]. As UKR develops, with the introduction of better design features and instrumentation, they are rivalling the TKR procedures. There a few studies that provide evidence that UKR prosthesis survive longer than TKR[13], [16].

While the majority of studies state that the UKR doesn't perform as well as TKR, but it outperforms TKR in short-term healing and functional parameters[10]–[12], [16], [17].

A study by Laurencin *et al.* (1991)[17], compared patient's preference of either UKR or TKR knee; with patella resurfacing on the TKR the preferred knee was the UKR (60% choosing the UKR and experiencing 23% having no difference) but without resurfacing most didn't notice the difference (54%) and those who did preferred the UKR knee (31%). UKR still requires improvement – there is a need to increase survivorship and to decrease variability from procedure to procedure. One

method of decreasing variability and increasing accuracy of UKR procedures is by utilising latest advances in orthopaedic tools. Manual methods of UKR have a wide variation between each surgery (compared to TKR) and are inaccurate of implant positioning and alignment[18]. This is increased when UKR is performed in minimally invasive procedure[18], [19], this is in contrast to a company funded study of the Oxford knee concluding that alignment is unaffected by a minimally invasive procedure[20]. Navigational assisted tools have helped surgeons to reduce UKR's variation and increase accuracy[21], [22]. Moreover, robotic orthopaedic tools can guide the surgeon where to cut and to prevent wanted tissue from being removed, this has been proven to improve the UKR's variation and accuracy more so than navigational assisted tools[23]–[25].

When accuracy is improved, the UKR survival outcome is also improved[26]. Therefore, combining a UKR prosthesis design that integrates with robotic orthopaedic tools can provide patients with long surviving prosthesis with excellent functional outcome that can rival TKR in isolated compartmental diseases for all patient age groups. As a result, this thesis seeks to readdress UKR prostheses design in the context of robotic orthopaedic tools where bone sculpting is more easily achieved and potential benefit to prosthesis fixation are possible.

Chapter 2

Literature Review

This chapter is a review of the information obtained from published sources: scientific literature from journal papers, articles, and conferences. The chapter begins with at general information about UKRs and how they are different from other procedures. This information was put in the design processing 'space' to guide the investigation to other aspects of UKR in relation to designing a novel UKR with improved performance. Throughout the investigation, the recorded information was up-dated as new information appeared; this information was referred to as the investigation progressed. The investigation then focused on established designing processes, this is detailed in the second part of this chapter.

2.1 Unicondylar Knee Replacement (UKR)

2.1.1 UKR Versus TKR

There are two schools of thought when it comes to knee arthroplasties (see figure 2.1-1): only fix the damaged part and try to leave healthy tissue alone[27]; or if one part of the knee needs to be replaced then the whole knee needs to be replaced because damage or arthritis will/has spread across the knee[28]. The UKR

procedure involves removing articular surface of one unicondylar compartment of the knee and is replaced with prosthesis components; this matches the first school of thought mentioned. The TKR procedure will involve the removal of articular surface across the knee to be replaced with the prosthesis components; this is the second school of thought mentioned.

Figure 2.1-1: Image of a UKR and a TKR
The images shown are of Stryker Ltd.'s knee prostheses take from a source online[260]. The left is the unicondylar knee replacement (UKR) and the right is the total knee replacement (TKR)

In Marmor's study[28] of 87 UKRs, only 18 reflected a poor outcome while 70% had satisfactory results at 10 years or more. From the study, 8 had to be replaced due to disease: 6 was established to be improper selection as the disease was too great for UKR, and 2 had degeneration of the uninvolved compartment of the same knee. Argenson in 2002[29] observed that the success of an UKR was down to patient selection; the 54 cases in their findings, and the 8 cases in Marmor's

study, had to have revision surgery shortly after an UKR procedure due to continued degeneration of ailments. Hence, patient selection is key whether to choose TKR or UKR, the parameters include: patient's BMI lower than 32, health of cartilage throughout knee, and no spreading disease[30].

Patients are out living their prostheses, especially with younger patients receiving knee arthroplasty. There is a limit how many times a patient can get a revision of a knee arthroplasty, because each revision involves removing more bone for the preparation for the revised prosthesis. Factors, such as presence of cement, will determine the volume of additional bone to be resected for the preparation. If each arthroplasty removes the minimal volume of bone, then theoretically a patient can have more revisions, if it was necessary, this would reduce their chances of outliving all their prostheses. This is another advantage of UKRs, that they are designed to have minimal bone removal in each compartment[6], [31], [32]; by doing so any revision procedure may provide a higher chance of success[33]–[36], though there a couple of reason papers that reject that claim[37], [38]. Arno *et al.*[30] credit the onlay style of UKRs with excellent results along with bone preservation. Aleto[39] and Halawi[36] recommend, in general, a UKR revision to a TKR implant is better than a TKR revision to a TKR implant due to the minimal bone loss in the UKR procedure. Additionally, choosing the UKR ideally means that a patient can undergo 2-3 revisions because they can have a UKR revised to a TKR – this revised to a primary revision TKR – this revised to a secondary revision TKR (generally a secondary TKR

revision is often discouraged). However, if the patient gets a TKR they lose the extra revision options.

UKRs in some of the literature have a revision rate greater than a TKR[40], [41] despite having good to excellent outcome in long-term survival[42]. There are a couple of reasons for this. The first is that early procedures of UKR had inadequate surgical techniques: positioning, bone preparation, cementing method, and improper patient selection[15], [42]. A potential problem with UKR is it can be difficult to create a strong fixation because the smaller area[30].Over the years the technology, techniques, and implant design has evolved, which has reduced the revision rate of the UKRs[43], [44]; Kulshrestha *et al.*[44] randomised study suggests at the 2 year follow-up of UKR and TKR have very similar performance.

Niinimäki *et al.*[40] used national registries to report the performance of UKRs compared to TKRs. Almost half UKRs in the study failed due to aseptic loosening (46.8%), compared to 26.7% aseptic loosening in TKRs. Their study had a breakdown of the different prostheses makes and the top performing UKR prosthesis is the Oxford with survival ratings of 90.4%, 83.7%, and 76.9% at 5-, 10-, 15-year respectively. The TKR results for the best performing prosthesis percentage stayed in the 90's from 5 to 15 year results; the worse performing TKR was still performing better than the Oxford prosthesis at the 5-, 10-, and 15-year marks (94.3%, 89.2%, and 83.2%, respectively). Conversely, the study on the performance of Oxford implant in the 1999[45] had survivorship of approximately 95%, 90%, and 85% at the three marked periods; additionally the Oxford had a survival rate of 84% (±9%) at

the 22 year mark. Even if there was a conflict of interest (it is not stated if there is) with the Oxford paper, it is comparable to Van der List at al[46] 2015 review into UKR (of any make) survivorship: 92.8%, 88.6%, 84.1%. A possible explanation for the difference in results is the lack of information provided by the national registries; the indications, implant design, and patient demographics aren't always stated[40], [46]. Registries also take into account the hospital statistics in terms of procedure volumes; Badawy *et al.*[47]found a correlation between UKR procedure volume and complications. The turning point is 40 UKR procedures a year, less than that there is an increase risk to dislocation, instability, malalignment, and fracture. This is also supported by previous works by Baker *et al.* and Noticewda *et al.*; they state that the UKR procedure are more challenging and by having surgeons familiar to the system improves the survival rates[12], [16]. Therefore, when looking at survival ratings it is important to note what information might be missing (national registries), and who are the excluding (cohort studies) to obtain a better idea how the procedures and prostheses perform.

Gulati's[20] study into the Oxford UKR states that UKR's have a larger range of acceptable alignment compared to TKRs; the notion is that alignment of TKRs is related to leg alignment thus if miss-aligned can cause abnormalities. The UKR's alignment is mostly component thickness, which has limited effect on the whole leg alignment. Referring back to Niinimäki's study, UKR failure rate due to malalignment is 6% and TKR is 9%[40]; implying the main cause of failure is aseptic loosening.

Other benefits the UKR has to offer includes (not limited to): faster recovery time, shorter hospitalisation, reduced thromboembolic risk, reduced morbidity, reduced mortality, increased ROM, preservation of soft tissue, preservation of natural knee kinematics, increased patient satisfaction[48]. The shorter hospitalisation and recovery time provides potential for UKR procedures to become a same-day out-patient procedure for a select range of patients[49]. An investigation from Walker's research, Yildrim *et al.*[4], showed that partial arthroplasty, such as medial UKR and patella trochlea, can produce kinematics that are similar to the natural knee during crouching. Since patients are expecting their natural kinematics after a UKR, then they be able to return to their recreational activities with UKRs. Two studies have found the number of patients returning to sport after TKR and UKR, with the UKR having a higher rate: Bradbury *et al.*[50] study had 65% of TKR patients returning to sport while Fishers *et al.*[51] had 93% UKR patients.

With all these benefits UKR has to offer, there is potential for this system to be more cost-effective over TKR procedures[41]. This was calculated using a Markov model and it included factors such as UKR higher revision rate; but it does rely on the clinical effectiveness and thus it might only be cost-effective with high-volume centres as they have fewer complications associated with UKRs. Overall, choosing between UKR and TKR for a patient is multifactorial and there still isn't a clear-cut rationale for one over the other.

2.1.2 Mosaicplasty

Mosaicplasty is a procedure aimed at encouraging knee cartilage to form a new surface naturally within scar tissue. This is less invasive than UKR and removes less tissue from the knee thus if a patient goes through with mosaicplasty then they are still eligible for arthroplasty if they need further intervention. This is done by drilling out damaged cartilage and replacing the holes (4-8mm diameter and 15-20mm deep[52]) with circular autogenous cartilage grafts from healthy non-weight bearing regions of the knee[52]–[54] (typically from the periphery of supero-lateral trochlea or superomedial portion of the tochlea[52]). This procedure can be done either by across the knee incision or by keyhole surgery, depending on the position of the damaged area[53]. There are alternative procedures that include autologous chondrocyte implantation (ACI) and autologous periosteal graft; these procedures involve cultivating tissue from other body donor sites to replace the damaged cartilage in the joint[53], [55]. The NICE guidelines[53] stated the results from 3 studies on Mosaicplasty; the results for “excellent to good” outcomes ranged from 69% to 94% [53], [56], [57] (one report has 66% of “fair to good” results[58]). Mosaicplasty show better results when repairing damaged cartilage on the condyle rather than the knee cap[57]. ACI had 88% of “excellent to good” outcome results compared to 69% for mosaicplasty and had more patients (84%) with signs of healing after a year from the procedure than mosaicplasty (35%). The NICE guidelines[53] suggest the wide variance in mosaicplasty and its successfulness of the procedure is dependent on area and volume of replaced tissue; as a result their final advice is that

mosaicplasty is an acceptable procedure but the patient needs to be aware that there are still uncertainties and the other possible procedures. Indications are: patients under the age of 45-50[52], [55], symptomatic cartilage defects are less than 2-3cm[52], [55], [58], [59], full thickness cartilage defect in weight-bearing joints[53], not for patients showing osteoarthritis or inflammatory arthropathies[55]. The reported risks taken from NICE guidelines[53] including, but not limited to: 9.6% patients had knee lock, haematoma within the joint (2%) or haemoarthrosis (4%) and infection (<2%).

Robert (2011)[55] reported that the mosaicplasty procedure is difficult and demanding; grafts "…should be flush, radial and not aggressive to chondral cells…" and with maximum coverage of grafts that are pressed-fit. Before or during the procedure knee joint misalignment (> 5°) or instability should be corrected[55]. Bentle *et al.*[58] suggest possible reasons for some of the mosaicplasty failure: the differing articulate cartilage thickness of the donor and recipient sites along with the difference in structural orientation which could be preventing full incorporation of the graft; including the difference in curvature[55]. The other disadvantage is donor sites are filled up with a film of fibrocartilage[52], [55], [58] and between the mosaicplasty plugs there is formation of fibrocartilage[58].

A similar procedure to mosaicplasty is osteochondral autografts: the procedure is almost identical with the addition of including bone tissue in the removing and grafting of the cartilage tissue; just like mosaicplasty, the donor sites are often unaffected areas of the knee[60], [61]. There is also stem cell transplants as

another available alternative; studies here have shown that stems cells alone don't last long (95% die within two weeks[62]) without being transplanted with a scaffold that encourages cartilage formation and integration[63].

Non-biological grafts are another alternative procedure that only removes damaged tissue of the knee joint and replacing the gap with a filler material with a smoothed surface (like pot-holes on a road). This is a similar idea to inlay prosthesis (see page 27) and mosaicplasty but preserves local healthy tissue and does not damage other healthy tissue sites, respectively. There are numerous material types for non-biological inserts, from Bohner's[64] extensive investigation into the subject, with ceramics (inorganic non-metallic) being recommended for their biological performance unless in a high loading environment when a metal material is advised. The advantage of using non-biological grafts, on top of them being less likely to invoke an immune response, is that the final structure can be manipulated and are not relying on growth of tissue. This area could be perceived either as different to inlay prosthesis or as different type of inlay prosthesis design, such as it being a modular inlay prosthesis ranging from partial plateau coverage to full coverage. A design process needs to take place to look at the possibilities in this area and if it is a promising route to take.

2.1.3 Surgical Tools

Manual tools are used in most orthopaedic surgery, with and without navigational assistance; the tools used include, but are not limited to (figures 2.1-2 and 2.1-3): cutting jigs, drills, screws, oscillating saws. The manual system carefully placed jigs with the use of recognisable landmarks as guides for removing the bone ends leaving flat surfaces with defined edges.

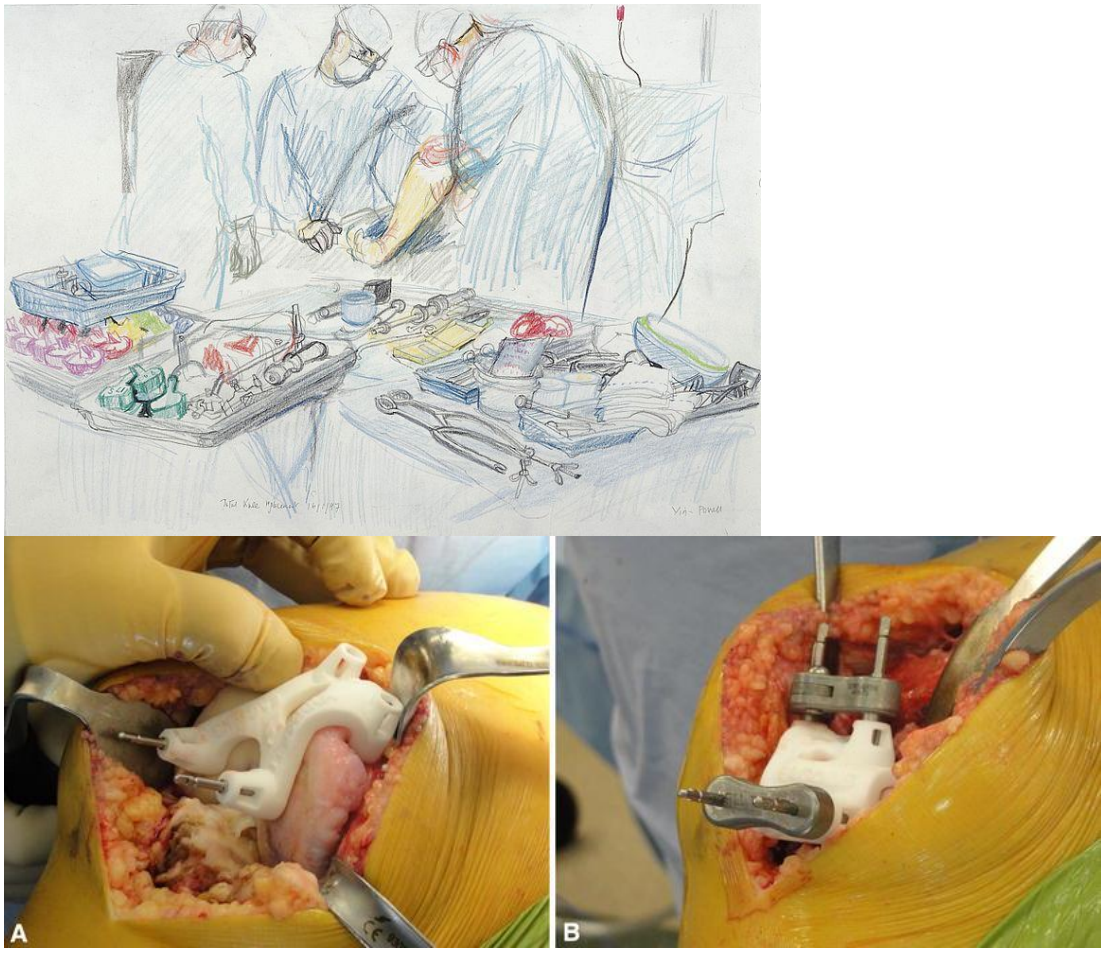

Figure 2.1-2: Images of Orthopaedic Knee Procedures
To the left is a sketch by Virginia Powell[261] that depicts a typical orthopaedic knee surgery using manual tools.
The bottom two images are of Biomet Inc. Signature™ Personalized Patient Care System[262], i.e. a patient specific cutting jig.

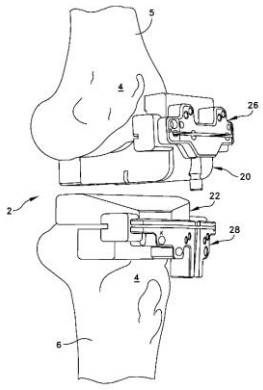

Figure 2.1-3: Schematic of Cutting Jig by Wright Medical Group Inc.
The image is from google patents for a patient specific surgical guide (jig)[263]*. The structures labelled 5 and 6 are the patient's bones (tibia and femur respectively). The additional structures are drilled in position and the slits seen in the schematic are where the oscillating saw cuts the bone.*

There are surgical practices that offer robotic aid to knee/hip replacement procedures. Currently the two robotic orthopaedic tools certified for use are RIO by MAKO (certified in 2006) and NavioPFS by Smith and Nephew (certified in 2012 by Blue Belt Technologies). The systems are similar as they both consist of stereo infrared cameras, light reflecting trackers, and a control unit; the main difference is the cutting burr. The RIO system, figure 2.1-4, is referred to as a stereo tactic system due the cutting burr being attached to a robotic arm - the surgeon can move the burr head to desired positions to remove bone tissue but the arm prevents the burr being moved into areas where bone is to be preserved. In the other system, the NavioPFS, figure 2.1-5, the burring tool is held "freely" in the surgeon's hand allowing the surgeon to position the burr in a desired spot – the system can prevent the surgeon from removing wanted bone/tissue by retracting the burr head into a protective sheath where it can't do any harm.

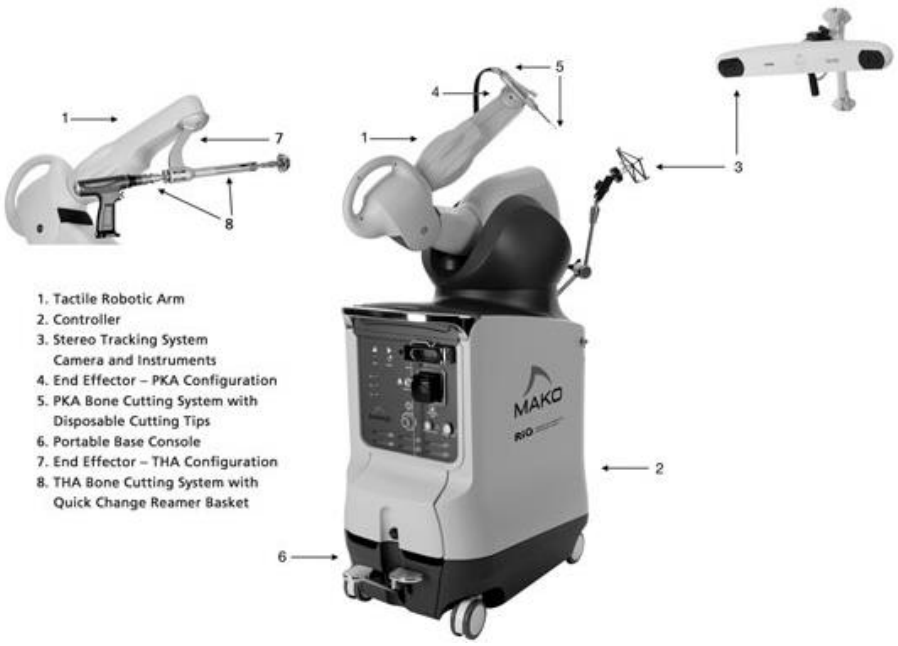

Figure 2.1-4: The RIO System by MAKO Crop.
The RIO system has stereo tracking with haptic feedback to allow accurate removal of bone tissue. Numbers 7 and 8 refer to the hip procedures. Source: 2012 10-K

Figure 2.1-5: Image of the NavioPFS Cutting Burr
The NavioPFS system has stereo tracking with a retractable burr head to prevent unwanted removal of bone tissue. Source: Lonner et al 2015[74]

Figure 2.1-6: Image of the Femur and Tibia Stereo Tracking Frames
All robotic technology system parts require a tracking frame to locate its position in surgery using inferred stereo sensors. This image shows the femur and tibia tracking frames in situ in the surgical procedure. Source: Lonner 2009[142]

There are another two methods of preforming knee arthroplasty that are currently not on the market: milling[65] and lasering[66]. The milling technique is a cross between the robotic tools above and the traditional methods. The articulating surfaces of the knee are exposed and a milling jig is positioned. The mill (similar to the burr head) is fixed to the jig and the bone is cut to the required depth and shape. This procedure creates a smooth surface finish on a flat surface, yet there is potential for a jig to create a curved surface. The laser technique is very much like the robotic system, with the burr head is replaced by a bone cutting laser.

The position and alignment of the prosthesis components could lead to better outcomes in terms of kinematics, survivorship, and wear patterns[67]–[69]. Navigational tools are one method to ensure proper placement and alignment of the components[21], [70]. They can work alongside conventional UKR and TKR methods by checking the placements of the jigs are correct before cutting the bone tissue. Navigational tools have been shown to significantly improve alignment over just using landmarks to place the conventional jigs[21], [70]. Alternatively, robotic orthopaedic tools can further enhance the accuracy and precision of prosthesis' positioning and alignment[23]–[25], [71]–[73]. Lonner *et al.*[74] found in their cadaveric study using the NavioPFS system, the prostheses were positioned within 1.3mm and 2° of the planned position, this is comparable to studies, including Picard's *et al.*[69] (potentially biases lean in favour of) NavioPFS system that had 1mm and 1° out from the planned position.

Since the above literature promotes the robotic technology to be accurate and precise, the question developed to: is the improved accuracy and precision justifiable in the prosthesis performance? Roche and Conditt in 2014[71] state that the early UKR failed due to surgical techniques that include malpositioning of the prosthesis and accordingly the MAKO can provide comprehensive 3D planning of component positioning and soft tissue balancing. In addition, they reported that the Rio system had improved the post-operative outcomes in the measured functions. Part of UKR procedure is to correct ligament alignment to correct the patient's varus-valgus deformities. Robotic tools can assist the surgeon understanding of the patient's ligament tensions by analysing the joint movement; this can prevent over- or under-correcting the tension balance[71], [74], [75]. Robotics can also assist in intricate surgeries, such as lateral UKR[76] by providing pre-op planning and/or in-op planning. Furthermore, the kinematics of the knee after arthroplasty can be similar to natural knee by the robotic technologies' accurate placement of the prosthesis[4].

At present the two techniques, oscillating saw and burr drill, produce different surface finishes. The oscillating saw method leaves a fairly smooth surface finish and the time to remove the tissue is not dependent on the volume of bone tissue being resected. The burr drill leaves a surface finish that is bumpy and pitted and the time required is dependent on the volume of bone needed to be resected (and the complexity of the final shape). Surgeries using the Rio system, take twice as long (in total, including factors on top of bone removal) as the conventional methods[77] (20 mins and 10 mins respectively). The burr method generates heat

friction that can accumulate in the bone tissue. There are ongoing studies on cell survivability comparing an oscillating cut surface and a burred cut surface. One particular study illustrates with appropriate cooling by irrigation, the cell validity after cutting or burring the bone are both viable[78]. With related to these two techniques, one area of interest will be the bonding property of bone cement to bone and implant.

The advantage of using a burr is the accurate intricate removal of hard tissue but the main disadvantage, as mentioned, is the generation of heat and time required to remove bulk tissue. Surgeons have been known to remove the tibia plateau (the main tissue bulk to be removed) using manual tools in order to save time, see chapter 3 *Personal Experience Exploration*. This chapter also discuss other problems noted from first-hand experience from using a burring system.

The cost of using robotic orthopaedic tools is a concern because they are expensive equipment in terms of capital and running expenditures. Using the Markov model, Moschetti *et al.*[68] concluded that it is cost effective on the conditions that the centre carries out more than 94 UKR procedures a year with a 2-year failure rate less than 1.2%.

The use of a burr cutting drill opens the scope for prosthesis designs as it removes the need for cutting jigs. The cuts can become intricate and surgery specific (surgery for cartilage damage might not suit the same procedure to surgery for arthritis). One possible reason for the lack of diversity of prosthesis designs that work with robotic orthopaedic tools is that these tools are fairly new and are only

just making their way into main stream surgery. This leads to the second reason of professionals not being familiar with the system. This brings about the third possible reason, a novel approach will be fraught with issues and pitfalls[71]; this might prevent professionals being willing to take the risk especially when they are happy with the conventional method and results. If the novel approach is broken into stages, then issues are fixed one stage at a time thus reduces the overall risks. This is how BBT NavioPFS system entered into the market (potentially without conscious of this approach); it relied on the current implant technology to sell their system that provides precision and accuracy of implant placement. By utilising robotic systems, it opens up potential re-design of implants to improve their performance.

2.1.4 Bone Cement

Bone cement is a colloquial term for the substance used in orthopaedic surgery to join bone to bone or bone to implant; this is normally polymethylmethacrylate (PMMA). This substance is different from the PMMA used in dental procedures and more so from Plexiglas. Charnley is one of the first to introduce PMMA into orthopaedic surgery in the 1950's[79] – today it is still used and is regarded to be the "gold standard" in hip and knee surgeries. The term bone cement can also be applied to calcium phosphate (CPC) and glass polyalkenoate (GPC) used in orthopaedic surgery, these substances are less commonly used hence

bone cement throughout this document refers to PMMA type unless stated otherwise.

PMMA bone cement is an acrylic polymer formed by polymerisation when a liquid monomer and co-polymer are combined[80], table 2.1-1, below, shows the contents of Heraeus bone cement[81]. Bone cement is often sold in a range of viscosity properties which represents the 'doughy-ness' of the cement in the working stage, see chapter *6 Experimentation of Fixation Techniques*; with Heraeus the options are low, medium (regular), and high. In addition to the viscosity properties, bone cement can have anti-biotics added to the powder component – often it is gentamicin or tobramycin[82], [83].

Table 2.1-1: Heraeus Palacos®R bone cement component contents

Liquid:		Powder:	
Monomer	Methyl methacrylate	Polymer	Poly(methlacrylate, methyl methacrylate)
Accelerator	N,N-dimethl-p-toluidine	Initiator	Benzoyl peroxide
Stabiliser	Hydroquinone	Radio-opacifier	Zirconcium dioxide
Colourant	E141 (Green)	Colourant	E141 (Green)
		Optional	Antibiotic

2.1.4.1 Preparation

Bone cement goes through 4 phases: mixing, waiting, application, and setting. It is highly recommended by the Heraeus manual[81] to add the powder to the liquid to prevent powder nests and to keep a uniform polymerisation reaction

and the components need to be thoroughly mixed in the first 30 seconds. The mixing of components can be done by hand or in designed mixing apparatus – Heraeus calls theirs the Palamix. The waiting state commences after the mixing stage, in this stage the substance is still fairly liquid like state which take from 15-150 seconds to change to a 'doughy' like putty – the time is dependent on the room temperature and mixing method. When the bone cement becomes doughy it is ready to be applied to the bone – this is the working stage of the cement which last between 3 to 5 minutes (again dependent on the room temperature and mixing method). The viscosity stated for the bone cement refers to the 'doughy-ness' of the cement at this stage. High viscosity cement has a 'dough' state that is firm which is easier to work with by hand and in bulk volume. In contrast, the low viscosity cement's dough is more fluid and maybe harder to work with in some conditions it works well with small joints and fracture type surgeries. The cement's dough viscosity has an inverse relation to the cement penetration into the bone matrix[79], [82], [84], [85]. When applying the cement, it can be done by applying the cement by hand or a delivery system (often integrated with the mixing system) to the bone and the cement is either pressed down by thumb/fingers or by pressurisation; by apply pressure could improve the cement penetration[85] but this could be limited[86], [87]. The final stage is the setting stage that is approximately 4 minutes; here the bone cement temperature rises somewhere between 40°C[88] to 82-86°C *in vivo*[80] while it hardens.

Formerly mentioned mixing method, there are a number of options to mix the components together: by hand or by appropriate mixing apparatus which can be either mixed under vacuum conditions or atmospheric conditions. The cement properties during and after curing are dependent on the mixing method used. Porosity of bone cement has been widely talked about in the literature, the bubbles that contribute to the porosity, microporosity and macroporosity, is produced by a combination of 5 different sources during the cement preparation: air is entrapped when the powder is poured, air is entrapped in mixing, air is entrapped when working with the dough, the air that is initially surrounding the components before mixing, and when the cement heats up during curing that causes boiling and evaporation of liquids[89]. Some have argued that the porosity can create local stresses that initiate crack formation, while other have suggested that they dampen in the growth of cracks in the bone cement. Overall there is a general consensus that the number and size of bubbles need to be reduced. One method to reduce the extra formation of bubbles in the cement is to mix the components under vacuum conditions[90], [91]. Plus under vacuum conditions the working state is longer and the peak temperature is reduced[92]. Other methods that can control the porosity of the cement are the mixing apparatus (hand, pump, centrifugal etc.), application method (through a pump, syringe etc.), and chilling the components prior to mixing.

The thickness of the bone cement under the implant has been reported in terms of shock absorption and micro-motions. Bauer[93] states that a thick cement mantle for the implant is better than a thin cement mantle, although Ramaniraka[94]

suggests that mantle should be between 3-4mm and any thicker or thinner will increase destructive micro-motion.

The preparation of the bone determines the fixation strength of the cement to the bone[84], [85], [95], [96]. Once the required bone tissue has been removed, the exposed bone needs to be cleaned from debris and blood. This permits a full contact of the cement to the exposed bone surface but the penetration of the cement into the bone matrix is dependent on the cleaning method. Majkoski *et al.*[97] establishes that the interstitial tissue in the bone matrix acts as the barrier, preventing the cement from penetrating into the matrix and that high pressure lavage is efficient to remove this tissue to allow penetration up to 7.9mm. The other methods used in the study was unprepared, brushed with irrigation, pulse lavage, and high-pressure lavage with brushing irrigation; the former two only allowed penetration up to 0.2mm and 1.4mm (respectively) and the latter one was insignificantly different from the high-pressure lavage alone.

2.1.4.2 Cement Interface

There is a split in opinion on the purpose of bone cement used in orthopaedic surgery; common belief is that it is the glue for affixing implants to bone surfaces but the other belief is that bone cement is more of a shock absorber[93] and space filler than a glue [80], [86]. Many studies have looked into the strength of the bone to cement interface and they state that bone cement has no intrinsic adhesive properties[85], [86], [98]–[100] or that PMMA is unable to bond to living bone[101], [102]. The bone actually interlocks with the bone surface and a good bond is

dependent on the cement penetration into the bone matrix to form interdigitation[82], [87], [95], [96], [99], [100], [103]–[107]. Without interdigitation, the cement bond strength is dramatically reduced[98], [103], which supports the theory that bone cement isn't really glue for affixing bone in these conditions but it can be avoided with good bone preparation – by using a high pressure lavage and completely drying the bone before cementing[80], [97].

As the bone cement's primary means of attachment to bone is through interdigitation which has led to the belief among surgeons that there is no adhesion between PMMA and implant because the cement doesn't penetrate the surface to form the interdigitation bond. However, Davies and Harris[108] have dispelled this belief with their research and showed that there is bond between (grit-blasted finish) implant and cement. This bond has a tensile strength around 5MPa – this is quoted to be seven times lower than the ultimate tensile strength of bone cement.

However, there is still debate as to whether a smooth or rough surface would have better adhesion with bone cement[93], [109], [110]. The argument for retaining a smooth surface is to reduce debris generated when the cement adhesion deteriorates and starts to cause wear. This question is still to be fully answered[93]. Ramanirake[94] results show that a smoother implant surface finish increases slipping and decreased debonding. The paper also states that improving the cement to implant interface has a significant increase of slippage at the bone to cement interface which could promote early failure of the implant. A smooth surface can allow certain implants, like femoral hip components, to self-tighten[110],

this has been shown not to cause significant damage to the cement mantle[111]. From several studies reported in Lennon *et al.* 2003 article[110], the debonding will occur in both smooth and rough surface implants as a results the rough will have increased wear damage; their results don't confirm their hypothesis that a rough implant surface will have lesser cement mantle damage than smooth implant surface. However, Verdonschot and Huiskes'[111] research suggested that implant roughness does not reduce the damage generated in the cement mantle even though the mechanical behaviours were different. All this put together points in the direction of admitting that the cement and implant interface will separate and thus to improve survivorship of the implant, a smooth surface that prevents wear particle generation might be the approach to use.

As already discussed, there are a couple of methods that can increase the cement penetration into the bone matrix: cement viscosity, bone preparation, pressurisation. Increasing the interdigitation has a linear increase on the strength and the stiffness of the bone to cement interface; same applies to the contract area of the bone to cement interface[86], [95], [105]. According to Majkowski[112], the strength does not increase after 3 to 4mm of penetration. The literature seems to be in agreement that the bone to cement interface is essential for long term viability. The interface of the bone to cement has been reported to be 2.5 times stronger in shear than in tension[86] and this is independent on interdigitation. Halawa[85] reports that the bone remodelling that occurs next to the bone to

cement interface has limited effect on improving the shear strength. The majority of cracks occur in the cement body and not the bone matrix[86].

2.1.5 Implant Models

There are various UKR designs featuring different aspects, providing their own advantages and disadvantages. This section will cover the topical different implant categories.

2.1.5.1 Inlay and Onlay Prostheses

Inlay and onlays are two methods of implantation of the prosthesis on the proximal tibia, see figure 2.1-7. A typical onlay prosthesis requires the full removal of the compartment's tibial plateau (this includes removing meniscus, cartilage, cortical and subchondal bone) to create a seat for a metal tibial component with an interlocking bearing, which is normally made from polyethylene. Inlay prostheses also removes the tibial plateau but leaves the subchondal bone and the cortical rim, which creates a shallow seat for an all-polyethylene bearing to fit[113]. Almost all UKR prosthesis manufacturers design an onlay prosthesis for several reasons: onlays are widely used which means if a surgeon/practice chooses a different manufacturer, the skills are easily transferred (less time to relearn). This in turns makes it an accepted design since there is long-term history with statistics making it harder to introduce a different (inlay) design, since it doesn't have the guaranteed status as a widely accepted (onlay) design.

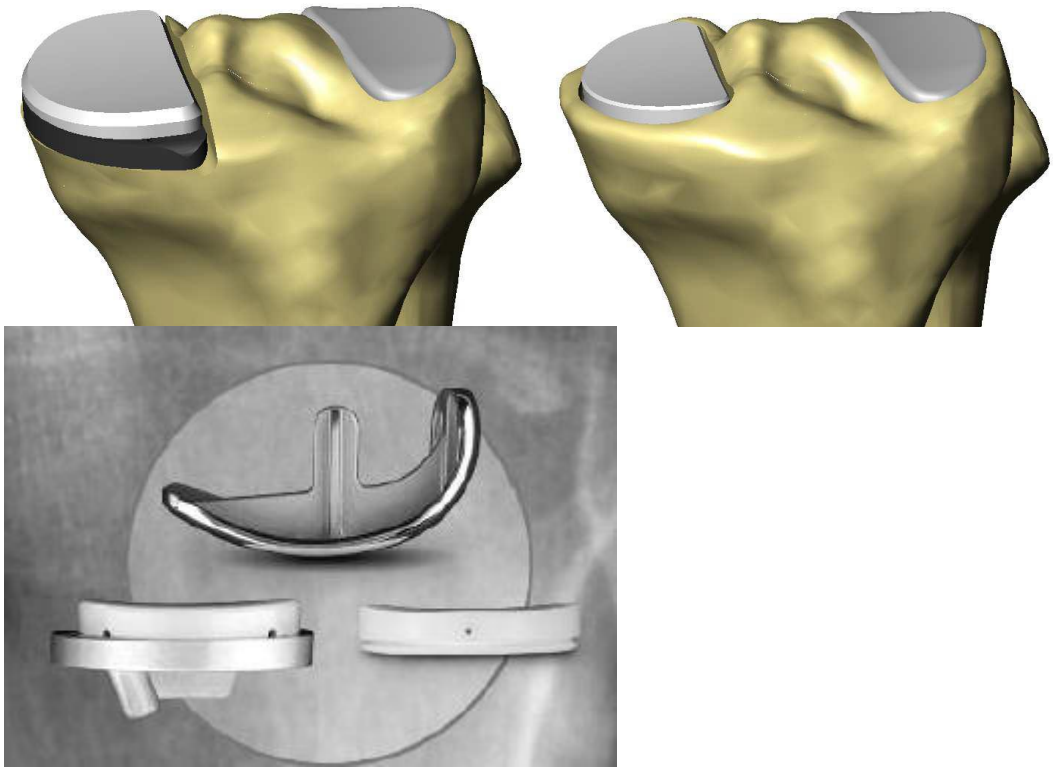

Figure 2.1-7: Images of Onlay and Inlay UKR Prostheses
Top left is an image of an onlay prosthesis and top right is an image of an inlay prosthesis; both indicating the volume of bone removal.
The bottom image is of MAKO's onlay and inlay prosthesis, left and right respectively.

Furthermore, onlay prostheses as a whole do not need special equipment and each manufacturer provides the same rudimentary tools and jigs, whereas the inlay prosthesis needs more guidance and will be more patient-specific due to the difference in knee anthropometry. This makes inlays less straight forwards and costly in tools, and surgical learning. Robotic tools are making an appearance in operation theatres; this means that inlay implants can be developed and adopted since the system takes care of patient-specific nature of the method and increases transferable skills. Similar to the introduction of UKR, inlay prosthesis may have a bumpy start as surgeons and patients would like to have guaranteed satisfaction.

Inlays have the potential to reduce post-operation pain and recovery time because it preserves more bone including the medial tibial cortex and nociceptors of periosteum[114], [115]. So far studies relating to inlay prosthesis are overall negative: poorer results, pain, more stress/strain and disfavoured procedure compared to onlay prosthesis[116], [117]. There are a few studies that demonstrate inlay prosthesis can have improved performance by tweaking the design such as creating channels for the cement[5]; this is a similar trend when onlay UKR were making an appearance to a world of TKRs.

In an annual summary produced by MAKO[5], it claimed that MAKO's onlay prosthesis are implanted with 2-3 times more accuracy with at least 3 times more reproducibility compared to standard onlay prosthesis procedures. The numerical results (these are not stated in the report) for the inlay prosthesis also had improved accuracy in each category. Inlay prosthesis are made of polyethylene and have the benefit of preserving cortical bone on the outer edge of the tibia. However, in finite element models, the inlay prosthesis has been found to generate a peak stress 6 times and strain values almost 13.5 times greater on the tibial surface as opposed to the onlay prosthesis[5]. It was not specifically stated in the work why the inlay causes a greater stress concentration but the understanding was the inlay's reduced surface area compared with the larger surface of the onlay, together with the unstated loading conditions applied to the FEA could produce the higher stresses recorded. Due to the numerical value, they suggested that the best prosthesis design option is the onlay design over the inlay design. The report then

goes on to suggest improvements for the inlay prosthesis design. If a cement channel is added to help with fixation along with a dovetail channel to improve lift-off resistance, it will result in 10 times stronger laboratory push-out tests.

Walker *et al.*[118] used computer models to determine how stress and strain of the tibial components create on the underlying bone. Using their strain values, they established that the inlay tibial component produced peak stress directly beneath the loading point whereas the onlay implant distributes the load under the metal implant so there is less peak stress values. The meniscus also plays an important role of distributing load; it spreads the load so there isn't a point-load to create high stress peaks. From these findings, the inlay prosthesis designs need to incorporate a method to spread loading.

Suero *et al.*[119] investigated the effect of different UKR tibial components on the mechanical alignment. Their results showed that patients with metal-backed onlay tibial component had better post-operation results than inlay all-polyethylene tibial components; it is their belief that the thicker construction of the onlay components is an important factor for alignment. Gladnick *et al.*[120] in the same year, found that onlay prosthesis had better pain relief compared to inlay prosthesis at the two years follow-up. They also observed a trend that onlay prosthesis has improved functional performance and fewer surgical procedures. The pain could be due to the procedure exposing raw nerve endings, Gleeson *et al.*[121] suggests that reaming could be a cause of pain. Gladnick *et al.*[116] two years later still advises a metal-back onlay UKR over other designs due its better clinically performance.

Thompson[96] argues that the inlay fails as a result of inadequate cement penetration due to the current onlay technique being difficult for inlays prosthesis, therefore an alternative cementing process is needed. The new cementing technique is to create a thicker cement–cancellous-bone interdigitation by the use of a pulsed lavage technique. Plate *et al.*[122] argues in favour for inlay designs even for patients with BMI greater than 32Kg/m^2; though it is noted that have a higher revision rate compared to the onlay designs.

The innovative idea from Chaudhary and Walker[123] was to switch the material of the tibial and femeral components around so that a thin metal plate (with and without an A-P keel) is inserted to the tibial plateau; and the condyle has an all-polythylene inlay. The idea for this is that the thin metal tibial component can preserve the dense and stiff bone near the surface, which is ideal for the loading to distribute across the bone. The FEA results revealed that the polyethylene tibial inlays had elevated stress and strains. These are factors associated to: tibial loosening, non-uniform bone re-modelling and pain. The metal tibial inlays showed a distributed stress and strain, 2mm with keel had better distribution than 3mm without keel. This innovated reverse of the materials seems to be an effective solution to solve the distribution of loading problem that inlay prostheses have, which can lead to failure of the prostheses.

Chaudhary and Walker's study is very similar to Hori and Lewis' study in 1982[106]; their thought process was to match local tissue mechanical properties to create a prosthesis and obtain a silastic rubber between bone and cement. The

mechanical properties of articular cartilage (estimated modulus of 330MPa) come from the fluid interaction of the synovial capsule (hydrostatic pressurisation of tissue). This is due to an avascular tissue that receives nutrition via diffusion from the synovial fluid, whereas fibrous tissue (estimated modulus of 2MPa) interaction is unclear and needs further investigation because of the rich vascular supply and lost fluids are replenished quickly[106].

There is a potential to do inlay procedures for a select group of patients in the hope that they don't need to be revised. This has a two-fold benefit if the inlay prosthesis does require a revision[122]. First the upgrade would have a higher chance of success due minimal bone removal. Secondly there are still the option of revising to an onlay prosthesis, again this preserves bone tissue removal.

2.1.5.2 Cement and Cementless Prostheses

Bone cement (PMMA) is an option to ensure fixation and load transfer of the prosthesis to the exposed bone. The other option is to use prostheses that have a surface that encourages growth of bone which then bonds the prosthesis onto the bone matrix.

There are different opinions and theories on whether cement should be used or not; some believe that cement is harmful[159], [160] and others think that cementless is the inferior option[161]. Depending on literature findings, the cementless prostheses can be either just as effective or less successful than the cemented prostheses[42], [107].

There are concerns that cement can cause necrosis of bone tissue (caused by thermal, avascular, or micro-fracture damage) - this can happen up to 3 weeks post-operation[160]. The research by Linder *et al.* [162] suggested that the monomer trauma from the bone cement did not add to the minimised surgical trauma; the important issue for acute tissue trauma was the preparation of the prosthesis bed and inserting the bone cement. Necrotic tissue adjacent to the cement is resorbed and initially replaced with an immature, poorly organised soft tissue between bone and cement; this tissue can take up to 2 years to mature and still not be uniform[160]. Mann *et al.* in 2012[163] concluded that biocompatibility or thermal necrosis are not issues when it comes to bone resorption because the bone continued to have a strong interdigitation within the same samples. Both cement and cementless produce similar fibrous tissue[106]; it has been suggested the important factor for the differential of the reform tissue is mechanical stimulus[106], [160]. Carter *et al.*[164] developed a graphical hypothesis for the different mechanical stimulus on the bone, figure 2.1-8; fibrocartilage is due to compression and it is virtually devoid of factors that could shorten its longevity. Oonishi *et al.*[165] deduces that cementless prostheses that form a chemical bond to bone will lose the connective tissue but cement prostheses (and cementless prostheses that don't form a chemical bond) have the connective tissue broken down by the presence of high-density polyethylene (HDP) wear particles which will cause loosening at the interface.

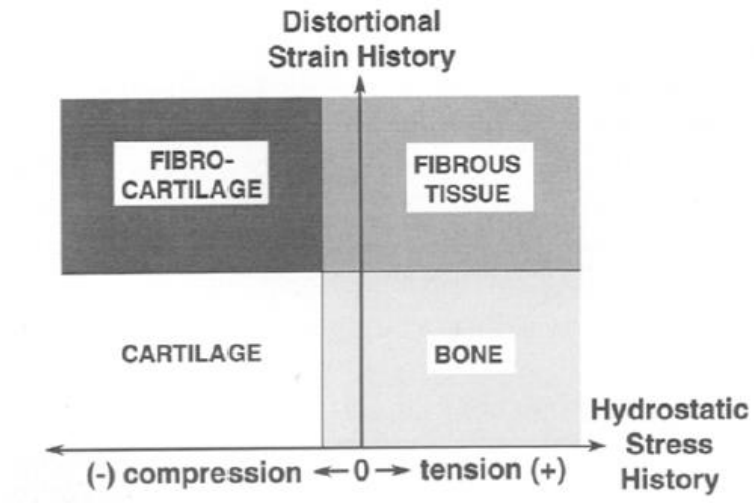

Figure 2.1-8: Schematic of Tissue Differential in response to Mechanical Stimulus
The schematic is taken from Carter et al 1988 paper[164] shows which tissue is developed under the different stimuli.

Cemented prostheses have the advantage of being 'very secure immediately after surgery'[165], while cementless options take time before the bond is fully formed between bone and prosthesis. As cited in Sara and Pal's paper[79], the research found there is not deterioration in static or compression-fatigue behaviour when the cement is stored in bovine serum at 37°C for 2 years and the fracture toughness is increased when stored in bovine serum compared with air. However, these results are contradicted by Oonishi finding of the bond strength of the different types of prostheses over time, figure 2.1-9 exhibits that has the cemented prosthesis having the highest strength initially but over time it degrades to approximately the same strength as an untreated cementless porous prosthesis. During the degradation of the bone cement, there is a cross over point where the cementless options the bond strength grows; in the case of porous coated with HAP (hydroxyapatite) appears to be just as strong as the initial strength value of cement.

Aseptic loosening is the leading cause of cemented UKR[40], [67]; cementless prostheses have a reduced risk of aseptic loosening over time[43], [166]. Furthermore, a cementless UKRs on have a reduced surgical time compared to cemented UKRs[43], [166], on average 9 mins[67].

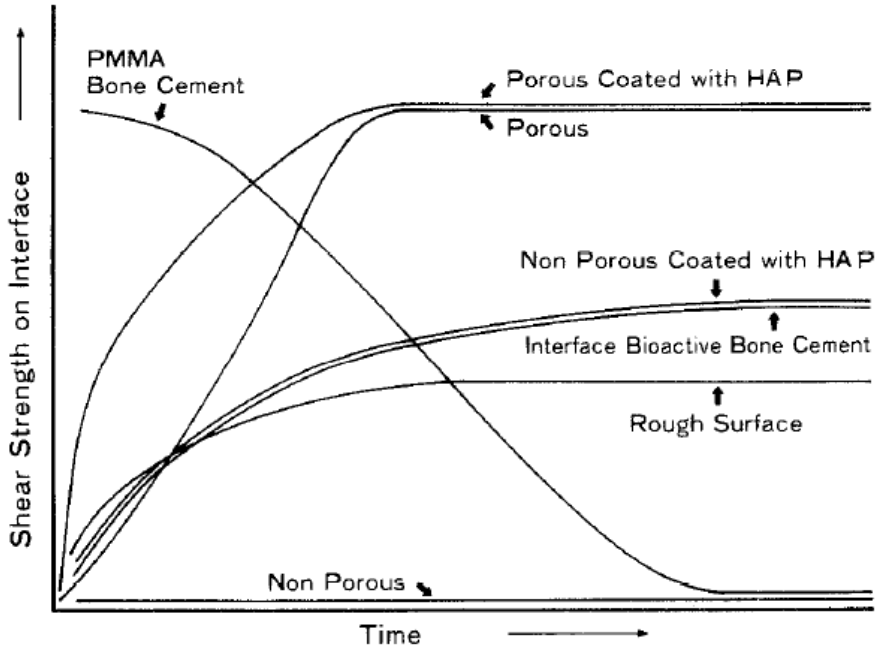

Figure 2.1-9: Interface Strength Over Time
A schematic from Oonishi et al 1990 paper[165] dipictating the loss of strength of bone cement over time while osseointegration cementless prostheses increase in strength over time.

Cemented prostheses may prevent micro-motion from happening but it is down to the cementing technique[42], [106]; the techniques that provides deep penetration are best fixation for micro-motion[107]. Cement that has only penetrated 0.25-0.5 mm into cancellous bone is not sufficient to resist distraction forces or prevent stem from acting like a piston[106]. However, this again is short-term, as mentioned above, the cement degrades over time. Cementless prostheses that have a chemical bond to bone have no pain due to micro-motion[165].

Cemented prostheses are good for the initial fixation, as discussed, this is good for elderly patients as they can get back to full recovery and will only need one or two revisions. Whereas younger patients also can benefit from the faster recovery but since cement loosens in the range of 10 to 20 years[167] and having more than 1 revision is not ideal, the patients can outlive their prostheses; this is another push for cementless options[93], [168], [169].

Reports suggest different percentages for the appearance of physiological and pathological radiolucency lines[36], [42], [107], [170], [171] but all agree there is a less frequent and smaller in size radiolucencies lines in cementless prostheses. Additionally some authors report the absence of radiolucencies lines after 2 years[43]. Freeman *et al.* [159] observed that the radioluceny at the bone to cement interface has a different appearance from a bone to cobalt chrome interface (cementless). It appears that macrophages are attracted to PMMA in a similar way as to other prosthesis material[159], [172]. The number of macrophages is positive in relation to the fibrous tissue found. It has also been suggested that this attraction is due to the presence of miniature beads or cement shed from surface or slow leaching of monomers and the formation of radiolucence lines at the bone-cement interface[159], [170]. However, the use of radiolucent lines to determine if the prosthesis is successful isn't a useful predictor[170], but could still be used to determine the effectiveness of fixation of a prosthesis.

An interesting study on cement and cementless total hip replacements was presented at GlarMOR 2014 (Glasgow Meeting of Orthopaedic Research)

conference; they compared the death rate between the two types of hip replacements. It was speculated that the older, frailer hip replacement patients are less likely to survive hip replacements that use cement, indicating that the cementless option is recommended for this select group of patients. The study showed that on the day of surgery the patients that had the cementless replacement had a greater chance of surviving. The chances of survival then became the same as cemented from day 1 (the day after surgery) till day 30, where the cemented replacement had a greater survival outcome. This kind of study doesn't take into account many factors, it merely generates figures of patient death. Therefore, it is possible for a hidden cause to be present which isn't obvious from the statistics.

From the readings, it is still ambiguous if cementless prostheses are more effective than cemented prostheses. Cementless can reduce the unwanted factors that cement comes across (tissue damage, immune response, death) but it creates its own disadvantages by reduced initial stability of the prosthesis which is desired for positive mechanical loading. It has been reported that the cementless option is suitable for UKR but not for TKR because of the mechanical environment of the interface. The loads under the tibia in UKR implants have been reported to be chiefly compressive and the shear stresses minimal because the tibial-femoral joint isn't constrained (especially with mobile bear type implants)[166].

Finally, the choice between cement and cementless may need to be assessed on a patient specific basis to provide the best selection for their condition and lifestyle[107].

2.1.5.3 Medial and Lateral UKRs

In theory, UKR procedures should be able to replace either a damaged medial or lateral compartment of the knee. Yet the number of UKR procedures is not equally split between medial and lateral[43], [173]. This is partly due to osteoarthritis rarely forming in the lateral side of the knee: McAlindon *et al.*[174] looked into the formation and development of osteoarthritis in a group of volunteers over 55 years of age in the Bristol area of England. Figure 2.1-10 contains three Venn diagrams of the percentages of observed osteoarthritis in the volunteers and in all three subgroups, the lateral compartment exhibiting osteoarthritis is no higher than 6.7% while the medial side ranged from 7.9% (no knee pain subgroup) to 30.5% (men with pain subgroup). It was also observed that the development of medial compartment osteoarthritis increases with age in men, whereas in women it is the development of patellofemoral osteoarthritis increases with age. These results are comparable to other studies finding that the occurrence of isolated lateral osteoarthritis is in the range of 5-10%[43], [148]. Observations by Brown and Shaw[175], showed that the medial condyle carries 60% of the load compared to the lateral condyle, this could partly explain why one compartment, as shown in McAlidon *et al.* finds, has a greater incidence of isolated osteoarthritis.

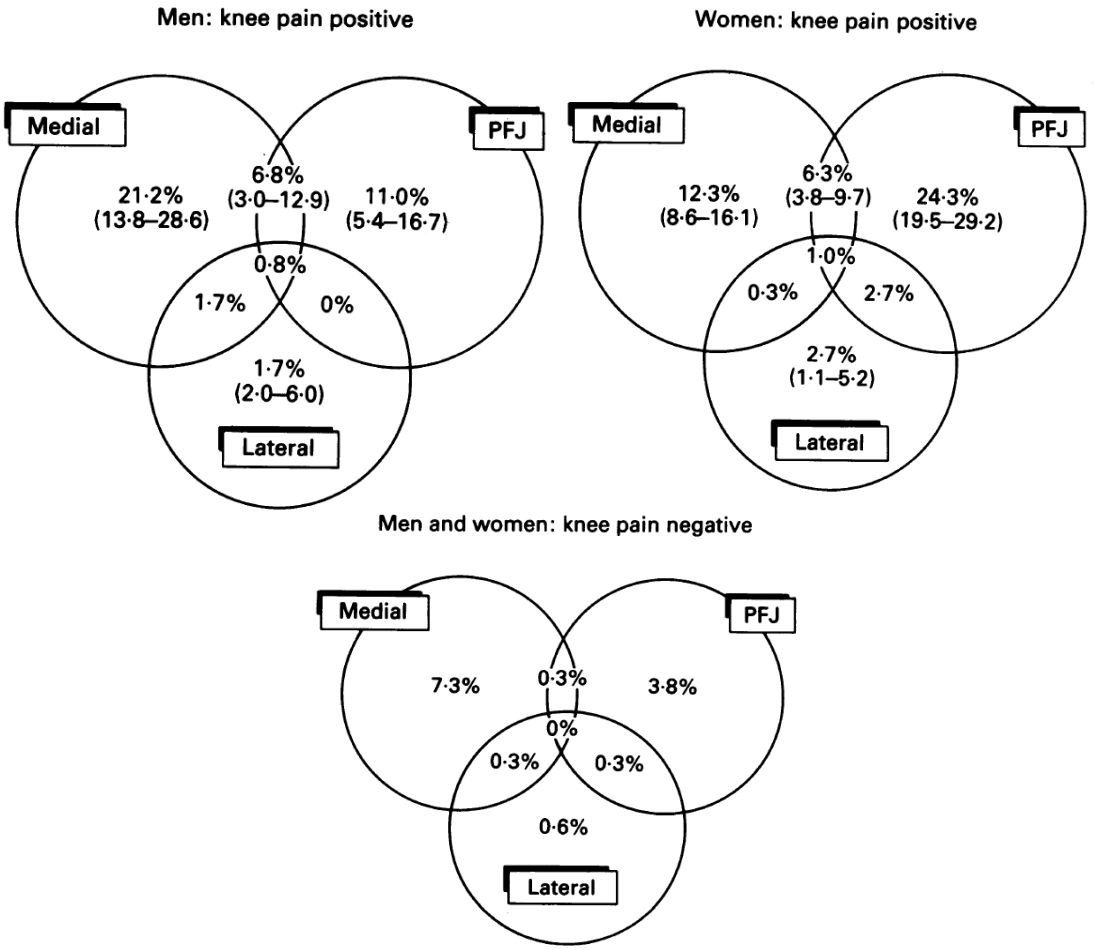

Figure 2.1-10: Three Vein Diagrams of the Frequency of Osteoarthritis in the Knee Compartments
The vein diagrams are from McAlindon et al 1992 paper[174]. It shows the percentage of the osteoarthritis present in knee compartments of the study's participants.
PFJ = patellofemoral joint

The other reason for the unequal split of medial and lateral UKR is due to confidence in the performance of the lateral UKR. One paper found that 38% of lateral UKRs have femoral loosening but were unable to fully identify the triggering factors[176]. Scott *et al.*'s[177] study concluded that they could not support that lateral UKR perform better than medial UKR due to their finding of 2 out of 12 (16.7%) lateral UKRs failed compared to 1 out of 88 (1.1%) medial UKRs. Cameron *et al.*'s paper[178] states that the lateral UKR in their study had an 'unacceptably high failure

rate' which was thought to be caused by two factors: the lateral side of the knee is point-to-point basis softer than the medial side by approximately one third and this resulted in sinkage of the implant, and secondly, the valgus deformity is unable to be corrected properly with the releasing of the soft tissue. Owing to the poor results stated in these and other comparable studies may suggest why some surgeons do invest time into offering lateral UKRs.

Though there are many papers, especially recent, that contrast the results from above. A follow-up study by Insall and Aglietti[179] observed that the lateral UKRs outperforming the medial UKRs and similarly, Laskin[180] states that UKR should only ever be used in post-traumatic arthritis cause on the lateral side of the knee. A current paper by Halawi *et al.*[36] state that the survivorship between medial and lateral designs are similar. In a 5 to 16 year follow up paper of 54 lateral fixed UKR by Lustig *et al.*[173], only 4 (out of 49) patient's underwent a second surgery (1 revision to TKR and 3 a medial UKR) and there was no surgery undertaken for femoral wear or infection. Their conclusion was that the lateral UKR is also a reliable option along with medial UKR for their patient selection. Finally, a (cohort) review paper by Van Der List *et al.*[46] did not find any significance between their direct comparison on medial and lateral UKR at the 5, 10, and 15 years follow ups.

More recently, there have been many suggestions that the kinematics in the lateral tibial-femoral compartment is different from the medial side[46], [76], [148], [150] which requires different techniques of soft tissue balancing[76], [150] and preparation of the bone tissue[150]. Overcorrecting the ligament tissue is a problem in lateral

UKR; up to 11% of lateral knees are overcorrected compared to 4% of overcorrected medial knees[76]; this is partly due to the difficulty of predicting joint alignment in lateral UKRs, and partly due to surgeon transferring medial UKR principles to the lateral UKR procedures. Khamaisy *et al.*[76] suggest robotic orthopaedic tools can assist in controlling the alignment of the joint but this still doesn't remove the difficult nature of lateral UKR.

It has been frequently stated in the literature that lateral UKR have a good track record with a fixed bearing design over a mobile design primarily due the biomechanics of the lateral compartment[46], [76], [148]–[150]. Unlike the medial side, the lateral tibial-femoral compartment is loose at high flexion – the low conformity of the fix bearing is forgivable in this condition than the mobile bearing[148], [151].

Overall it seems that patient selection is key for both medial and lateral UKRs to be successful, for example, a number of the failures mentioned in the literature had revision due to continued development of the disease across the knee joint which has been an indication for concern for TKR not UKR. The contentious debate over medial and lateral results may be down to definitions of failure and the selection criteria for the study/reviews[29].

2.1.6 Radiolucencies

A commonly observed feature in patient's x-rays are radiolucencies, or radiolucent lines, they frequently appear at the interface of UKR and TKRs' between the prosthesis and bone interface on the tibia[20], [171], [181]. A typical x-ray with

radiolucencies can been seen in figure 2.1-11; the lines that can be seen under the prosthesis that is brighter than the surrounding bone tissue is the trait of the radioluencies. These radiolucent lines appear on x-rays when it is parallel to the interface and aligned by an image interface. Radioulucencies lines can be shadowed by implant features, such as keels[182].

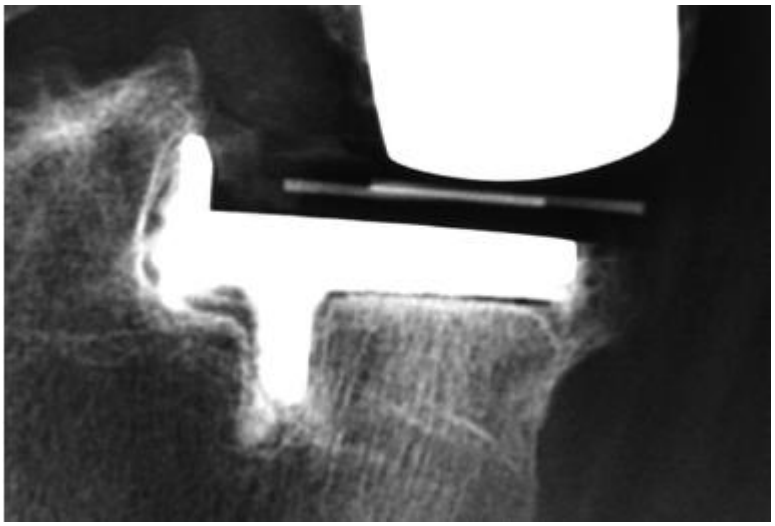

Figure 2.1-11: Example of Typical Radiolucent Lines in a UKR X-ray
The white lines present in the tibia under the UKR tibial component are the radiolucent lines. These can been see at perpendicular x-ray angles. Image taken from Gulati et al 2009 paper[187].

The aetiology of how radiolucencies are formed isn't clear, there are a few theories: the bone is resorbed due surgical procedure and/or the exothermic reaction of the bone cement[20], [181], [182] then, depending on the mechanical loading, the replacing tissue can form these radiolucency [181], [182]; the micromotion of the prosthesis creates sclerotic lines that form part of radiolucency[183]; and could be the result of macrophage induced osteoclasis of bone tissue which is replaced by fibrous tissue[159], [184]. Freeman *et al.*[159] study disproved the theory that it is caused

by blood and debris from the bone preparation because their study had thorough cleaning before cementing; and Kendrick *et al.*[182] disproved the theory that polyethylene debris is associated with formation of radiolucencies because the polyethylene debris are not present in UKR less than 7 years, while radiolucencies form within the first year of the operation. From the remaining theories suggest a recurring theme of the bone being resorbed and replaced with a mixture of fibrous tissue with bone tissue through the matrix[20], [182]. As a result, this is an area of less dense bone tissue with lines of dense unorganised bone tissue. Radiolucencies are usually formed during the first 1-2 years post-operation[20], [171], [182]. During this period the patients report pain and only a few continue to have pain after the 2 years, therefore there could be a correlation between the pain and the formation of the radiolucency[185]. At this stage these are two independent statistics that seem to correlate, and Gulati *et al.* findings suggests there is no association[20].

Radiolucency lines have been divided into two groups depending on their physiological appearance in radiographs[186]: physiological and pathological. The physiological radiolucent lines are usually less or equal to 1mm in thickness; they have a sclerotic margin that makes them well defined, lines run parallel, and normally develops and consolidates during the first/second post-operation years. The physiological type is common and isn't associated with significant problems. The pathological radiolucencies are usually bigger than 2mm in thickness and don't have a sclerotic margin which makes them poorly defined and progressive[20], [182]. Even though pathological radiolucencies are present, it alone shouldn't a be key

indication that a prosthesis has failed[159], [171], [181], [182], [187] or is the cause of pain[20]. Kendrick's paper[182] affirmed that the prostheses with radiolucencies that suggested loosening and pain where in fact securely attached to the bone through interdigitation; same for all other diagnosed radiolucencies. It is unclear if the presence of a radiolucency line could be used to determine positive outcome of prostheses[181]. In a later section *2.1.13 Physiological Response*, it is discussed that all prostheses produce radiolucencies but it is their formation that differentiate the clinical outcome.

The fibrous tissue from animal samples in Hori and Lewis study[106] was noted to be mat-like structure, in the perpendicular plane it was fibrous in appearance with fibrocytes dispersed in collagen fibre running in parallel to the interface; in the parallel plane collagen fibre patterns was observed to be woven into sheets that are randomly distributed. It was posited that this structure allowed the tissue to withstand large compressive loading normal to the sheets and tensile loads parallel to the sheets. Though the tissue structure is made up of parallel sheets then the shear resistance is properly very low as the sheets layers will slide. The tissue has a rich vascular supply and potentially this allows the replenishment of the lost fluids quickly *in vivo*.

A paper (Simpson 2011)[188] looks at the location of the pain with UKR to be under edge of the tibial plate and has associated it as a high stress zone created by the lack of mechanical compression loading causing a typically low bone density at the tibial tray wall and bone interface. Their computer simulated models suggest

that creating a mechanical tie to this wall to increase compression load to in turn increase the strain energy that encourages the formation of bone. This paper lead to a creative brainstorm of prosthesis designs

2.1.7 Physiological Response to Knee Arthroplasty

How the body interacts with the implantation of a prosthesis plays a major role in the success of the procedure - the above section *2.1.12 Radiolucencies* has already touched one area of this subject. Most researchers think that prosthesis loosening is due to bone resorption, a body response to a foreign object (potentially of any size[131]), while other suggested causes include material failure[189], [190].

Murray *et al.*[190] did a study to observe the release of mediators from macrophage response (primary immune response) after being exposed to different types of material. Macrophages in suspension release mediators for bone resorption but when they are adhered to a surface they release significantly more bone resorption mediators. Six different materials (table 2.1-2) were tested for bone resorption mediators, ranging from smooth glass to PMMA. Hydrophilic surfaces cause the macrophages to releases 2.5 times more mediators than on hydrophobic surfaces; similarly rough surfaces release 2 times more than smooth. Combining the two surface properties, it was found that rough hydrophilic surfaces stimulated the most bone resorption mediators and PGE_2 (inflammation mediators released by damaged cells) than smooth hydrophobic surfaces (and there was no significance of the middle 2 combinations). The final observation from the paper is

that the physical surface properties are more important than the chemical properties of the implant material.

Table 2.1-2: Surface properties affecting bone resorption mediators[190].

Material	Contact angle (degrees)	Surface type	Bone resorption
Glass	100	Smooth	Max
Stainless Steel	20	Smooth	
PTFE	100	Rough	
Epoxy Resin	70	Rough	
HDP	90	Rough	
PMMA	60	Rough	Min

In a similar style study, Rich and Harris[191] observed the preferences macrophages and fibroblasts, which tended to be different to each other. Where the macrophages migrated towards hydrophobic and accumulated on the rough surfaces, fibroblasts acted to the opposite surfaces properties. Initial further investigation carried out by Rich indicated that macrophages have a stronger adhesion to hydrophobic substrata.

Murray then went on to study the inflammation and toxicity of PMMA (bone cement) and high density polyethylene (HDP) [189]. It was concluded that with only 1.5 times greater level of lactate dehydrogenase (LDH, a cytoplasmic enzyme) than the known non-toxic materials, that these substances are not toxic. However, they have an inflammation effect (including the release of PGE) that is less than zymosan (substance from yeast cell walls). Inflammation response causes damaging effects

on the cells that prevent them from functioning properly and can lead them to being resorped; PGE is the prime indicator and the activation of bone resorption.

Vestermark *et al.* observed the formation of sclerotic bone rim (SB rim) under two conditions, stable and unstable. They described a stable condition one where the cement mantle and prosthesis is not loose and unstable conditions is when they are loose. SB rim has been theorised to be the body's way of isolating the prosthesis from the bone marrow (as the prosthesis is being treated as a foreign body). The first formation of the sclerosis is to separate the prosthesis. The secondary formation of the sclerosis forms close to prosthesis in response to mechanical stimulus and this further stabilises the prosthesis[183]. In the unstable conditions, the SB rim is more distinct, continuous, thick and located further from the prosthesis. It was also observed that it requires higher and ongoing formative activity on both surfaces (prosthesis and bone) with little to no resorption being observed. In stable conditions there was more than one SB rim, these were thinner with radial trabeculae connections between each rim - the resorption and formation occurred at the same rate. Bechtold *et al.* found that stable implants have been shown to cause less inflammation and irritation[192] which is supported by Giori *et al.*[160], reporting that unstable interfaces are metabolically active which secrete PGE_2 and collagenases. From these results it can be seen that resorption is a good activity if coupled with formation and not associated with inflammation.

It has been observed that bone tissue located near/on prosthesis surfaces are better at anchoring[192]; this allowed Swider *et al.*[193] to the following

hypothesis, “Bi-directional bone growth from implant surface towards the bone and bone towards the implant. This will associate with high mechanical fixation so when bone is only growing towards implant surface fixation will be inferior”. This hypothesis was supported by their study; therefore, the suggested prosthesis designs are strategies to promote bone growth at prosthesis surface, this is called clinical corollary. They also remarked that the SB rim has limited effect on the implant shear stiffness.

2.1.8 Failures of UKRs

In order for UKRs to improve their clinical and functional performance, their failure needs to be addressed, this is easier51 said than done because there many factors involved[194], [195]. In part two of Bauer and Schils’ 1999 article[196], it states that there are 6 different mechanisms of failure: infection, implant wear, inappropriate mechanical load, interface fatigue failure, implant motion, and hydrodynamic pressure. However, Vince[195] in 2003 states that there are 9 failure mechanisms: aseptic loosening, (tibial-femoral) instability, patellar complications, structural failure, infection, extensor mechanisms, stiffness, fracture, and un-diagnosable. Callaghan *et al.*[194] believes that the modes of failure have changed over time and now the common modes of failure are instability, infection, osteolysis, and failed fixations; and the major causes of early failure is malalignment and instability due to inadequate previous procedure techniques. Vince[195], believes restoring stability requires more than constraining the prosthesis.

There is no clear definition what period for early failure refers to, but from the literature it is anything from 12 months to 5 years post-operation[197], [198]; this links in to studies claiming to be short-term at around 5 year follow ups. Early UKR procedures have been noted to have early failures that were due to lack of knowledge and technique which have been improved over the years[15], [199]. With the above information, it can be said that early failure can be down to two factors: poor design of implant allowing wear[151], [200], overloading[39], [201], insufficient fixation[151], [201], and/or unsuitable material[151], [200]; or UKR was not an appropriate indication due to progression of disease[39], [177], [200], [202].

Possible reasoning for chronic pain following a UKR surgeries maybe caused by degenerative bone re-modelling and/or micro-damage as a results from high strains induced by implantation parameters[185]. Simpson *et al.*[188] discussed the increase experience of pain in cemented and cementless UKR patients; they theorised that the main source comes from an increased strains on the proximal tibia. Over time, estimated up to 12 months, the bone is remodelled and the subsequent pain subsides[185], [188]. From Simpson's FEA investigation, it was hypothesised that if there is a mechanical tie on the vertical tibial wall, then the strain is reduced and potentially the pain too. Therefore, pain within the first 12 months should not be an indication the UKR has failed, it should be managed to give the UKR to settle and remodel.

Potential causes of early failure are polyethylene wear with and without loosening, and the progression of arthritis[39]. Strict patient selection should be

implemented to exclude patients that may have continued spread of arthritis across the knee as their disease can cause early failure of the UKR.

It has been reported that polyethylene wear occurs in 83% of revised implants[203]. There are a couple of wear mechanisms in UKRs, polyethylene wear is most noted in the literature because the rate and pattern can reduce the life of the implant[204]. It has been suggested by Aleto[39] *et al.* that polyethylene wear and degeneration is caused by polyethylene-sterilisation cause detrimental influence to the material's mechanical properties[39]. Along with other possible causes including: a thin polyethylene bearing, the modularity design in fixed bearing prosthesis, and if bony defects causing mechanical overloading. Palmer *et al.*[151] and Akizuki *et al.*[204] supports that polyethylene thickness and material's sterilization process does account to polyethylene wear. Although the thickness claim was reject by Bartley *et al.*[203], they state that polyethylene thickness does not affect the wear rate. Both Palmer and Akizuki papers suggest that polyethylene wear is the primary result of the implant deficient conformity of the articular surfaces that generates high local stresses. Sublaxation also caused localised high contract stresses, particularly at the thinnest parts of the poly[203].

Saenz[201] study into early failure of all-polyethylene implant lead to the conclusion that they failed partly due to non-uniform stress distribution across the tibial component unlike the metal back tibial component. Plus other features, such as thinner and shorter keel, also contributed to the poorer performance by reduced fixation that lead to loosening. Saenz paper does not reflect the findings Aleto[39] all-

polyethylene which had a 10 year survivorship of 91-93%; Saenz paper did note a conflict of interest.

Loosening occurs when the material fails or resorption of bone[190]. Osteolysis is multifactorial including particle wear debris, wear from articular surface, post-impingement, cementless and polyethylene[194]. Schmalzried *et al.*[205] observed that the surgeon is the most important influence to determine if aseptic loosening will occur. A retrospective review remarked that more than half of revised UKR had loosening in one or more of than compartments[206].

There is less information in the literature about failure of the femoral component, this might be partly due to the femur is less likely to fail to aseptic loosening[202], [207]. Unlike the tibia component the concern is the tissue area under the component, it needs to be able to withstand high stresses; yet on the femoral component the concern is to prevent a posterior notch to create unnecessary stresses on the component[208]. In addition, the literature it has also been noted that the tibia soft tissue is more likely to be subluxed than the femur[177]. The femoral component of the Mark implant originally had a tab on the anterior part but it was noted to be difficult to insert and the revision from it required unfavourable extra bone removal[177].

2.1.9 Knee Outcome Reports

Knee scores were developed as a way to assess the outcome and performance of hip and knee replacements[209]–[211]. The scores are calculated from

a questionnaire assessing different parameters of the replaced knee. It is filled out by the patient and/or clinician depending on the scoring system. For example, the Oxford knee score (OKS) are answers provided by the patient and the American Knee Society Score (AKSS) is filled out by the clinician.

Hospitals and clinical trials needed a way to measure the outcome of knee arthroplasties for comparison. Initially scoring systems were completed by surgeons who assessed the function of the knee and asked patients questions on other parameters such as pain. One of the earlier scoring systems is now known as HSS (Hospital for Special Surgery), published by Insall in 1976[212], and is used in many hospitals and studies. The two sections of this system covers pain, stability during standing and specified movement, and ROM. Even with HSS' (and other similar systems such as KSS - Knee Society Score) popularity, they haven't been proven to provide adequate psychometric parameters[213] – that is to say the surgeon isn't able to reflect on the actual patient's senses (e.g. pain). Additionally, during trials the potential for surgeon bias is not eliminated.

The OKS was developed in 1998 to assist and remove biasness from randomised prosthesis trials[209]. In this revised scoring system the patient answers 12 questions with a rating between 0-4 (4 is the best); thus making the score range between 0-48 (48 best knee performance). Western Ontario and MacMaster Universities Osteoarthritis Index (WOMAC) is another patient based scoring system[213]. Since these systems are completed by the patient, the scores should, theoretically, be more reflective of the true outcome. However, these systems can

be affected by the patient's pre-existing joint problems [214], and by their expectation[211], [215].

Since there isn't a gold standard knee scoring system, caution should be used when applying and analysing the results. Along with other clinical aspects, the knees scores should help paint a picture of general knee function.

2.1.10 Meniscus

The meniscus plays an important role in load transference between femur and tibia. One of the study from a New York University (NYU) research group used miniature transducer to determine load transfer mechanisms[216]. Under no loading condition the contact is primarily on the meniscus (at 0° contact is on the lateral aspects and moving to the posterolateral aspects at 90° flexion); the area often in contact with the meniscus is the (cartilage of) medial tibial spine region. Conditions with loads up to 150kg: the meniscus on the lateral side of the joint appears to carry most of the weight and on the medial side the load is shared between the medial meniscus and exposed cartilage. From this study, it can be observed that the contact area increases with load as the meniscus enhances the stability of knee, this is also supported by recent works[217].

The meniscus transmits almost half of the forces that go through the medial side of a normal knee (based on contact area and pressure); highest pressure arises from the spine and central area of the condyle which suggests a relationship between the extent of contact with the meniscus.[218]. In moderate to severe

osteoarthritis, knees are likely to have meniscal damage which leads to the loss of its mechanical function - along with this a reduction in cartilage volume can further affect the ability of the meniscus transferring load. One study found there is an association with meniscus tear and osteoarthritis along with the increase time of relaxation after stress with the increased severity of osteoarthritis[219]. Arno *et al.* showed that the reduction of cartilage volume was related to the reduction of meniscal contact and height. They also concluded that the increased reduction in cartilage volume reduced the meniscus function of loadbearing or protection that could increase wear progression[218].

In early studies, the NYU group, investigated the difference in contact area with and without the meniscus. The average contact area (throughout flexion) with load of 1.5kN the present of meniscus is ca. 1,770mm^2 and without the meniscus the average contact is ca. 1,500 mm^2 without loading [216], [220], [221]. Later works investigated where the centre of contact points are located on both the tibiofemoral and patellofemoral joints of the knee and where, if any, potential overlap in high flexion[221], [222]. This research was to aid the further understanding the mechanics of the knee and thus help with joint design and implants. The results from these investigations can be seen in appendix 1 (page A1).

2.2 Key Message from Literature

The review process pulled together a considerable volume of information regarding UKR prostheses.

The different types of prostheses in the market is important to know along with how they were designed to tackle a perceived problem and, in cases with the right indication, how the prostheses were successful. The other driving point of knowing the different designs currently on the market was to establish if there have been different approaches to prosthesis design that utilises burring and robotic technology. As far as the literature review indicates, the profile of the bone to prosthesis interface (referring to this as the "undercarriage" of the prosthesis) for a standard prosthesis is flat with one or more anchoring features. Thus, there is potential for development in this area, not only to make the procedure easier to use with a burr, there is possibility that an undercarriage profile that isn't flat could be beneficial in terms of performance and survivorship of the prosthesis.

The physiological response to the prosthesis is an important aspect for survivorship of the prosthesis. This project will mainly look at the bone's response to mechanical stimuli, which can be altered by different prosthesis designs and material. However, other physiological aspects could be looked into for this project and for future work to improve the survivorship of the prosthesis.

The information from this chapter and the primary information gathered in the next chapter (*Personal Experience Exploration*) will be combined to assist the formation of the project's brief specification, discussed in chapter *4 Design Process*.

Chapter 3

Personal Experience Exploration

The scientific literature does not contain much information derived or obtained from personal experience. The design processes reviewed in the previous chapter acknowledge that acquiring information from personal experience will enrich the understanding of the product or system and further emphasise the key topics for the design process. Knowledge from personal experience isn't just from direct usage of the product or system, it can be obtained from indirect methods such as direct communication with current and potential users. Personal experience type of information is less quantifiable, if at all, and as a result isn't generally published in literature.

Gaining knowledge from experience, such as a user diary, one can empathise being a user to understand from their frame of reference. With communication, supplementary knowledge can be gained from different frame of references. This information can further clarify the strengths and weaknesses of the product/system that are mentioned in the literature as well as to reveal aspects that are not notable in the literature alone.

Whilst in the literature there is discussion about the workflow, training etc., this information lacks the personal experience of the surgeon in the operating theatre, and there is even less information from the supporting staff perspective. A unicondylar prosthesis' end use and goal is to keep the patient mobile and pain free; yet it is the surgeon and the support staff who are using the technology and implanting the prosthesis. This investigation explores what it is like using the NavioPFS system, being in an orthopaedic operating theatre, discussions with professionals, reading patient forums, reflecting on stakeholders, and official reporting sources. The information gathered in this chapter and literature review chapter was gathered and sorted in the next design stage, chapter *4 Project Aim and Specification*, and was used to assist the investigation direction and brief.

3.1 Personal Reflection of Robotic Orthopaedic Tools (User Diary)

The first step in understanding the system is to use the system, which is referred to as a user diary. By operating robotic orthopaedic tools in a close to surgical scenario will provide valuable knowledge that may not be able to be obtained from reading the literature. During this exercise, the thoughts were recorded for reflection; the observations included: how easy it was to perform each process, what could be changed to make the process better, what activities were difficult to do, etc.

For this, user diary used a robotic orthopaedic system (NavioPFS, Blue Belt Technologies, Pennsylvania, United Sates) using artificial bones (Sawbones Europe AB, Malmö, Sweden) without soft tissue. The in-depth understanding came from

learning how to use the system and continued practise with the system (there were several occasions for demonstrating the system to the department's visitors). The following is recollection that is split into three main areas: set-up, burring, and surface finish.

Set-up

It was noted that the system takes a while to set-up as all the parts need to be assembled, calibrated, and virtual modelling and fitting. The NavioPFS is a modular system that can be broken into various sections to allow it to be used in different theatre set-ups and for the surgical parts to be sterilised. The drawback of this modular system is time to assemble and make sure all parts are connected and working. After being assembled, the next stage is calibration of the system. This process also takes a bit of time to complete and it requires a sort of knack to waving the apparatus in the air as if one was performing a magic show. Part of the calibration, which leads on to virtual modelling, is the locating the (patient's) knee. The system uses two sources of information the first is by identifying markers drilled strategically placed on the femur proximal to the knee and the tibia distal to the knee; the second is the bony landmarks of the knee. This information allows the system to know where the knee is, its orientation, and estimate size and ratios for the virtual modelling. To complete the virtual model, the calibrated apparatus is skimmed across the knee surfaces for the system to create a 3D meshing of the knee. The last set-up step is the virtual fitting of the prosthesis' components. The virtual 3-D model allows the surgeon to consider which component size, their

optimal position, and any possible soft tissue corrections of the knee to be made. The majority of these 4 set-up steps are all done in theatre with the patient. It occurs after incision into the knee but before removal of tissue by burring.

Using the Robotic Tools to Burr

During burring, it was noted that the removal of bone tissue is easily done in most areas of the knee and with a degree of high accuracy; though it is only fast when there is a low volume of bone to remove. Therefore, increasing the volume increases the time – unlike the conventional bone tissue removal. There are some design features that don't work well with the hand-held burr, such as drilling straight holes for the pegs, as this requires a steady hand with a lot of practise to get the hand piece exactly aligned along the axis. Using a burr to cut bone tissue can be a slow process if it is the especially first time. After some practise, it gets a little easier but there are still difficult to reach areas of the knee and difficult features to burr. The whole procedure and interface is straight forward; it seems that almost anyone can use the system, which is good as it means it is user friendly and reduces training time.

Figure 3-1-1: Surface Roughness after Burring and Sawing
Photo of artificial bone (Sawbones) exhibiting typical roughness after burring (left) and sawing (right).

The finished surface roughness can be described as bumpy and/or pitted, figure 3.1-1; it isn't very practical or possible to create a smooth surface finish using the NavioPFS' burring method of bone removal. This finish could have the advantage of having a greater adhesion property with bone cement – further investigation was suggested to validate this.

Reflection

Overall, it seems that the NavioPFS system (and potentially other similar systems) has a potential issue of lengthier tissue removal. However, from the literature, these systems are only a faction longer than the conventional method of an oscillating saw. There is strong potential for a prosthesis design to reduce bone tissue removal volume together with burr friendly features to reduced surgery time (and may improve other aspects of UKRs).

Conclusion

- The burr can be time consuming if a large volume of tissue is needed to be removed.
- Preparing the bone tissue for features, such as flat surfaces and pegs, can be difficult to obtain with a burr.

3.2 Personal Reflection of Orthopaedic Surgery

The previous section provided valuable first-hand experience of the NavioPFS system but it lacked context. The setting was in a spacious room without a patient, and personal safety equipment was a lab coat, gloves, and goggles. This is different from what real surgery is like. It is preferable to do a user diary in a real-life context so the knowledge is built from first-hand experience but in this case that was impractical and unethical. Therefore, to gain context, the operation of robotic orthopaedic tools was observed during orthopaedic knee surgeries.

Two surgeries took place on a February morning in 2014, the surgeon was the same for both operations. The first surgery was a cemented TKR using navigation assistance only and the second surgery was a cemented UKR (Zimmer, Stryker) using the Blue Belt Technology's NavioPFS system. Each surgery took approximately 90 minutes from start to finish and neither experienced complications during surgery.

The operating room was a standard clean room equipped for surgery. In the middle of the room was a blue rectangle marked out directly below the ventilating

system attached to the ceiling. This rectangle marks out the operating zone where there is continuous clean filtered air being pumped from the ventilating system above thus keeping the particles down to the floor and outwards to the rest of the room. Only surgeons and scrub nurses can enter this space once they are fully scrubbed and wearing full protective scrubs (including head visor). Everyone else present in the room is required to wear a facemask. These precautions are there to minimise the risk of exposing the patient to particles and contaminants which can lead to complications. Therefore, it is necessary even though it can uncomfortable for the surgical staff and at times it limits the surgeon's movement.

Navigated TKR Procedure

The procedure for the TKR that morning involved an incision across the knee, the knee joint was then "opened up" by clamping aside tendons and the patella – they remained clamped to the side for the best part of the surgery. Guidance pins were drilled at various landmarks and their position was confirmed by the navigational system, then the jigs were positioned and pinned into the bone. The jigs provide guidance for the oscillating saw. Before cutting, the positions of the jigs were double checked with the navigational system – "measure twice and cut once". After the prosthesis was aligned (using dummy implants) and the tissue balance performed, the whole knee area was washed for the preparation of cementing the prosthesis. The cement was mixed in a vacuumed vessel, as soon as the last ingredient was added the timer was started. Time is an important factor when working with bone cement as the cement needs to be mixed for a certain

length of time before it is ready for use and then the surgeon has a limited working time with the cement before it begins to cure.

Robotic Orthopaedic UKR Procedure

The UKR procedure was almost the same as the TKR procedure but it utilised a robotic-assisted orthopaedic tool, the NavioPFS from BBT (at the time), instead of an oscillating saw and navigational guidance. The other difference was that the second procedure was a medial UKR, the incision made was smaller and on the medial side of the knee (patella and other soft tissue clamped to the side). There were extra people present in the theatre, they were the BBT representatives. They are on stand-by in all NavioPFS system related procedures so they can provide support to the surgeon and talk through any problems they may encounter. During the procedure the representatives only had to provide help for simple interface or technical problems. The NavioPFS system was fully covered by protective plastic sheets including the screen – this was not ideal as it created a glare on the touch screen but this is going to be fixed with an actual custom-built touch screen cover. As the theatre was being prepared for the UKR procedure with the robotic system, the body language and comments made by the nurses suggested scepticism. Amongst the nurses, there were some who were not in favour of the new robotic orthopaedic tool in the theatre. This notion is perceived to extend from the statement that: “if it is not broken don’t go changing it”.

The surgeon used the burr to remove bone tissue with ease from the femoral condyle and the holes for the pegs. When it came to the tibia, the surgeon burred a few holes across the plateau down to the desired depth; then used the oscillating saw to remove the plateau. I asked one of the BBT representatives about this and they replied that it is common for some surgeons to modify the procedure in this way to reduce burring time of the tibia part of the preparation. A personal speculation at that point is that the tibia component can be altered to encourage surgeons to use the full potential of the NavioPFS system.

Reflection

The operation is performed in a tight space while wearing layers of protective clothing which adds up, restricting the surgeon's movement. Having a semi-active tool such as the NaviosPFS in surgery helps give peace in mind that there is less chance for human error but it can add to the restrictions. In surgery, the time to remove bone is perceived to be directly linked to the volume of bone that needs to be removed. Plus, if there are any tricky shapes for bone removal, it may also increase the time required, though this could be reduced if there is practise because the surgeon did not seem phased at removing the peg holes. Therefore, at the prosthetic side of the surgery, the prosthesis' components could be designed to work with the system to fully utilised the potential of robotic orthopaedic tools.

Conclusion

- Perceived the time to prepare the bone tissue is proportional to the volume required to remove
- There is room for the system and prosthesis to evolve to further complement each other.

3.3 Interviews with Potential Users

Another way to obtain context is to communicate with users. This can be done by questionnaires, interviews, discussions etc. The method depends on the number of users and resources available along with what information is required from the process. This investigation reached out to one surgeon at the Golden Jubilee, this meant that one-on-one discussions were practical use of resources. The pursed information ranged from initially wishing to learn a bit about orthopaedic tools in surgery to feeling on the developed concepts. The latter discussion with the surgeon is mention in chapter *8 Concept Selection*. The one-to-one discussions with the surgeon were left to be informal as it meant everyone would be comfortable and will allow free-flow of speaking. Before meeting with the surgeon, a range of questions were prepared to keep the discussions on track to make most of the time and not miss any desired information. In appendix 2 (pages A2-3) was the list of questions brought into the interview, not all of them were asked but they were useful to have in the informal discussion. The following is the review of the initial discussion.

Background Information

The interviewee was a consultant from the Golden Jubilee Hospital, Glasgow, and specialises in lower limb joints – primarily the knee, hip, and ankle. The Golden Jubilee was one of the few hospitals that had the NavioPFS system for clinical trials but they have finished up with the initial contract. Blue Belt Technology was bought by another medical device company, resulting in the NavioPFS system not currently (at the time of the interview) in use at the Golden Jubilee.

Robotic Technology

The consultant believes that the technology has come a long way but the implants are still to catch up with the technology. The orthopaedic technology is useful and provides consistency but there is yet to be an open platform that allows more than just one implant model to be used. For example, the two main competing systems of robotic technology are the RIO system (original owner was MAKO, and the new owner is Stryker) and the NavioPFS (original owner was Blue Belt Technologies, new owner is Smith and Nephew). These systems can only use Stryker's or Smith and Nephew's (before the acquisition, ZUK (Zimmer Unicondylar Knee)) implants, respectively.

UKR prostheses

When asked about the priorities for a prosthesis, the main factors stated were: the contracts between hospital and supplier, and the cost of prosthesis. The

choice of supplier contractor is decided by the consultants as a collective. Their main justifications for choosing would be based on documented track records (this includes that a fixed prosthesis is better than a mobile one) and their preference of systems. After a knee replacement surgery, the patient may think the implant is satisfactory or better but clinically it might not seem satisfactory (via x-rays); or vice versa which is apparently more common.

Unicondylar implants have good functional outcomes but they are not as durable as total knee implants. Plus, the surgery is more of a soft tissue balancing operation which makes it a less forgiving procedure thus indicating that technology is vital for success – UKA can be performed manually, but doesn't always end up being successful.

Procedures with Robotic Technology

The consultant mentioned the main advantage of the NavioPFS system is the absence of an arm (that is with the competitor system, MAKO) that can restrict the already confined space of the surgical area. The robotic technology furthermore helps with the soft tissue balance which, as he already mentioned, is important in UKA. Then goes on to say that the awkward and annoying part of the robot system is the pegs, getting the angle of attack and keeping it steady.

The consultant was asked about changing the burr head, the interviewee felt that it would be annoying but its highly likely not to be a rejected idea just as long as the surgeon doesn't have to change tools as that may mean more *'faffing*

around'. The consultant continues this argument to say that when the surgeon is in surgery wearing all the personal protective clothing, he/she/xe has constraints in their movement and time in theatre amongst other factors. Therefore, the tools and instruments need to be intuitive and user friendly to both surgeons and supporting staff.

The tools and instrument requirement is not just this surgeon's opinion, it was also mentioned later by an expert in designing medical devices for orthopaedic surgeries. On a visited to the department, the designer stated*: "the perfect surgical tool is the tool that surgeons don't notice";* the need for intuitive tools and instruments seems to be a trait that is desired for surgery. Therefore, for orthopaedic robotic tools to be utilised to their full potential, some changes need to be made to the prosthesis and to the system. Ways in which the prosthesis can help would be to reduce the volume of bulk tissue removal, and by having easy to burr features.

Reflection

The discussion with the consultant clarified the key conclusions from the user diary and surgical observations: reduce volume of tissue removal, change features such as pegs to be burr friendly, and to further integrate the prosthesis and robotic orthopaedic tools. The consultant also made the point that prostheses are still to catch up with the current technology, thus verifying the strong potential of

this investigation to improve UKR prosthesis by generating novel designs to be used with robotic technology.

3.4 Patient Online Fora

To appreciate the patient's point of view, online patient forums were accessed via the internet; these forums are part of orthopaedic knee surgery experience and are used by post-, and pre- operation patients. The NHS suggests patients to use https://patient.info/; though this lacks information regarding UKR procedures. However, a more useful online forum for all knee related issues was discovered: https://bonesmart.org/. This online forum has different levels of administration and monitors that are all active in moderating and providing support. There is also a dedicated FAQ section for knees, it has almost all information a patient (pre- and post- operation) would need; this includes what to expect in terms of progress and feelings at the different post-operation stages. From reading the threads the important recurring theme for patients is for them to appreciate that the progress rate they experience fluctuates throughout recovery and they mustn't compare themselves with other people's recovery. Another recurring theme was the quoted "#ODIC" which stands for Overdid It Club – this is when a patient has done too much activity that they have aggravated their knee tissues causing pain. When this happen, or other issues arise, users and moderators are at hand to give advice (most of the time it is RIMES (Rest, Ice, Medicate, Elevate, and Stretch) and take it easy for a while).

On the online forums members can start threads with any topic they have on their mind. Most of the time it is questions related to issues the patient has come up against and they are un-sure about it or they just want some re-assurance that things are ok. Members can use the space to post their progress and express their happiness with their procedures; others use the forums to vent. Both of these aspects are useful sources of information for different types of people: for future patients to read past patient experiences to recognise possible outcomes; and then for health specialists so they can provide a better service that includes information they offer and for them to manage expectations – using a hyperbole as an example, they should not allow the patient to expect they can to run a marathon 2 days post-operation. Universally, forums are a great supportive social environment for everyone and should not be over looked. It brought home the effect this project could have on patients, as the novel design approach could potential improve the prosthesis and thus bring quality of life to patients.

3.5 MHRA

MHRA (Medicines and Healthcare Products Regulatory Agency) are responsible for regulating all medicines and medical devices in the UK by ensuring that they work and are acceptably safe. There were 21 health notifications, appendix 3 (A4), regardless reported problem or recall of any knee replacements.

The majority of the 21 notifications were due to manufacturing mistakes (which are unfortunate to happen and not fully reflective of poor prosthetic design or prosthesis type). The MHRA was relocated to the government website in January 2015. The original search in October 2013, there was no alert hits from 2010 to 2013. On top of prosthesis problems, there was a number of field safety notices concerning instruments used in arthroplasty, including: corrosion properties with the potential threat of contamination of particles into the patient and malfunction.

The HMRA alerts highlight the importance of not overlooking manufacturing processes, it can be easy to go through a whole design process and have a valuable product but if the manufacturing the product does not to follow the required specification for any reason then it can result in failure of the valuable product. This investigation will keep in mind the requirements for manufacturing as it will be necessary for future work on novel prostheses to have manufacturing as part of the design process to reduce possible manufacturing errors.

3.6 Stakeholders

When designing a product or a system it is important to consider all the groups involved and what they have 'stake' in. The following is a list of the recognised stake holders and what they require from the product.

- Blue Belt Technologies.
  - At the start of the project, BBT were their own company and their goals were to improve the NavioPFS system to make it better and more versatile to appeal to hospitals for purchase. At the moment, the market

is very new and their main financial property is their IPs. They are almost in direct competition with MAKO.

- Smith and Nephew.
  - They acquired Blue Belt holdings in 2015, which implied their business model focussed around the sale of NavioPFS systems to hospital along with their own implant range. This makes the NavioPFS less versatile as only Smith and Nephew implants can be used with the system currently. Nevertheless, this might not be a hindrance as Smith and Nephew are a fairly substantial company with many collaborations, links, and contracts within health care establishments worldwide.
- DJO Surgical.
  - At the start of the project it seemed that DJO surgical were going to produce a line of unicondylar implants to work with the NavioPFS. This would make them stand out from other unicondylar implant producers on the market, a strategy that could lead to the increase of sale due to a wider range of implants.
- University of Strathclyde.
  - They have the promotional NavioPFS system to use for research and promoting the department with the agreement that they store and look after it for Blue Belt Technologies between their priority uses of the system. Industrial connections and research is valuable to the university as it is a source of publicity and income. They can afford to carry-out side projects to present their resourcefulness to Blue Belt Technology, and for

Blue Belt Technology this partnership acts as an economical resource of research/innovation.

- Patients, relatives, and carers.
  - They want an implant that won't hinder their health or their active lifestyle. They would like to visit the hospital the least number of times and with the least number of surgeries (but still feel satisfied with the level of care received). They also want a fast recovery so they can get back to everyday life as soon as possible. They are very much in the end stage performance of the product and they are the group of people everyone wants to keep happy and healthy. Patients like to be (or at least feel) in control because their health is important to them. Therefore, to have choices on treatments available to them puts them in control and thus at ease.

- Hospitals.
  - They want patients (and surgeons) to choose their hospital for operations and procedures; most people, if they can choose, will base their decision on the hospital's accreditation. Part of this accreditation comes from: using state of the art medical devices and up-to-date procedures, patient care, patient recovery, providing alternative choices for the patient, top qualified surgeons, and on-going surgical training and research. They might have alliances/contracts with medical device manufactures but

they will always be monitoring their competitors, shopping around for the best product (compared to cost) available on the market.

- Doctors (including primary care givers, nurses etc. but excluding surgeons and their team).
  - They want the best for the patient and for them to get better as soon as possible, and they like to give the patient options so the patient feels they are in control. They are likely to support an operation that is minimally invasive and doesn't require an arduous post-operation care routine.
- Surgeon (including surgical team).
  - Their concern (after patient care) is their stats because that is how their "worth" is judged. Some care about being part of a trial, as it can show that they are willing to train and change with the medical world. They want a theatre system that can provide constant results and is easy to use; they have a lot going on in the operating theatre and with protective clothing; they don't have much space or freedom for anything complicated. Also, if it is an easy system then the scrub nurses will be easy to train and be able to anticipate the surgeon's needs.

3.7 Key Message

The information found in the personal experience research uncovered information that was not included in the scientific literature. The knowledge of the context how the product is used allowed some insight into attributes the product

requires. For example, the surgeon has restricted movement in theatre and thus all tools used need to be as intuitive to allow the surgeon to pick up to use. Furthermore, after a discussion with a surgeon, it was brought to consideration that everything in the theatre must be intuitive to use by all theatre workers; for instance, how it is removed from packaging and assemble needs to be intuitive for the assisting scrub nurse(s).

The most important finding is that until now prostheses needed to be flat faced because the cutting technology has been saws that can only cut straight edges. With robotic technology use of burrs, the prostheses are no longer requiring to be flat faced. However, the current robotic technology procedures often replicate straight edge cuts for the tibial component because there hasn't been a parallel development of prosthesis design. Furthermore, using a burr to replicate straight edge cuts isn't the most efficient use of the system; it requires more time, and often surgeons take short cuts.

The advantage of using a burr is the accurate intricate removal of hard tissue but the main disadvantage, as mentioned in the literature, is the generation of heat and time required to remove bulk tissue. To save time, surgeons have been known to create short cuts, such as removing the tibial plateau (the main tissue bulk to be removed) using manual tools. After learning to use the NavioPFS system on sawbones, it was noted that some bone removal is harder than expected. For example, drilling the holes for pegs is difficult because the burr has to be held

steady along the axis of the hole; and the tissue is difficult to remove at the posterior area of the tibial plateau.

Chapter 4

Design Process

Humans are natural problem solvers but the use of creative methodology, such as a design process, can enhance this natural ability. Summer and Whites[223] outline the importance of choosing techniques to find solutions to problems. Evans[224] believes there is always a methodology (conscious or subconsciously) being applied to problem solving and when creativity is applied the problems are more likely to be resolved.

A design processes is a systematic approach intended to guide either an individual or a team to a product or system, and it implements creativity at key stages. While there are “no strict rules for creation”[225] – the design process is a guideline how to proceed through a complex problem of developing a product or system. There are many already established design processes that are used worldwide. This investigation reviewed 5 selected design processes: Total Design, Double Diamonds, Product Design and Development, and verification and validation models; elements from these processes were utilised in this project’s design approach.

The scope of this investigation was to commence a new approach to UKRs designs. To do this required systematic approach i.e. a design process. There are numerous existing design processes that are well established, most are aimed to produce a product as a solution. The following five are regularly adopted processes: Pugh's – Total Design; Ulrich and Eppinger – Product Design and Development; Design Council's – Double Diamond; Waterfall; and V-model. The latter two processes have been adapted by the US Food and Drug Administration (FDA) and Canadian Medical Device Bureau (MDB) to be applied to medical devices and by following either methods whilst adhering to ISO standards, the generated medical device will make it to market with the required certifications.

All these design processes seem to cover many of the same steps to yield a final marketable product(s); for example, they all have: formulation of a brief, concept generation, and concept evaluation stages. These five processes and a concept generation tool known as TRIZ were explored. Time scale and resources for a medical device to get to market is beyond the possibility of this investigation, as a result the above processes where not always applicable for this investigation's design process. Therefore, this investigation carefully chose the design elements from the explored designs processes to create a tailored design process that will attain the aim of this investigation. This chapter covers the key stages of the investigation's design process.

4.1 Overview

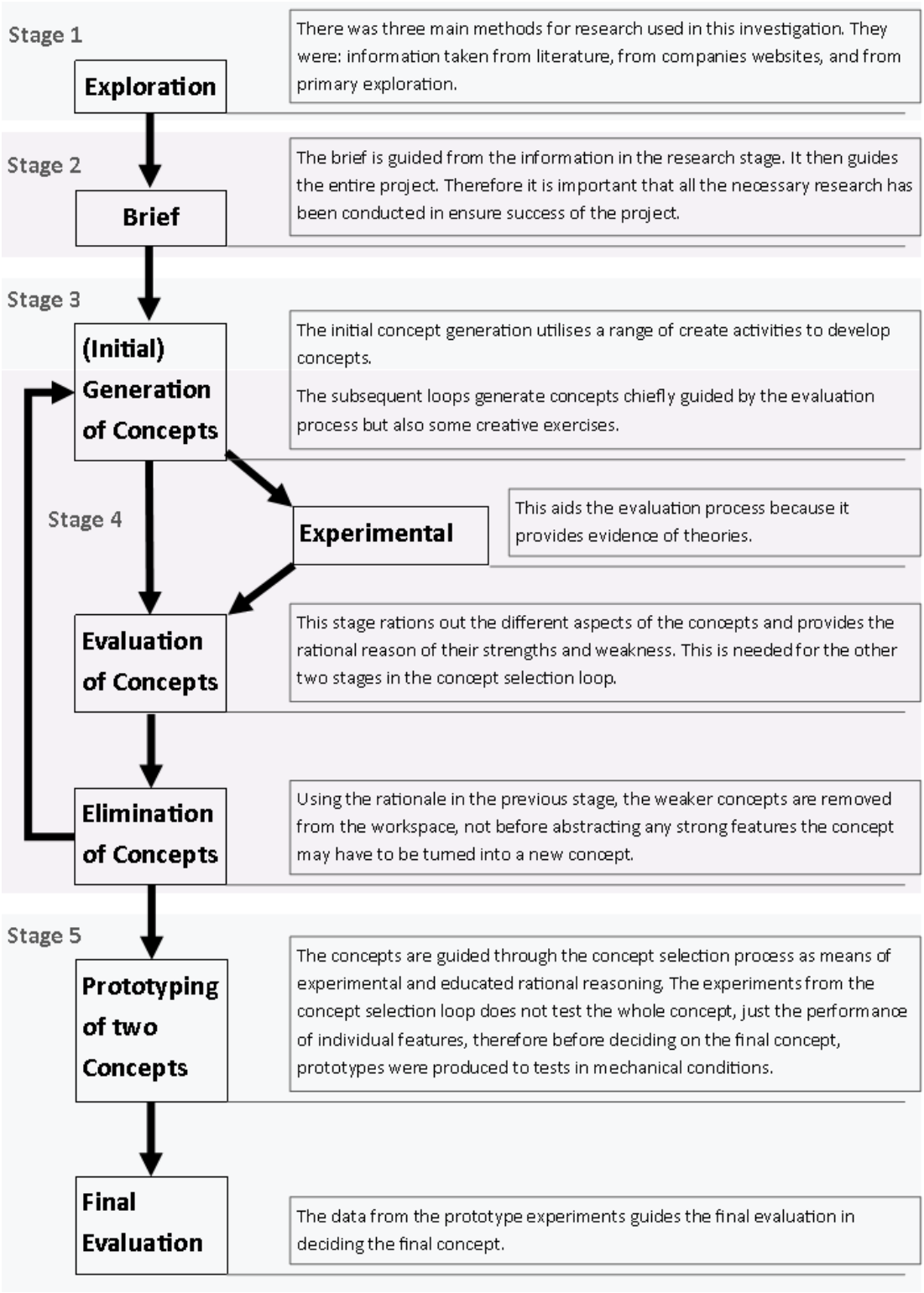

Figure 4.4-1: Project's Design Process

4.2 Stage 1: Exploration

The objective of the exploration stage is to gather information and to understand the product so to make informed and rational decisions throughout the investigation. The information and understanding was gathered from three sources. The first was from literature, this is where the scientific community present their work for others to utilise and build on. Information from this source is recognised by most professionals to be reliable due to the peer review nature of publish articles. The second source of information for the exploration was market analysis of current UKR products; most of this source is located on websites of the companies that manufacture prostheses. The last source of information was from experience by exploration; because the first two sources lack a subjective perceptive of the UKR process. The information for the exploration source can come from personal experience, such as user diary, or from talking to others about their experience, such as interviews. The work carried out in the exploration stage of the project is predominantly presented in chapters *2 Literature Review* and *3 Primary Source Exploration*.

Log books were introduced at this stage in the design process to keep track of all the information gathered. This proved to be handy as was a recorded of what had been done, what was planned to be done, and allowed reference back to any information. Two set of log books were used, the first set (4 books used) was recording researched information and other relevant investigation information; the second set of logs books was information obtained during experimental work and development, this was not till stage 4 of the design process. To help find

information the log books were numbered in their chorological order, and for locating the information a contents page was constructed and updated at the beginning of each book.

The exploration began with the scientific literature and prosthesis manufacture's websites to find general information on UKR and how it is different from the other procedures. Starting from this point, the information that was brought into the work space was all relevant and built a picture of UKRs and the procedures. Plus, this approach permitted the research space to know which areas that were worth branching out to and the best source to gather the information.

4.3 Stage 2: Project Brief

The second stage was forming a project brief, utilising the information from the previous stage – as suggested by the Double Diamond design process[226]. The brief is heavily relied on because it is basically the key summary of the research; it acts as the preliminary (supporting) evidence for concepts that adhere to the brief. Pugh's Total Design[227] is the most laid out, fully comprehensive brief that takes on 32 elemental design attributes that all concepts will/may need. It does go into a lot more detail in some areas where this project wasn't required to go through but by making notes in these areas, it could be the footing for future work. Therefore, this project used Pugh's PDS methodology for its project brief, found in section *5.3 Product Design Specification – PDS*, and it is the basis of the verification process[228]–[230]. The validation process comes from the review and evaluation of the concepts:

it draws key design aspects from the PDS to assess if the concepts are fulfilling them and thus mostly following the PDS.

4.4 Stage 3: Initial Concept Generation

Concept generation is about producing ideas, and preferably with no or partial limitations[227]. Ideas can come directly from research, as the information is interpreted the ideas formulate and take form into concepts. Nonetheless, this process has its limits and hence other processes are utilised to generate more ideas and concepts. The process known as TRIZ[231]–[233] can be utilised in many ways to suit the user(s) in design processes. This investigation's design process primarily used TRIZ's 40 principles[234] to enact thought scenarios that will lead inspiration to generate concepts.

Nonetheless, as stimulating as TRIZ is, the process can be a little stale for a singular user, stale thought processes does not always generate out-of-the-box inspiration to be conceptualised. Consequently, this project also did group concept generation with two different group types this project has defined as fresh group and skilled groups. The fresh group are made up of individuals of post graduate students with the field of knowledge out-with the orthopaedic, and engineering fields. The skilled groups are made up of individuals with knowledge in orthopaedic and/or engineering fields. The advantage of having the fresh group increases the number of out-of-the-box inspirations as they won't be limited to information they already hold, plus this group did not contain 'skilled' individuals which reduces the possibility of the (fresh) participants feeling threatened by sharing potentially

'ridiculous ideas'. These 'ridiculous ideas' can be used directly or used abstractly to be turned into possible concepts that may not have been considered. The skilled group maybe a little limited to their knowledge but their ideas have little more foundation as they know principles, so the ideas need less work to turn into a possible concept. These processes are covered in depth in chapter *6 Concept Generation*.

4.5 Stage 4: Concept Selection Loop

Concept review starts after the first cycle through the concept generation. This starts an iterative loop of evaluating (with support from experiments), elimination, and generation. This loop takes on the board concept selection flow that is illustrated from Pugh's Total Design[227]; thus, the loop is aimed at refining the concepts through continual concept generation and evaluation.

It is this iteration of converging and diverging phases, which Pugh believes superior to many other approaches that only implements a single convergence (like in the double diamond, and the product design and development processes):

"A major advantage of controlled convergence over other matrix selection methods is that it allows alternative convergent (analytic) and divergent (synthetic) thinking to occur, since as the reasoning proceeds and a reduction in the number of concepts comes about for rational reasons, new concepts are generated."[227].

The output of the initial cycle of the concept generation was a large number of concepts, so they need to be organised and filtered because some of the concepts contained ideas that were out-with the scope of the project, but they

weren't rejected because there are some good ideas in a few of them. The remaining concepts were further sorted whether they were suitable according to the brief, and if not, they were reviewed to possibly gain any inspiration before they were discarded or put a side for a different project. As a result, this step acts as a verification of this design process.

The remaining concepts are evaluated and reviewed by entering them into a design matrix, either an evaluation, or weighting and rating matrix which includes the key aspects (a partial verification since it only has part of the brief for evaluation) from the brief. These matrices can highlight strong concepts or features within a concept so that these ideas can be fed into other concept ideas for developing stronger concepts. Not only can it highlight strong, but it can also highlight weak concepts and features that can be eliminated after any promising features or inspirations are taken or altered from them. The design matrices are used every iteration of the concept selection and they are very good at initial weeding of concepts, but it can lack experimental and practical aspects, which can limit its effectiveness after a few iterations. Consequently, tests were conducted at different stages to provide data into the evaluation process. The tests include: two types of FE analysis, interviews, user diary, and prototypes; these tests act like a validation in the design process. Utilising tests and the design matrixes, the project was able to eliminate from over 200 concepts in total to 2 strong final concepts. The concept selection processes can be found in detail in chapter *10 Concept Selection*.

4.6 Stage 5: Prototyping and Evaluating

When the concept selection is down to two potential concepts then the two concepts, along with a model of a standard UKR, will be constructed from 3D metal printing for the purpose of experimentation. The tests were generated to compare the concepts with the UKR standard prosthesis. Ulrich and Eppinger would call these alpha prototypes[235] because they are not manufactured in accordance to the final product but is similar enough to be used for representable tests and trials. The experiments provided support for choosing the final design of novel UKR this investigation proposes is a strong fundamental design. The final results are not just for the final strong concept, but all the other potential concepts developed along the way as they can still hold promising aspect that may not have been notice in this investigation or the investigation thought unable to be implementable

4.7 Key Message

The research into the above established design processes highlighted the importance to have clear methodology with a clearly defined project brief. It was noted that the design processes follow a similar systematic approach of getting a brief/aim to the market. The different approaches had their different strengths and there is not “one fits all” design process that can be applied to every (design) situation. Furthermore, there did not seem to be a design process that was specifically tailored to an academic pursuit of knowledge without necessary taking a product to market. Following a design process that is not tailored to fit the appropriate goals may hinder finalising the conclusion. Therefore, this project

employed a bespoke design process influenced by established design processes, concluding with recommending a prototype.

Chapter 5

Project Aim and Specifications

The standard UKR system uses an oscillating saw to cut and remove bone tissue to replace with a prosthesis with flat interfacial surfaces (this system is sometimes paired with a navigation system that guides the saw cuts). The straight surface interface might not be the best approach for load transfer from the prosthesis into the remaining bone structure; it also might not provide the most efficient bone preservation that could benefit cutting time, kinematics, or the inevitable revision of UKR to a TKR. Whereas, the burr head of the robotic technology can create different shapes that could take on these advantages. UKR procedures often involve rebalancing of the surrounding soft tissue so to improve the patient's gait, this can be done using the robotic technology as it can analyse the soft tissue to help with the rebalancing that the standard navigational system can't do.

Currently, there isn't a prosthesis that fully utilises the above advantages the robotic system has to offer; this is due to a number of factors including system usability and integration. In order to address this, both a problem- and solution-oriented approach will be adopted. This is beneficial as together the approaches

provide reasons why this technology should be used, problems that could be fixed, and resolutions for integration problems. Therefore, this thesis generates and evaluates UKR concepts yet maintaining the main goal of prosthesis design.

5.1 Aim

To explore, by creative design processes and informed by experimental data, design features that can be incorporated into a novel UKR implant design that will improve performance predominantly in the areas of fixation, and load transference, as a consequence of the enhanced cutting capability of robotic orthopaedic tooling.

To gain full potential of the robotic orthopaedic tools available to surgeons, there is a need to re-examine unicondylar knee arthroplasty techniques. The literature, experimental data and creativity exercises can generate ideas to enhance UKR implant performance. The creative exercises will focus on the key areas that could be improved or developed by the use of the robotic orthopaedic, for example, minimal bone removal, customisable, different shapes, and surface texture. Selected ideas will be investigated and possibly tested, chiefly in the areas of fixation and load transfer. Fundamentally, the implant designs need to be appropriate for implantation with, for example, the NavioPFS.

This thesis focusses on the tibial component design because, from the research, there are more possible improvements to be made with a novel tibial component than a femoral component.

5.2 Research Synthesis

The following approaches were taken to collect and analyse the information gathered: constructive writing, mind maps, road maps, and discussion. The constructive writing mainly took on the form of a review of both literature and documented experiments which allowed the information to be organised and presented within the context of the project. The prime advantage of this was to help separate the relevant and irrelevant information. Mind maps provided a visual focus of the information in context to the investigation; two central mind maps were generated in the investigation. The first one was constructed in a software programme called MindGenius (East Kilbride, Scotland), it provides the visual overview framework of the constructive writing phase and can be seen in figure 5.2-1. MindGenius helps to understand the areas that have been researched and it helps to indicate the areas that need to be looked into or that could be researched further. The second mind map had the central cloud titled “UKR” and was hand constructed, see figure in appendix 4 (page A10).

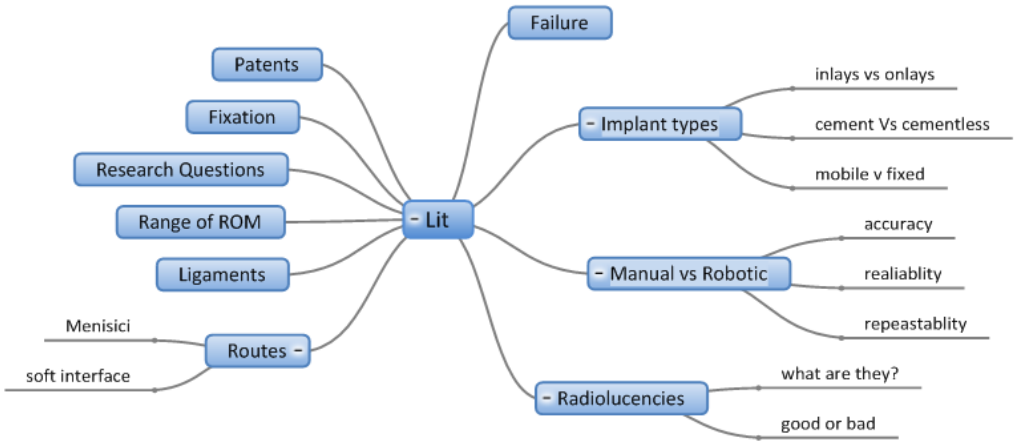

Figure 5.2-1: Mind Map of the Information Gathered
During the research stage information covers different areas relating to UKR.

Initial ideas developed during the reading of the literature. These ideas assisted the formulation of branches of different possible UKR design themes. The subjects in each theme were written in bubbles surrounding the branches. There were some bubbles that related to two branches either directly or indirectly. The benefit of the mind map wasn't stating the relevant areas in literature but how the literature can be used in creating a novel UKR design that is favourable and was valuable for discussions where to take the project. During the course of the project, branches, bubbles, and notes were added, both versions are represented in figure 5.2-1 and appendix 4. In parallel to the mind maps, an ambitious road map was composed for the development of the project's new UKR, appendix 5 (pages A11-12). This the thesis would only cover the first portion of the road map, this is the creativity and experimental works for further development of UKRs with the use of robotic orthopaedic tools. The main focuses will be fixation of the implant to the bone as well as find a shape that will transfer the load across the implant-(cement)-bone interface. All the constituents of the implant design will ideally have a seamless interface with the NavioPFS to increase surgeon's willingness to fully comply with the system.

5.3 Product Design Specification – PDS

As mentioned in chapter *4 Design Process*, Pugh's Total Design discusses documentation, the product design specification (PDS) that acts as a project brief, guiding the project down the right lines to provide a product. This documentation is sub-divided into 32 attributes (see table in appendix 6 (page A13)). However, this project is only the beginning phase of producing a product for market, and it

doesn't require 21 of these attributes. Therefore, only 15 (including a couple of unrequired attributes) of these are considered here in table 4.3-1. The PDS was updated when new data arrives or when new decisions are made; the initial PDS can be found in appendix 7 (A14).

Table 4.3-1: Final PDS

List Number	Description of Specification
1.00	Overall to have better performance than current UKR
1.01	To have better anchorage
1.02	To have better integration/reaction to the bone tissue
1.03	To have the surgeon fully use the robotic system
1.04	To remove the least bone possible
1.05	To transfer loads evenly
1.06	Can be "upgraded" to a UKR or TKR
3.01	To be made out of biocompatible material
3.02	To be made out of reliable material
3.03	If possible, have a material that will help healing, anti-rejection, and/or anything else I can think of
3.04	Working temperature range of 35-42°C
4.01	No surgical or invasive maintenance
4.02	If possible, to have non-invasive maintenance to extend the life of the product
5.00	Better and/or cheaper than the competition
7.00	Avoid patents
7.01	Use information gather from the literature review
8.00	Avoid patents
9.00	Follow standards (see section 10)
9.01	Tests are safe to perform in the university labs
10.01	Must fully comply with CE mark (and FDA)
10.01	Must fully comply with Medical Device regulations
12.01	Tests are reproducible
12.02	Tests are possible within resources (most likely pull-out/compression and cyclic)
15.00	Last the remaining years of the patient
18.01	Either have all products manufactured before (and possibly modified in theatre) or have it 3D printed with in the surgery ca. 30 mins
19.01	Patient to match requirement to allow them to have UKR
19.02	Hospital staff fully trained
21.01	Needs to be surgeon friendly (see subset of criteria)
21.02	To be integrated with NavioPFS
21.03	Doesn't need other tools (or at least no specific tools) than the NavioPFS
29.01	Packing process needs to sterile
29.02	Packing keeps the product sterile
29.03	Opening the packaging is compatible with operating room procedures
29.04	Clear labelling
31.01	Range of sizes to fit majority of the population
31.02	Small as possible (while keeping the anatomical features it is replacing) so to preserve bone

5.4 Design Process

Established design processes provided the investigation with a number of logical directions to get a product to the market but since, they were all mostly based on a stage serial model, the key stages were very similar. These models tended to focus on different stages in the design process and they all aimed to get a final product. Yet the goal of the established models is to get a product to market yet this was not part of the projects brief and thus it would be like quitting halfway through a design process; not having a clear ending point could pro-long the project unnecessarily.

Therefore, this investigation's design process will rationally use aspects from 5 previously discussed design processes to generate a process tailored to this project. The resulting design process consists of nine steps in a stage serial based design model, seen in figure 4.4-1; during the creative and evaluation stage of the process there is iteration loop that was terminated when 2 final concepts were selected.

5.5 Key Message

Referring to the design process (figure 4.4-1), the information acquired in stages 1 and 2 were fed into the remaining stages of the project design process. Consequently, stages 3 (chapter 5) and 4 (chapters 6, 7, and 8) had the necessary guidance for the constructive creativity to achieve the project goals while trying to limit constraints. Furthermore, stage 4 will also provide some supportive evidence (in chapters 6 and 7) for concepts generated in this investigation. Lastly the last

stage of the project design process will take the final concepts from the concept selection loop, stage 4, to test and evaluate against the market standard UKR prosthesis design.

The next part of the design process, concept generation (stage 3) is covered in the next chapter. This chapter will utilises creative exercises and techniques to generate as many novel ideas as possible.

Chapter 6

Concept Generation

This phase of the design process required to be creative in order to formulate as many ideas and concepts as possible by doing so the chances of finding potential solution are increased[223].

Creativity doesn't come from nothing, it needs to be exercised and played with so it doesn't become overused, tired, clichéd, repetitive etc. Creative exercises can be thought of the designer's tools that can draw out creativity, but like a tool box, there are many exercises for different creative purposes and intentions. Hence, just like a Swiss army knife can't make up a full tool box, there isn't a single creative exercise that can act as a full concept generation process. Not only are exercises important, human interaction plays a role in the exercises. The people can be other members in the team or sub-team, people in the same field, (end) users, colleagues and/or friends, or have no connection to team or project; each of these groups (and possible other grouping) bring their own aspects to the creative exercise. The benefit of having the interactions with different types of people encourages a large number of ideas generated and collaborated[236], as well as increasing the chances of inspiration occurring; both of which adds to the number of concepts being

produced. This in turn can increase the chances of a concept that fully fulfils the design brief.

The following are the different creative exercises that were utilised in the project. This chapter covers how they were used and who were involved in helping creativity. The generated concepts were then organised for concept selection in chapter 8. In addition to organising the concepts, the concepts were reviewed to construct experiments to provide validation for concept selection rationale.

6.1 Creative Techniques

Creativity can come from one word notions, take the word dynamic as an example – it is one of the 40 principles in TRIZ. This word was applied to a prosthesis design and lead to two questions: “can the prosthesis have moving part(s) to reduce wear?”, or “Can the prosthesis have a positive movement to help ROM or wear?”. These questions were combined with ideal, theories, and boundaries that formed concepts: “If the movement is passive then there isn’t a need for actuators – things like springs and rollers”, “Reduce gliding that will cause wear with roller balls”, or “reduce the normal forces with slopes” etc. The concepts included ♫(15)5: Have the roller balls within the meniscus bearing and the material goes all the way round like a conveyer belt. During the process, the one word ideas did not just come from the TRIZ’s principles, there was batman idea (δ_i) that created a concept of the tibial component being a cap and fixing to the sides of the tibia.

6.2 Inspiration from the Literature

The formation of ideas doesn't always have a clear commencement date; it can happen before, during, or after the research phase. Normally ideas start flowing during the research stage because the information is being interpreted while the mind is thinking how it fits into the problem presented. It can be a little limited as information is still being drawn into the design space yet it is useful in two main aspects: the first the inspiration can lead down a research direction which gathers more information for the design space; secondly it maintains interest and activeness of the brain to stimulate possible ideas. The recording of all the ideas, inspirations, or possible routes is good practice otherwise good potential ideas/concepts can be lost and not thought of again; so they don't get evaluated the concept selection stage of the design process. All ideas were recorded in the log book for future referral. Example of ideas is in table 5.2-1.

Table 5.2-1: Example of Ideas Generated by the Literature

Idea	**Description**
Modular based	This is to have a prosthesis that can interlock to increase in size, this allows the surgeon to only remove unhealthy tissue and leave healthy tissue rest untouched.
Mosaic	This is to remove unhealthy bone and cartilage to be replaced with sections to be inserted into the holes as anchors to hold an interlocking mosaic like cover over the tibial plateau.

6.3 Inspiration from the Personal Experience Exploration

The gathering and analysing of the qualitive evidence, just like the literature review in the above section, inspires the creative ideas. The ideas were generally solutions that came from identifying problems or nuisances with the system and

prosthesis. The main problem that appeared in the different qualitive gathering activities was the difficulty of using the burr drill to remove bone tissue, in particular the time required. These thoughts and ideas were brought into all the creative exercises below and into the evaluation of the concepts.

6.4 TRIZ

As mentioned in chapter *2.2 Design Process,* TRIZ is a very useful comprehensive suite of tools for developing and redesigning. This investigation utilises creativity by applying the part of TRIZ that identifies 40 principles for problem solving, the list can be found in appendix 8. This creative exercise can be done as a group or solo, the following work only did the latter because performing TRIZ it was reflected to be optimum as a solo exercise; plus there were other group exercises being conducted to pull in influences from a range of people. The 40 principles can be used in many approaches, therefore making TRIZ a malleable and can be utilised in many ways to suit the user. In the case of this project it was used as inspirations to form ideas then concepts; for example, the curvature principle, number 14, was applied to reduce time to remove bulk tissue of the tibia. The resulting ideas were:

- (3(14)1): Have an inlay that is curved thus reducing excess tissue removal;
- (3(14)2): Have a curve on the prosthesis to direct forces from the femur to areas of the tibia that can withstand and adapt to these forces rather than break or resorped; or

- (3(14)3) Use curves to allow healing around the prosthesis while reducing volume of tissue removal.

These ideas were implemented in many of the concepts for example, the concept U1 had a curve (dome) to save tissue removal, and concept S2 had a curve (hemisphere) to direct forces. Then concept BQ had a curve direct forces, reduce tissue removal, and to secure the prosthesis in place.

The project took two approaches for the use of TRIZ; identifying problems and the overall system. The first approach was to identifying problems in the system, they were perceived to be:

- The robot takes up space in the operating theatre

  The area around the surgeon's operating field is in high demand and everything here needs to work with the surgeon for the operation.

- New Skills and Learning
  - Surgeons will need to learn how to use and interact with the new cutting tool and new technology. This might be a big ask for a sub-group of surgeons for various reasons. The interaction of the tool and technology needs to be intuitive to keep the learning curve a minimum to promote the suitable use of the system.
- Surgeons may not always use the system properly

  - This information originated from the surgical technical support for the NavioPFS system saying that in surgery some surgeons may take the shortcut of using the oscillating saw to cut the straight edge on the tibia plate in order to save time and effort.
  - This is linked with the problem above and below.

- Time taken to remove bulk volume of bone tissue
  - Unlike the oscillating saw that can cut through once to remove a big volume of tissue, the burr needs to remove each volumetric unit of tissue. As a consequence, to remove a deep volume of tissue with a burr makes it ineffective and inefficient method.
- Restrictions of the hand-held device
  - The burr is a little bulky to hold and to use it in the tight space environment of the operating field and within the incision of the patient's knee; it makes reaching the posterior points of the knee joint hard to get to while only removing the desired tissue. On top of that, the tool is held in the hand for a longer period of time than the oscillating saw and the surgeon's hand might get tired during the procedure.

Each of the above problems was taken one at a time to apply each of TRIZ's 40 principles. This was a good approach as it highlighted key problem areas as well pointing out which of the above would take the project out of the scoop of the

brief; for example, the first point is it takes up space in the operating theatre and the operating zone but this is primarily a system problem not an implant problem and the interaction of the system isn't necessary down to the interaction covered by the brief. The number of ideas from this approach was 46 of the 71 but a lot of them were outside the scope of the project. The second approach wasn't limiting the thought to key problem area but just looking at the system and the implant as a whole to apply each of the TRIZ's 40 principles. Table 5.4-1 has examples of ideas generated from TRIZ; these are found with all the ideas generated from this project in appendix 9 (pages A16-30).

Table 5.4-1: Examples of Ideas Generated from Using TRIZ

Idea	**Description**
♫(♫)2	Have the material release positive modulators into the synovium fluid that will help to fight/prevent tissue damage from wear (particles).
♫(4)3	The prosthesis' shape on the articulating surface is designed to help load transfer for walking and running etc.
2(6)4	The prosthesis be its own glue This can be done by: Have the underside a soft and malleable material to mould into the burred surface for a snug fit. Have the underside pre-glued like an envelope.
5(37)1	Have a compacted material that expands to fill the space.
4(2)4	Eliminate the need for pre-made and trial prostheses. The prosthesis is positioned on the prepared tissue and the burr cuts the prosthesis into shape and polishes the surfaces.

6.5 6-3-5

This is a group based creative exercise, requiring ideally 6 participants but can work in the range of three to seven participants. This exercise was performed twice with two groups of types of participants: fresh and skilled, as mentioned in chapter *2.2 Design Process*. The fresh group for this exercise was made up of 5 participants that were of post-graduate level (biomedical engineers) whose field were not surgical orthotics and engineering. The skilled group was made up of 3 participants (including myself) of various academic statuses within the field of engineering and/or surgical orthopaedics. Group exercises can produce many more possible ideas than a solo exercise and no two groups will come up with the exact output. Therefore, by performing the 6-3-5 exercise twice and with two group types, provided and influenced the project with many possible ideas that may not have been produced solely or with technical aspects.

The basic process of 6-3-5 was as follows: the participants were given a sheet of paper with a blank table made up of 3 columns and the number of rows the same as participant number, please see appendix 10 (page A31). The group had 5 minutes to enter an idea or concept in the top row of their current sheet of paper; ideally filling all three but it did not matter how many ideas were generated in the 5 minutes. After the 5 minutes, the sheets were passed to the next person around the table. The group had 5 minutes to fill the next row of boxes with ideas before passing the sheet around the table again. This was repeated by the number of participants.

The instructions given to the two groups taking part in this creative exercise were the same apart from this slight difference: the fresh group were told to read previous ideas/concepts and further enhance, modify, or develop them; the skilled group were told to read the ideas above and come up with 3 ideas/concepts related or unrelated to the above concepts. The reason this happened was due to a misunderstanding, the instructions for the exercise were written down in shorthand to be read out to the participants, appendix 10 (page A32), but during the delivery there was some miscommunication. This was both beneficial and unfavourable: it limited the space for some additional ideas in the fresh group but it helped some of the participants who were struggling to provide initial ideas to work with other participants' ideas to draw out inspiration. Furthermore, meaningless one word ideas, like 'Batman', were expanded to being less abstract and lead to practical ideas.

This exercise is dependent on the input factors, the two primary inputs are the type of participants and the brief they are given. The fresh group may not have the knowledge or foundation in engineering or orthopaedics but they have their own field of knowledge that could be brought to the table; for example their field have similar situations/problems and could transfer their methods of problem solving. Also, the fresh group can (and did) open the opportunity to diverse ideas that included plenty that were abstract. These can either be suitable and have potential or not at all be applicable; because these ideas were fun to come up with it kept the process energetic. The skilled group was different, as the majority of

participants were lecturers at academic level in the engineering field and one of them was in the orthopaedic and living tissue field; all these factors meant there were strong ideas presented that were supported by both fields. There was less of a thought process to turn them into working concepts but there was the limitation on the diversity of ideas. The following two tables, 5.5-1 and 5.5-2, have the ideas generated from the two group types, see appendix 10 pages A33-37 for fresh group and pages A38-40 for the skilled group; these are also listed in appendix 9 (page A16 30). When presented next to each other, the differences of ideas generate from each group type are apparent.

Table 5.5-1: Example of Ideas Generated by 6-3-5 with 'Fresh' Participants

Ideas	**Description**
$\varepsilon(_i)$	Chewing Gum ideas. These ideas range from sticking the prosthesis with chewing gum to using the chewing gum as shock absorber.
β_4	3D print new prosthesis directly onto the knee.
γ_1	Apply a sticker to replace the gliding properties of the bone.

Table 5.5-2: Example of Ideas Generated by 6-3-5 Exercise with 'Skilled' Participants

Ideas	**Description**
π1	Have channels and groves on the back of the prosthesis that matches with the bone grooves.
σ6	Have a snap-fit like pegs that hold the prosthesis in place by undercuts
π 4	Have hammered in pegs that have barbs to prevent pull-out

6.6 Technical Aspect Creative Exercise 1

This is both a group and solo based creative exercise that looks at the different functions of products/systems and solves any problems with a technical point of view. The previous exercises are good at generating all types of ideas and concepts but they can be too abstract for what is needed whereas the technical aspect is a little more grounded approach, calling on knowledge and experience from the participants; because a solution doesn't need to be some farfetched way of thinking, a well-established approach can be the solution. Consequently, it made sense to have the skilled group as the contributor to this exercise; there were three participants (including myself) all at the time were doctorate students with engineering under-graduate degrees and two (including myself) of them also had a project within the surgical orthopaedic field.

To start the exercise, a table was produced with 4 columns and 13 rows, see appendix 11 (page A41); in the first 10 cells in the first column had each of the implant's function: integrated with bone, reduced wear, transfer loading, cement or cement-less, anchoring of implant, ease of implant, native kinematics, prevent pain, longevity, and impingement at 155°. The remaining 3 boxes were left blank for any functions that might be thought of during the exercise and to give space for extra ideas to be jotted down. The functions were discussed separately to allow a full understanding of the current function and possible areas to enhance or solve, during the discussion any ideas and/or concepts that were formulated were noted in the blank boxes. This creative exercise doesn't outline a time limit, as given in the 6-3-5 exercise. Although in future use of the technical aspect technique, the use of

time management would be suggested to allow the participants to cover all the functions; if there is time left over, then the participants can go over each function or revisit high potential functions.

This exercise didn't produce many different ideas like the 6-3-5 did as it strides a little for 'quality' ideas, not to say that the previous exercises produced inferior ideas. The point of this exercise is to get into the nitty-gritty of problems to seek ideas that have support from the available knowledge and theories from the research. This exercise takes advantage of talking out the problem to others that opens up to sharing knowledge and theories, in turn stimulating more recall of information; all of this can lead to different theories behind ideas that is set out to solve the problem. Therefore, as this exercise needs to draw on knowledge and theories, the participants need to know the information; it was apparent that the group needed to have participants with knowledge in the required fields. Table 5.6-1 below has a few examples of the ideas generated from the Technical aspect approach, the full outcome can be seen in page A36.

Table 5.6-1: Example of Ideas Generated by Technical Aspects Exercise with 'Skilled' Participants

Idea ID	**Description**
Wear 1	Injectable material.
Integrated 2	Reverse peg.
Kinematics 1	Have the patient determine the shape if the prosthesis by using their kinematics to shape it.

6.7 Technical Aspect Creative Exercise 2

Another creative (solo) exercise was self-devised for this project, it shared some traits from the technical aspect exercise 1 (previously discussed. The exercise starts at listing functions that could enhance the mechanical performance of the implant, they were: knee joint loading, fixation/anchoring, wear, commonly damaged area of – knee and implant, bio-reaction, and kinematics. Afterwards, a long thought out rational was stated for each of the functions drawing in information from the literature review. The gathering of previous researched information in a set area reminds the brain of principles and ideas it had already learnt; plus, it frees up the mind giving it the time, space, and RAM to think for the generation ideas and concepts. Below, in table 5.7-1, are two examples of the ideas produced in this constructive exercise.

Table 5.7-1: Example of Ideas Generated by Exercise

Idea ID	Description
$б_2$	Have a material in the middle of them implant to keep the pressure on the femoral component.
$г_5$	Have a conveyor belt system to the surface is always moving with the femoral component and thus does not wear.

6.8 Discussion

All the creative exercises above were providing many different (and many of the same) ideas but many of them will not be used for the final concept or experiments. That was the point of the exercises; it was to get a surplus of ideas and

concepts that may never get past the first round albeit by doing so the process has included as many ideas and concepts as possible because often there is more than one solution to a problem yet some may be more applicable and/or cost effective than others. Accordingly, there might be concepts that would be more applicable to solve the problem that designers may not think of straight away and if the designer doesn't try to look for other possible solutions could lead to the product/system failing to live up to the brief thus overall failure of the project. Therefore, it is important to try and find as many solutions as possible even if they might be exceedingly abstract as it is all part of the process that might lead to the well-fitting solution; this leads onto the next section below, 6*.8.1 Gathering and Organising*.

6.8.1 Gathering and Organising

The creative exercises used in this chapter had the ideas written down everywhere: some were noted within the log book and other sheets of paper that the participants filled out. Each idea was given its own unique identification reference. The identification references were noted all together in the log book with a little sentence or drawing next to it to summarise the idea, see appendix 9 (pages A16-30). Going through the summarised list of over 150 ideas, it was noted that there were ideas/concepts which had 4 different groups: not connected to the system or implant; system related but not implant related; implant related but not system related; and both implant and system related. Only the latter group will satisfy in full the project's brief, yet some ideas from second last one listed (implant

but not system related) was relevant to this project and could be used along with other concepts that emerge from this project. Therefore, the ideas and concepts were then listed in their own categories: non-implant related (page A11-12), implant design not connect to NavioPFS (page A13-16), implant design for NavioPFS (page A17-24); the lists can be found in appendix 9. Each list was fed into a positive, minus, and interesting (PMI) matrix, see appendix 12 (A43). This matrix helps with evaluation of ideas, the lay out is of a table with each idea entered in each row in the first column. The subsequent columns allow space for writing out anything positive, negative, or interesting (respectively). The PMI matrix for the former group included two more columns with the headings “possible to implement?” and “possible for the implant?”; this was to help with extracting any possible ideas and translate them into an implant related idea. Similarly, for the other two groups’ PMI matrix had the following additional columns: “test it?” and “further investigation”; this was to evaluate if an experiment can be devised to test the idea’s theory and then to add any additional notes of where the idea could be thought further in. Ideas from the former two categories were not brought forward to the next stage as they did not fit the project brief but the evaluation from the PMI matrix assisted to determine if any ideas had features that can be extracted or adjusted to generate ideas for the latter category. Furthermore, the ideas and concepts in the first two categories can be the beginning of other possible projects/research.

The ideas that are brought forward were then expanded to develop concepts; this process was to logically assess the idea in terms of practicality, the notes from the PMI matrix, and the benefits it can bring to the prosthesis. These concepts were then given identification numbers and were put through the concept selection process discussed in chapter 10, ideas from the concept generation require some experimental testing in order to validate if the principles will work in reality. The next chapters, *8 Experimentation of Fixation Techniques* and *9 Virtual Experimentation of Concept Ideas*, describes experiments that are investigated; the results are fed into the 10 *Concept Selection* chapter.

6.9 Key Message

This chapter generated the initial ideas for testing and evaluating. Generating ideas needed creative tools and interacting with individuals to generate the initial 150+ ideas; these ideas produced 58 concepts that comply to the investigation's brief and PDS. The next chapters, 8 *Experimentation of Fixation Techniques* and *9 Virtual Experimentation of Concept Ideas*, will be testing some of the features applied to the concepts which will aid the following chapter's evaluation.

Chapter 7

Experimental Techniques and Materials

The follow techniques and materials were using the experimental work found in chapters 8, 9, and 11.

7.1 Material and Equipment

This is the list of all the material and equipment used in this investigation.

7.1.1 Log Books

The notes from the literature review and personal experience exploration were recorded in the investigation's log books. This was helpful for referring to information needed in other parts of the investigation. In addition to these notes, the log book recorded the experiments performed and the results.

7.1.2 Animal Tissue

The bones used in experiments in chapter 8 were fresh-frozen bovine tibias. The sample were obtained from a local abattoir on the day the soft tissue was removed from the hind legs. The knee joints were still intact, the femur and tibia were connected (primary) by the ligaments. The knees were a random mix of left

and right. When the samples were defrosted overnight, the remaining soft-tissue was removed and discarded with the femur. The remaining tibia bone was cut using a hand saw between 20-35cm distal to the tibial plateau - which was then cut off approximately 1cm distally to expose the cancellous bone.

7.1.3 Laboratory Equipment

The laboratory contained standard equipment including power tools:

- pillar drills,
  - Model
- band saw,
  - Model
- hand saw,
- oscillating saw,
  - Model
- glass beakers,
  - This was needed for mixing the cement as plastic beakers would dissolve
- measuring apparatus.

7.1.4 Software

The following software was used:

- Wavematrix (Instron, Massachusetts, United States)
- BlueHill (Instron, Massachusetts, United States)
- MatLab (The MathWorks Inc, Massachusetts, United States)
- Microsoft Excel (Mircosoft Corp., Washington,United States)
- SolidWorks versions 2015 and 2016 (Dassault Systèmes, Vélizy-Villacoublay, France)
- Geomagic (North Carolina, United States of America)
- SPSS (IBM, New York, United States)

7.1.5 Instron

All the experiments in chapter 8 used the E10000 Instron tensile machine (Massachusetts, United States). Unless stated otherwise, the top grip was programmed, using either the Wavematrix or BlueHill software, to apply tensile tension on the samples at a constant rate of 5N/s till an adequate displacement was achieved.

7.1.5.1 Loading Condition

Unless stated otherwise, this is the loading condition to applied to the sample. The loading was set to 300N/min and stopped when the system surpassed 0.5mm, this was when the cemented samples broke apart i.e. failure. The grip displacement was recorded by the Instron and the video extensometer recorded the strain of the material using the two TipEx dots on the samples. The system

produced a CSV file of the captured measurements: load, displacement from crosshead and video extensometer, and time.

7.1.6 Pegs

For the peg extraction experiment, pegs made form steal rods. There were three diameter rods (4, 5, 6mm), all sizes were cut to a length of 60mm and the edge was smoothed with a file to give it a slight fillet.

7.1.7 Anspach Burr

Half of the samples in the surface texture experiment needed a roughen surface similar to one created by using robotic tools. The NavioPFS system's burr head is driven by an anspach unit (details). In the experiments 6mm NavioPFS burr heads were connected to the anspach unit as it wasn't constrained by the user interface and had a smaller lab space foot print. The foot pedal controlled the operated the burr head and it controlled the rotation speed. There was no rotational speed limit applied and the foot pedal was full depressed in operation. To get the desired texture, the burr was skimmed along the surface which created little pits and groves that were observed in bone after use of robotic tools.

7.1.8 Epoxy

The experiments used artificial cortical material that has similar mechanical properties to human cortical bone. From Sawbones 4th generation range, epoxy rods of 20mm, and 35mm diameter were purchased; the rods modified into the desired specimen by the workshop.

7.1.8.1 Epoxy Jacks and Plugs Samples

The partial cement experiment had the 20mm diameter epoxy rods, plugs, inserted into the 35mm diameter epoxy rods, jacks. The jacks and plugs are from 6 groups; each group has a general shape but with slight differences - as seen in figures 7.1-1a and 7.1.b. In general: the 35mm rods were cut to lengths of 47mm, then a 20mm fin cut in one end of the rod and a 20mm or 27mm diameter hole cut (depth 20mm or 16mm) on the other end; and the 20mm rods were cut to a length of 40mm, with a 20mm fin cut at one end of the rod.

Table 7.1-1: Cement Samples Names with the Description and Cement Application	
Sample's name	**Description of the sample**
1 – Fully	The plug is an unaltered 20mm diameter 9 mm deep epoxy and the jack has a central hole of 27mm diameter 9mm deep. The cement is applied all around the plug before inserting it into the jack.
2 – Rib	The 20mm plug has 3 concave ribs running the circumference, ca. 1mm radius. The jack has a central hole of 20mm and is 9mm deep. The cement is only applied to the ribs before the plug is inserted.
3 – Wall	The plug is an unaltered 20mm diameter 9 mm deep epoxy and the jack has a central hole of 27mm diameter 9mm deep. The cement is applied only to the side of the plug before inserting into the jack.
4 – Channels	The plug and the hole in the jack are the same size (20mm diameter and 9mm deep). Around their circumferences' there are 2 concave 1mm ribs that are aligned when the plug is fully inserted. The cement is only applied to the ribs of the plug.
5 – Extruding	The plug is the same size as before but has the addition of 2mm extruding circle of 10mm diameter central on the base. The jack has a 20mm diameter hole that is 9mm deep; the base of the hole there is another hole of 10mm diameter and 2mm deep, this matches the plug's addition. The cement is only applied to the hole of the jack.
6 – Intruding	This is the opposite of sample 5. The plug's base has a 10mm diameter hole of 2mm and the jack has a circle of 10mm diameter extruding 2mm from the base. This time the cement is only applied to the plug's 10mm hole.

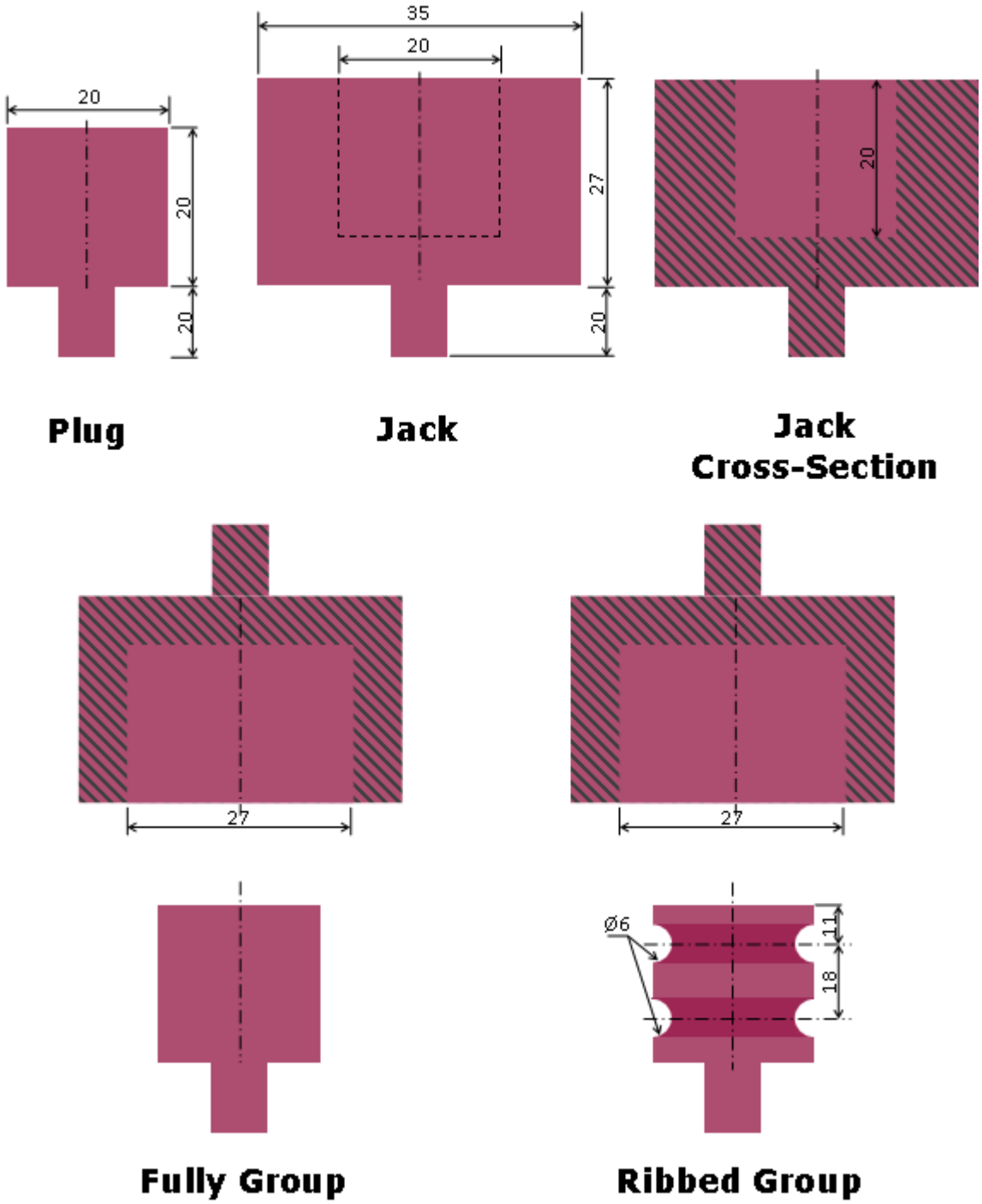

Figure 7.1-1a: Illustration of the Partial Samples, part 1.
The top row illustrates the standard sizes of the plug and jack, these are the sizes used unless stated otherwise. The illusion of the Jack to the right on the top row is a cross-sectional view as if cut down the middle; the hatched area represents where the material would be cut.
The bottom two rows illustrates the jack and plug configurations of the fully and ribbed groups.
Illustrations are not to scale.

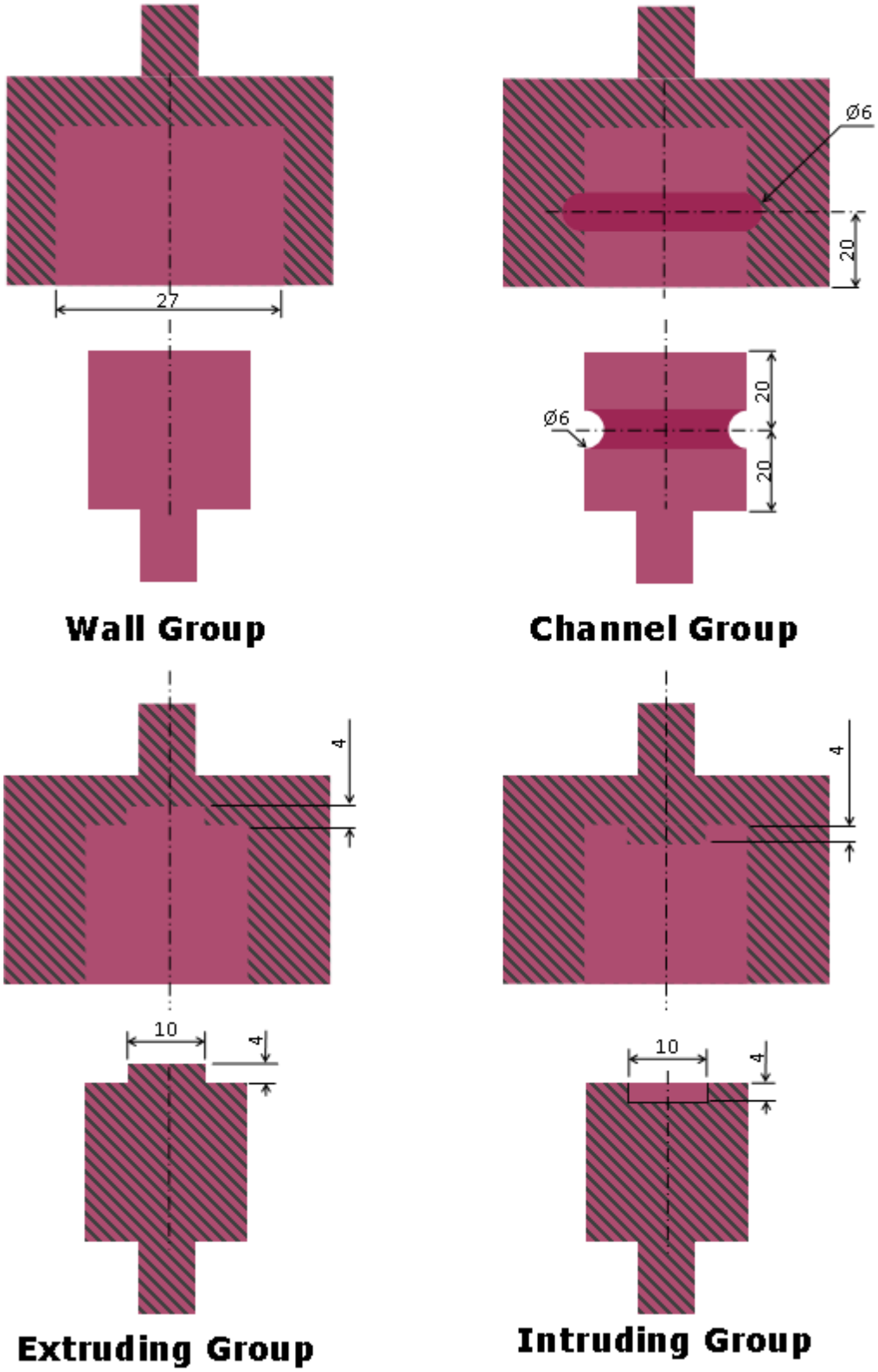

Figure 7.1-1b: Illustration of the Partial Samples, part 2.
The top pair illustrates the jack and plug configurations of the wall and channel groups. Likewise the bottom pair illustrates are of the extruding and intruding groups. Not to Scale See figure 7.2-1a for sizes and definition of cross-sections.

7.1.8.2 Epoxy Tensile Pull-Off Samples

The epoxy rods in the surface texture experiments are very similar to the plug samples above: the 20mm diameter rods were cut to a length of 40mm and a 20mm fin cut on one end, see figure 7.2-1. The side opposite to the fin was left as the smooth cut of the band saw or was roughen using the burr detailed in section *7.1.7 Anspach*.

7.1.8.3 Epoxy Shear Pull-Off Samples

The epoxy rods are prepare just like above, length of 40mm with a 20mm fin, with the additional cut on the end opposite of the fin seen in figure 7.2-1. On the side of the additional cut is surface the cement is applied to, shown in figure 7.2-1, and half the samples have this surfaced roughened using the technique described in section *7.1.7 Anspach*.

7.1.9 Bone Cement

The bone cement used in this investigation experiment was PALACOS R (Heraeus Medical GmbH, Germany), which is a PMMA of XX viscosity (unless stated the PALACOS® was used instead which has a viscosity of XX). Cement mixing procedure was conducted under a ventilation hood as there were vapours from the liquid monomer (MMA) and double gloves were worn to prevent any contact to the skin. using the

7.1.9.1 Mixing Contents as Packaged

The method of mixing the bone cement used the PALAMIX® (Heraeus Medical GmbH, Germany) mixing system. The constituents were removed from the sterile packaging and placed in the workspace under the ventilation hood along with the samples in their respective set-ups. All extra equipment that is required is also placed under the ventilation hood within the workspace as they there is a limited working time frame of the cement.

The bottle of the liquid monomer was snapped open and poured into the mixing tube via the liquid filtering part of the funnel (from the PALAMIX® system). Once the bottle is fully emptied, the powder component was added through the wider part of the funnel into mixing tube. As the cement is added, the timer is started as the cement has set mixing, waiting, and working periods before it begins to cure. Promptly, the funnel was removed and mixing tube's lid and plunger was screwed tightly and pumped 17 times in a figure of eight style twist, this took approximately 30 seconds that is required for the mixing stage. The lid and plunger were removed and after 30 seconds, when the timer says 2 minutes, the cement is ready to work with.

After the cementing samples together, the leftover cement is pushed into two syringes that have the nozzle-end cut off and are left to cure to create two cement rods with a diameter of 4.5mm and roughly 20mm in length. All samples are left to cure for at least 24 hours before being removed from rigs or syringes.

7.1.9.2 Mixing smaller volumes

This procedure is used to mix the same ratio (1ml:2g) of the above cement constituents but in smaller quantities for the smaller batch sizes in the pressured and bovine cementing procedures.

Under the ventilation hood, a scale was set up to measure out 4g of the powder component from PALCOSE®R cement into 10 plastic containers. The liquid monomer is poured into a glass stopper jar (no plastic or rubber as the monomer degrades these materials), via the filter part of the funnel provided from the PALAMIX® system; the stopper prevented spills and evaporation of the liquid monomer.

A glass pipette was used to measure out 2ml of the liquid monomer and transferred to a 25ml glass beaker. One of the plastic containers that contain 4g of the cement powder was emptied into the glass beaker and the timer was started. The components were mixed with a small metal spatula for 30 seconds before it was collected together from the edges of the beaker and waited till 2 minutes on the timer when the cement was ready to be used.

7.1.10 Microscope

In the surface texture experiment, the something microscope (details) was used to evaluate the interface between the cement and epoxy. Random tensile and shear pull-off samples were selected after they were tested to be cut along the

plane of the fin, as indicated by the dotted lines in figure 7.1-2. The surface was wet polished with very fine sandpaper.

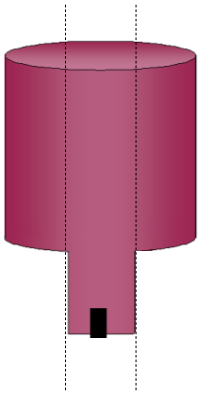

Figure 7.1-2: Illustration Where the Sawbones Epoxies were Cut for the Microscopy Analysis
The dotted line was where the epoxy was cut. Not included in the image is the cement attached to the top of the epoxy.

The two materials appeared as different shades of grey, and the black area indicate possible voids at the interface or in the material. Voids at the interface are potential areas where the cement and epoxy are not in contact and thus reduced surface area of affected adhesion. To obtain the scale, a steel rule was placed on a sample and the image was captured for future reference.

7.1.11 Manufacture of the Prototype Samples

The MAKO prosthesis was 3D scanned and exported to SolidWorks, as described in section *7.1.12.1 Prototype Prosthesis*. The modelled MAKO was altered to create the two novel prototypes designs. All three models were exported as .stl

format, and sent to Shapesways (New York, United States of America) to be 3D printed in aluminium in duplicate.

7.1.12 FE Modelling

7.1.12.1 Prototype Prostheses

The MAKO's prosthesis was used because it is very similar to all the other UKR prostheses out in the market and thus it was a good guideline to compare the prototypes against the market design in general. The MAKO prosthesis' components were scanned using a 3D infrared scanner in 3 orientations. This created overlapping meshes that needed to be stitched together using software Geomagic. The stitched meshes of the components were exported individually to SolidWorks as a dumb solid stereolithography (.stl) files. The parts then had references assigned to them so there were able to be ordinated and worked. The MAKO prosthesis did not have any alterations added to it after being imported into SolidWorks, figure 7.1-3.

The MAKO prosthesis was the foundation to build the prototypes, the peg features were removed and replaced with the flange features (as prescribed from the design of BQ and T6.2), for images and for nomenclature of the features see figures 7.1-4 and 7.1-5. The surface for BQ was generated using surfacing tools in SolidWorks, this allowed for a both undulating and curved surface.

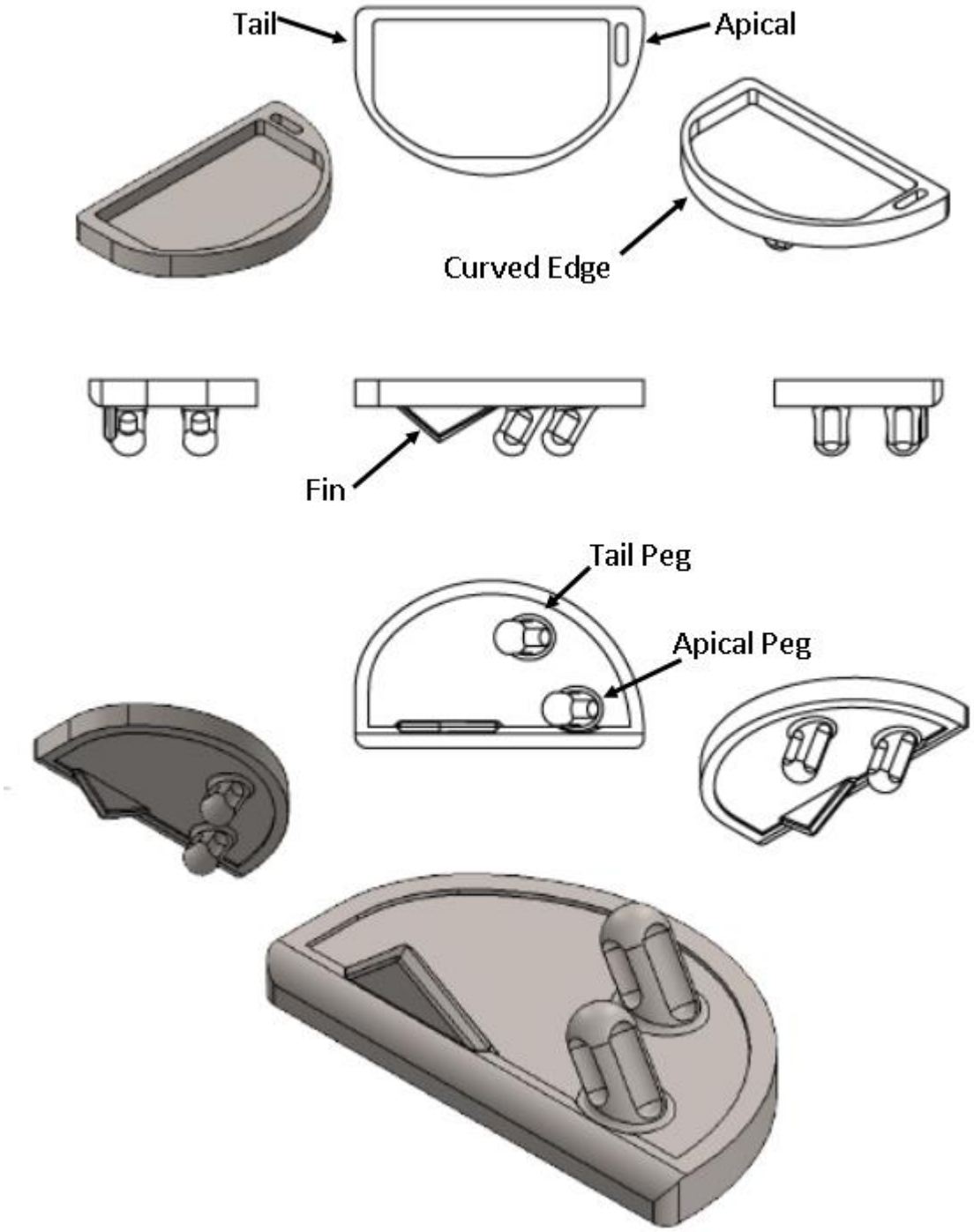

Figure 7.1-3: The Model of Original Prototype
The figure has the model in different orientations. The model was based off the MAKO UKR prosthesis size 6. The location subfigure shows the nomenclature of the original prototype used in the report.

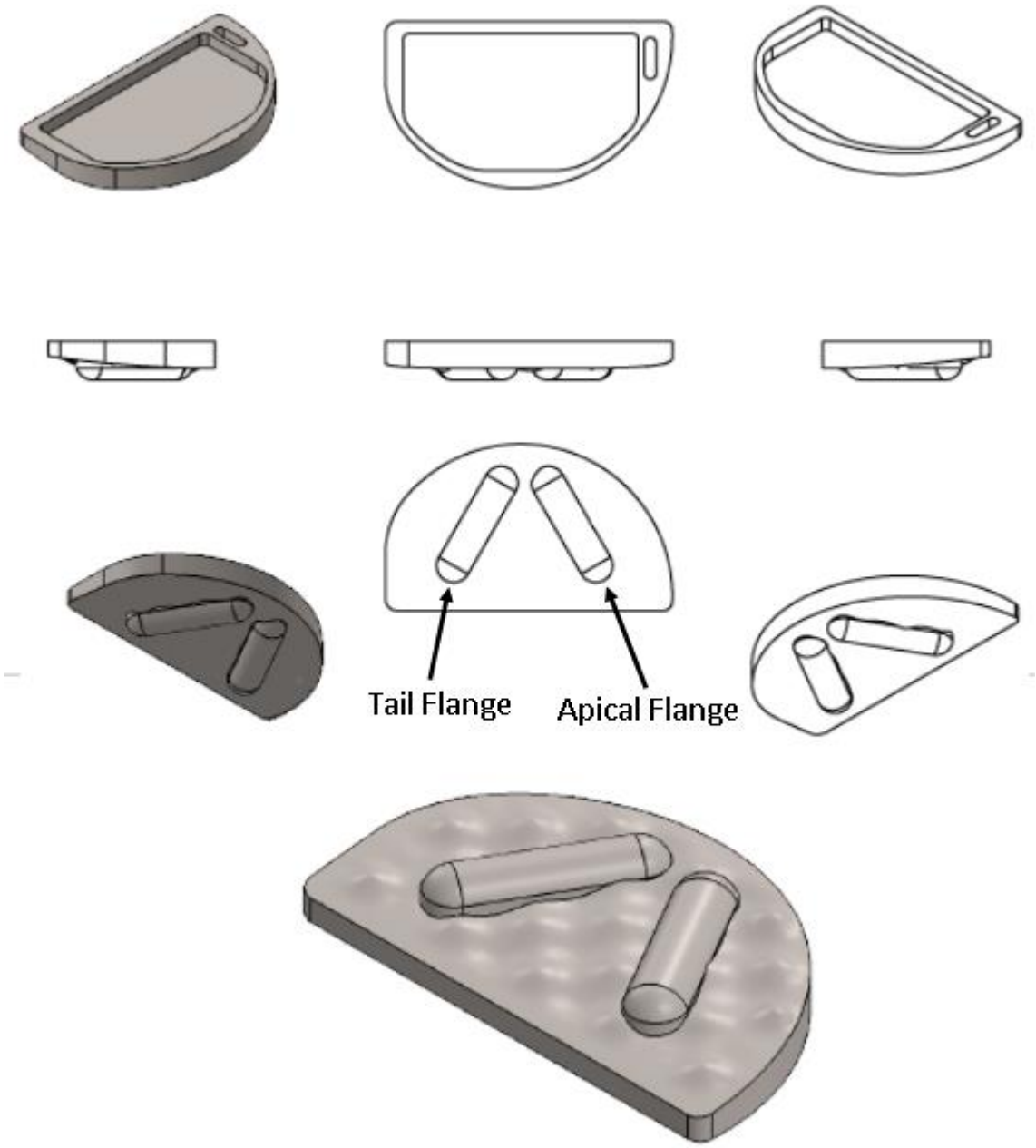

Figure 7.1-4: The Model of BQ
The figure has the model in different orientations. The location subfigure shows the nomenclature of the BQ used in the report.

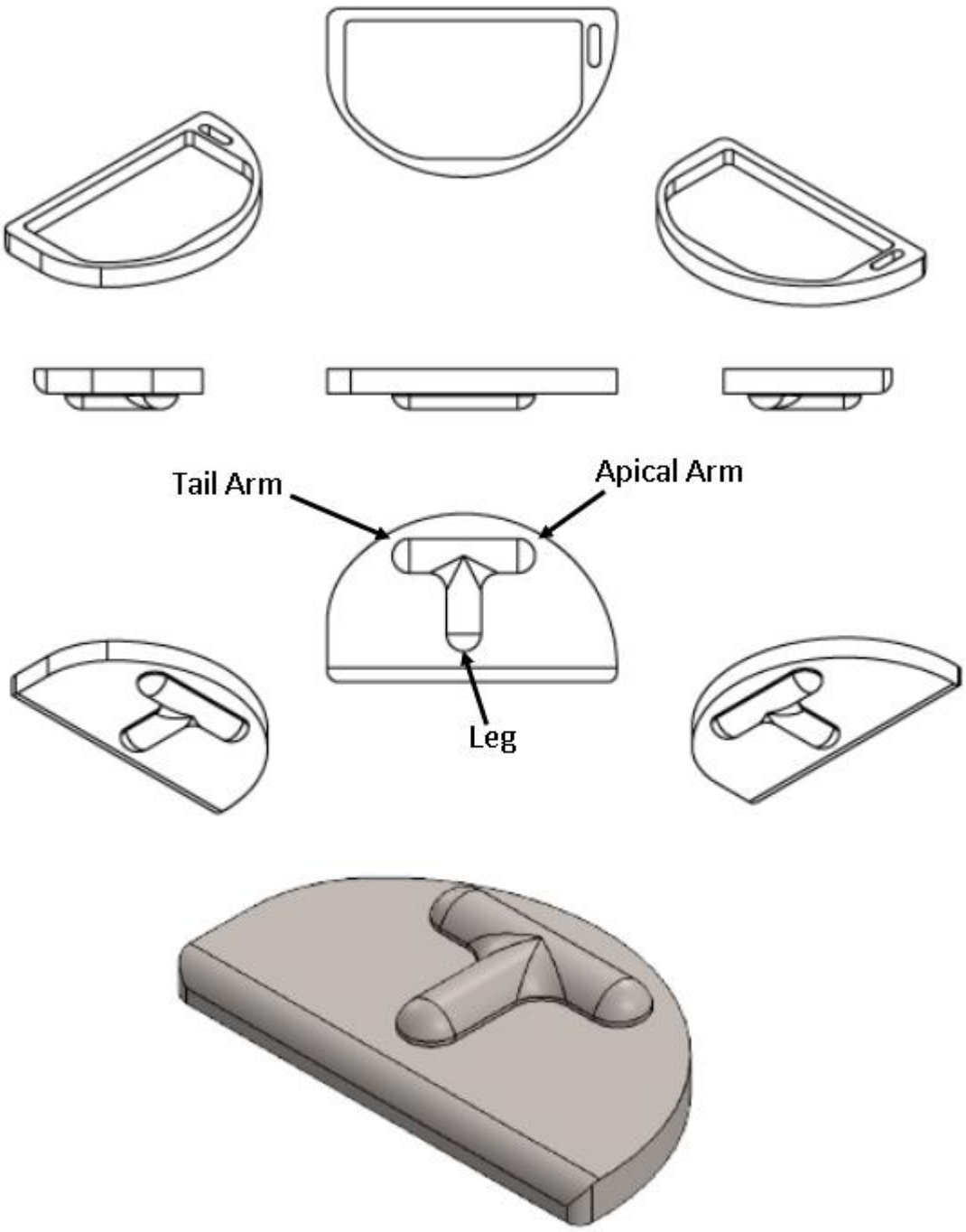

Figure 7.1-5: The Model of T6.2
The figure has the model in different orientations. The location subfigure shows the nomenclature of the T6.2 used in the report.

7.1.12.2 Right Tibial Knee

For the FEA models, the generation 1 tibia model[237]–[240] was downloaded from open knee (simtk.org). The file type was a '.stl' file, which was converted into a SolidWorks part model (without feature recognition). Using the flat surfaces on the medial and lateral side of the model reference points were made, these SolidWorks references were used in all following models.

The tibia plateau was 'cut' by positioning the prosthesis or cement part model on the tibia part model, then using the subtraction feature in SolidWorks. This feature removes erases a solid volume were the prosthesis/cement part model is positioned, thus creating the negative profile on the tibia part model which allowed for no interference of parts in the assembly model.

7.1.13 Foam Blocks

The foam blocks are made from one part Pedilen Rigid Foam 300 (617H32=2.300) and one part hardener (617P21=4.600) both from Otto Block GmbH (Duderstadt, Germany). Each block was made individually by completely incorporating the above components and pouring into a 60x60x30mm mould with metal walls and a 3D printed base with the negative imprint of the prototype design (sprayed with releasing agent, name from Otto Block), see figure 7.1-6. Once cured and left overnight, the foam blocks were cut 5mm from the base to be flushed into the holding box.

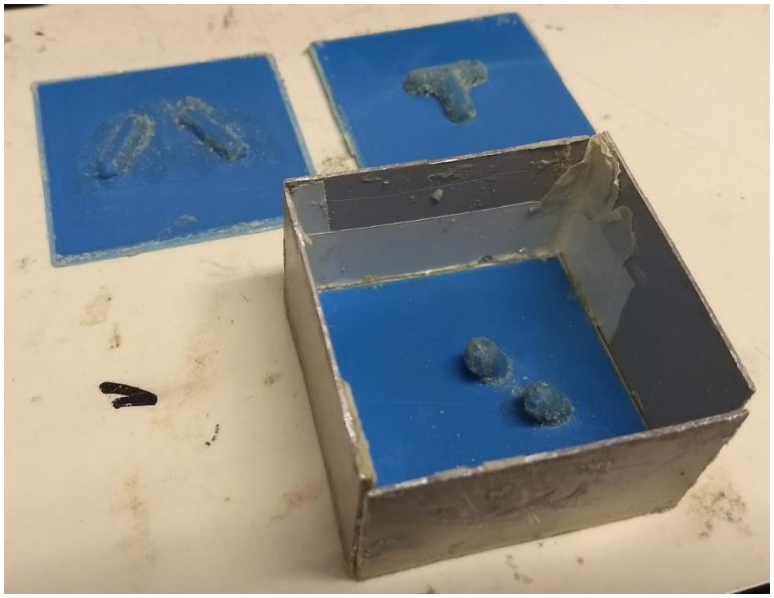

Figure 7.1-6: Pictures of the Foam Moulds with the 3 Bases
The walls of the moulds are made from scrap metal tin taped together with the base using electrical tape. The top picture is original design, middle picture is the BQ design, and the bottom picture is T6.2 design.

7.1.14 Holding rigs

7.1.14.1 Holding rig 1

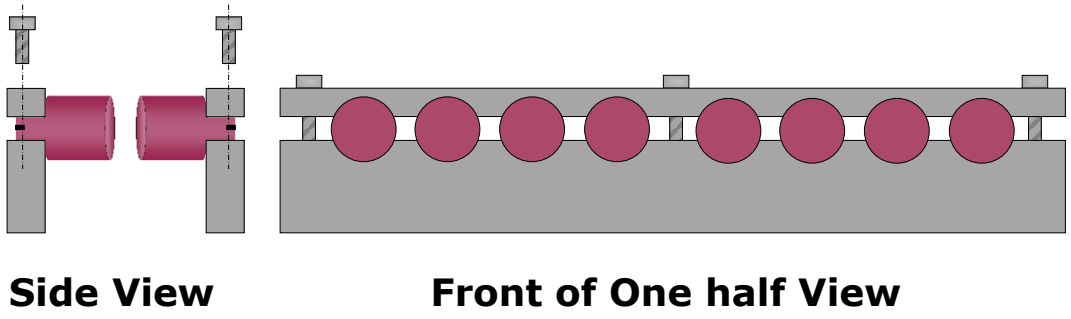

Figure 7.1-7: Illustration of the Holding Rig Set-up.
To the left is side view of both holding rig ready for cementing. To the right is one half of the holding rig that has all 8 (in this example) smooth epoxies.

7.1.14.2 Holding Rig 2

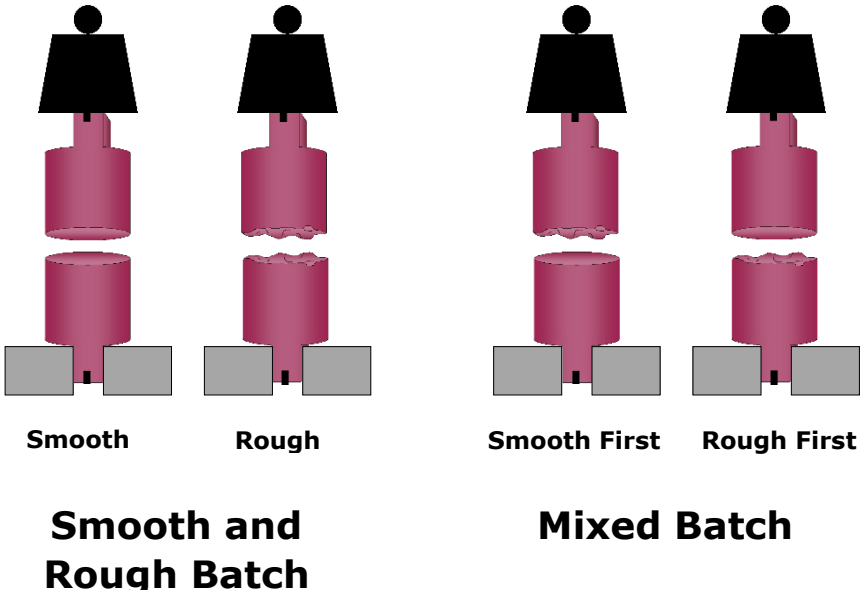

Figure 7.1-8: Illustration of the Metal Holding Blocks and the Sawbone Epoxy Batch Samples *The left hand side is the batch with the smooth and rough groups and on the right is the batch with the mixed group in the two orientation.*

7.2 Methods

7.2.1 Chapter 8

This chapter's experiments were concentrated on finding answers to questions proposed in the concept development stage: these were concerning on prosthesis fixation.

7.2.1.1 Peg Extraction

Bovine tibia were prepared as detailed in *7.1.2 Animal Tissue*. A pillar drill was used to produce nine holes on each bone sample (sizes range from 3mm to 6mm, see table 7.2-1); the holes were perpendicular to the plateau surface and to a

depth of 20mm. A 60mm length peg with a filleted edge was then inserted, sometimes requiring a hammer, 20mm into hole leaving 40mm of the peg exposed to allow for gripping. The distal tibia was secured in a vice bolted to the Instron E10000; the arrangement was such that the sample position could be altered so that the peg and the grip were vertically aligned. Wavematrix software was used to apply a constant rate of 5N/s, stopping once the peg had displaced 25mm upwards, i.e. when the peg had been fully extracted.

The maximum extraction loads were taken from the force-displacement data and analysed using two-way ANOVA attributing the variance in extraction force to peg size and peg-hole discrepancy (i.e. 1, 0.5 and 0mm diameter smaller than the peg diameter).

Table 7.2-1: Group IDs and Sizings

Group ID	**hole size (mm)**	**peg size (mm)**
h3p4	3.0	4
h35p4	3.5	4
h4p4	4.0	4
h4p5	4.0	5
h45p5	4.5	5
h5p5	5.0	5
h5p6	5.0	6
h55p6	5.5	6
h6p6	6.0	6

7.2.1.2 Partial Cement

Following the cement mixing procedure on page 129 (*Mixing Contents as Packaged*), the cement was applied to the samples in the following manor before the plug is inserted into the jack. For the control sample, the cement was liberally applied to the full surface of the plug component so it was had thickness of around 2-3mm. For the grout, ribbed and undercut samples the cement was liberally applied to the rounded side of the plug taking care not to allow add cement to the flat base of the plug. The anchor sample had the cement carefully rolled, by finger, into a *ca.* 4mm rod to then be placed around the indented groove of the plug component. For male plug the cement was carefully applied to only the extruding circle of the base of the plug and vice versa with the female plug (cement only to the extruding ring).

Each batch was left in holding rig 1 for at least 24 hours before they were lined up in the Instron grips and pulled apart with the Instron loading condition, on page 122, without the video analysis and the displacement was set at 9mm after the first sample. Each design had two samples for testing except the angle design because of cementing error. The comma-separated values (CSV) files were imported and stored in MatLab; the find peaks function found the ultimate load and displacement. The loading of the samples would have produced a mix of tension, shear, and compression. Difference between the samples is the cementing application, the samples are similar to each other – a 9mm deep plug is inserted into the jack that is 9mm deep and its diameter ranges 0-2mm bigger than the

plug's dimeter. Therefore, the results expressed in load and displacement can be used to compare the cement's adhesion strength of the different cementing techniques. In addition to the quantitative results, there were observational notes taken for qualitative analysis. Due to the limited sample numbers, ANOVA analysis can't be relied upon; the statistics analysis used was average means, standard deviations, and co-efficient of variance (CV).

7.2.1.3 Effect of surface texture

7.2.1.3.1 Cement rods

Each end of a cement rod sample was placed into the Instron's grips leaving around 15-20mm between the grips. The cement samples, 68 in total, were pulled in tensile as mention in the *Instron Loading Condition*, page 122.

From the CSV files produced by the Bill Hill software, a MatLab (The MathWorks Inc, Massachusetts, United States) code read and stored the data for processing. The code also retrieved information on the grip distance from an excel worksheet. In each sample's data, the maximum load was calculated by find peak function in MatLab; the displacement at this found data point was the ultimate displacement. The loads were converted into stresses by dividing by the cross-sectional area (15.9mm^2); the ultimate stress was then calculated from the maximum load with the same conversion. Likewise, the crosshead displacements were converted into strain percentage by divided by the grip length from the excel worksheet. The curve of the graphs starts off initially as elastic-linear relationship. With the continuation of tensile force, the curve becomes non-linear at an

undefined yield point. The Young's modulus was calculating by taking 2 points on the straight section of the stress-strain curve and calculating the gradient of straight line between the points. The two points were acquired by dividing the data length by 3 and 5 - this was to avoid initial measurement errors and be certain that the gradient calculated was still within the linear portion of the curve. The yield stress and strain were calculated by finding the intersection of a line with the calculated Young's modulus as the gradient and off-set by 0.02% strain and the sample's stress-strain curve. A one-way analysis of variance test was used to test the hypothesis that a mechanical property did not vary between the batches.

The first cement batch followed the cement mixing procedure and used the high viscosity cement (PALACOS®R) and it produced 2 smooth epoxy tensile pull-off samples and 2 cement rods. The second cement batch followed the cement mixing procedure to produce the same sample types but instead of the high viscosity cemented, it used the medium viscosity version (PALACOS®M). The mechanical properties of each viscosity types were compared to each other by analysing average of means and a One-Way-ANOVA test in SPSS software.

7.2.1.3.2 Tensile and Shear Epoxy Pull-off without pressure

The epoxy samples were held in holding rig 1 (see figure 7.1-7) that was designed to hold to eight pairs (all either tensile or shear sample types). Pairs where one of three groups: rough, smooth, and mixed – see figure 7.2-1. When the cement is ready, mix according to (*7.1.9.1 Mixing Contents as Package*), the cement is rolled into little spheroids that were around 15mm in diameter. The cement

spheroids were placed on the samples on the unfixed side of the holding rig; for the mixed category, the surface roughness of the samples on the unfixed holding rig was recorded for later analysis. The samples are then pushed together in the holding rig and left for at least 24 hours at room temperature before testing in the Instron, *7.1.5.1 Loading Condition* page 122.

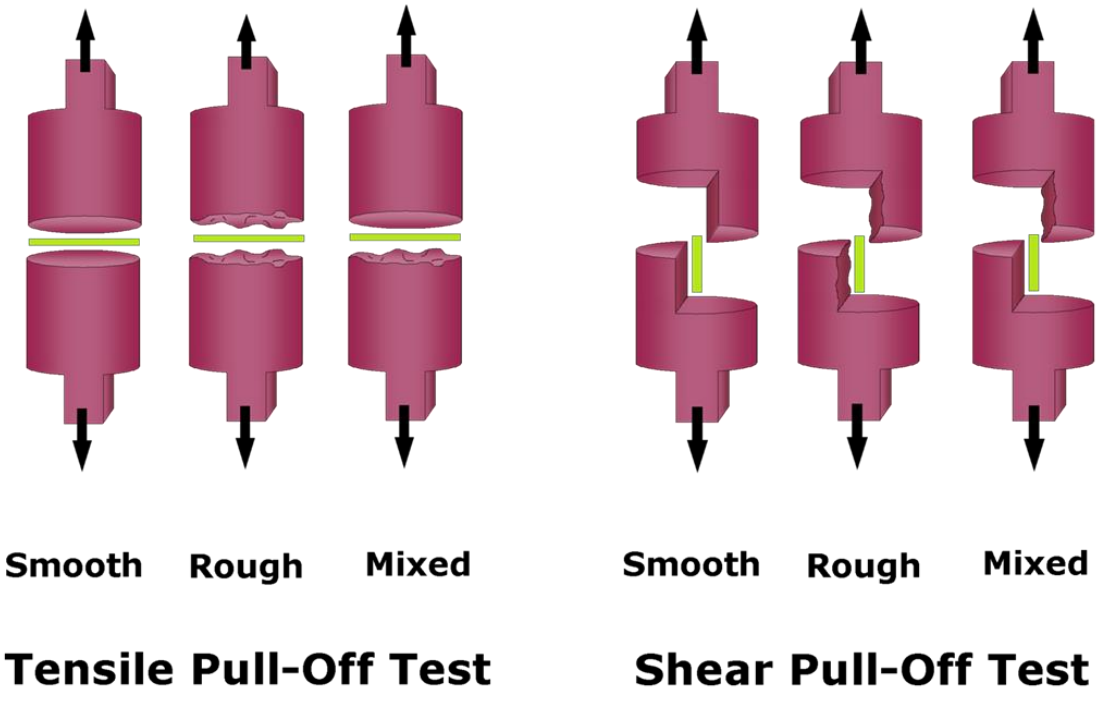

Figure 7.2-1: Illustrations of the Sawbone Epoxy Sample
The samples on the right are the design and arrangement for pulling in a tensile fashion and on the left are the samples designed and arranged for pulling in a shearing fashion.

The cement thickness fluctuated with every sample and it was difficult to measure on the rough surfaces; it was unclear where to take the measurements from and the difference was as much as 1mm in some samples, this would have had an error range of 0.167% to 0.25% when calculating the stress and strain. The cross-

head displacement included the displacement of the epoxy. Nevertheless, the epoxy displacement at each stress value would be the same for all samples. Additionally, the Young's modulus of the epoxy is approximately 15 times (16GPa) greater than the Young's modulus of the cement and so the epoxy displacement is ignored. The data was fed into a similar MatLab code above and it found the maximum load and displacement in the method. The gradient of the linear part of the curves was obtain by visual inspection: from the graph 4 points were picked in the middle of straight contour to obtain 4 gradients (the load divided by the displacement) in which the average was taken from. A one-way analysis of variance test was used to test the hypothesis that a mechanical property did not vary between the batches. Then a two-way analysis of variance to test if group and/or batch had an effect on the mechanical properties.

To test if the surface roughness affects the adhesion properties a two-way ANOVA test was performed on the stiffness, ultimate stress, and ultimate strain, with the null hypothesis being that the groups, batches and their interaction do not affect the adhesion property. Following that, independent t-Tests were performed three times comparing the groups in pairs against each other.

Analysing the interface, the mixed group provided information to the side the interface failed. This, along with the side the cement was initially attached to, were put through two Chi-square tests under two hypotheses: "the surface the cement first adheres to has a stronger bond than the other surface" and "the rough surface has a stronger adhesion than the smooth side".

7.2.1.3.2.1 Cement viscosity

The following was done for the first four tensile samples, 2 of smooth epoxies sandwiching medium viscosity cement and 2 samples with high cement viscosity. A MatLab code read and stored that data from the CSV files along with an excel worksheet with the recorded in the testing log. The maximum load was calculated by find peak function in MatLab; this also returned the ultimate displacements at the ultimate load. The loads and displacements were converted into stress and strain by dividing by 314 (cross-sectional area of the epoxies) or by the length in the excel file (respectively). The ultimate stress and strain were calculated in the same conversion. The curve of the graphs starts off initially as elastic-linear relationship; with the continuation of tensile force, the curve becomes non-linear at undefined yield point. The Young's modulus was calculating by taking 2 points on the straight section of the stress-strain curve and calculating the gradient of straight line between the points. The two points were acquired by dividing the data length by 3 and 5- this was to avoid initial measurement errors and be certain that the gradient calculated was still within the linear portion of the curve. The yield stress and strain were calculated by finding the intersection of a line with the calculated Young's modulus as the gradient and off-set by 0.02% strain and the sample's stress-strain curve. The mechanical properties of each viscosity types were compared to by analysing average of means and a one-way-ANOVA test in SPSS software.

7.2.1.3.3 Tensile Epoxy Pull-off with pressure

Each batch in this method used two tensile pull-off epoxy pairs in an up-right configuration, each pair was held by the fins using two metal holding blocks, see holding rig 2 (figure 7.1-8). Before cementing the base epoxies were secured to the holding blocks by a rubber bands and a paper guide was taped around the circumference; this acts as guide to ensure the two epoxies being cemented line up and it prevents the cement spilling out which in turn caused pressure during the cementing. Also prior to cementing, the top epoxies had weights, 523g each, attached to the fins, as indicated in figure 7.1-8; this utilised gravity to apply a constant pressure. In the case of the mixed group, the bases samples had one smooth and one rough, this was recorded in the testing log to keep track which surface the cement contacted first.

The cement was prepared using the small volume cement mixing procedure as described in *7.1.9.2 Mixing Smaller Volumes*. The cement was halved and each half was placed on the sample in the holding blocks. The top pairs were gently placed on top of the cement and push gently down the paper guides making sure they were straight. They were left like this for 10 minutes, while been continually monitored to make sure they weren't falling to one side. After 10 minutes, the weights and holding blocks were removed and the samples were set aside for at least 24 hours before testing in the Instron, *7.1.5.1 Loading Condition*.

The CSV file was imported in to MatLab and the following information was extracted. The ultimate load was calculated by using the find peak function, this

also returned the ultimate displacement. From the initial straight curve in the load against displacement graph, 4 points were picked in the middle, the points load was divided by the displacement and the 4 values were averaged out to give the stiffness of the samples.

A one-way ANOVA was performed in SPSS, the variances were the adhesion properties and how they were affected by the different batches. The groups were pair up three times to run independent t-tests (on SPSS) between them to see if the batches affect the groups. Between the rough and smooth a paired t-test was calculated in Excel because each batch had a sample from each group. Standard analysis was also calculated: average mean, standard deviation, and CV.

7.2.1.3.4 Bovine Pull-off with pressure

Bovine tibias were prepared as detailed in *7.1.2 Animal Tissue*. One half of each of the tibia compartments was slightly burred to simulate the surface roughness from a robotic assisted surgery. The exposed cancellous bone was cleaned to remove debris and as much interstitial tissue from the bone matrix by using a modified water spray and a stiff bristle brush. The samples were dried using lab tissue paper and the secured in a vice by the distal end of the tibia. Weights were added to the fins of two smooth epoxies of the pull-off design (523g each), see figure 7.2-2.

Figure 7.2-2: Illustration of the Bovine Experiment Set-up
The illustration is not to scale and only shows one epoxy from a batch of two. Knee imaged taken from google free-use imagine search.

The cement was mixed using the small volume cement mixing procedure section *7.1.9.2 Mixing Smaller Volumes*, the cement was then halved. A cement half was placed on a smooth epoxy which was then carefully sandwiched on either the sawed or burred prepared area of the tibia to allow the cement to adhere the epoxy to the bone with the aid of the weights. The second epoxy was adhered in by the same process but on the other prepared area on the same side of the knee. During the first 10 minutes, the samples were monitored to keep the epoxy from tilting off balance. This cementing procedure was repeated for the other side of the knee.

An hour after cementing, the samples were pulled off using the Instron, *7.1.5.1. Loading Condition*. However, the size of the clamp and alignment problems prevented all the samples from being suitably tested. Only 4 samples (2 rough and 2 smooth) from the 4 knees produced results. This lead to using the sawn off tibial

plateaux to be used in the experiment too. Each cut-off had one half of the surface roughed up with the burr to mimic the surface texture left behind after burring. The exposed cancellous bone was cleaned, using the same modified spray and brush as before, and dried using the lab tissue paper. The cement was prepared using the small volume cement mixing procedure before being halved between two epoxy samples to be cemented on both sides of the cut-off. During the first 10 minutes of curing the sample were monitored to stay upright and they also had weights of 523g secured to the fins. After an hour, the samples were pulled off using the Instron, *7.1.5.1. Loading Condition*. This method produced 4 samples each of smooth and rough.

The data from the CSV file was opened by MatLab code and it found the ultimate load at the displacement at ultimate by the find peaks function. The gradient was obtained by taking the average of 4 points in the middle of the linear part of the curve; from the 4 points the load was divided by the displacement, this is taken to be the gradient since the curve originated at origin.

The statistics values (average mean, and standard deviation) of the 3 mechanical properties were calculated along with a two-way ANOVA (variance being group and batch) and a paired t-Test of each batch.

7.2.2 Chapter 9

7.2.2.1 Simple shapes

In SolidWorks, 20 simple undercarriage shapes were created, all shapes are described in appendix 14 (page A74). The shapes were assembled on the medial side of the downloaded and prepared knee modelled in *7.1.12.2 Right Tibial Knee*.

7.2.2.2 Material Properties

The modelled profile was assigned as pure titanium as some prostheses in the market use this material for the metal components; the mechanical properties used were the stored values in the SolidWork's library. Modelling both cortical and trabecular bone was not possible from the open source model of the knee without significant effect. It was deemed unnecessary to more accurately model the underlying bone since FEA model were to be used comparatively, and not for absolute values. The tibia's material properties were manually entered with the values of cortical bone, seen in table 7.2-2.

Table 7.2-2: Material Properties of the Profile and Cortical Bone

Part	*Profile*	*Knee*
Material	Titanium	Cortical
Elastic Modulus (GPa)	115	6.91
Tensile Strength (MPa)	900	99
Compressive Strength (MPa)	875	106
Poisson's ratio	0.3	0.3

7.2.2.3 Meshing Parameters

A global meshing parameter was applied to the whole assembly. Standard 4-point Jacobian elements were used with a global size of 4.36mm and tolerance of 0.218mm.

7.2.2.4 Boundary and Loading Conditions

The bond between the part's interfaces of the assembly was assumed to be ideally bonded. The flat base of the tibia had a fixed geometry applied so it had no degrees of freedom. The two simulated conditions of the assembly are 750N axial load applied to the top surface under equal distribution of the profile, or 750N shear load applied to the top surface of the profile.

7.2.2.5 Plot Generated

A von Mises plot is used to analysis the stresses experienced in the elements of the virtual tibia, the colour scale was set at dark blue for 0MPa and red for 10MPa. The iso-clipping tool provided insight into the model by only showing the prescribed range of stress within the model. In the von Mises plot, the dark blue areas were considered as areas for potential stress shielding and the hot colours (in particular red) were considered as areas for potential stress concentration.

7.2.3 Chapter 11

7.2.3.1 Prototype Experiment

The following was set up on the foot-base of the Instron, see figure 7.2-3. This allowed the Instron to apply a regulated increasing downward force on the implant which creates a shearing action on the interfaces of the components. The force applied axially to the prototype-cement-foam arrangement to insured the whole system remains in the arrangement for shear forces and to mimic a person's loading going through the knee joint.

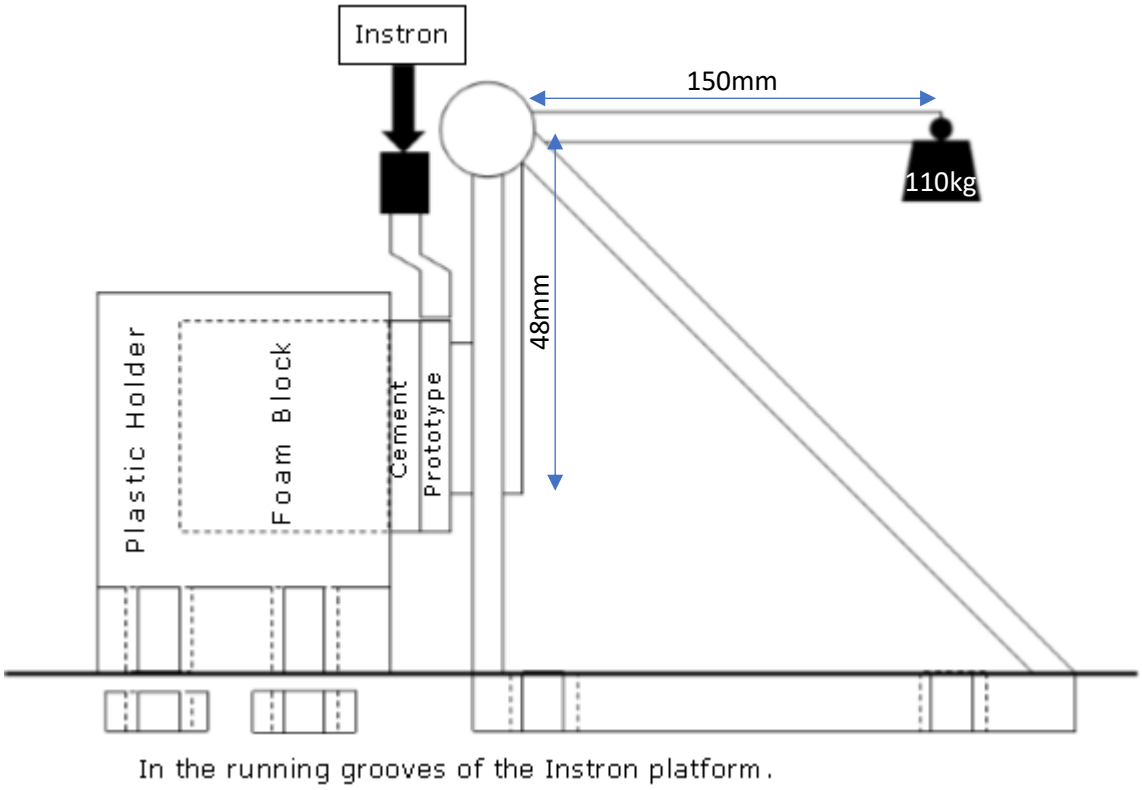

Figure 7.2-3: Diagram of the Instron Prototype Setup.

The 3D printed prototypes were cemented one at a time, following the cement mixing procedure on page 129 (*Mixing Contents as Packaged*), onto the corresponding foam blocks and were left for at least 24 hours. The samples were inserted into the above configuration so they had a force of 33.79N onto the foam block – this was the maximum force able to be applied to the samples using this rig. The Instron was programmed to 'push' down at a loading rate of 300N/min as shown in figure 7.2-2 until 1.5mm displacement – 'initial failure', then till 5mm displacement – 'failure'.

The CSV files from the Instron were read into a MatLab script that extracted the maximum load values and the corresponding displacement value at that maximum. From the graphs, the stiffness was calculated from taking 4 points from the middle of the initial linear curve, dividing each the load against the displacement and taking the mean average of the 4. Because the models were a complex combination of tension, compression, and shear the stresses and strains are not replied. The load, displacement, and stiffness can be compared as the systems were similar to each other in terms of cemented area and loading conditions. The sample size was for each design and displacement was 2 (except for the T6.2 with displacement of 5mm only had one sample) so that the statistical analyses used were mean average, standard deviation, standard deviation error, and coefficient of variance.

7.2.3.2 FEA representing Prototype Experiment

This analysis used the prototypes models that were created using the method on page 132. The foam blocks were modelled as 60x60x25mm box in SolidWorks. The features of the prototype were 'cut' onto the top surface by the subtract overlap feature in SolidWorks mentioned in page 136. The peg and flange features (not including the MAKO's fin) had the diameter increased by 1mm to allow space for the cement. The MAKO's fin did not have the feature increased so it created a perfect fit between the foam and prototype because the designed is meant to be hammered into the exposed cancellous without pre-drilling as a result there would be hardly any cement between the fin and the prosthesis. The cement body was created by positioning the prototype 1mm vertically above the complementary foam, see figure 7.2-4, the parts were aligned as they would in the assembly (1mm apart) and a solid body of same outline as the prototype filled the space.

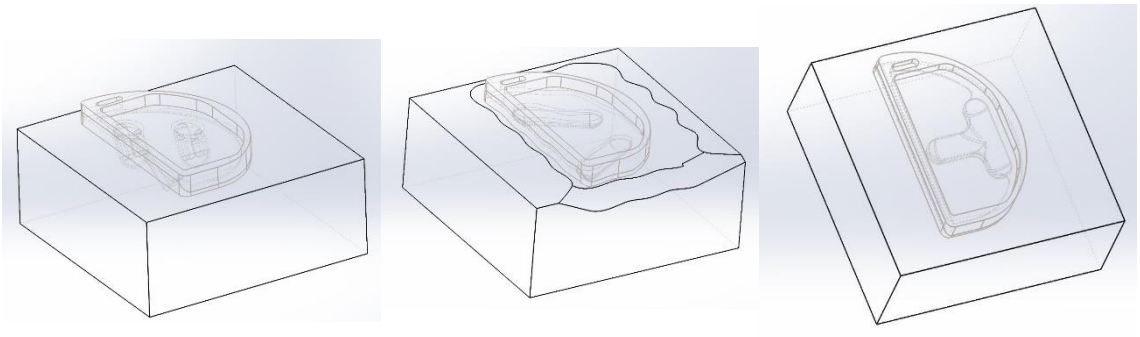

Figure 7.2-4: The Positioning of the Prototype and Foam
Left is the original prototype, middle is BQ prototype, and right is the T6.2 prototype.

7.2.3.2.1 Material Properties

The foam during prototype experiment was tested in the Instron under compression conditions to obtain the compressive properties (compressive elastic modulus, yield and buckling), these were used in the modelling, see table 8.2-3. The standardised properties of titanium (ASTM F136) were input properties for the prototype, this material is very similar to the prosthesis material currently on the market. The PMMA material properties were already stored in SolidWorks' materials library. All the materials were assumed to be linear elastic isotropic, the same in every direction.

Table 7.2-3: Material Properties of the Models

Part	Prototype	Cement	Foam Block
Material	Titanium	PMMA	Foam
Elastic Modulus (GPa)	105	2.77	0.0420
Tensile Strength (MPa)	825	61	42.9 (guessed)
Compressive Strength (MPa)	900	105	42.9
Poisson's Ratio	0.3	0.3	0.3

7.2.3.2.2 Meshing Parameters

SolidWorks has a global meshing function which was used to create Jacobian 4-point elements, size seen in table 7.2-4. On the interface surfaces (i.e. the 'cut' foam surface, all cement surfaces, and the underneath surfaces of the prototype) had a controlled meshing conditions by using the built in function of SolidWorks, also seen in table 7.2-4.

Table 7.2-4: Meshing Parameters			
Global Meshing		**Mesh Control**	
Maximum element size	4.3110843	*Element size*	1
Minimum element size	0.10	*Ratio*	1.5
Minimum number elements in a circle	3		
Element size growth ratio	2.1		

7.2.3.2.3 Boundary and Simulation Conditions

The walls and base of the foam block had a fixed geometry boundary condition, i.e. it was not able to displace. This represented the rig the foam block was placed into during the experiments.

A load of 33.79N is applied on the recessed surface of the prototype, this matches the same force applied in the experimental method. The apical tip edge of the prototype had a prescribed displacement to create a shearing action across the interfaces, similar to the shearing motion in the prototype experimental work. The prescribed shear used in the simulations were 0.1mm, 1.5mm, and 5mm; the latter two match the experimental displacement applied but this is created large displacement in the finite element analysis as a result and the former was included to have a model that didn't trigger a large displacement. Figure 7.2-5 displays the applied boundary conditions.

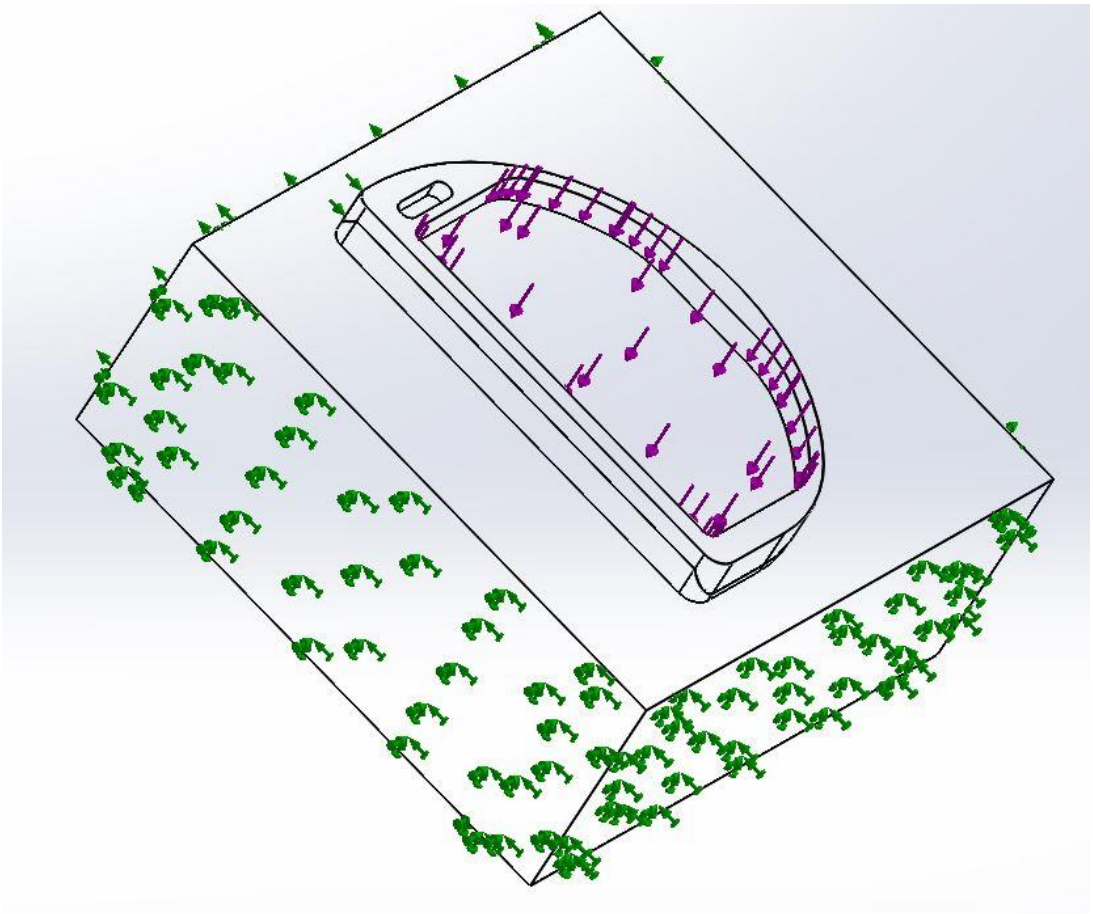

Figure 7.2-5: Boundary Conditions applied to the Box FEA models

7.2.3.2.4 Plots Generated

Von Mises, von Mises iso-clippings, triaxial, shear, and strain plots were generated to extract information. The von Mises plots the overall stress the element experiences, it is used to determine where the material might start to yield due to the combination of stresses; the colours on the plot represent the different levels of stress. The scale for the von Mises was set to include the yield value of the foam (42MPa); the red represents von Mises stresses of 42MPa and above therefore any red areas indicated areas that may yield. The iso-clipping uses the same scale as the von Mises but only plotted a selected range; this allows insight

into the model under the surfaces. Two types of iso-clippings were obtained, the first used the 1.5mm shear displacement condition only showing the elements in the red and orange range of the scale (set to be 30MPa and above). The second iso-clippings took an objective range for each model (under 0.1mm shear displacement condition) that showed the stress distribution from the stress concentrations. The triaxial plot represents all the axial forces summed together, unlike the von Mises, the values don't include the shear stresses and they have a pole, i.e. the value is expressed with ±sign to indicate if the stresses are in tension or compression. The triaxial plot was of the 0.1mm shear displacement and had the upper colour, red, set to 42MPa (and greater) and the lower colour, blue, set to -42MPa (and lesser). Two iso-clippings of the triaxial plots were taken, one for the top end of the tensile stresses and one for the lower end of the compressive stresses. Peak values were expressed on the foam block by an in-built SolidWorks option, these displaced maximum von Mises stresses were entered into a table, table 11.2-1. From the table, it was noted that the values for each prototype were linear, and the location of the peaks are were the same. It can be assumed that all the simulations are going to express values to scale; the screenshots then were of the 0.1mm simulation.

7.2.3.3 FEA modelling of Prototype

The knee used was the same one modelled in *7.1.12.2 Right Tibial Knee*; and the prototype models are the same as the ones modelled in the above sub-section *7.1.12.1 Prototype Prosthesis*. For each model, the knee was altered 4 times: the medial condyle side of the knee was altered for the prototypes with cemented and

without cement, and the lateral side of the knee was altered for the prototypes with cement and without cement). The prototype in the medial and lateral were both the same, just rotated 90°; when expressing the anterior and posterior aspects it is of the knee and not of the implant (unless stated otherwise). The cementless models had the prototypes imported into the part file and positioned on the tibia all at the same distance (approximately 7mm on the lateral side and 6mm on the medial side) away from the condyle surface; at this position, the cut covered the majority of the tray, with as little overhang of the prototype. The combine function in SolidWorks 'cut' away the prototype from the tibia this left a solid model fitting the prototype perfectly without interference occurring (i.e. a solid within a solid), see figures 7.2-6 to 7.2-9. For the models with cement, the prototypes were again imported and 'cut' away from the tibia but this time positioned 2mm higher than the cementless models. The pegs and flanges on the tibia were increased by 1mm in diameter to allow coverage of cement. The cement was modelled for each part by the same method as described in the previous section *7.1.12.2 Right Tibial Knee* – that is by creating a solid between the tibia and prosthesis then using the combine feature to remove everything apart from the cement layer.

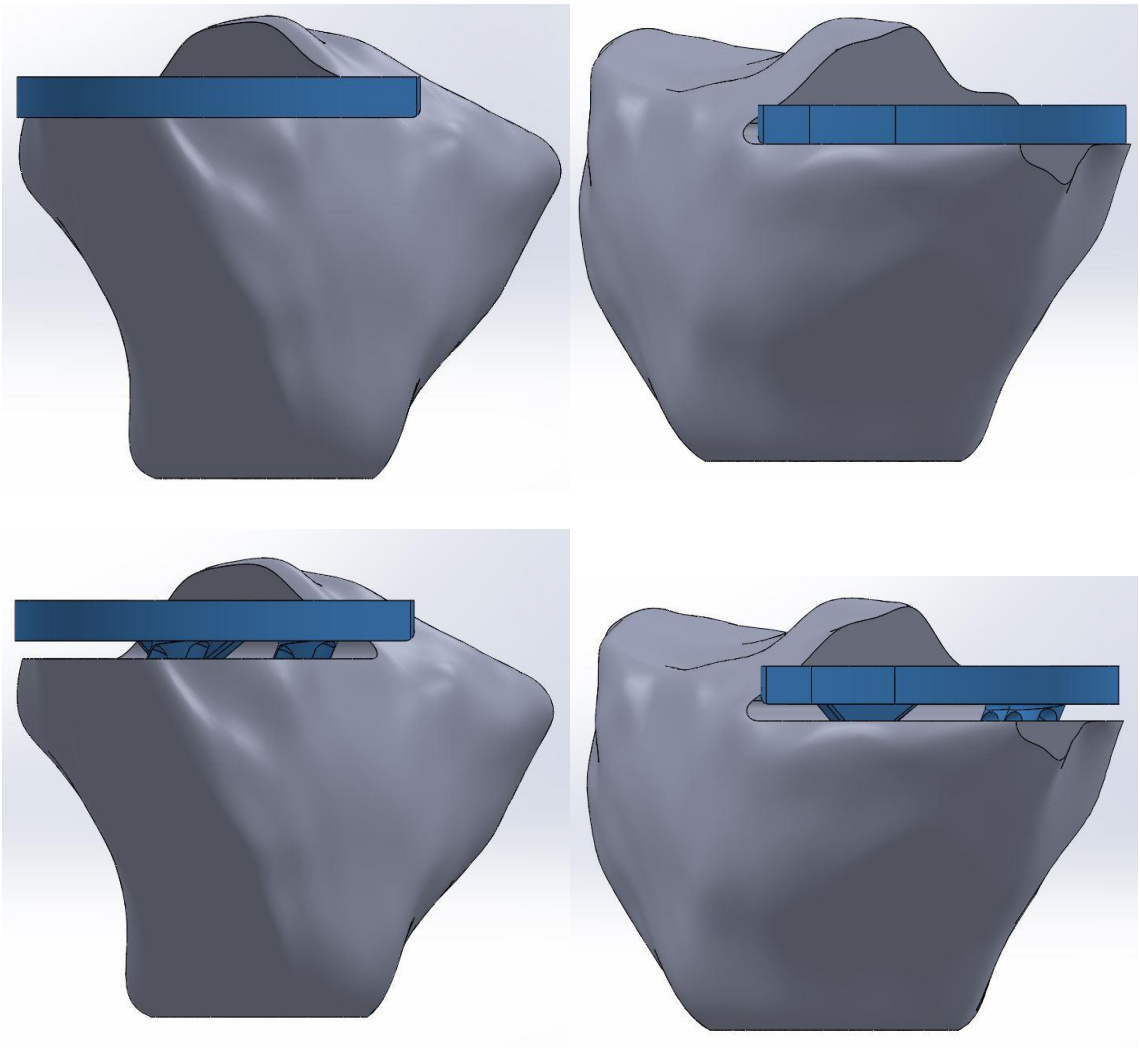

Figure 7.2-6: Positioning of the Original Prototype on the Tibia
Top left is on the lateral side without cement; bottom left prototype on the lateral side with space for cement; top right is the prototype on the medal side without cement and bottom right is the prototype on the medial side with space for cement.

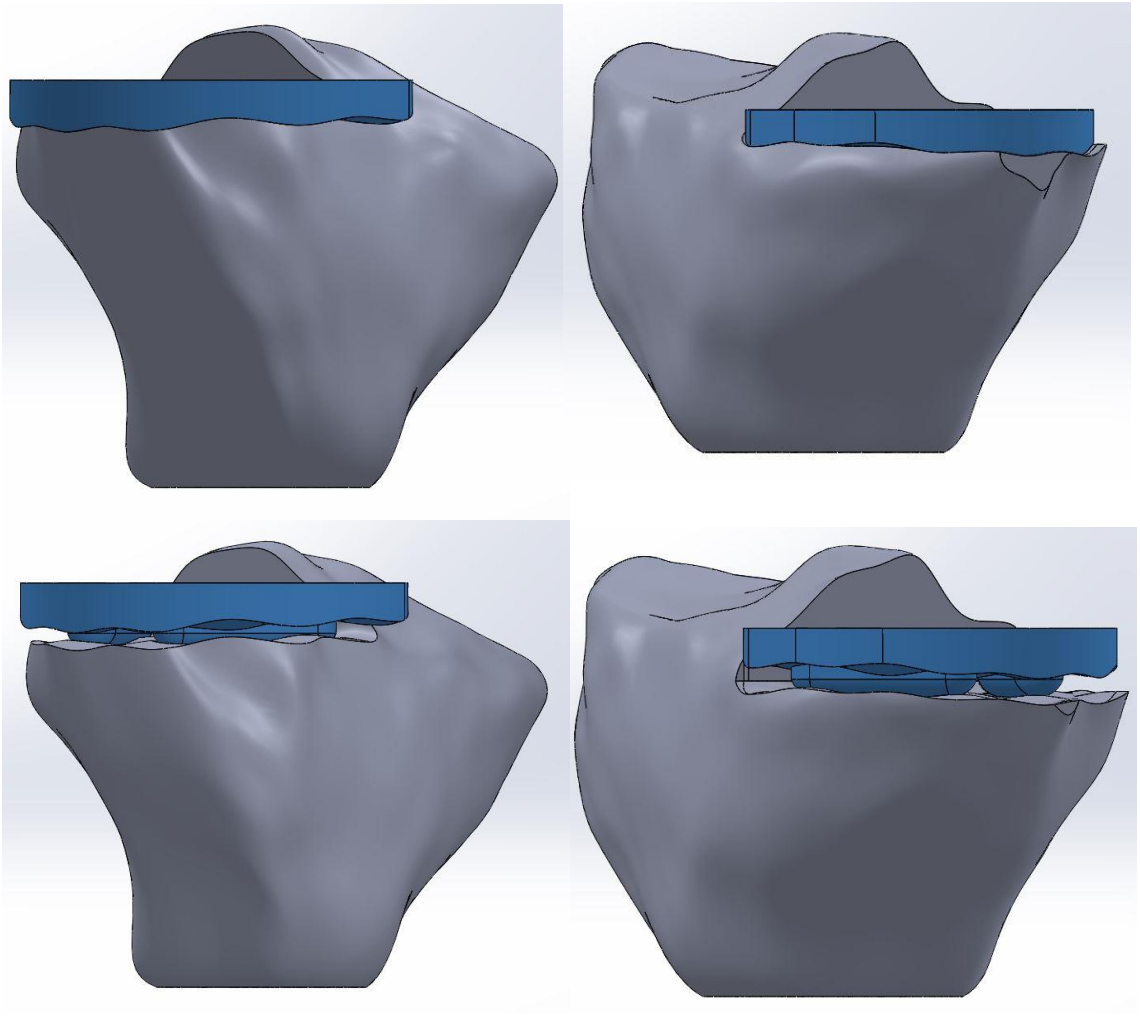

Figure 7.2-7: Positioning of the BQ Prototype on the Tibia
Top left is on the lateral side without cement; bottom left prototype on the lateral side with space for cement; top right is the prototype on the medal side without cement and bottom right is the prototype on the medial side with space for cement.

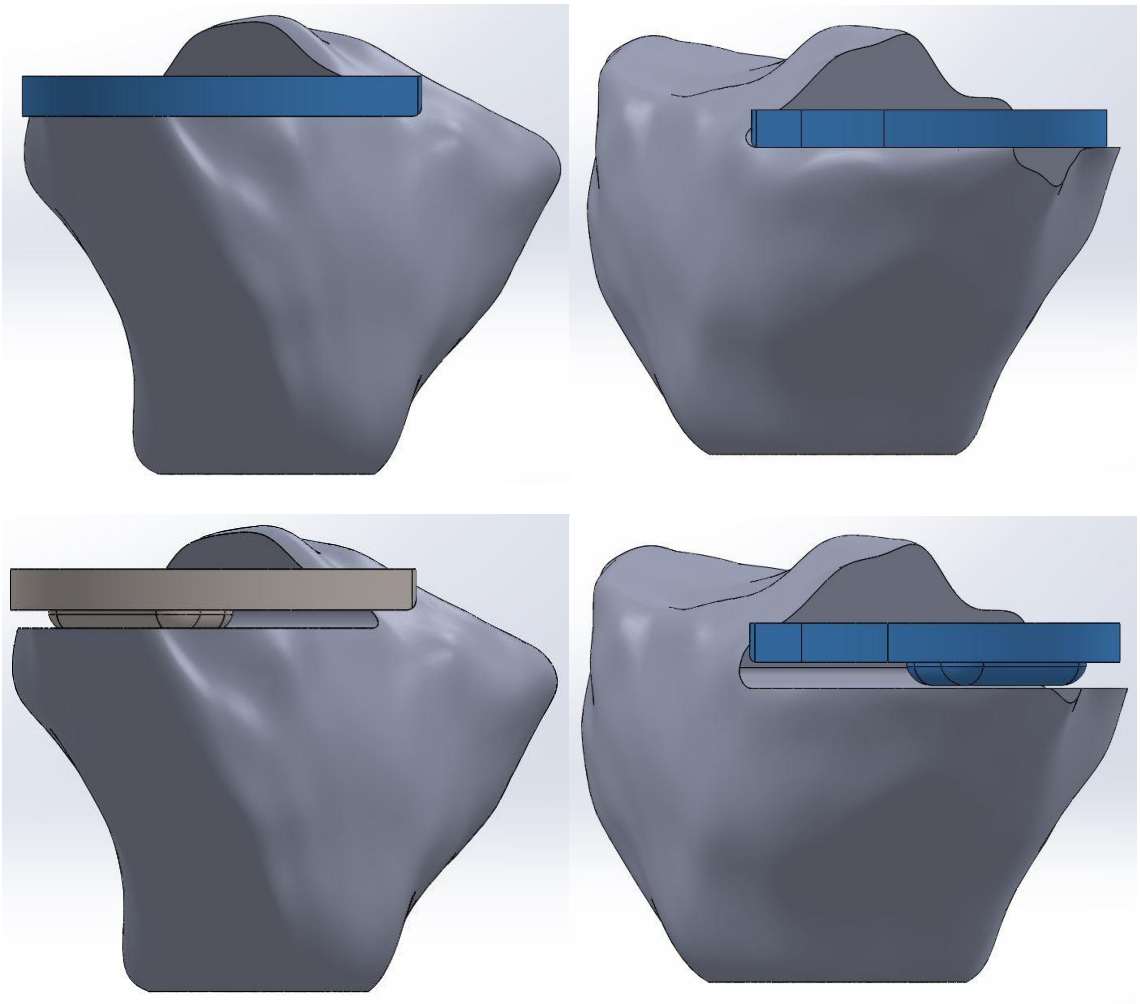

Figure 7.2-8: Positioning of the T6.2 Prototype on the Tibia
Top left is on the lateral side without cement; bottom left prototype on the lateral side with space for cement; top right is the prototype on the medal side without cement and bottom right is the prototype on the medial side with space for cement.

7.2.3.3.1 Material Properties

The standardised properties of titanium (ASTM F136) were used for the prototype. The PMMA material properties were already stored in SolidWorks' materials library. The bone model was of cancellous bone; the Young's and mechanical strength was calculated by Cowin's[241] equations with the information of a woman with osteoporosis bone density. All the materials were assumed to be

elastic isotropic, i.e. the properties same in every direction, see table 7.2-5 for the material property values.

Table 7.2-5: Material Properties used for the Prototype Models

Part	Prototype	Cement	Knee
Material	Titanium	PMMA	Cancellous
Elastic Modulus (GPa)	105	2.77	0.1035
Tensile Strength (MPa)	825	61	3.42
Compressive Strength (MPa)	900	105	3.42
Poisson's Ratio	0.3	0.3	0.3

7.2.3.3.2 Meshing Parameter

The meshing parameters are the same as the above FEA analysis, see table 7.2-6. The surfaces the meshing control were the surfaces of the cement, the 'cut' surfaces of the tibia, and the underneath surfaces of the implant – this and the global mesh can be seen in figure 7.2-6.

Table 7.2-6: Meshing Parameters

Global Meshing		**Mesh Control**	
Mesh type	Curvature based	*Element size*	1
Elements	Jacobian 4 points	*Ratio*	1.5
Maximum element size	4.3110843		
Minimum element size	0.10		
Minimum number elements in a circle	3		
Element size growth ratio	2.1		

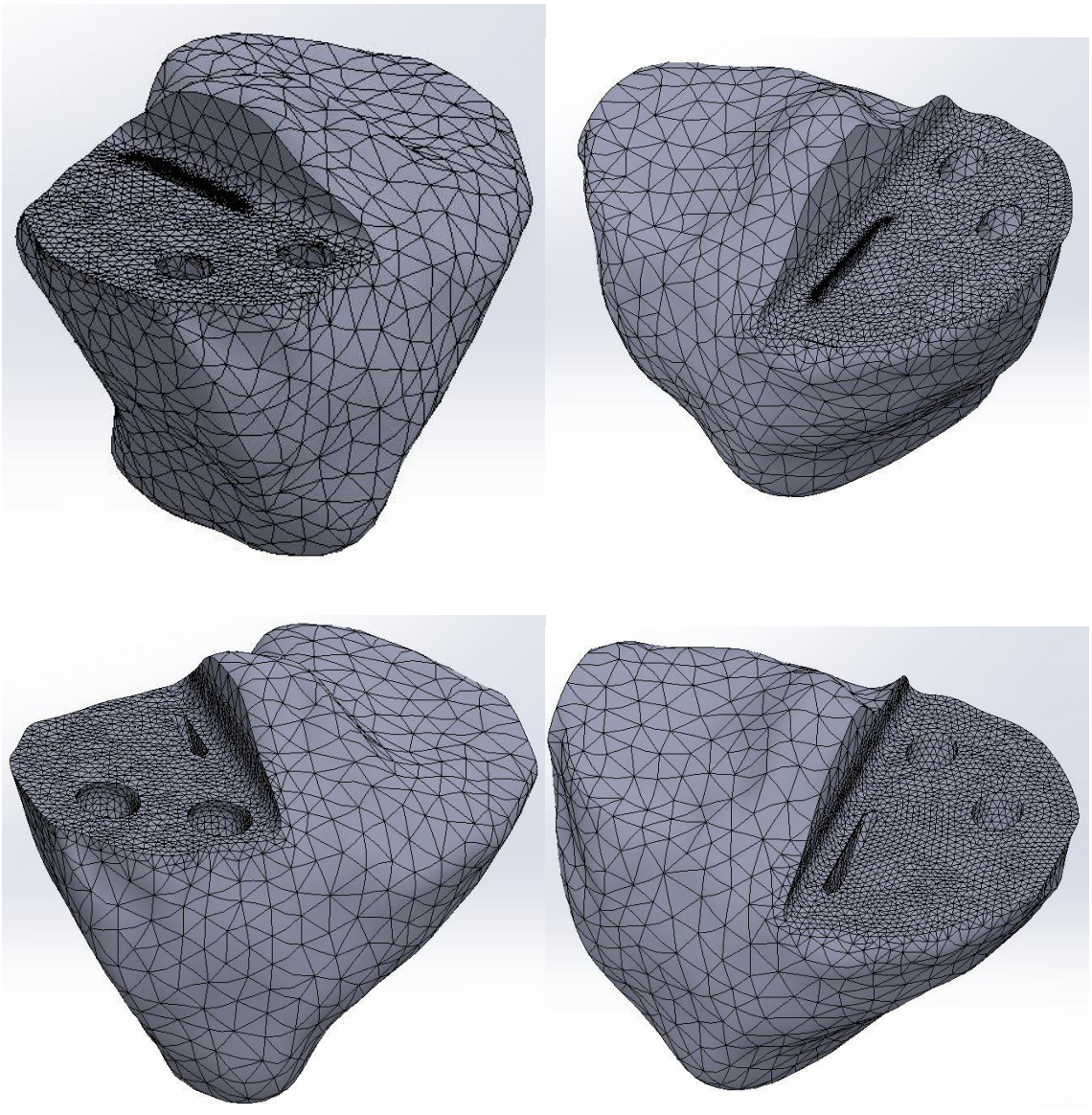

Figure 7.2-9: Meshing of the Original Prototypes with cement
Top left is on the lateral side without cement; bottom left prototype on the lateral side with space for cement; top right is the prototype on the medal side without cement and bottom right is the prototype on the medial side with space for cement.

7.2.3.3.3 Boundary Conditions

The base of the tibia had a fixed geometry boundary condition, i.e. it was not able to displace. There were two conditions applied to all of the models: condition A had an axial load, of 750N applied to the recessed surface of the

prototype; condition B had an axial load and shear displacement of 0.1mm, the axial load was 33.79N applied on the recessed surface of the prototype. Condition B matches the same force applied in the experimental method. In total, there was 8 simulations for each prototypes, see table 7.2-7 and figures 7.2-10 and 7.2-11.

Table 7.2-7: Table explaining the 8 Simulations

Condition	**Location**	**Description of the condition**	**Cemented**	**Code**
Condition A: An axial load of 750N	Lateral (AL) figure 7.2-10	This is model is on the lateral side of the knee with and without cement. The prosthesis has an axial load.	Cement	ALC
			Cementless	ALN
	Medial (AM) figure 7.2-10	This is model is on the medial side of the knee with and without cement. The prosthesis has an axial load.	Cement	AMC
			Cementless	AMN
Condition B: An axial load of 33.79N and 0.1mm shear	Lateral BL figure 7.2-11	This is model is on the medial side of the knee with and without cement. The prosthesis has an axial load and a shear displacement of 0.1mm.	Cement	BLC
			Cementless	BLN
	Medial BM figure 7.2-11	This is model is on the lateral side of the knee with and without cement. The prosthesis has an axial load and a shear displacement of 0.1mm.	Cement	BMC
			Cementless	BMN

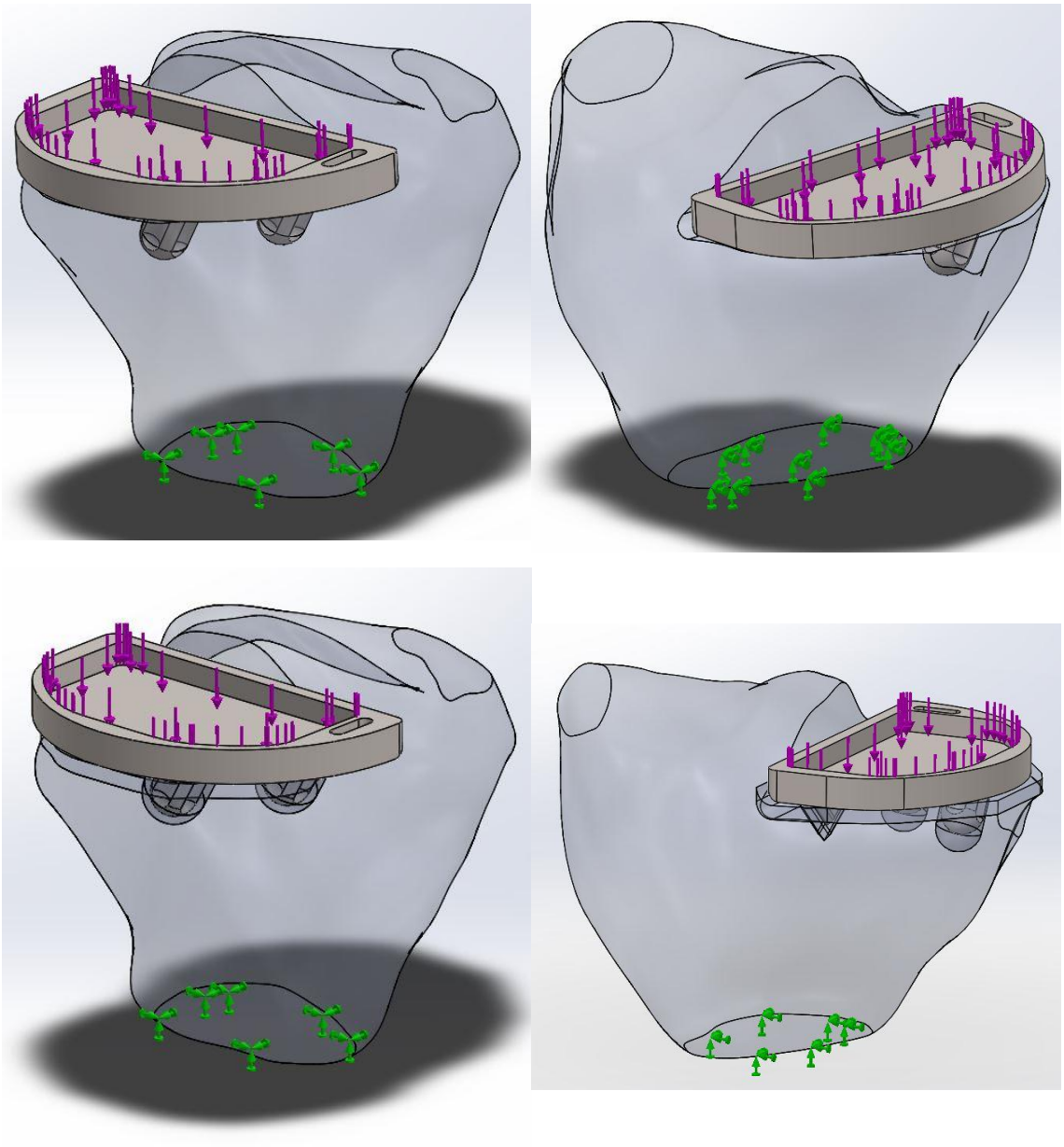

Figure 7.2-10: The Original Prototype Displaying the Boundary Condition for A Conditions*. The four images show the condition A on the lateral and medial side of the tibia: upper left is the lateral non-cement (ALN), upper right is the medial non-cement (AMN), lower left is the lateral cement (ALC), lower right is the medial cement (AMC). The green arrows indicated that the base surface has fixed displacement and the purple arrows indicate the surface with the applied 750N load.*

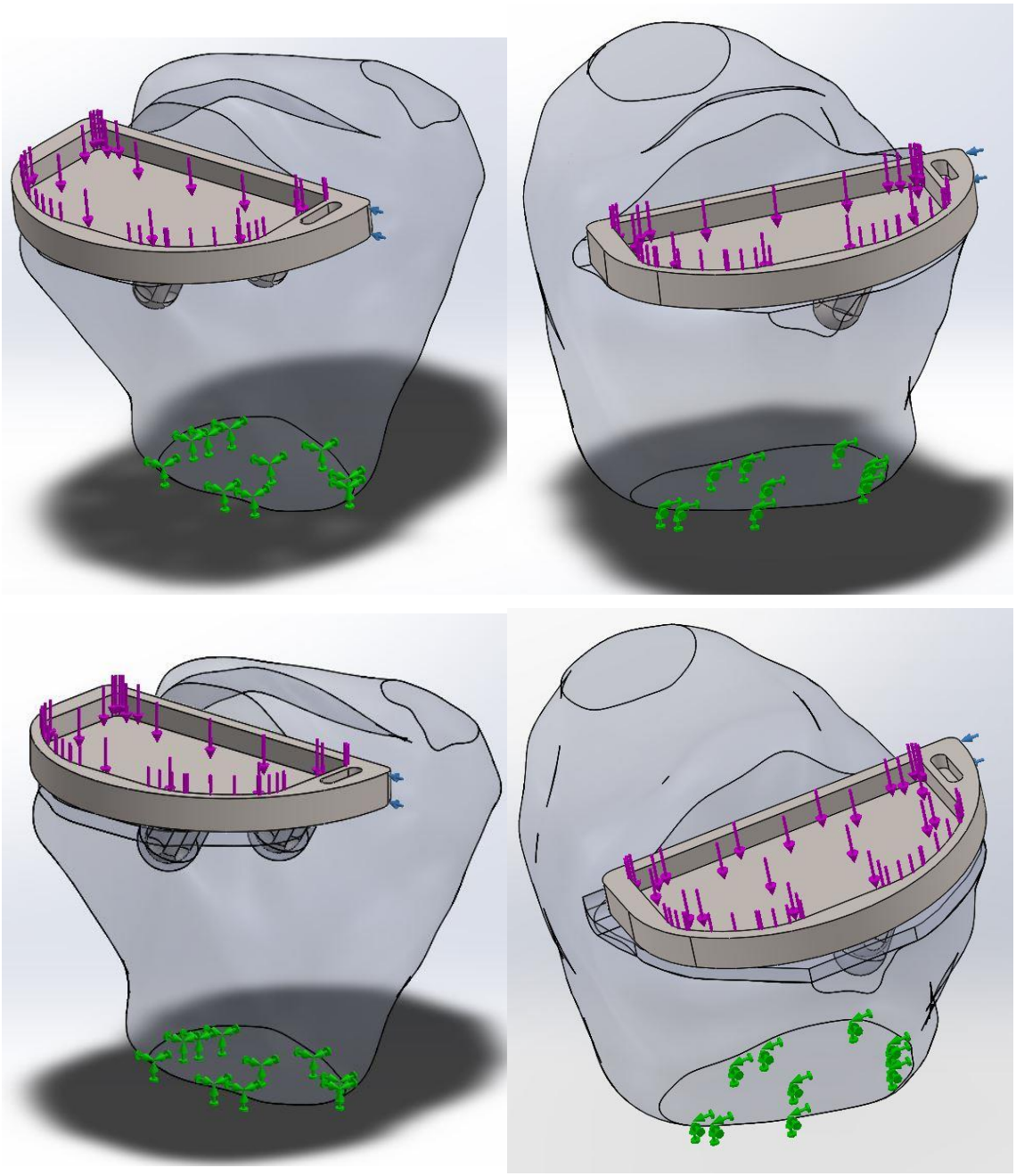

Figure 7.2-11: The Original Prototype Displaying the Boundary Condition for B Conditions. *The four images show the condition B on the lateral and medial side of the tibia: upper left is the lateral non-cement (BLN), upper right is the medial non-cement (BMN), lower left is the lateral cement (BLC), lower right is the medial cement (BMC). The green arrows indicated that the base surface has fixed displacement, the purple arrows indicate the surface with the applied 33.69N load, and the blue arrows indicate the edge with the prescribed 0.1mm displacement.*

7.2.3.3.4 Plots Generated

There were three types of plots used to extract the information from the FEA results; these were von Mises, strain equivalent, and triaxial. The von Mises proved the overall stress the elements were experiencing, the colour scale was set in the range between 0 and 3.4MPa except in condition B iso clipping; the stresses were lower in this condition and thus to help the interactive iso tool the scale was altered to be from 0 to 0.5MPa. The standard von Mises plot provided the information where the material might begin to yield and any surface location of stress concentration; the colour scale was set in the range between 0 and 3.4MPa (dark blue for zero and red for 3.4MPa and higher). The maximum von Mises stress experienced by the tibial elements was obtained from SolidWorks and noted in table 11.3-1; likewise for the maximum strain equivalent value noted in table 11.3-2.

The interactive iso-clipping demonstrated the distribution of the stresses together to show any under the surface stress concentration and stress shielding; the two images for each model taken had one of just the red to yellow scale display and the other image of von Mises stresses less than 0.1MPa (i.e. dark blue). Triaxial plots represent the sum of axial forces present in the element, thus it can suggest if the elements are in tension or compression. The scale for the triaxial forces was set to be from -1MPa (dark blue) to 1MPa (red). The interactive iso clipping displayed the potential location of the polar axial forces in the tibia.

.

Chapter 8

Experimentation of Fixation Techniques

The exploration and the initial concept generation process (stages 1 and 3), postulated a number of experimental questions and hypotheses to investigate. As part of stage 4 of the design process, this chapter will cover questions relating to fixation as this is a promenade point relating to improving the integration of the prosthesis with the robotic orthopaedic tools. The results of this chapter and the following chapter (9 *Virtual Experiments of Concept Ideas*) were fed into the evaluation process in chapter *10 Concept Selection*.

The follow three Laboratory experiments were identified as possible investigations that could complement the concept selection process in relation to issues surround fixation.

These were:

- How small pre-drilled holes affect the pull-out strength;
- How the surface texture affects the cement adhesion strength; and
- Can partial cementing be used instead of a fully cemented prosthesis.

The results from the above experimental work were then fed into the design matrices which was advantageous as the concept selection stage not only requires analytical reasoning, it can require investigations to support the reasoning behind the concepts. In addition, the results were able to provide some insight into the use of robotic orthopaedic tools and to open up new potential directions of prostheses using robotic orthopaedic tools technology. This chapter will cover each of the above questions in turn.

8.1 Peg Extraction from a Pre-drilled Hole

8.1.1 Introduction

Press-fit pegs designs are one method designed to improve initial stability of a cementless and cemented prostheses. The theory is if a peg is forced into a hole smaller than it size then the wall of the hole holds the peg in place and thus holds the prosthesis in position. The standard testing measurement for extracting peg and screw designs is called the pull-out strength; this is the force required to extract the peg or screw.

This experiment investigates press-fit assumptions of improving initial stability of cementless knee replacement implants. The pull-out strength (the force needed to pull out a design) of different size pegs in different size pre-drilled holes in cancellous bone of the bovine tibia plateau has been assessed experimentally.

It is assumed that peg and bone's interface are experiencing static friction conditions but as the load increases there comes a point where the applied load

overcomes the static conditions. At this point the peg moves across the bone's surface the force required to retain the movement is lower than the initial force needed to put them in motion. Therefore, the maximum load will be the force required to instigate movement of the peg and this will be described as the pull-out strength

8.1.2 Aims

To characterise the dependency of peg extraction force (pull-out strength) required on the size of peg and hole.

8.1.3 Results

Table 6.1-2 displays all the results and figure 8.1-1 depicts the variation in mean extraction force with group ID. Two samples were not included because during set-up, the samples became misaligned and thus were not able to be included in the results.

Table 8.1-1: Displays Samples Results and Mean values

Group ID	Test 1	Test 2	Test 3	Test 4	Test 5	Test 6	Mean	SD
h3p4	420.7	596.1	316.2	197.5	85.8	431.7	637.2	182.2
h35p4	376.0	636.0	74.7	376.6	44.1	-	301.5	245.4
h4p4	163.9	62.8	192.6	172.7	94.5	-	137.3	55.7
h4p5	1,395.8	1,112.8	225.5	380.9	194.5	870.0	696.6	503.2
h45p5	378.3	80.0	142.9	673.4	901.9	894.8	511.9	364.8
h5p5	61.0	305.5	505.9	497.5	839.9	189.4	399.9	276.6
h5p6	211.4	250.9	843.6	2,880.3	2,047.7	672.1	1,151.0	1,078.1
h55p6	132.9	158.1	1,251.2	2,284.7	256.7	1,518.0	933.6	890.9
h6p6	469.4	104.9	318.6	438.0	405.4	60.3	299.4	175.9

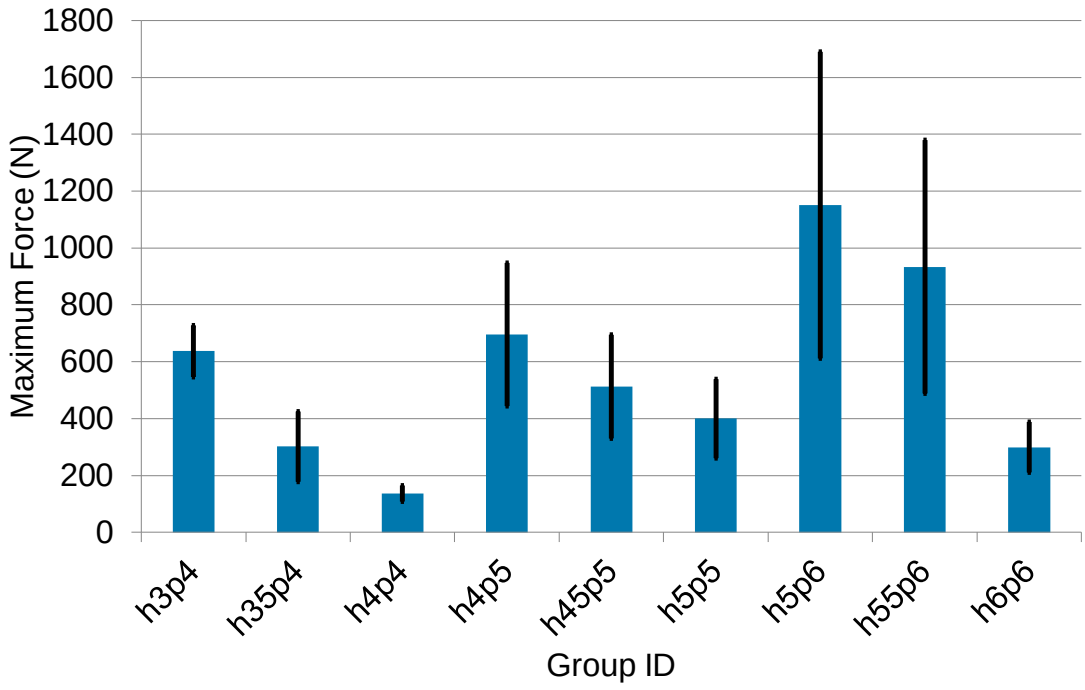

Figure 8.1-1: Graph of the Groups Mean Extraction Force
The groups name indicates the size of hole and peg, please see table 6.1-1. The graph includes a standard deviation, represented by the black line.

The two-way ANOVA suggests that the peg size ($P<0.02$) and peg-hole discrepancy ($P<0.045$) both have a significant effect on the extraction force strength, with the peg size having potentially a greater effect. The interaction between the two variables on extraction force was insignificant. As peg size increases, the required extraction force also increased. Similarly, as the peg-hole size discrepancy increases, the extraction force required increases too. Therefore, the maximum extraction force required (1,151N) was exhibited by the 6mm peg in a 5mm hole. However, for all combinations of peg and hole size, significant variance existed with a coefficient of variance (standard deviation divided by the mean) approaching 1 in some cases.

8.1.4 Discussion

The results from the tests showed the following trends: the pegs inserted into holes of the same size had the lowest extraction force compared to the pegs inserted into a smaller hole. The largest extraction force came from the 6mm peg in the 5mm hole; similarly the lowest extraction force was from the 4mm peg in the 4mm hole. It is hypothesised that as peg size increases, a larger volume of bone is compressed, due to the larger surface area, and thus a greater friction force is experienced, created by the compressive stress in the bone. Since friction is proportional to a coefficient of friction and the normal force acting perpendicular to a surface only, it is independent of surface area. Therefore, any increase in extraction force is only attributable to an increased normal force on the peg.

The experiment represents of a surgical prosthesis with pegs being positioned into a pre-drilled hole that is smaller than the peg's diameter. However, the experiment doesn't model full in vivo conditions, the main factor would be the lack of bodily fluids that constantly keeping the bone tissue hydrated and nourished. The nourished part of the bodily fluids helps with healing and re-growth and thus can be ignored for the results in this experiment because this experiment was investigating the initial pull-out strength of the pegs prior to bone re-modelling. It also has been reported in the literature that the mechanical properties holding the pegs will loosen over time[93], thus method is only for initial fixation to allow the osseointegration to provide full fixation.

This experiment took the assumption that the bone's material behaviour is not affected by its moisture content. Bone is a known viscoelastic material, as in it behaves in a combination of a fluid and a solid, thus its mechanical properties can be affected by moisture content[106]. It is likely that some stress relaxation would have occurred, which may add to the observed variance.

Bone is unique material because when it is in vivo it adapts the local microstructure due to the loading that area experiences, this means the microstructure is not uniform throughout bone, notably so in cancellous bone. The testing area used was any available the cancellous bone on the tibia plateau, from the medial to lateral condyle of the tibia both of these condyles experiences a different loading pattern this means they will have a different microstructure[242], [243] and thus density has an effect on the pull-out strength[244]. The experiment

randomly placed the different size holes and pegs throughout the plateau to overcome the uniform material properties of the bone; this can explain the large range of pull-out strength in each group. Another method not used in this experiment is to only use one of the condyles for the testing area, as this will provide similar material properties and will avoid the wide range of results.

While preparing the samples it was observed that the cut of the bone was not the straightest and artefact free as desired. It was deemed that this was not a major concern: the distal cut was just to make the samples smaller so to be able to use the equipment; the proximal cut was to expose the cancellous bone without the harder bone (cortical) affecting the results and to provide a base for a uniform depth. Not all cuts were parallel to each other, this was corrected by adjusting the bone in the vice so the cut surface was parallel and the peg was perpendicular. This made the peg to be pulled out in a fairly straight pull-out but alignment error still existed. In a couple of the tests there was migration of the sample bone in the vice where the clamping force wasn't enough to keep the bone from moving when force was applied. The data from these samples were removed from the analysis. This could be avoided by having an improved holding rig designed to hold the bone and keep it from moving while in tension, this would be advised for future work.

The majority of other work done on initial pull-out strength is on screws designs – how the different types of thread affects the pull-out strength[244]–[247]. Other works have included how the bone's microstructures and density affect the pull-out strength[244]; and there is some work that has been done on how different

size pegs(/screws) in pre-drilled holes affect the pull-out strength. A study done on different peg designs affect the pull-out strength in avian cortical bone[247] showed that pegs have a lower pull-out strength than same size pegs with a thread (positive and negative) design, intuition will naturally think that so the results from that study provided no surprise but does clarify why not many studies have gone into pure peg pull-out strength. The advantage of this study on size of pegs (without threads) is its simplicity; screws (or pegs with thread designs) as the diameter increases it increases the surface area, more so than just a plain peg (cylindrical surface area plus the thread surface area) and it can increase the number of thread ridges. Therefore, a different peg size in pre-drilled holes study will purely look at the importance of diameters on the pull-out strength.

8.2 Partial Cementing Experiment

8.2.1 Introduction

Most implants are cemented to prepared bone tissue and it provides attachment of the prosthesis to bone almost imminently. This is unlike osseointegrating implants – these prostheses become fully attached by the process of bone tissue forming in and around the implant, known as osseointegration[123], [248]; this takes time to achieve. Cemented implants prevent this process from happening, it creates a physical barrier that bone tissue can't penetrate. Cemented implants are, in theory, ready to take working load immediately after surgery but after time the cement has the potential to degenerate[165]. Whereas the

osseointegration implants, the strength of the implant attachment will grow as osseointegration develops and full strength will be maintained by the bone regeneration process[165], [248]. A number of ideas from the *Concept Generation* chapter tries to use the best of both worlds approach by including a cemented and non-cemented areas of the prosthesis. The cemented areas will provide the initial attachment of the prosthesis to bone which is ideal[249] for allowing for a strong osseointegration of the bone tissue into the prosthesis via the non-cemented areas thus having initial and potentially life long attachment of implant to the host's bone tissue.

This laboratory experiment was designed to determine the initial strength of partial cementing because the downside of only apply cement to part of the prosthesis is that the cement area is reduced. It is observed in the literature that cement adhesion strength is related to the surface area to the interface – therefore some of the literature warns against inlay prosthesis due to a smaller surface than the onlay. The samples try different approaches to increase the cement adhesion strength with the reduced cemented surface area. It was theorised that if there is adequate fixation and on the osteo-porous part of the prosthesis is in contact with the exposed bone tissue with no cement present, then over time osteointegration will happen.

8.2.2 Aims

The aim of this experiment is to determine if partial cementing can provide a strong initial attachment as a fully cemented design. Five different partial cementing designs were tested against a fully cemented design. This might be potentially useful in inlay type prostheses.

8.2.3 Results

The first sample of the fully group ran until a displacement 1mm, this was repeated 7 times, as seen by the different colours in figure 8.2-1. In each cycle, represented by the colours in figure 8.2-1, the applied tension increased linearly and the samples respond linearly until a maximum point when the tension drops suddenly- this is possibly a fracture within the interface. The first cycle has a maximum force of approximately 670N, and then the maximums decrease for the next two cycles before the highest peak in the fourth cycle of just under 800N, can be seen in figure 8.2-2. The second batch method was changed to have the displacement run up to 9mm, thus it only produced one peak before failing: 1,640N, as seen in figure 8.2-3, which is greater than the previous batch.

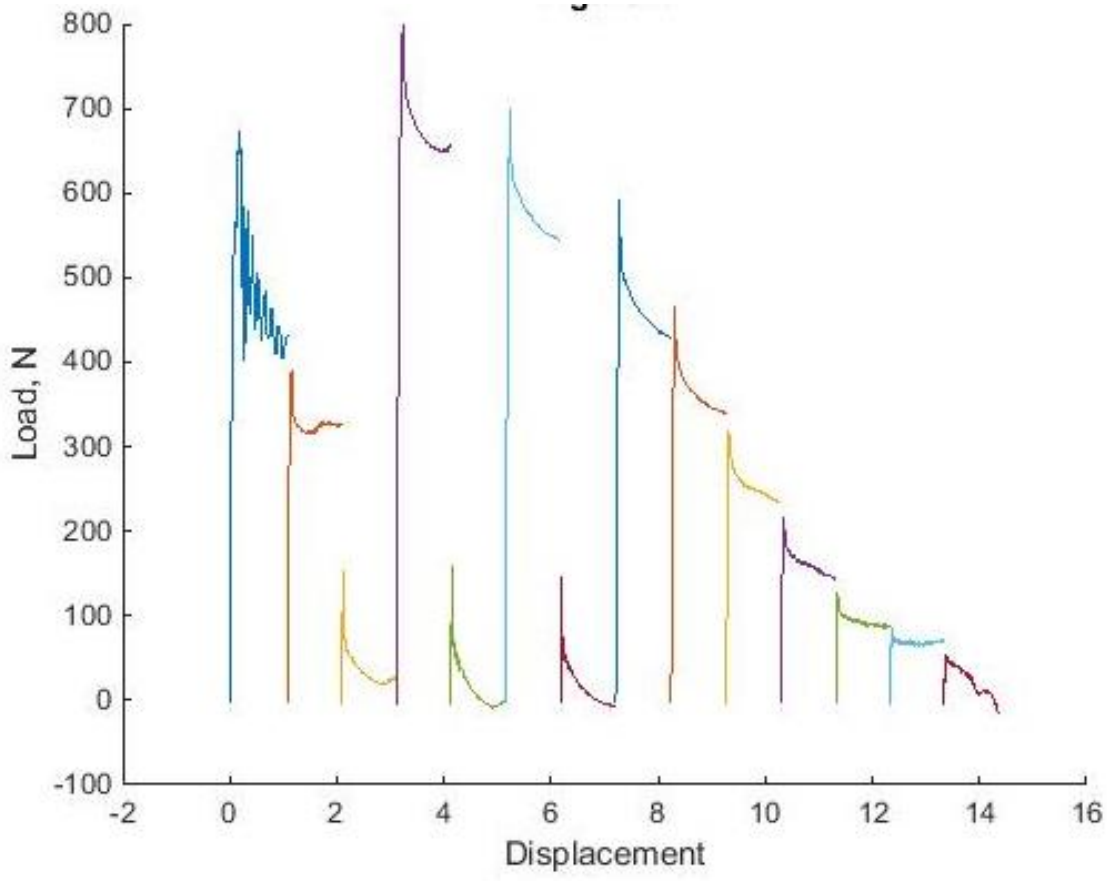

Figure 8.2-1: Load Against Displacement Graph of the First Batch Fully Group
The different colours represent each cycle sample experienced.

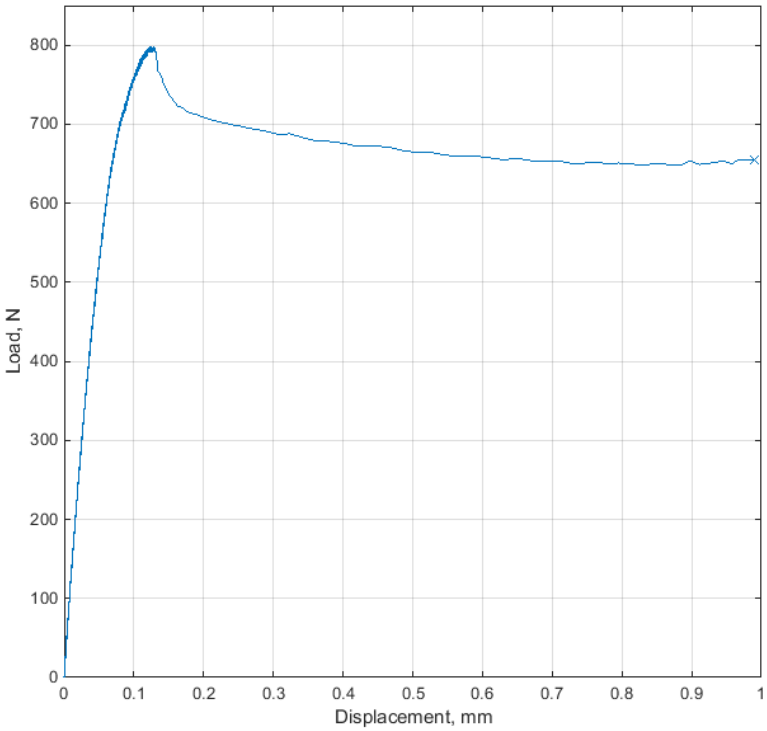

Figure 8.2-2: Load Against Displacement Graph of the fourth cycle of the First Batch Fully Group

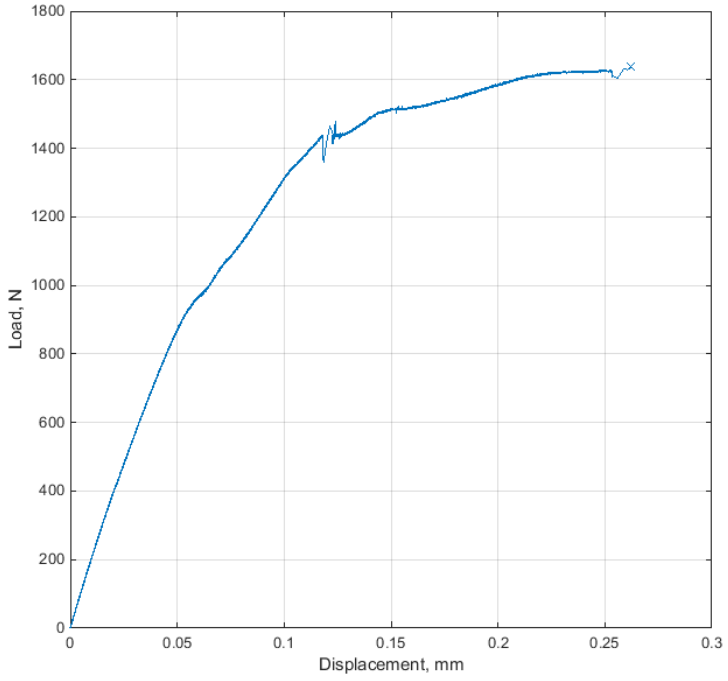

Figure 8.2-3: Load Against Displacement Graph of the Second Batch Fully Group

Both batches of the fully group had the cement stayed inside the hole of the jack all intact and is smooth to the touch. Batch one's sample, had full coverage of cement on the bottom of the jack but the walls had cracks at joining of cement and had a small area with no cement coverage at all, as seen in figure 8.2-4. In batch two, both the bottom and the walls of the jack was fully covered, also seen in figure 8.2-4. The plug was not able to be pushed back into the hole of the jack for both batches

Figure 8.2-4: Photographs of the Fully Group After Testing
On the left is the jack from the first batch and on the right is the jack from the second batch.

The two batches of the rib group had a constant load increase till full failure. Figures 8.2-5 and 8.2-6 are the displacement against load graphs of batch one and two respectively - the peak load of each batch is approximately 1,320N and 2,020N, respectively.

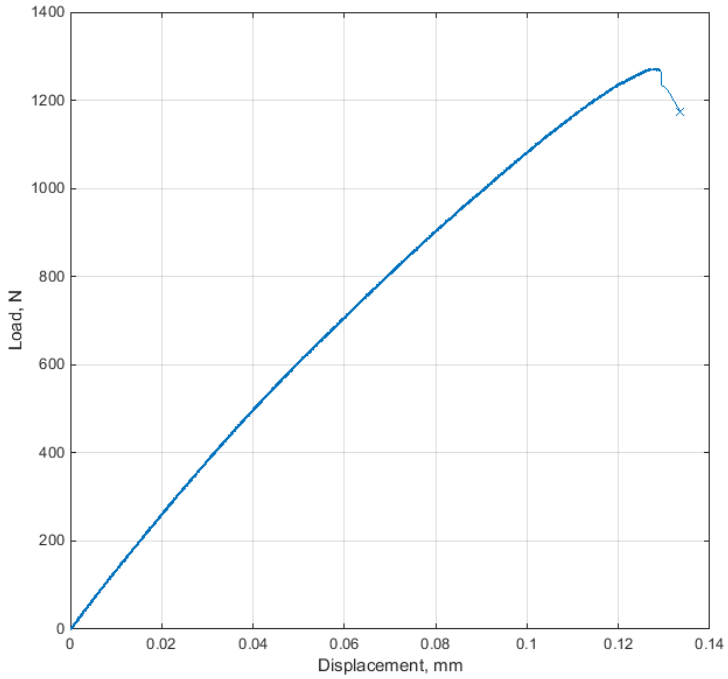

Figure 8.2-5: Load Against Displacement Graph of the First Batch of Rib Group

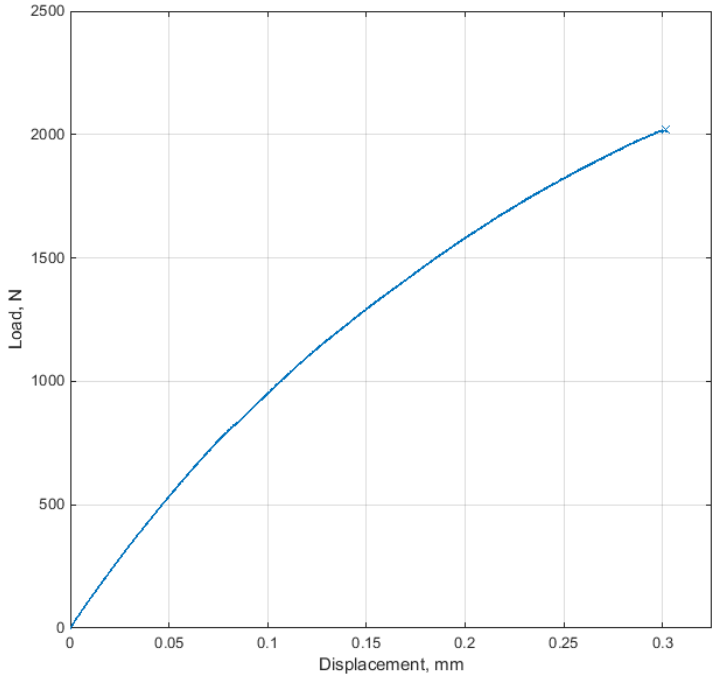

Figure 8.2-6: Load Against Displacement Graph of the Second Batch of Rib Group

The cement in the group rib came out with the plug fully intact and was not smooth, true for both batches. There was no evidence that the cement got to the base of the jack but there was cement around the bottom of the plug below the bottom rib. Photos post-test can be seen in figure 8.2-7. The first batch's plug was easily pushed in and pulled out of the jack's hole and the second's plug was easily pushed back in but difficult to pull out – the load required was recorded again on the Instron at approximately 50N.

Figure 8.2-7: Photographs of the Rib Group After Testing
On the left is the jack and plug from the first batch and on the right is the jack and plug from the second batch.

Both batches of the wall group had a constant load increase until failure. Figures 8.2-8 and 8.2-9 showcase the displacement against load graphs of batch one and two respectively. The peak load of the first batch is approximately 1,700N and the second batch has 4 peaks with point of failure has the maximum load of approximately 700N.

The group wall had the cement fully intact inside the jack after failure and was smooth to the touch for both samples. Neither of the samples had a uniform coverage of cement on the walls as in the photos in figure 8.2-10. Both of them had no indication of cement on the jack's base. The second batch plug was noted to be difficult to push in and pull out of the cement covered jack.

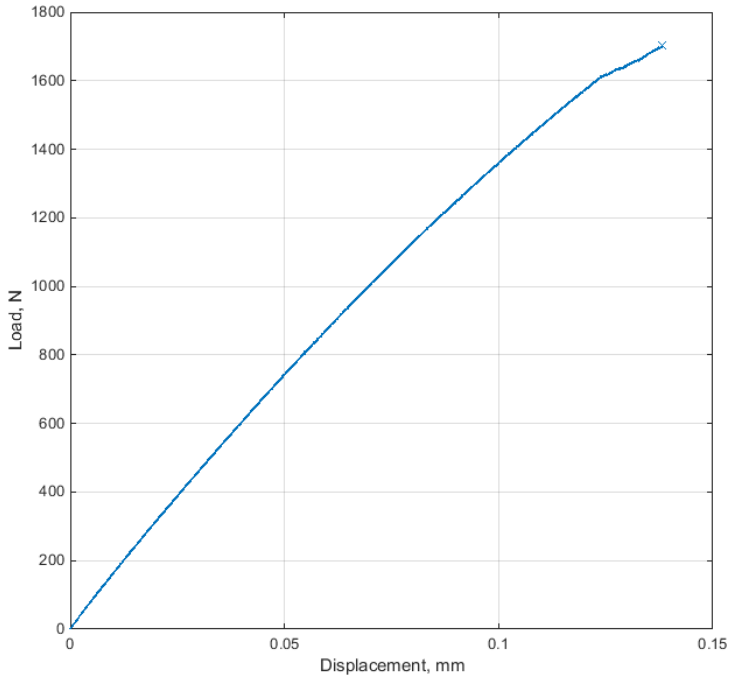

Figure 8.2-8: Load Against Displacement Graph of the First Batch of Wall Group

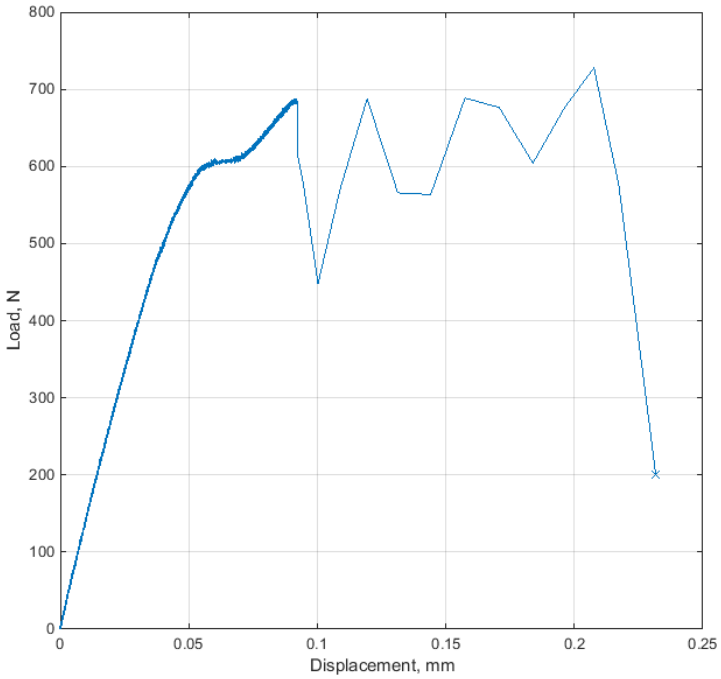

Figure 8.2-9: Load Against Displacement Graph of the Second Batch of Wall Group

Figure 8.2-10: Photographs of the Wall Group After Testing
On the left is the jack from the first batch and on the right is the jack from the second batch.

Figures 8.2-11 and 8.2-12 represent the displacement against load graphs of batch one and two respectively of the channel group. Batch one has the expected displacement against load shape, as the force increases the displacement increases linearly up till the perceived yield of ca. 800N till maximum loading of ca. 1,300N. On the other hand, batch two (figure 8.2-12) has a different behaviour with dip in force just after the perceived yield point just below 400N before rapidly climbing the maximum loading of approximately 500N.

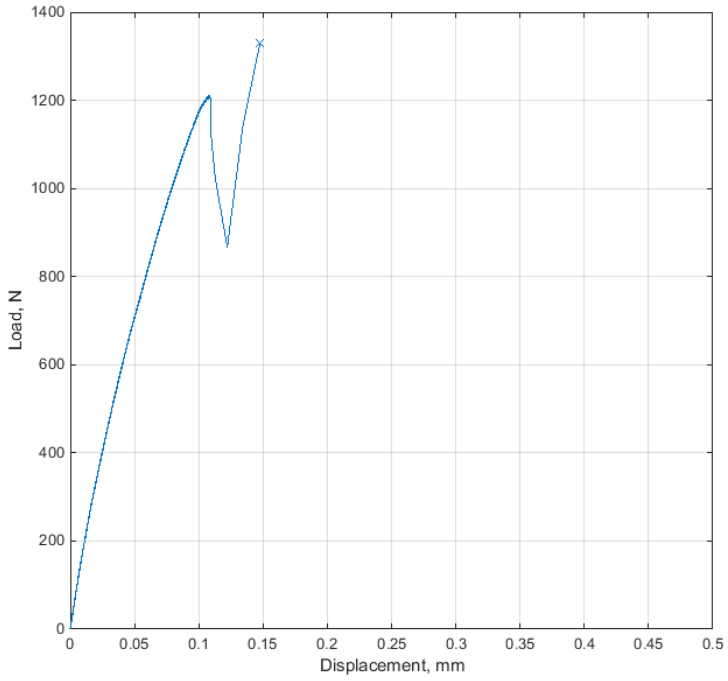

Figure 8.2-11: Load Against Displacement Graph of the First Batch of Channel Group

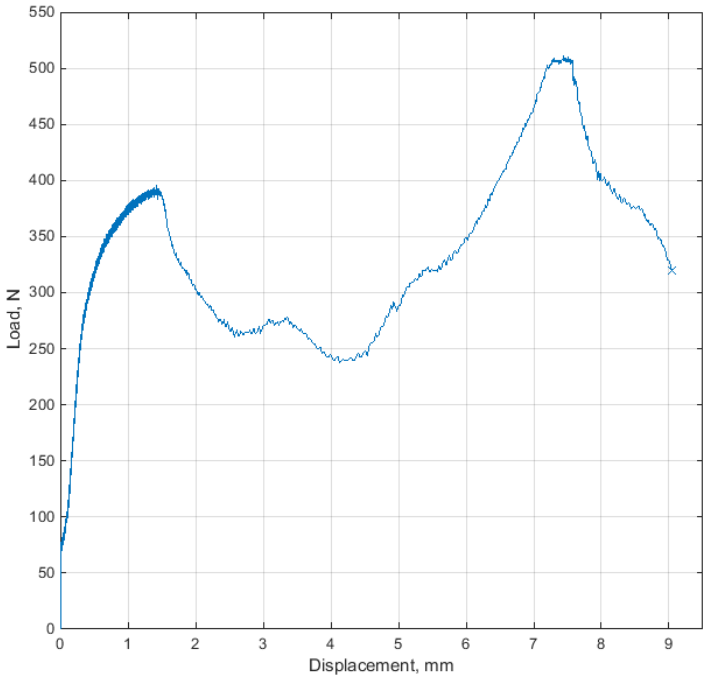

Figure 8.2-12: Load Against Displacement Graph of the Second Batch of Channel Group

It was recorded for both batches for the channel group that the cement did not stay intact but was split between the plug and jack and in addition the cement was flaky and easy to peel, this can been seen in the photo in figure 8.2-14. There was cement above the rim of the jack with none in the rim and the small epoxy had cement majority in the rim and some on the wall above and below the rims. There was no cement present on the bottom of the jack in either batch.

Figure 8.2-13: Photographs of the Channel Group After Testing
On the left is the jack and plug from the first batch and on the right is the jack and plug from the second batch.

The displacement against load graphs for extruding batch one is shown in figure 8.2-14 and batch two shown in figure 8.2-15. Both batches have a similar displacement-load curve yet with batch one has a maximum load of ca. 17N.

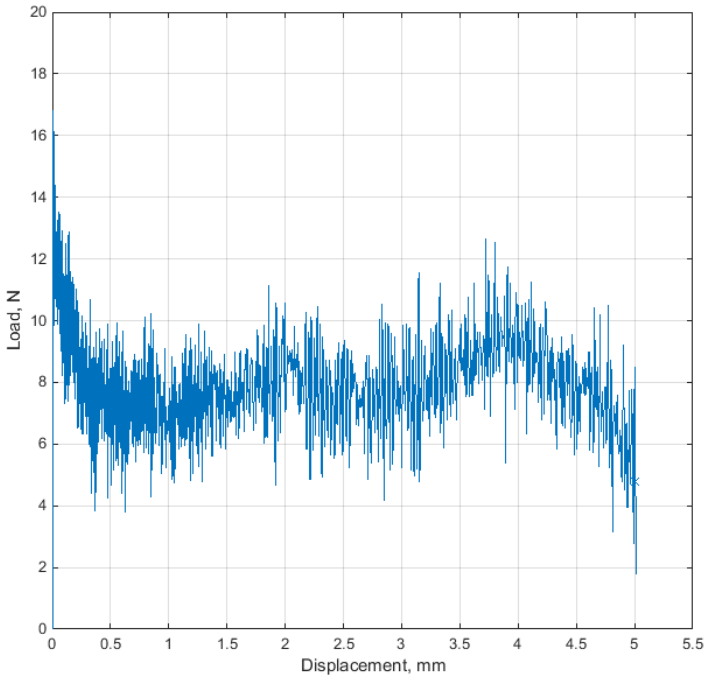

Figure 8.2-14: Load Against Displacement Graph of the First Batch of Extruding Group

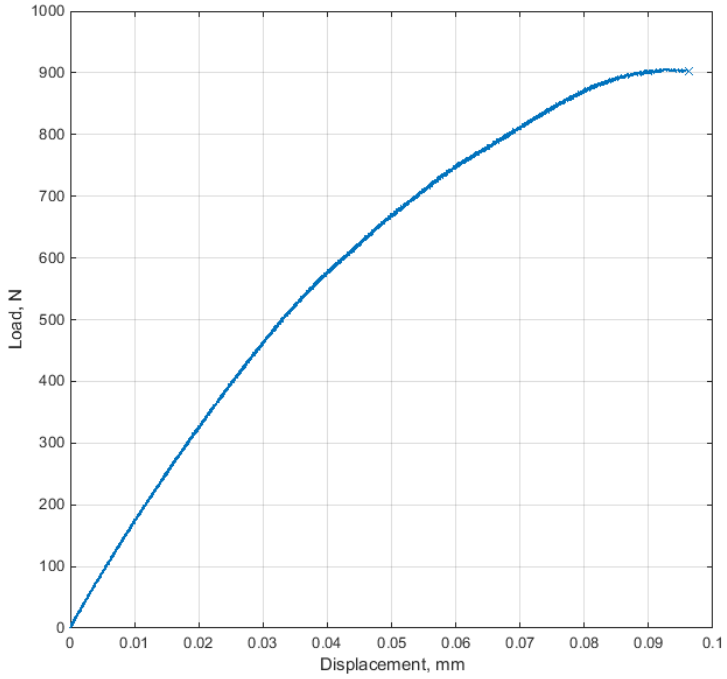

Figure 8.2-15: Load Against Displacement Graph of the Second Batch of Extruding Group

Figure 8.2-16: Photographs of the Extruding Group After Testing
On the left is the jack and plug from the first batch and on the right is the jack and plug from the second batch.

The cement in the extruding group remained in the jack for both batches, as seen in figure 8.2-16 photos. The cement surrounds the hole on the jack's base, as designed intended but the walls below the hole had cement that was also smooth. Up the side of the jack's wall had areas covered in cement that was a little flaky in areas. Plus, in the first batch there was a small area of flaky cement at the bottom of the hole where cement was not designed to be. The cement on the base of the

jack in the second batch was broken up into quarters, it was also noted with the second batch that the cement on the walls required harder pushing in and pulling out the insert compared to when it was later removed.

Intruding group's batch 1 and 2 displacement-load graphs are represented in figures 8.2-17 and 8.2-18, respectively. The maximum load for batch one is 270N and for batch two it is ca. 1,850N.

The location of the cement body was different in each batch for the intruding group, the difference can be observed in figure 8.2-19. In batch one the cement remained in the jack, it covered all the raised plateau and majority of the lower surround base that wasn't intended to have any cement. The cement in the second batch was in the well of the plug with some protruding up the well wall, up to 2mm above the main body of cement. The base of the jack had cement surround the plateau, covering approximately half this area.

Table 8.2-1: The Max Loading for each and the Statistics

Sample number	**Batch 1 (N)**	**Batch 2 (N)**	**Average**	**SD**	**CV**	
1 -fully	797.8	1,638.3	-			0.129
2 -rib	1,323.8	2,019.1	1,671.45	492	29.4	0.2205
3 -wall	1,701.9	727.8	1,214.85	689	56.7	0.173
4 -channel	1,330	510.9	920.45	579	62.9	3.7925
5 -extruding	16.8	907.8	462.3	630	136.3	0.05
6 -intruding	271.3	1,867.5	1,069.4	1,130	105.7	0.5245

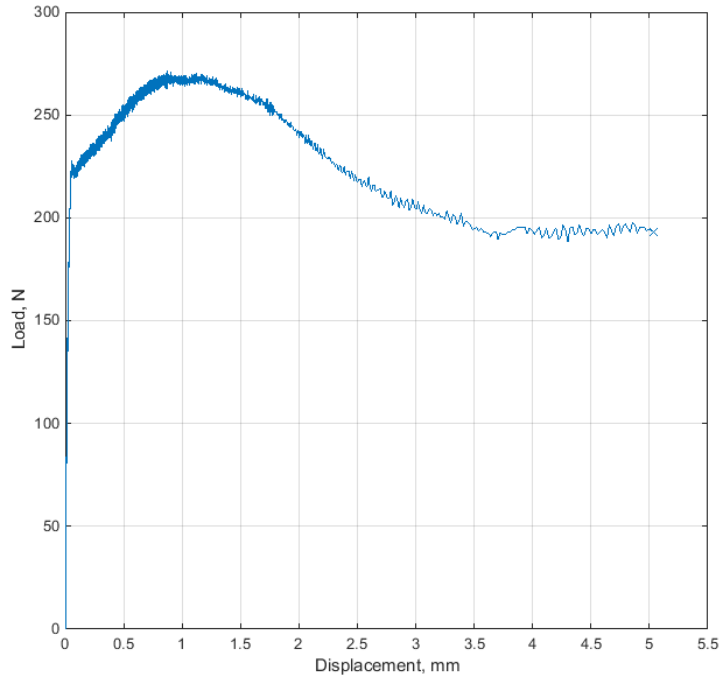

Figure 8.2-17: Load Against Displacement Graph of the First Batch of Intruding Group

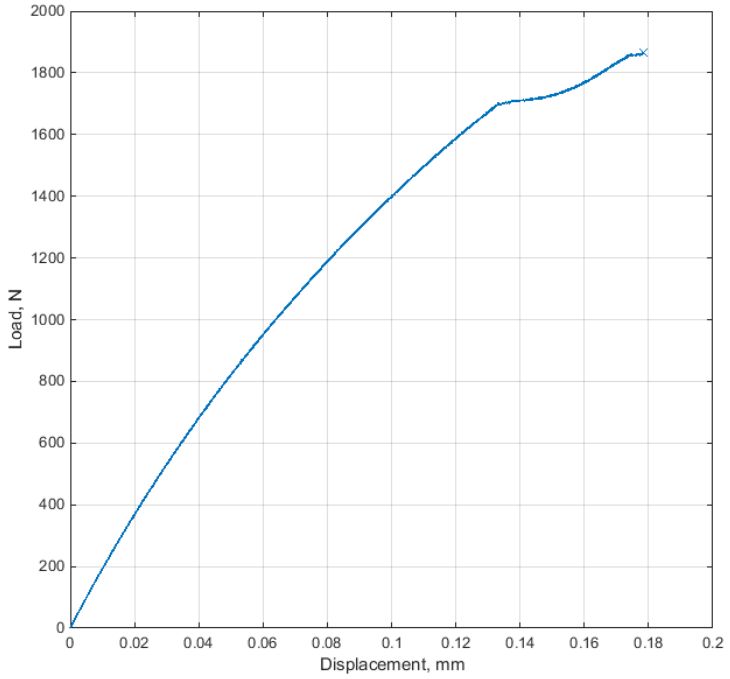

Figure 8.2-18: Load Against Displacement Graph of the Second Batch of Intruding Group

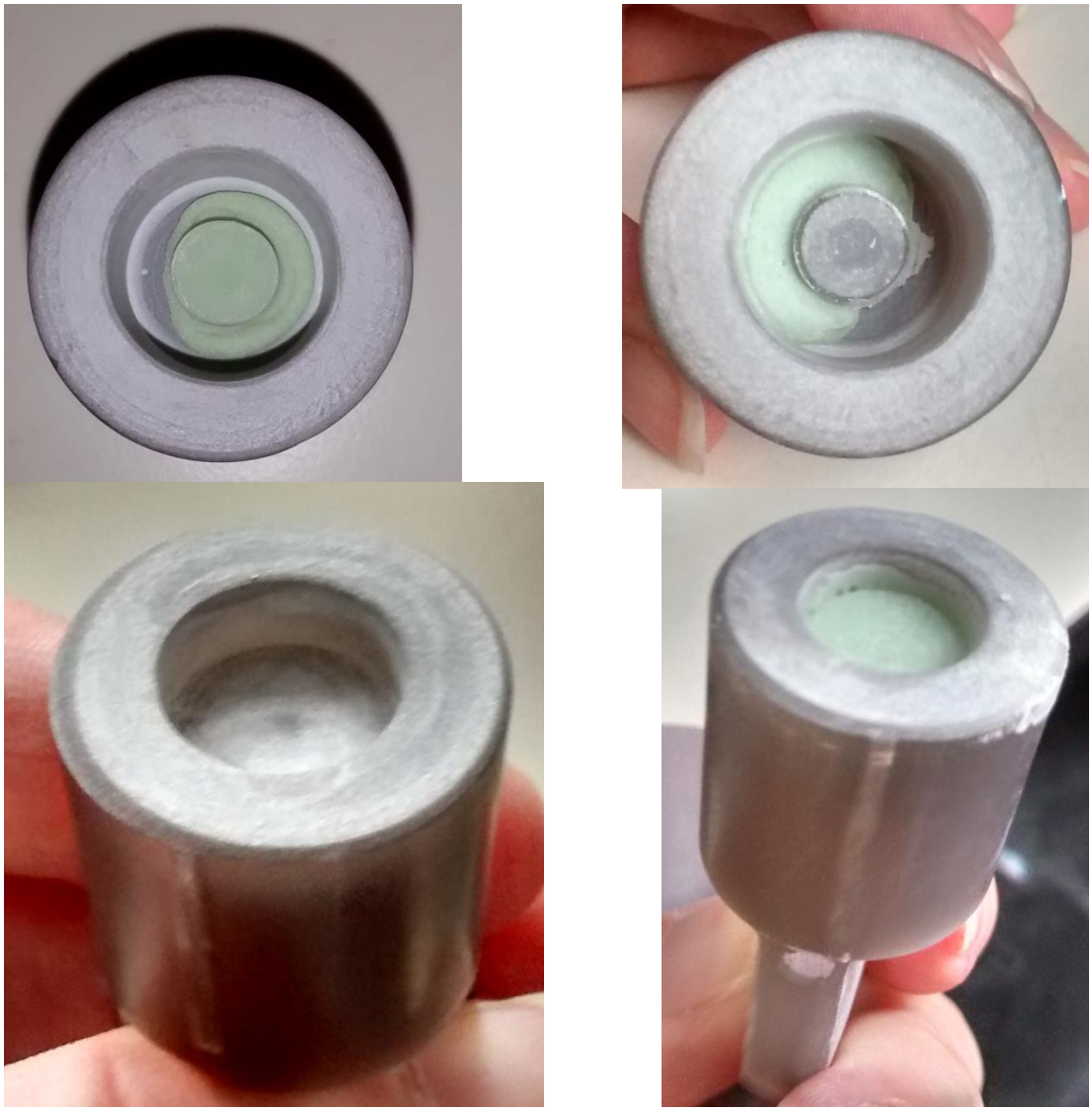

Figure 8.2-19: Photographs of the Intruding Group After Testing
On the left is the jack and plug from the first batch and on the right is the jack and plug from the second batch.

8.2.4 Discussion

This experiment has its limitations because it is just a preliminary investigation into a new field of prostheses. As far to my knowledge, this work hasn't been discussed before in the literature, nor has the idea of combining a prosthesis with cement and cementless systems. However, the sample sizes are too

small to give definitive conclusions but they provide analytical thoughts as to where to go with this prosthesis idea. Inlay prostheses may benefit from these designs as the jack and plug a very illustrative to the knee bone and inlay prosthesis (respectively). It has been reported in the literature, the main fixation problem with onlay prosthesis is there isn't enough contact area to of the bone to the cement to make the bone strong enough for the implant[96]. This idea of partial cementing with areas to oesointegration might not work so well with onlay designs; though this hasn't been fully investigated yet, but it might be partial cementing can be possibly done with inlay and TKR prostheses. The information from this investigated can be applied to fully cemented prostheses; the features that make a strong partial cement adhesion could be added to fully cement to potentially create a stronger adhesion that the partial.

The two batches of the fully group can't be compared to each other because the first batch did not apply load until failure, unlike the second batch. It is assumed from the first batch that each peak represents a fracture occurring allowing the two epoxies to displace. With this in mind, the first batch suggests the minimum force required for the initial crack to occur but it is not the maximum force required for full failure. The forth peak is the maximum force that was applied to the sample but since there was already previous failure, this is assumed to be less than the required force to pull apart the sample – this explains why the second batch's maximum load is greater than the first batch. Therefore, the fully group initial failure occurs approximately 650N but the minimum required single loading force is

approximately 1,600N if fully covered in cement. Only this group had information to indicate when initial fracture occurs, but it does provide an estimated maximum load under a single loading before failure.

All the groups have a range between the two batches of approximately 1,000N; plus, the extruding and intruding groups, the CV values are over 100%. There are two possible reasons for the variation of maximum loading in the two batches: cement procedure and cementing application. The cement used in these samples were mixed up on different days, as discussed previously in section the surface texture discussion, cement properties can differ with different batches due to uncontrolled variables. The cement application was the same in both samples but the different between the batches could be a learning curve in favour of the second batch.

The wall group's maximum load average is lower than that of the fully group; this could be due to the exclusion of cement on the bottom of the plug. Couple this with the rib group's maximum load average within the same 100N of the fully group, by adding the ribs to the plug seems to have a similar adhesion strength as a plug fully covered in cement. The channel group has an average less than a thousand Newton's, suggesting that having corresponding ribs on the jack to create channels performs slightly worse than the wall group. The extruding group has the worst maximum average than the other groups and the difference between it and the fully group is over a thousand Newton's; if the 16N is removed this group performs just as well as the channel and wall group. The intruding group – which is

similar to the extruding group, area and cement position – its average is not as low as the extruding group but similar to the channel group. In the results there are only a handful of samples that have maximum load above 1638.3N.

The rib, channel, extruding, and intruding groups had cement in areas unintended for cement; in the case for rib and channel groups it did not affect the area required to be cement free (the base of the plug). It seems that the extruding and intruding design might not appropriate features to use in a prosthesis intending to have both cement and cementless attributes; the rib and channel designs might be suitable depending how they are applied. The opposite can be said for the wall design, as it had no evidence of cement in the unintended areas, suggesting their potential of initial cementing without the cement protruding into areas designed for oestointegration.

The fully, wall, and rib groups had cement surround the circumference, when the plug was removed it was either unable to be pushed back in (fully group), or if it was it took a bit a force to then pull it back out (this was recorded for one sample to be 50N). This suggests that there is potential radial pressure in holding the plug in place. This is the theory is reinforce by the graph for the second batch wall group, figure 8.2-9. There seems to be a plastic range present at approximately 600N; at approximately 690N the sample seems to have failed but the graph continues to oscillate between 450N and 730N. This pattern could signify the radial pressure on to the plug preventing it from being free extracted from the jack.

The extruding and intruding groups have a disadvantage, if the cement fails initial attachment there is less chance of their features holding the plug in place. There is a dramatic difference between the intruding groups maximums load, the first batch failing at a load around 100 times smaller than the fully cemented group. The second batch, the cement cracked and on one side of the cement was attached to the jack and on the other side of the crack the cement was still attached to the plug. This could explain partly why the load is much greater the first batch.

From the extruding and intruding samples, it can be concluded that applying cement to only a small area on the bottom flat surface is not practical as the cement is most likely going to spread to surround the flat area. Plus, if failure of the cement interface happens before oestointegration, there is nothing in the design of these samples to prevent the insert from being fully removed with almost no effort.

There was one other design that was not tested due to failure of the epoxy; this design was to have the internal walls of the jack and plug to be slopping, it increases in diameter distally. This design may be advantages because the plug can be inserted into the jack before applying the cement which will, theoretically, add a mechanical wedging aspect to keep the plug in the jack, consequently could increase the pull-out strength. Plus, this design could involve pressurisation of cement during working and curing to increase the penetration of the cement into the bone matrix. The down side is the shape is tricky to cement and from the user diary, undercuts of the bone are difficult to attain.

From the results, the rib design is an overall good design candidate because the maximum load is equivalent to the fully cement group plus it is easier to apply cement and shape required to cut the bone. Therefore, the rib design is the main front runner as a potential feature in prostheses with the intention of both cement and cementless.

8.2.5 Conclusion

The results suggest that a prosthesis could be designed to be partially cemented while retaining the same pull-off strength as a regular cemented prosthesis. These results furthermore, suggest that the pull-off strength of a regular cemented prosthesis could be increased with the same techniques used for the partial cementing. The findings of this preliminary experiment were integrated into the concept selection and evaluation cycle of the design process.

8.3 Effect of Surface Texture Experiment

8.3.1 Introduction

The cement-bone interface is vital for the longevity of any implant design[250]. The cement's main adhesive strength comes from the ability to penetrate the bone surface to create interdigitation[99], [251]. This phenomenon is dependent on bone preparation factors to create a strong interface[85]. Burring the bone leaves a surface roughness, which can be described as rough and pitted; this is different compared to traditional sawing and thus could affect the cement's

adhesion strength. From the literature, the bone cement's adhesion is stronger proportionally with contact area[250].

This series of experiments was to establish if surface texture had an effect on the adhesion strength of cement. This in principle increases the surface area and thus drove the following hypothesis: that a roughed surface, as a consequence from burring, will provide a stronger adhesion due to the greater surface area compared to a smooth surface.

8.3.2 Aims

The main aim was to ascertain whether surface texture affected cement adhesion under tension and shear forces. This was accomplished using artificial bone samples from Sawbones Europe AB (Malmö, Sweden) and real bone samples. A secondary aim was to establish if applying constant pressure during curing of the cement will have an effect on the adhesion strength. The viscosity of cement was considered as a factor.

8.3.3 Results

8.3.3.1 Cement Viscosity

The two cement viscosities, medium (M) and high(R), are compared under tensile and tensile pull-off conditions; the mechanical properties are shown in tables 8.3-1 and 8.3-2.

Table 8.3-1 Cement rods under tensile					
Cement Viscosity	**Young's Modulus (MPa)**	**Ultimate Stress (MPa)**	**Ultimate Strain %**	**Yield Stress (MPa)**	**Yield Strain %**
Medium	1,800	47.9	5.01	30.4	1.89
Medium	1,580	47.2	4.74	31.3	2.18
Medium mean (SD)	1,690 (158)	47.6 (0.539)	4.87 (0.190)	30.8 (0.590)	2.03 (0.206)
High	1,490	45.8	5.56	38.6	2.11
High	1,650	49.9	4.82	33.7	2.24
High mean (SD)	1,570 (114)	47.8 (2.92)	5.19 (0.529)	31.1 (3.63)	2.17 (0.0872)

Table 8.3-2: Smooth epoxy Tensile pull off					
Cement Viscosity	**Young's Modulus (MPa)**	**Ultimate Stress (MPa)**	**Ultimate Strain %**	**Yield Stress (MPa)**	**Yield Strain %**
Medium	139	17.4	15.0	12.7	9.31
Medium	156	16.7	13.2	10.1	6.69
Medium mean (SD)	147.6 (12.0)	17.0 (0.531)	14.1 (1.25)	11.4 (1.79)	8.00 (1.85)
High	187	7.43	4.82	6.53	3.69
High	191	5.90	3.50	5.37	3.02
High mean (SD)	188.89 (2.38)	6.67 (1.09)	4.16 (0.938)	5.9 (0.820)	3.35 (0.474)

The mechanical properties of the cement rods between the two viscosities under tensile conditions vary slightly but are not significantly different ($P>0.05$) in 4 of the mechanical properties: Young's modulus, ultimate stress, yield stress, and yield strain; ultimate strain was significantly different with the two groups ($P<0.045$).

Under tensile pull-off conditions the mechanical properties between the two viscosities have a greater variance, with all 5 mechanical properties rejecting the null hypothesis in the one-way-ANOVA analysis ($P<0.05$). This means that viscosity does not significantly affect the cement properties but does affect the adhesion properties significantly. The high viscosity has a significantly higher Young's modulus and significantly lower ultimate stress and strain, and yield stress and strain values than the medium viscosity.

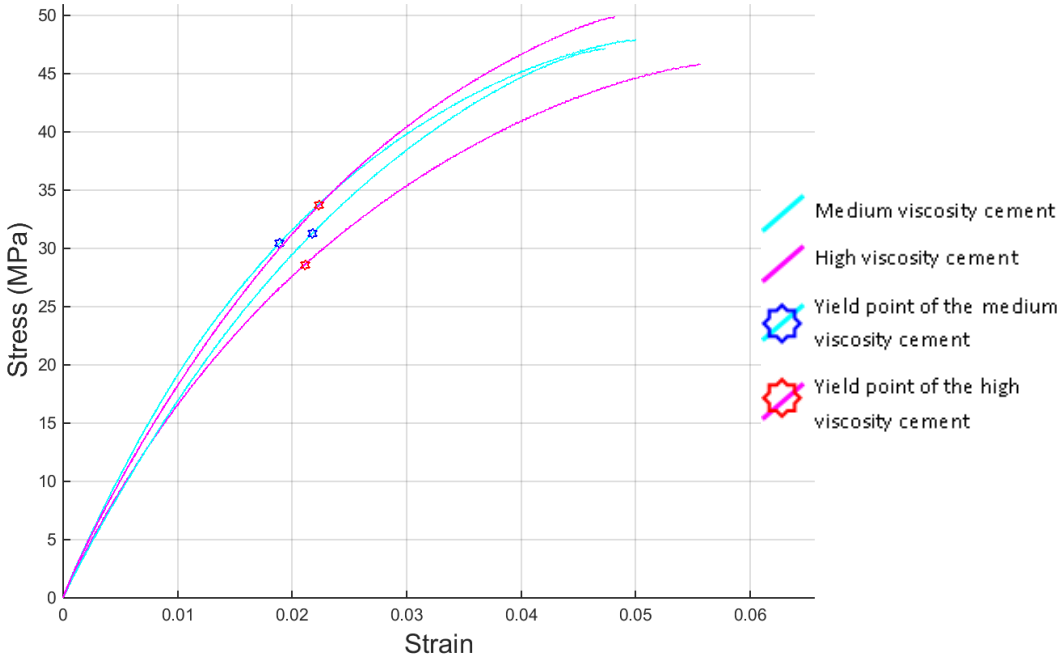

Figure 8.3-1: Stress-Strain Graph of the Cement Rods under Tensile Conditions
The blue lines are the medium viscosity samples and the magenta lines are for the high viscosity samples. The points are the calculated yield at 0.2% strain.

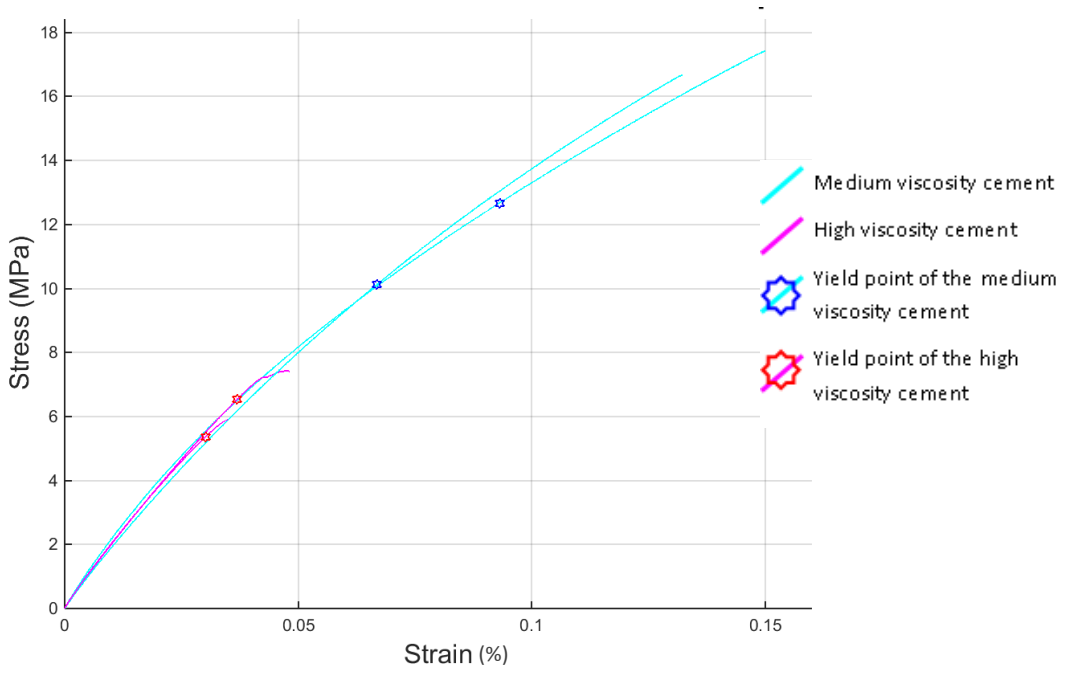

Figure 8.3-2: Stress-Strain Graph of Tensile Pull-off from two Smooth Sawbones Epoxies
The blue lines are the medium viscosity samples and the magenta lines are for the high viscosity samples. The points are the calculated yield at 0.2% strain.

There is a distinct difference of the mechanical properties between the cement rods and the pull-off conditions; plus, the difference between the viscosity under pull off conditions can be visualised in figures 8.3-1 and 8.3-2. The Young's modulus is approximately 10 fold off and stresses (ultimate and yield) is a 4 fold in favour to the cement rods; the strains are approximately either 1 or 5 fold difference.

8.3.3.2 Cement Rod Properties

To compare the tensile mechanical properties of the cement between the batches standard statistical analysis was carried out, all the sample data are in figure 8.3-3 and the means are presented in table 8.3-3, below.

A one-way analysis of variance test was used to test the hypothesis that a mechanical property does not vary between the batches. This analysis did not find any significant differences ($p>0.05$) in Young's modulus, yield stress and strain, and ultimate stress and strain between the batches and they can be considered equivalent. This shows that the cement mixing procedures provide statistically equivalent samples in terms of mechanical properties, and that batch number does not need to be considered when analysing the results of mechanical tests which involve other variables.

Table 8.3-3: Tensile Mechanical Properties of the Cement Rod (n = 86)

	Young's Modulus (MPa)	**Ultimate Stress (MPa)**	**Ultimate Strain %**	**Yield Stress (MPa)**	**Yield Strain %**
Mean of all	1,610	41.4	4.40	28.0	2.00
SD	213	6.89	1.33	3.25	0.245
Standard Er	28.2	0.853	0.2	0.414	0.0312

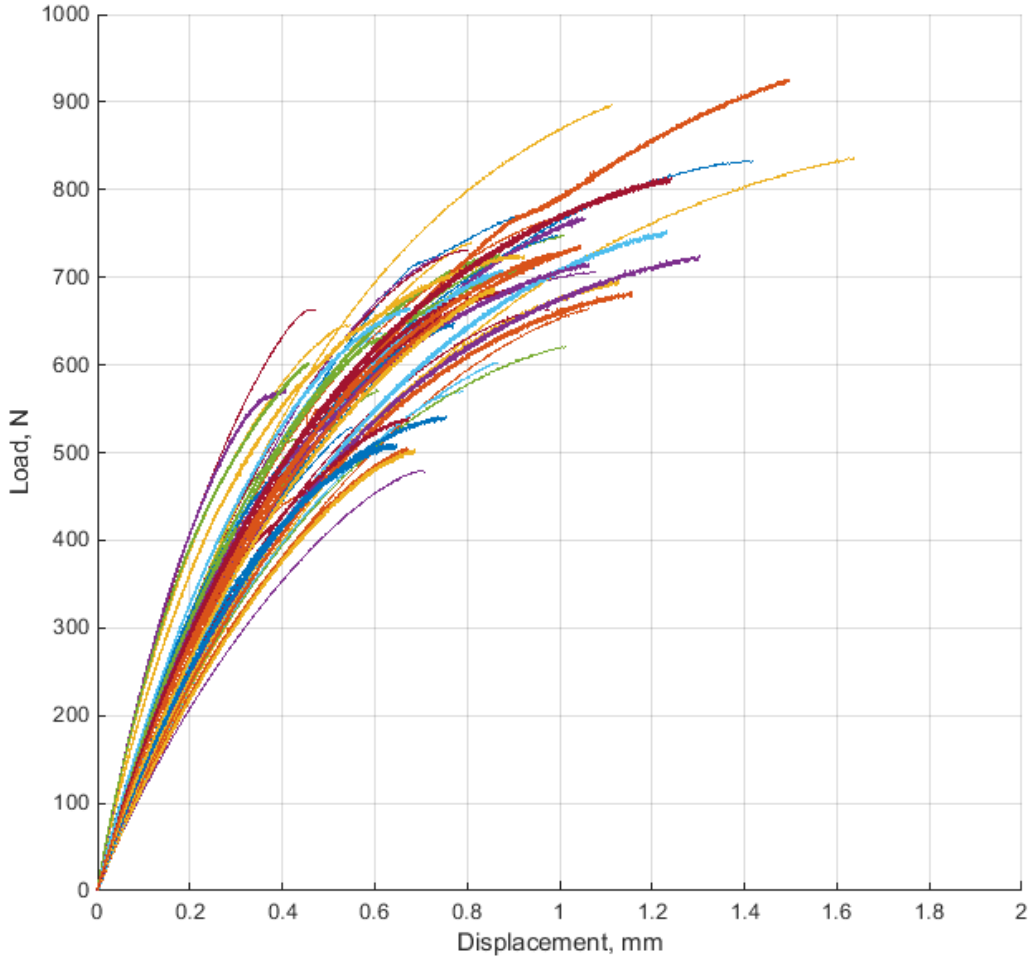

Figure 8.3-3: Stress-Strain Graph of all the cement Rods Under Tensile Conditions
Each line represents a sample.

8.3.3.3 Tensile Epoxy Pull-off Tests without Applied Pressure

The load against displacement graphs of the three data groups can be found in figure 8.3-4 to 8.3-6; from the individual sample graphs, it is easier to observe that the materials exhibit a linear to plastic material with yield point hard to defined. It is from these graphs that adhesion property data were obtained. The means of each group's adhesion properties are displaced below, table 8.3-4; the count is the number of samples that were included into the analysis (some samples

had alignment issues and thus were not able to be included in the results since they wouldn't be in full tension conditions).

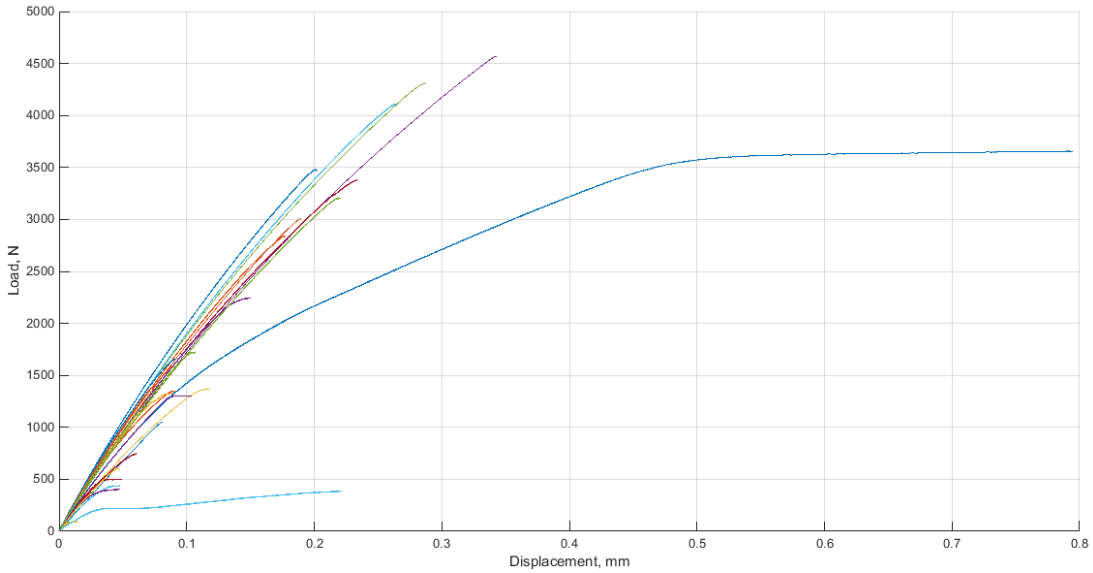

Figure 8.3-4: Smooth Group Load Against Displacement Graph
The different colours represent each sample tested

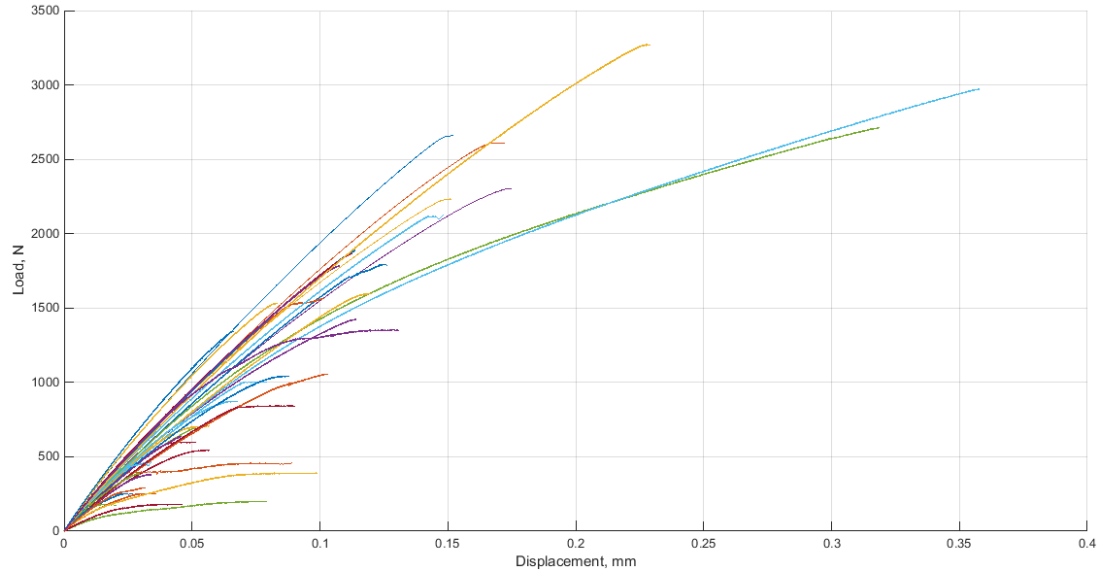

Figure 8.3-5: Rough Group Load Against Displacement Graph
The different colours represent each sample tested

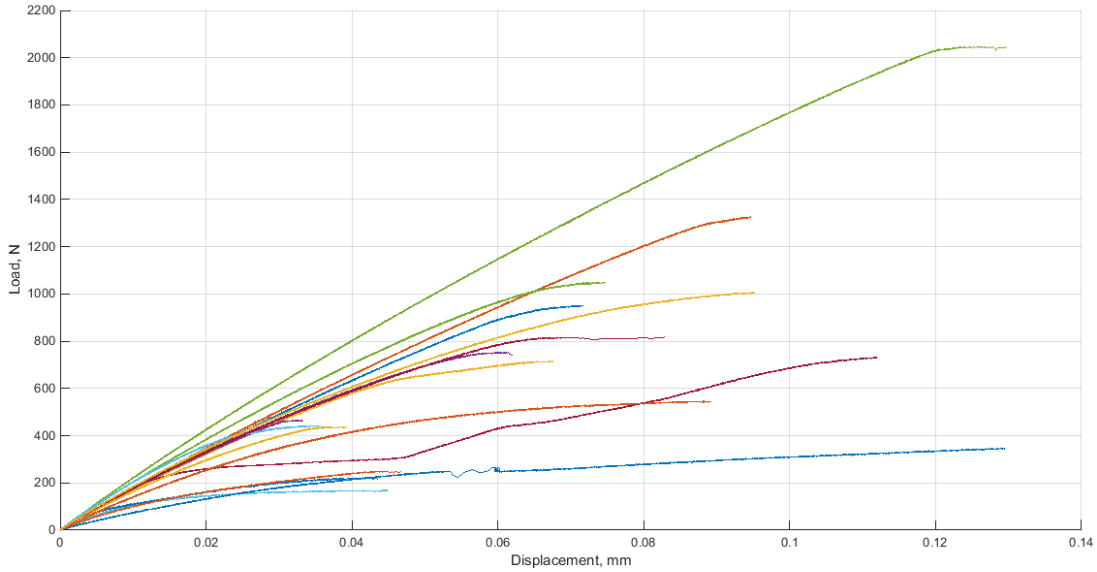

Figure 8.3-6: Mixed Group Load Against Displacement Graph
The different colours represent each sample tested

Table 8.3-4: The Adhesion Properties of Non-Pressure under Tensile Pull-off Conditions

	Count	**Stiffness, N/mm (SD)**	**Ultimate Load, N (SD)**	**Ultimate Displacement, mm (SD)**
Rough	39	16,700 (3,790)	1,180 (869)	0.137 (0.208)
Smooth	23	17,800 (2,830)	1,930 (1,460)	0.164 (0.166)
Mixed	17	15,700 (3,520)	724 (471)	0.0733 (0.0321)

From the one-way-ANOVA analyses the batch had a significant effect ($P<0.045$) on the ultimate load values. Building on the picture the two-way-ANOVA analysis showed that batch, group, and group interaction with batch has a significant effect ($P<0.01$) on the ultimate load. Additionally, the one-way-ANOVA analyses of the group effect on the adhesion properties and it was only the ultimate

load was significant effected by the group (p=0.001); the smooth group had a higher ultimate load and the mixed group had the lowest. The independent t-tests showed that all three groups their ultimate load was significantly different to each other (P<0.002).

Table 8.3-5: Chi Square Test Based on the Original Hypothesis under Tensile Conditions

Categories	**Number of samples**	**Chi Square value**	**Critical value**
Rough	22	0.1098	
Smooth	19	0.1098	
Sum	41	0.2195	3.841

Table 8.3-6: Chi Square Test Based on the Revised Hypothesis under Tensile Conditions

Categories	**Number of samples**	**Chi Square value**	**Critical value**
Same	35	10.3	
Other	6	10.3	
Sum	41	20.5	3.841

Two Chi squared tests were perform from the mix group data using the two hypotheses proposed. The original hypothesis, table 8.3-5, was that the rough surface would be stronger than the smooth, thus the cement would stay adhered to the rough group after failure. For the rough and smooth category, the null hypothesis was failed to be reject thus there was no confidence (p>0.05) that the surface affects adhesion. However, the revised hypothesis, table 8.3-6:- was the

order of application affect the failure surface; the null hypothesis with confidence of $p<0.05$.

8.3.3.4 Shear Epoxy Pull-off Tests without Applied Pressure

The material under shear conditions exhibits a linear to plastic behaviour before breaking, again the yield point is ill-defined; examples of individual sample data can be seen in loadagainstdisplacement graphs in appendix 13 (PPI). The table below is the means for the groups with the above calculated adhesion properties and the count is the number of samples that were included into the analysis (some samples had alignment issues and thus were not able to be included in the results since they wouldn't be in full tension conditions).

Table 8.3-7: The Adhesion Properties of Non-Pressure under Shear Pull-off Conditions

	Count	Stiffness, N/mm (SD)	Ultimate Load, N (SD)	Ultimate Displacement, mm (SD)
Rough	11	4,550 (2,430)	394 (291)	0.179 (0.112)
Smooth	21	5,870 (2,540)	585 (401)	0.161(0.0716)
Mixed	11	4,028 (1,750)	383 (302)	0.144 (0.0810)

The one-way ANOVA test showed that the batch has a significant ($P<0.01$) effect on the stiffness and ultimate load. The three independent t-tests did not

demonstrate a significance ($P>0.045$) between the adhesion properties with the different groups. Though the two-way ANOVA did show a significant ($P<0.002$) effect of the group and the batch on the stiffness and ultimate load; the interaction

of the group and batch also had a significant (P<0.001) effect on the stiffness of the samples.

Table 8.3-8: Chi Square Test Based on the Original Hypothesis Under Shear Conditions

Categories	**Number of samples**	**Chi Square value**	**Critical value**
Rough	20	10	
Smooth	0	10	
Sum	20	20	3.841

Table 8.3-9: Chi Square Test Based on the Revised Hypothesis Under Shear Conditions

Categories	**Number of samples**	**Chi Square value**	**Critical value**
Same	13	0.9	
Other	7	0.9	
Sum	20	1.8	3.841

Two Chi squared tests were perform from the mix group data using the two hypotheses proposed. The revised hypothesis (table 6.3-9) was the order of application affect the failure surface, with the first surface in contact with the cement will still have the cement after failure. It was concluded that the order of cement application did not affect the cement adhesion, because the null hypothesis was failed to be rejected using confidence (p>0.05). However, the original hypothesis (table 6.3-8) was that the rough surface would be stronger than the

smooth, the null hypothesis was rejected ($p<0.05$) and surface texture may influence the cement's adhesion under shear conditions.

8.3.3.5 Tensile Epoxy Pull-off Tests under Applied Pressure

The batch size of two allowed direct batch comparison between the rough and smooth groups seen in appendix 13 (PPI); similarly, the direct comparison can be made with the mixed group with the cement being first applying to the smooth side and then cement applied first to the rough side, graphs in appendix 13 (PPI). In all the batches under pressure during applying and curing, the pairs are the same initially in the elastic stage of the curve then some of the pairs differentiate while other pairs continue to match curve to break at different loads. In 3 out of the 5 mixed group batches, the cemented rough side first had a greater maximum pull-off load. The rough and smooth pairs were the majority of batches, 7 out of 10, with the rough group experiencing a greater pull-off load. Tables 8.3-10 to 8.3-12 are the results from the 3 groups. The batches had sample size of 2: the results from smooth and rough groups are displayed in table 8.3-10; the results from the mixed group are displayed in table 8.3-11; and the static data for all three groups are in table 8.3-12.

Table 8.3-10: The Smooth and Rough Results

Batch	Smooth/Rough	Max Load (N)	Comments	Displace at Max (mm)
1	*Rough*	*3,510*	*Rough by*	*0.500*
	Smooth	*3,370*	*141*	*0.465*
2	*Rough*	*2,500*	*Rough by*	*0.331*
	Smooth	*1,630*	*878*	*0.146*
3	*Rough*	*3,610*	*Rough by*	*0.536*
	Smooth	*1,700*	*1910*	*0.190*
4	*Rough*	*3,960*	*Rough by*	*2.14*
	Smooth	*2,250*	*1710*	*0.213*
5	*Rough*	*3,990*	*Rough by*	*0.646*
	Smooth	*3,400*	*593*	*0.511*
6	*Rough*	*3,900*	*Rough by*	*0.999*
	Smooth	*3,250*	*644*	*0.381*
7	*Rough*	*4,420*	*Smooth by*	*0.500*
	Smooth	*4,550*	*135*	*0.682*
8	*Rough*	*4,210*	*Smooth by*	*0.461*
	Smooth	*6,140*	*1930*	*1.00*
9	*Rough*	*3,070*	*Smooth by*	*0.300*
	Smooth	*4,420*	*1350*	*0.570*
10	*Rough*	*4,530*	*Rough by*	*0.531*
	Smooth	*3,840*	*694*	*0.415*

Table 8.3-11: Results from the Mixed Group

Sample ID	Batch	Cemented	Failed Surface	Max Load (N)	Displacement at Max (mm)	Initial Stiffness (N/mm)
1	1	Rough	Smooth	3,940	1.00	14,300
2		Smooth	Smooth	3,700	0.650	14,400
3	2	Rough	Smooth	4,000	0.999	11,000
4		Smooth	Smooth	3,700	0.702	10,900
5	3	Rough	Smooth	829	0.0790	13,200
6		Smooth	Rough	791	0.0810	15,400
7	4	Rough	Smooth	4,740	0.479	16,700
8		Smooth	Smooth	4,800	0.580	15,800
9	5	Rough	Smooth	4,470	0.511	15,200
10		Smooth	Rough	4,920	0.681	14,900
Average (SD)			Smooth	3,520 (1,390)	0.560 (0.288)	14,200 (1,940)

Table 8.3-12: The Statistical Data from the Groups

	Stiffness Value (initial) (N/m)			**Ultimate Load (N)**			**Ultimate Displacement (mm)**		
	Rough	*Smooth*	*Mixed*	*Rough*	*Smooth*	*Mixed*	*Rough*	*Smooth*	*Mixed*
Mean	15,200	13,500	14,200	3,770	3,450	3,520	0.695	0.700	0.560
SD	1,860	1,600	1,940	621	1,390	1,390	0.544	2.54	0.288
CV	12.2%	11.8%	13.7%	16.5%	40.3%	39.5%	78.3%	36.3%	51.4%
Paired t-Test	0.0776		-	0.431		-	0.296		-

From the one-way-ANOVA analysis on the mixed group, the batch effect on the adhesion properties had a significant affected on all three properties ($P<0.01$). A paired t-test between the cement applied to rough and applied to smooth in the mixed group show no significance on the adhesion properties ($P>0.05$). The paired t-test between the rough and smooth also show no significance ($P>0.05$) between the adhesion properties. The stiffness and ultimate load averages of all three groups seem have little variance and the groups values are close to each other.

The chi-square tests from the mixed group, see tables 8.3-13 and 8.3-14, failed to reject the null hypothesis in both cases. Therefore, there was no significant relationship between the surface texture or the order of cementing on the side of interface failure ($P>0.05$).

Table 8.3-13: Chi Square Test Based on the Original Hypothesis under Tensile Conditions

Categories	**Number of samples**	**Chi Square value**	**Critical value**
Rough	8	1.8	
Smooth	2	1.8	
Sum	10	3.6	3.841

Table 8.3-14: Chi Square Test Based on the Revised Hypothesis Under Tensile Conditions

Categories	**Number of samples**	**Chi Square value**	**Critical value**
Same	7	0.8	
Other	3	0.8	
Sum	10	1.6	3.841

A one-way ANOVA showed there was significant effect (P<0.045) of pressure on the ultimate load and displacement properties. The average stiffness, ultimate load, and ultimate displacement of the non-pressure are: 16,700N/mm, 1,280N, and 0.125mm (respectively); the averages for the pressure group are 14,300N/mm, 3,580N, and 0.652mm (respectively). With pressure tensile pull-off has the ultimate load and displacement (significantly) higher than the non-pressure tensile pull-off.

8.3.3.6 Pull-off Test from Bovine Cancellous Bone under Applied Pressure

The distal knees only 4 produced results due to set-up issues, please refer to table 8.3-15 for the four results. The first knee 3 samples were a pair on one of the condyles and a rough on the other condyle. The third knee had one result from a smooth sample.

Table 8.3-15: Results from the Proximal Surface of the Tibia

Sample number	Knee number	Max recorded Load (N)	Surface texture
1	1a	188.4	Rough
2	1a	1,966.7	Smooth
3	1b	177.9	Rough
4	3a	485.2	Smooth

Each plateau had a smooth and rough sample so to minimise the affect of the uncontrollable variables (bone quality and cement strength) on each batch. The results from the plateau pull-off are shown in table 8.3-16.

Table 8.3-16: Results from the Cut-off Plateau			
Plateau/batch letter	**Sample number**	**Max recorded Load (N)**	**Surface Texture**
A	5	138.3	Smooth
	6	25.4	Rough
B	7	376.4	Smooth
	8	254.1	Rough
C	9	14.2	Rough
	10	270.8	Smooth
D	11	119.4	Smooth
	12	172.8	Rough

All the samples had the cement breaking off as a whole from the bone surface and none from the cement to smooth epoxy interface. Sample 2 from the distal test is an outlier because it is the only one that failed around 2,000N which is four times greater than highest value (around 20 times greater than the other samples) of all the other samples. As a result, the samples from the distal version of this experiment do not have a cementing batch pair therefore they are excluded from the paired t-test; there was no significant between the adhesion properties and the surface textures in the pairs t-test analysis.

Table 8.3-17: The Statistical Data from the Results						
	Initial slope stiffness (N/mm)		**Ultimate Load (N)**		**Displacement at Break (mm)**	
	Rough	*Smooth*	*Rough*	*Smooth*	*Rough*	*Smooth*
Mean	467	1,180	117	226	0.311	0.992
SD	392	761	117	121	0.159	0.869
SD error	24.5	49.5	39.51	7.54	0.0100	0.0543
CV	83.9%	67.1%	100%	83.9%	51.2%	87.6%
Paired t-Test	0.287		0.183		0.156	

The average force to remove the cementing from the rough surface is 116.6N (138.8N including the results from the joint set-up) whereas the average force to remove the cement from the smooth surface is 226.2N (278.02N including joint set-up) – almost double the force. Three out of 4 batches the smooth surface had a larger force required to break the cement interface than the rough surface. However, the standard deviation and CV values are very high reducing confidence in these results.

8.3.3.7 Microscopy

The images of the microscopic interface are in figures 8.3-8 to 8.3-13.

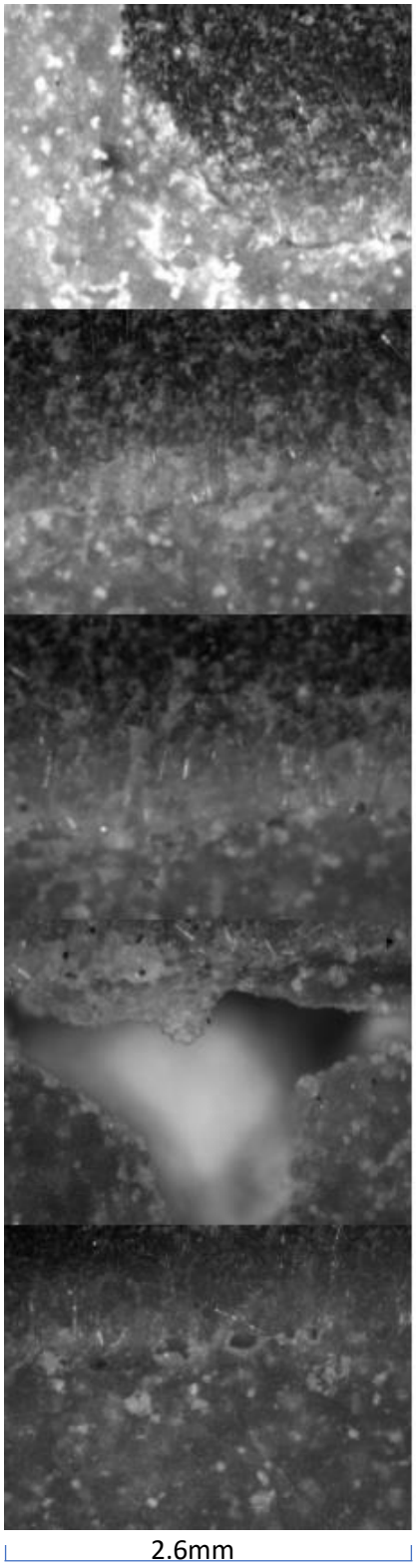

Figure 8.3-7: Rough Group without Pressure Microscopic Interface
Images were taken at 10x zoom at randomly allocated points along a sample's interface.

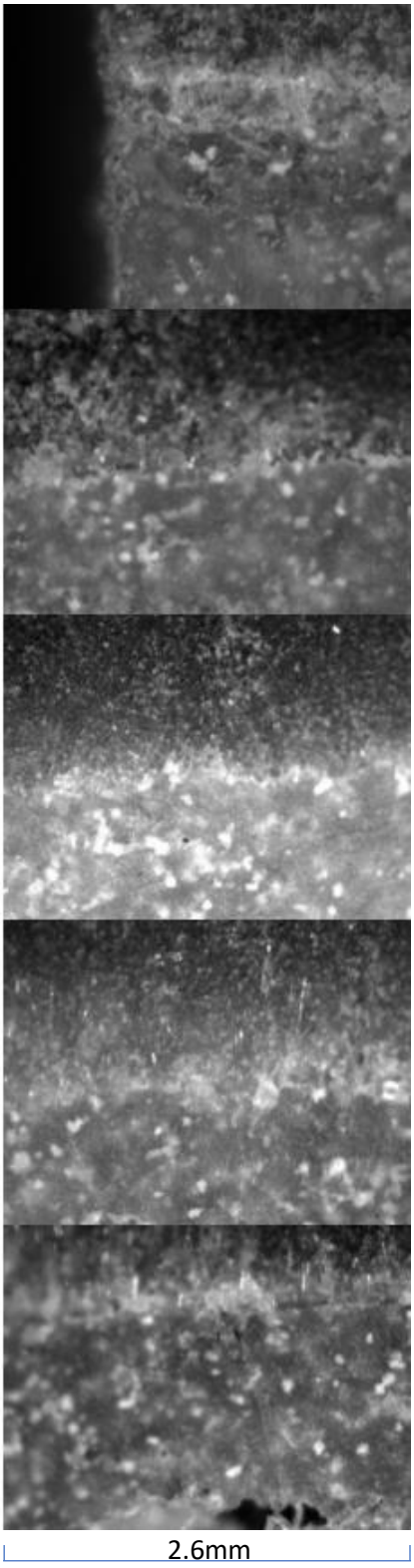

Figure 8.3-8: Smooth Group without Pressure Microscopic Interface
Images were taken at 10x zoom at randomly allocated points along a sample's interface.

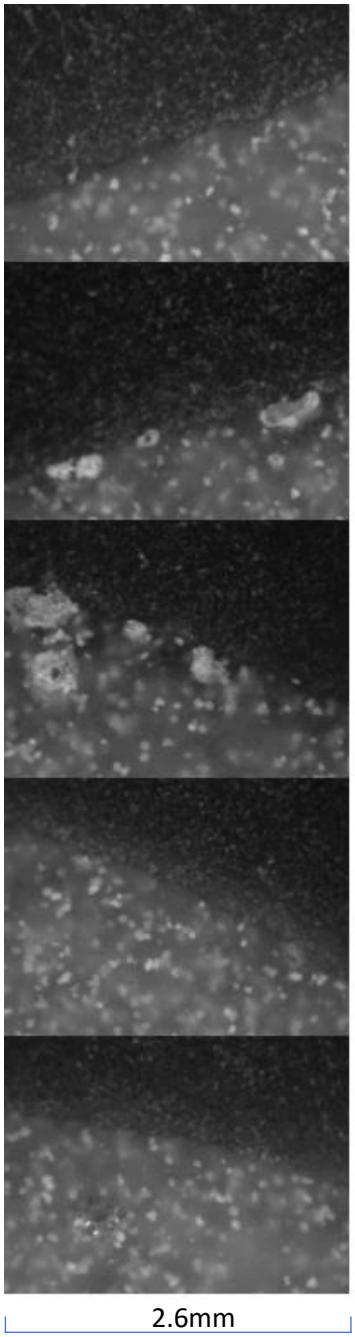

Figure 8.3-9: Rough Group with pressure Microscopic Interface Images

Images were taken at 10x zoom at randomly allocated points along the sample's interface.

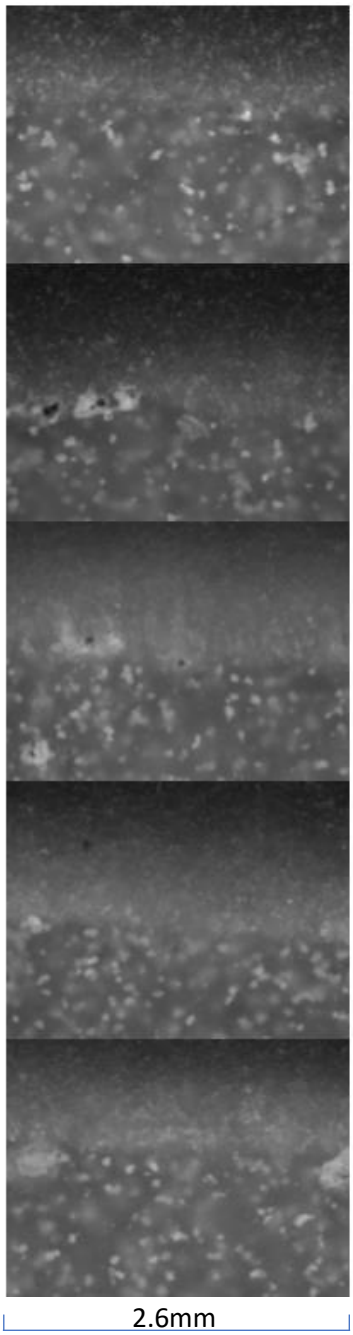

Figure 8.3-10: Smooth Group with pressure Microscopic Interface Images

Images were taken at 10x zoom at randomly allocated points along the sample's interface.

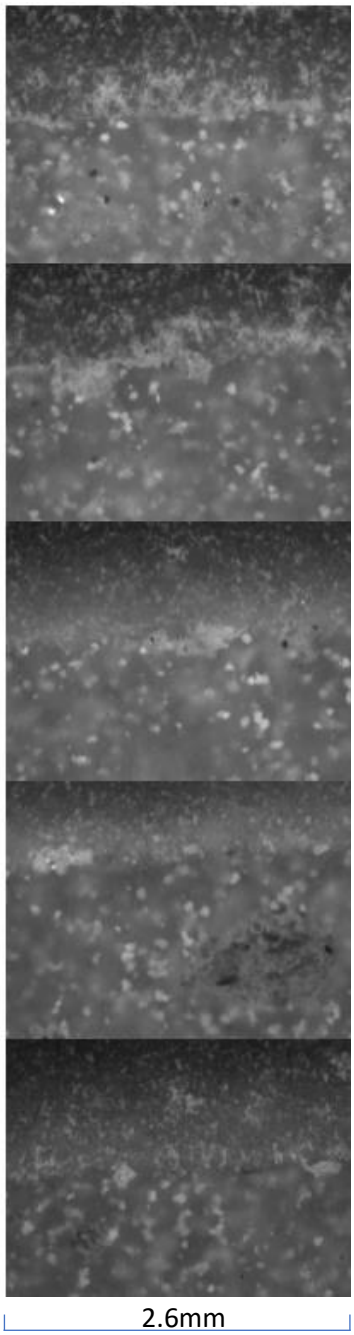

Figure 8.3-11: Mixed Group with pressure Microscopic Interface Images

Images were taken at 10x zoom at randomly allocated points along the sample's interface.

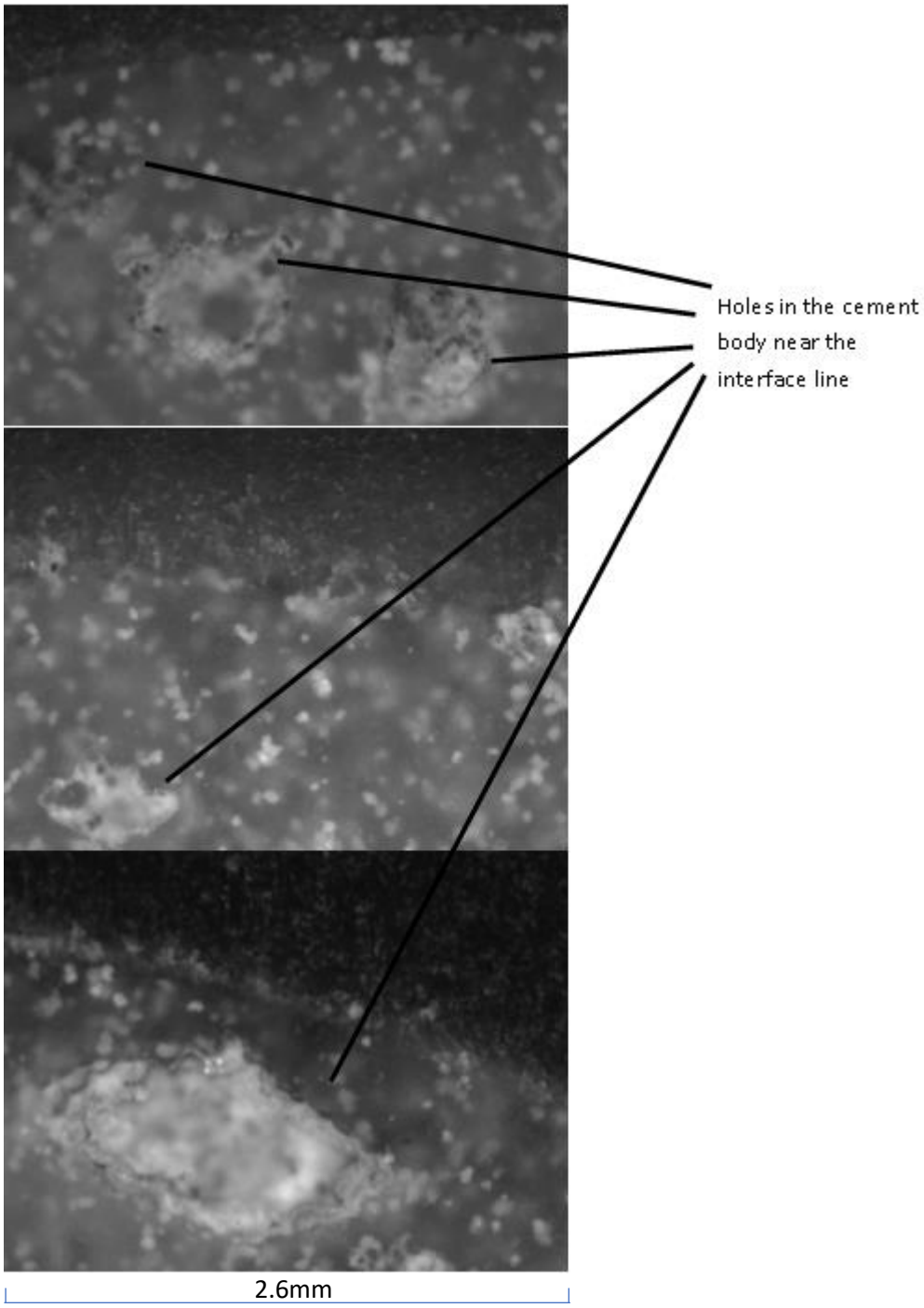

Figure 8.3-12: Voids in the Cement Body
The top row is from the rough group, the middle is from the smooth group and the last on is from the mixed group.

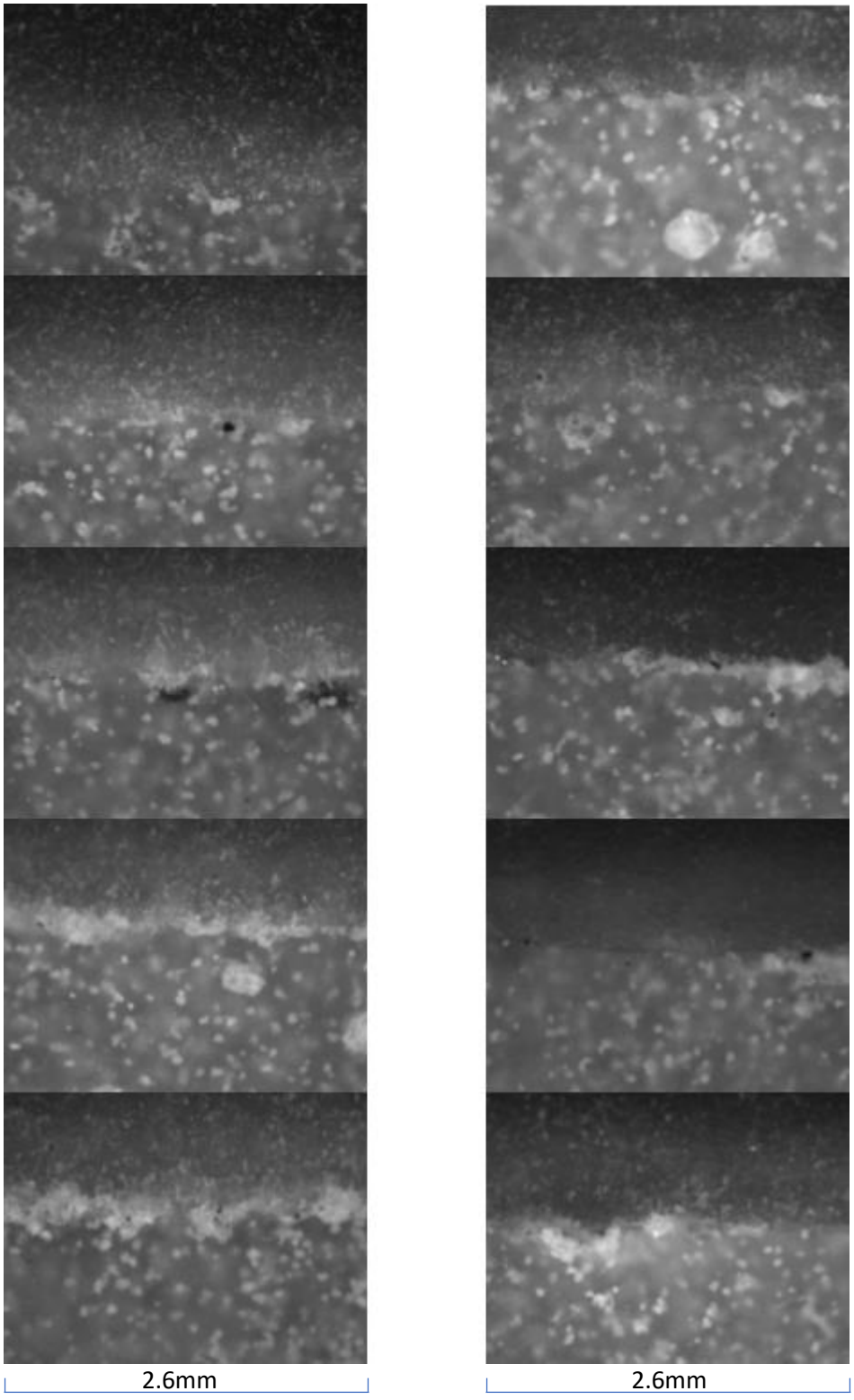

Figure 8.3-13: Bovine Group with pressure Microscopic Interface Images
Images were taken at 10x zoom at randomly allocated points along the sample's interface.
On the left is a sample.
On the right is a second sample.

8.3.3.7.1 Non-pressure

The rough group images are in figure 8.3-7 and the smooth group images are in figure 8.3-8.

The smooth group samples' interface shows a couple of voids, practically near the ends of the interface. Though the samples in the rough group show a few more voids that are also extend across the interface, again nearer the ends of the surface. There is a white indistinct line between the interface in both groups.

8.3.3.7.2 Pressure

The smooth, rough, and mixed groups images are in figure 8.3-9 to 8.3-11, respectively; all three groups images are very similar to each other. This time, the voids at each interval appears to be smaller and less of them. The interface is more define, this is often in the areas free from voids; every now and then there is the indistinct white line, particularly near voids. In figure 8.3-12, show the cement body not far from the interface has the presents of voids too.

8.3.3.7.3 Bovine

The three sample images are in figure 8.3-13. The voids present at the interface appear to be alike in size of the voids present in the pressure interface. Yet between the three samples, there is a little more variation on frequency, the left sample (top row of figure 8.3-13) has around 14 number in total from the 5 intervals, while the right sample has 6 number in total. The group has a variation difference is greater than the other groups.

8.3.4 Discussion

8.3.4.1 Cement Viscosity

The curves of the graphs produced can aren't the ideal elastic to plastic typical stress-strain curve, but they do have a linear elastic portion before an ill-defined yield point.

The results from the two viscosities of cement rods suggest that the mechanical properties are not affected by its properties in the working stage of cementing. However, from the pull-off tensile conditions, the viscosity does have a significant effect on the cement's adhesion properties. It is unclear from the results why viscosity property of the cement in the working stage results in lower stress and strain values with the more viscous cement. There are possible explanations that can be drawn from the information in the literature. The leading suggestion would be that the viscosity affects the flow of a substance over a surface, the higher the viscosity the slower it flows and less likely to fill small spaces. From the literature, bone cement is not always descried as a substance that is very adhesive, and it requires surface contact and even penetration into certain material (like cancellous bone) to increase its adhesion. Therefore, if the cement is not making full contact with the epoxy and there are more voids on the interface, then this might be the reason for the reduced adhesion strength. To further test this theory microscopic images of the interface were obtained to see if there are more or big voids at the cement to epoxy interface. Another possibility is polymeshrinkage during curing stage of the cement. If polymeshrinkage is greater in the more viscous

cement then it is possible that this too pulls the cement away from the surface more than the lower viscosity cement and this too will create more and larger voids at the interface. There needs to be a test to examine if the flow and/or the polymeshrinkage are the causes of different cement adhesion properties. Another possible reason is the surface properties of the two cement's viscosities, if the surface of the medium viscosity cement could have more of a 'sticky-ness'/chemical bonding factor that this could create a stronger bond to the epoxy over the high viscosity cement.

The cement always failed at the interface and not within the cement body, this could be to the observed cement to epoxy interface mechanical properties fail at 10 times lesser than the mechanical properties of the cement alone. Therefore, the mechanical properties of the cement do not affect the adhesion properties of the cement to epoxy interface. Mann *et al.*[87] estimated the adhesion strength (ultimate stress) of cement on bone under tensile condition to be approximately 1.35MPa which is approximately 10 times smaller than the adhesion strength of medium viscosity cement, and approximately 5 times smaller than the high viscosity cement value observed in this study. It appears to be the interface is a weak point in the composition as the cement can with stand higher tensile forces without breaking.

8.3.4.2 Cement Rods

This test was to observe how the tensile properties vary amongst the 68 cement samples from different batches. Because the cement properties can depend

on the mixing technique, this was to prove that the batches produced similar cement properties so that the cement results can be can be compared between batches. From the one-way ANOVA, there was no significant difference between the batches of the cement's mechanical properties. This was assumed to be the case for the adhesion pull-off tests. In the non-pressure tensile pull-off samples, the batch affects the ultimate load strength; in the non-pressure shear pull-off samples, the batch affects the ultimate load strength and stiffness; and in the pressure pull-off samples the mixed group had the stiffness, and ultimate load and displacement affected by the batch variable. The epoxy samples in the rough group had differing degrees of roughness, so to eliminate the rough surface as a variable, the smooth group in the non-pressure shear and tensile pull-off were analysis separately. They too had the significant effects of batch on the same properties: non-pressure tensile pull-off samples, the batch affects the ultimate load strength; and the non-pressure shear pull-off samples, the batch affects the ultimate load strength and stiffness. This means there is one or more factors that could be affecting the batch that the cement adhesion properties are extra sensitive to than the cement rod's mechanical properties. From the literature, the temperature of the room and of the cement components can have an effect on the cement's properties. Everything was stored and tested at room temperature, but from day to day this fluctuated due to factors such as the weather. Another possible variance source time during the working phase of the cement, all samples were cemented within the working stage time frame but some batches were faster to do and other batches took a little longer to cementing. This difference of a couple of minutes could play a factor on

the cement's adhesion because during the working stage of cementing the cement's properties are still changing and becoming solid.

Comparing these results to the literature, the mechanical properties of the cement rods are very similar. For example, the average Young's modulus of the cement rods is 1.6GP; Saha and Pal[79] calculated hand mixed PMMA to be 2GPa; yet Harper and Bonfield[252] had a higher range of Young's Modulus 2.26GPa – 3.53GPa. The average ultimate stress and strain of was 41.4MPa and 4.4%, respectfully; while Saha and Pal had ultimate stress at 30.8MPa and Harper; and Bonfield had ultimate stress ranging from 31.7MPa to 51.4MPa and ultimate strain 1.41% to 2.48%

8.3.4.3 Non-Pressure Tensile Epoxy Pull-Off

This test was performed to observe how the surface roughness affects the cement adhesion properties. With the analysis, the ultimate load was the only property to be effected by the batch, group, and batch-group interaction. This means that along with the batch significantly affecting the ultimate load the surface texture also significantly affects the ultimate load.

Since the smooth group has a larger ultimate load, it can be said that smooth group has greater adhesion strength than the other two groups. Intuitively, a rough surface will provide greater surface area for the cement to adhere to and, as discussed by Waanders (2010) and Skripitz (1999) [86], [100], the strength of the cement-bone interface is proportional to the contact area. From the microscopy photos, the smooth epoxy appeared to have smaller and less frequent voids at the interface compared to the rough interface. This could be one potential reason why

the smooth group has a larger ultimate load value as there is reduced contact area for adhesion for the rough group. There are a number of possible reasons why there are more voids observed in the rough than the smooth group: the cement is too viscous to fill the gaps; the epoxies samples were not pushed together adequately to bring the cement into full contact with all the exposed surfaces; or polyermerisation shrinkage occurred during curing stage of the cement[105], [110], thus pulling away from the surface. Additionally, to the voids present at the interface, the sharp edges on the rough surface interface introduced stress concentrations under loading, which provided ideal crack initiation sites, thereby reducing ultimate load value.

It is unclear why the mixed group had lower adhesion properties than the other two groups, intuitively it would have thought to fall between the smooth and rough group because it had a surface of each type. The results suggest that having a mixed group should properly be avoided, possibly having a bumpy bony surface with a smooth implant possibly should be avoided, but this needs further investigation. The chi squared analysis of the mixed group demonstrated that the texture had no effect ($P>0.05$) on the interface failure prediction whereas the order of cement had a significant effect ($P<0.05$) on the side of interface failure; this suggests that the time of the work stage of cement affects the cement's adhesion properties.

This work was able to be further investigated by applying pressure to the cemented sample during curing, this could demonstrate if the voids were partly

cause by inadequate pressure and, if they were reduced in size and frequency then, were they the reason for the reduced adhesion properties of the rough group.

8.3.4.4 Non-Pressure Shear Epoxy Pull-Off

This test is to observe how the surface roughness affects the cement adhesion properties under shear pull-off conditions. There were conflicting results from the two-way ANOVA and the t-tests of the significance value of the group affect had on the adhesion properties. This would be due to the t-test only comparing two at time rather than all three; taking all three at a time, the difference in the variances between the groups is wider but when only comparing two at a time then the variance is reduced. This means that between the three groups there was a significant different but it was not significant enough when comparing them as pairs. This means the stiffness and ultimate load were significantly greater in the smooth group than the other two groups; and likewise, the mixed group stiffness and ultimate load were significantly smaller than the other two groups.

Just like the non-pressure epoxy tensile pull-off tests, the there are three possible reasons for the smooth group performing better than the other two groups in terms of stiffness and ultimate load: inadequate pressure while cementing, polymerisation shrinkage, and sharp edges creating localised stress concentrations. It is unclear why the mixed group is again the lowest adhesion properties when it is expected to be between the other two groups because it has potentially a stronger and weaker surface. Again, this data could be a warning not to use a burred bony

surface with a smooth implant but further work is needed before any proper conclusions can be drawn.

Mann *et al.* (1999)[87] data suggests that the shear adhesion strength is stronger than the tensile adension, which appears to contradicts the work of this work as the adhesion strength under shear conditions is less than the tensile conditions. However, the shear and tensile pull-off adhesion values cannot be compared because they are expressed in nominal terms and not in dimensionless terms. However, the dimensionless adhesion properties suggested that (even with the errors in the calculation) the tensile pull-off were greater than shear pull-off property values. The difference between this experiment and Mann *et al.*'s was the material interfaces; Mann *et al.* investigated bone to cement interface that included cement penetration into the cancellous bone matrix this could very much increase the shear adhesion properties as the material in the penetration zone is a composite material. The work presented here investigated lacks a penetration zone, and thus there is no composite material zone that could potentially increase the shear adhesion. The results here can be used to relate the adhesion properties with the properties of a bone to cement interface that the cement failed to penetrate into the bone matrix. Plus, the results of the different surface texture could be assumed for a cement to bone interface with penetration.

From the mixed group, the chi squared analysis demonstrated that texture had an effect ($P<0.05$) on interface failure when under shear loading. This seems to contradict the above numerical data because it suggests that the rough surface has

a greater adhesion than the smooth surface. Therefore, further work is required to confirm this analysis.

8.3.4.5 Pressure Epoxy Pull-Off

The ANOVA analyses demonstrated that the batch still affects the cement adhesion properties. Yet the design in this experiment allowed for paired t-test analyses of samples in each batch and thus removing the batch variation; the follow two conclusions were extracted from the paired t-tests. The order of applying cement to a textured surface in the mixed group did not significantly affect the adhesion properties. Secondly, the surface texture does not affect the adhesion properties. This suggests that the adhesion properties between the three groups are very similar to each other and thus they are un-affected by the surface roughness. This is not support by the work of Skripitz (1999)[100] who have concluded with PMMA that a rougher surface has better adhesion force than a smooth surface but the adhesion property of PMMA to PMMA may have different effect than PMMA to other material.

From the microscopy, the voids at the interface were smaller and less frequent in both rough and smooth group than from the previous non-pressure results. Both the smooth and rough group had similar number of voids in the samples inspected and the voids were smaller in size. This strongly suggests the voids at the rough interface were the reason that the rough group did not perform as well in the previous non-pressure experiment. There were two suggestions why voids were present at the cement to epoxy interface, the first was there was

adequate pressure to have the cement to make full contact with the epoxy surfaces; the second was due polymerisation shrinkage. It is uncertain if either or both of these aspects were reduced in this experiment and further investigation would be needed to finalise which factor plays a more significant role. There was also the fact that the design of this experiment created extra compressive pressure in the cement due the presence of the paper guides, this would also played a role in reducing the voids present.

The mixed group from the pressure experiment seemed to show that the surface texture affected the interface failure; this was at the rough surface stayed had a stronger adhesion to the cement. However, the chi square test failed to show that there is a relationship between the surface texture and the interface failure, but the chi square value was close to the critical number plus sample size was small. Further work is required to increase the sample size. If there is a relationship between the surface texture and interface failure in the pressure experiments and not in the non-pressure experiments, the possible reason for this change was the only two samples were cemented in each batch, which means cement was applied practically at the same time (up a second difference due to human factors) thus eliminating the cement property changing over time factor[79].

The applied pressure has a clear and significant effect on the ultimate load and displacement properties, strongly indicating that applying pressure during the cementing of the samples increases the adhesion strength of the cement of all the

groups. This correspond to the work of Hori and Lewis[106], their work showed a pressure is needed for cement adhesion.

8.3.4.6 Pull-Off Tests from Bovine

This experiment does not return conclusive results due to the large variance observed in all parameters. Through with most of the paired samples, the adhesion properties were considerably higher for the smooth group than the rough group, and the same can be said for the average values in table 8.3-17.

This experiment had big limitation variation and small sample size; the main variation was due to uncontrollable factors of bone quality, and bone cleaning ability. The age, sex, and health of the bovine bone was unknown, these factors play a role in determining the density and other bone quality parameters, which can affect the adhesion of the bone cement. There wasn't access to a pressure or pulse water lavage this meant that the bone cleaning may have not been the same level for all samples. Both of these factors were aimed to be minimised by pairing up a burr and saw surface in the same batch and thus a pair t-test was performed. The sample size was originally meant to be 16 all from the distal tibia but the set-up of this experiment meant the cut off plateaus were need to provide more sample, but this still only produced 12 samples in total, 4 useable pairs.

Mann *et al.* in 1997 demonstrated the interface adhesion strength of bone to cement to be 1.28MPa. The work present in this investigation calculates the means of the smooth and rough groups ultimate stress (adhesion strength), were 0.720MPa and 0.373MPa (respectfully). The smooth group's ultimate stress is over

half the value of Mann *et al.*'s results, but factors such as vacuum cement mixing, may explain this difference. Another possible reason could be the feat that Mann used human bone whereas the experiment presented here used bovine bone.

8.3.5 Conclusion

The set of experiments described in this chapter had a positive impact on the investigation's design of concepts. The first conclusion is at the mechanical properties of cement is not affected by the different viscosity yet it does alter the adhesion properties. The results suggest that the less viscous cement may have a greater adhesion property.

The second conclusion is that applying cement with pressure is critical to increase the adhesion properties. The microscopic images suggest that the pressure applied reduces the size and frequency of voids at the interface; relating this to the adhesion property results suggests that voids play a part in reducing the cement's adhesion strength.

Lastly, there is not significant difference between the rough and smooth epoxy groups, yet the mix group has weaker adhesion properties than the other two groups. This suggests that the macro surface texture does not affect the cement's adhesion but when the surface textures are mixed then the cement's adhesion is reduced with the smooth interface failing first. This indicates that using the burr for removing bone tissue does not reduced the cement adhesion strength

and therefore it is still a viable bone removing method if the matching surface of the prosthesis has a similar macro texture.

Chapter 9

Virtual Experiments of Concept Ideas

At the end of the initial concept generation stage, there were a number of questions that desired to be answered. One important aspect was how the mechanical loading is influenced by changing the undercarriage profiles of the prosthesis. It was determined that the best approach to answer this question would be employ virtual modelling in the form of finite element analysis (FEA). The results from the virtual experiments were able to provide supporting evidence in the concept selection process in chapter 10.

9.1 Introduction

Currently the market uses a flat surface because this is only practical option for oscillating saw, but with robotic orthopaedic tools being used in knee arthroplasty, a burr may create different shapes. Long term factor for prosthesis survivorship is dependent on the prosthesis geometry and stiffness[93]. This factor taken into consideration in the concept generation process in the previous chapter, *6 Concept Generation* and it opened up the question what profile of the undercarriage of the prosthesis are best for transference of load to the tibia? It was debated that there were three load patterns to consider. First is the load

distribution in the head of the tibia, it was believed that the best distribution of the forces towards the outer surface of the tibia where the bone is in a cortical matrix structure; this tissue is better suited for the transference of load. The next best distribution would be a uniform distribution of the forces across the transverse plane. The second pattern to consider is stress concentration – in these zones there is a build-up of stress concentration being experienced that may be higher stress that is being applied systemically. Part of the material with stress concentration may fail and this can create new stress concentration zones that may subsequently, this will propagate through the material. The final load patterns to consider is stress shielding this is where localised areas experiences zero to low stresses compared to the rest of the system; in most materials this is not a design flaw, unless the material needs to be spared to make the system light or cost effective then design optimisation follows to prevent stress shielding. However, according to Wolff's law, if an area of bone does not experience loading the bone remodels itself absorbing the bone material to use in areas that experience loading. Therefore, if the bone under the prosthesis does not experience loading i.e. it is experiencing stress shielding, it then the bone tissue is resorbed and this could process could initialise aseptic loosening of the prosthesis for both cement and cementless types.

From the ideas in the design matrix, several them applied basic shapes for their engineering principles. For example, arches/circles radiate a uniform loading across the surface or a slope can direct a load to a stronger/securer point on the tibia. The profiles that were modelled are shown in table 9.1-1 in their intended

orientation on the medial side of the knee - the lateral side would in real life be slightly different because is more of soft tissue balance. The results from this experiment focusses on aspects which have affected in the design process and does not try to convey and/or explain the mechanics of each component-bone system. This section provides the evidence required for the design process in reducing the concepts to a final two.

9.2 Aims

To utilise finite element analysis (FEA) to observe the stress distribution within the proximal portion of the tibia when different prosthesis undercarriage shapes are loaded under axial and shear conditions. Von Mises plots are obtained from the FEA and are compared to determine the better undercarriage shapes to design a prosthesis around.

9.3 Results

As mentioned in the introduction, the results are only going to focus on the stress patterns that will inform the design process. All results in both conditions had high stress in the distal region of the tibia and had low stress in the medial half of the tibia.

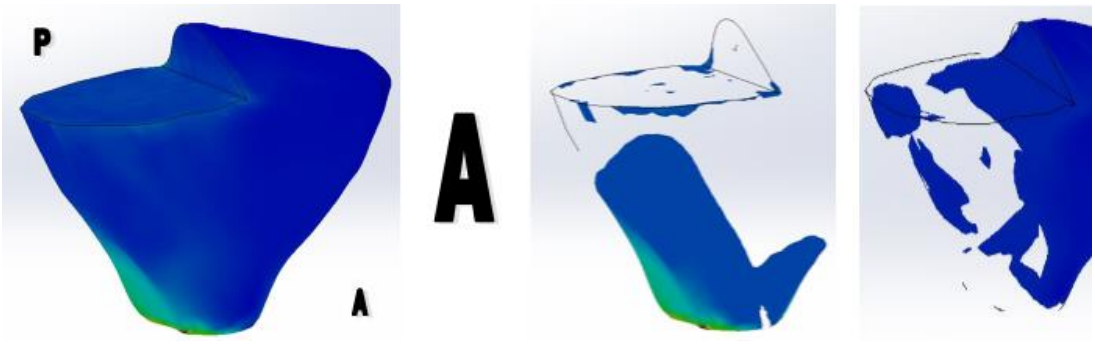

Figure 9.1-1: Von Mises plots of the Flat Profile under Axial Loading

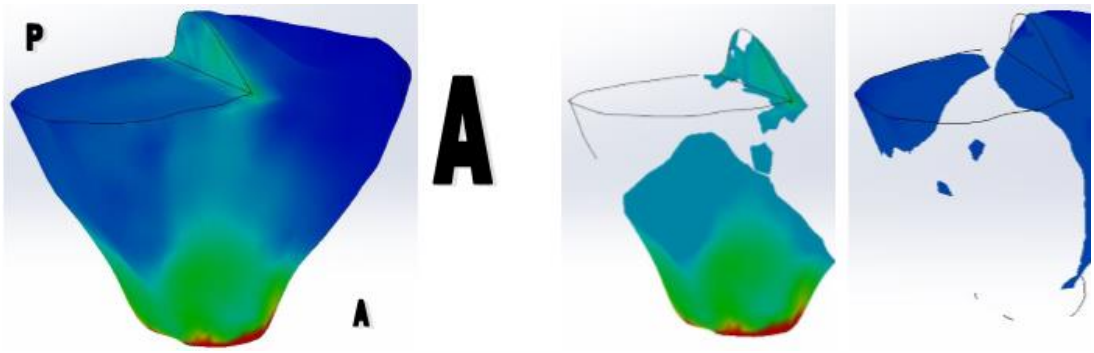

Figure 9.1-2: Von Mises plots of the Flat Profile under Axial Loading

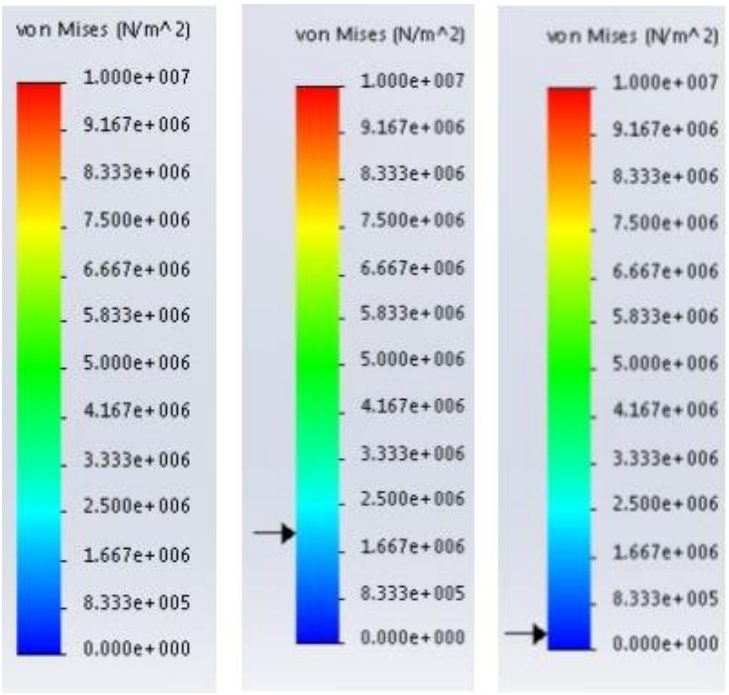

Figure 9.1-3: The Three Scales
On the left is the von Mises scale from 0MPa to 10MPa. In the middle is the same Von Mises scale but has an arrow that indicates the level the ISO clipping for the stress distribution. The right hand side is the Von Mises scale with the arrow indicating the ISO clipping for low stress.

9.3.1 Flat Undercarriage

9.3.1.1 Axial results

The 'hot' colours are primarily located on the distal part of the tibia (figure 9.1-1), yet some light blue zones around the rim of the cut away surface. The stress was distributed through the middle of the lateral side of the tibia. As the transverse plan plane travels distally, the stress increases. The dark blue areas are located on the outside surface of the tibia on and on the posterior bony landmark.

9.3.1.2 Shear Results

Looking at the von Mises of the tibia in figure 9.1-2; the hot colours are primarily located on the distal part of the tibia in both conditions.

Under shear conditions the cut wall has greater von Mises stress that range in the 3-5MPa range. The dark blue area is located on the lateral side of the surface tibia. The Stress is distributed down the outside surface of the tibia originating from the anterior and posterior wall corners.

9.3.1.3 Discussion

Under axial loading the stress pattern appears to be fairly good because there the 'hot' colours were not present in the area of interest which indicated that stress concentration is unlikely to occur; plus, the dark blue zones that indicate areas of low von Mises stress (though above zero), which could result in stress shielding, were not extensive on the lateral side of the tibia. The stress distribution is not of ideal scenario of directing the stress to the surface of the tibia yet it is does

have the stress almost uniform across the transverse plane which again indicated a low possibility of stress concentration and it the middle of the tibial head would take on an even load. Under shear loading the stresses appear to be travelling along the surface of the tibia; this is good indication that the cortical bone in vivo will be bearing most of the loading. This profile acts like a control for the other shapes because it mostly represents the market standard minus features such as pegs.

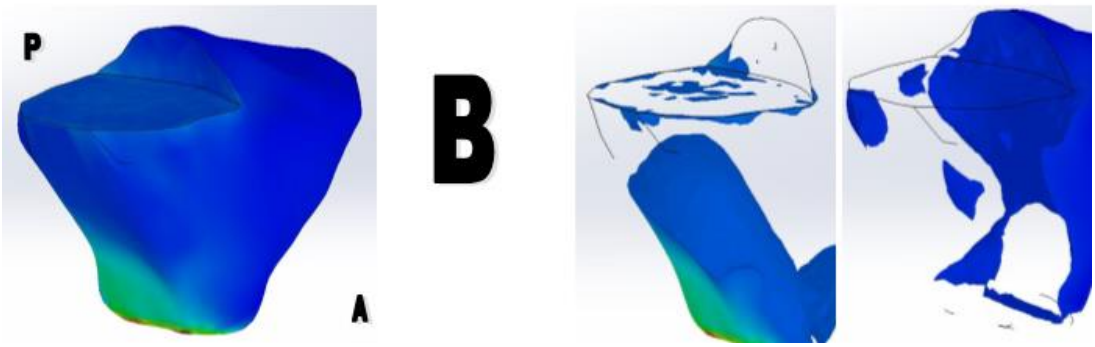

Figure 9.1-4: Von Mises plots of the Curve Profiles under Axial Loading

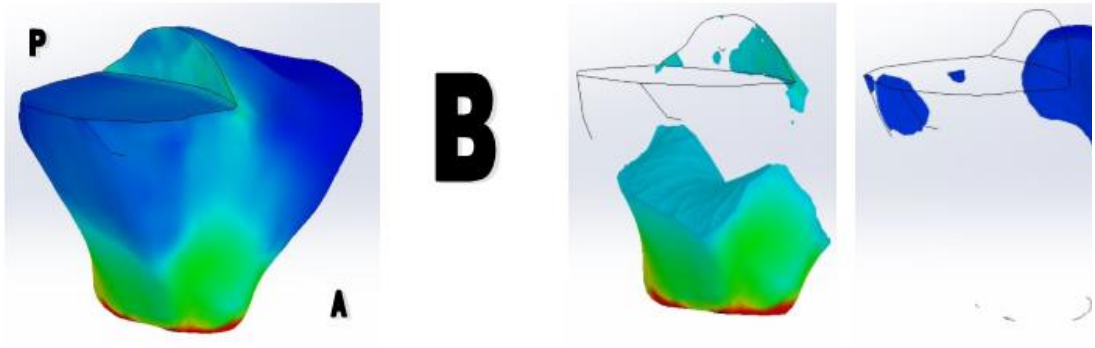

Figure 9.1-5: Von Mises plots of the Curve Profiles under Shear Loading

9.3.2 Flat with curved wall

9.3.2.1 Axial Results

The hot colours on the flat curve profile under axial condition is on the distal part of the tibia again but the light blue zones cover more of the cut away surface in figure 9.1-4. The dark blue colour zones are located on the outside surface of the tibia. The stress distribution is through the middle of the lateral side of the tibia, just like the flat profile, as the transverse plane travels distally the stress increases.

9.3.2.2 Shear Results

The hot colours in figure 9.1-5 are again on the distal part of the tibia and on the cut wall. Like the flat profile, the hot colours under shear condition are on the wall cut but It seems the magnitude is slightly lower than the observed magnitude on the flat profile. The dark blue zone is mainly at the bony landmark posterior of the tibia. The stress distribution goes down the outside surface of the tibia originating from the anterior and posterior corners of the wall cut.

9.3.2.3 Discussion

The addition of a curved tibial wall did not appear to significant change the stress patterns obtained from the von Mises plots in both conditions. Under shear stress, the anterior half of the cut wall is experiencing more von Mises stress than the control flat profile. That was to be expected as the curved wall provides some resistance to the shear loading and directs more of the stresses across the surface, figure 9.1-5. The downfall could be the wall edges break off because the thin profile.

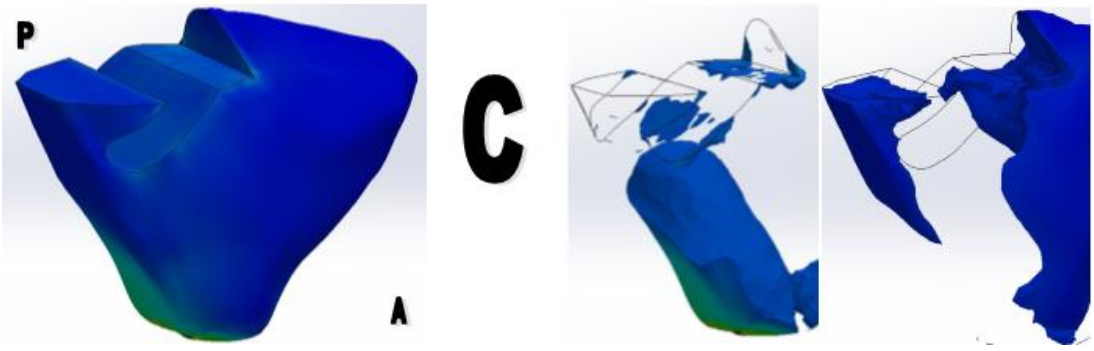

Figure 9.1-6: Von Mises plots of the Undercut Profiles under Axial Loading

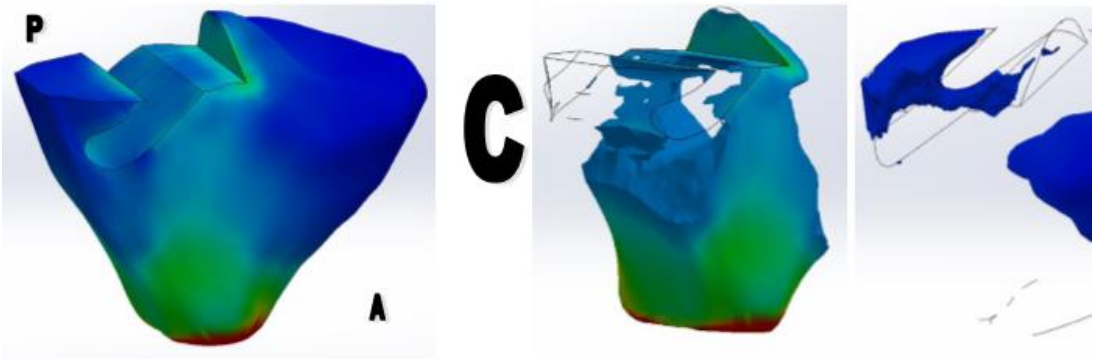

Figure 9.1-7: Von Mises plots of the Undercut Profiles under Shear Loading

9.3.3 Undercut

9.3.3.1 Axial Results

The axial loading condition in figure 9.1-6 has hot colours primarily on the distal part of the tibia; there is light blue areas located at the wall corners and in the middle of the slant. Almost the full volume of the lateral 'jut' does not experience high von Mises stress. The stress is distributed through the lateral half of the tibia either close to the lateral outer surface side or to the undercut slot.

9.3.3.2 Shear

The cut wall in figure 9.1-7, the wall corners, the jut edge, and the base of the undercut have at least green zones of von Mises stress under shear conditions. Like the axial loading condition, the lateral 'jut' created from this profile is almost entirely dark blue. The stress is distributed in two paths, the first is similar to the axial loading conditions and the second is from the anterior and posterior wall corners down the respective surface of the tibia before filling in the middle of the lateral half of the tibia.

9.3.3.3 Discussion

The stress concentration, indicated by the hot colours, was slightly worse in volume as a greater areas of the cut surface was shaded in light blue; the magnitude of the von Mises stress is only slight lighter shade of blue. The stress distribution is better because it directs stress to the lateral outer surface of the tibia, this suggests

there is a potential that the cortical bone might carry more of the loading as it is being directed towards the tibia surface.

The shear loading condition has the stress distribution more favourable because more of the stress is carried nearer the surface of the tibia where the strong cortical bone can carry the bulk of the load.

The main concern is the lateral ‘jut’ created by the profile because it is lacking von Mises stress in both simulated conditions. This may properly means that the bone density will decrease in the that can start the aseptic loosening of the prosthesis.

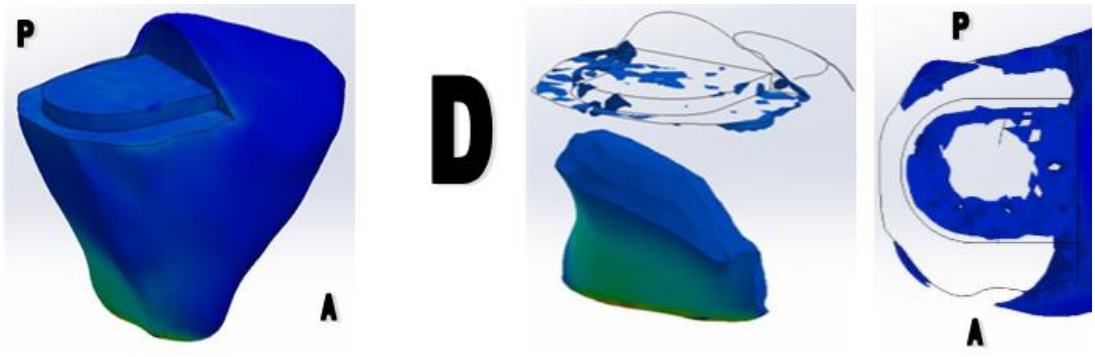

Figure 9.1-8: Von Mises plots of the Rim Profiles under Axial Loading

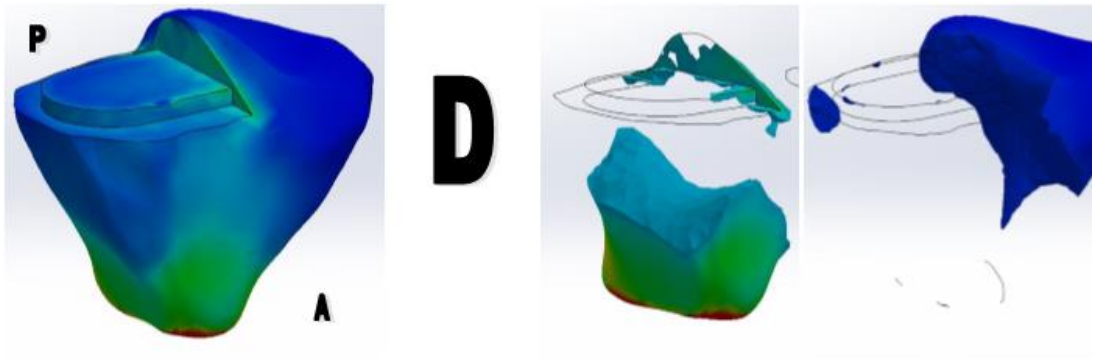

Figure 9.1-9: Von Mises plots of the Rim Profiles under Shear Loading

9.3.4 Rim

9.3.4.1 Axial

There weren't apparent 'hot' colours on the tibia in figure 9.1-8. The raised up kernel section had dark blue zones. The stress distribution is similar to the flat profile: through the tibial head near the posterior and outer surfaces.

9.3.4.2 Shear

The location of the 'hot' colours in figure 9.1-9 were along the wall and concentrated at the raised corners. The dark blue zones are dotted on the proximal surface: bony landmark, raised middle surface, and tibial surface. The distribution is like the flat profile: follows the tibial anterior posterior surface from wall corners.

9.3.4.3 Discussion

The distribution of the stress appears to be slightly better than the flat profile's stress distribution under axial loading condition because the stress seems to be directed more to the outer surface of the tibia but it was not as much as excepted; slight modifications to this design could direct more of the stress to the outer surface. There seems to be undesirable stress shielding on the raised kernel. The stress distribution, in shear loading condition is very similar to the flat surface.

Both of these scenarios are very similar to the flat shape but it did not as well perform as expected – this was to have all the stress distributed to the surface pf the tibia. This shape removes more of the bone tissue, in particular cortical bone tissue, which isn't ideal if the stress distribution isn't greatly improved.

Figure 9.1-10: Von Mises plots of the R10 Profile under Axial Loading

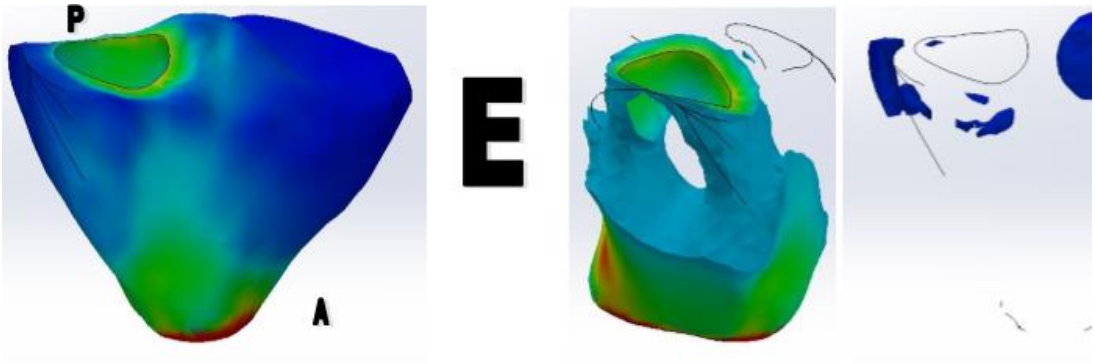

Figure 9.1-11: Von Mises plots of the R10 Profile under Shear Loading

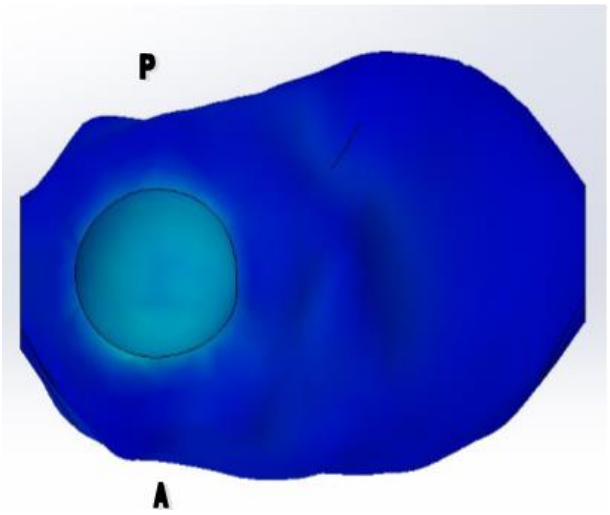

Figure 9.1-12: Superior View of R10 Profile
This figure is from the von Mises plot of the R10 under axial condition.

9.3.5 R10

9.3.5.1 Axial

The axial condition produces 'hot' colour von Mises plots (figure9.1-10) around the base of the sphere, seen in the superior view in figure 9.1-12. From this stress concentration at the base of sphere, the stress is directed along longitude axis. The proximal surfaces of tibia almost entirely dark blue.

9.3.5.2 Shear

The von Mises (figure 9.1-11) displays yellow concentration on the top rim of the spherical cut, and green on the anterior and posterior face of the spherical cut. The stress is directed down along the longitude axis from the two green stress zones. There are three zones of dark blue: the transverse line tangent to the base of the sphere cut, the posterior bony landmark, and the proximal lateral surface of the tibia.

9.3.5.3 Discussion

The von Mises shows the load is not uniform on the cut surface and thus creates concentration at the base of the sphere. The stresses travels through the middle of tibia, primarily on the theoretically weaker cancellous bone and not through the cortical bone on the surface of the tibia. The lack of stress concentration across the proximal outer surface of the tibia suggests that the cortical bone may experience resorption which is not be favourable as it will decrease the strength of the knee.

The stress concentration appears to be lesser in the shear loading condition than the axial loading condition. The stress distribution is also slightly better because the stress is covering more volume in the tibia but it is still transferring down the middle of the tibia, through the cancellous bone. The dark blue area is slightly better as it lesser in volume but it still located on the cortical bone which ideally should be loaded to preserve strength.

Matching the two simulations conditions together, the load is transferred primarily through the tibial cancellous bone, not ideal as this could mean there is reduced stresses going through the cortical bone and it leaves large areas of the tibial surface (i.e. cortical bone) stress shielded. The stress concentration is a concern in the axial loading.

Figure 9.1-13: Von Mises plots of the R15 Profile under Axial Loading

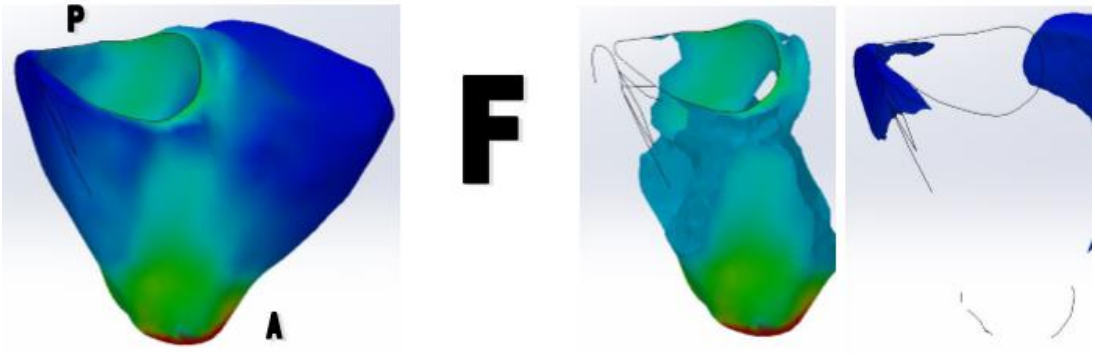

Figure 9.1-14: Von Mises plots of the R15 Profile under Shear Loading

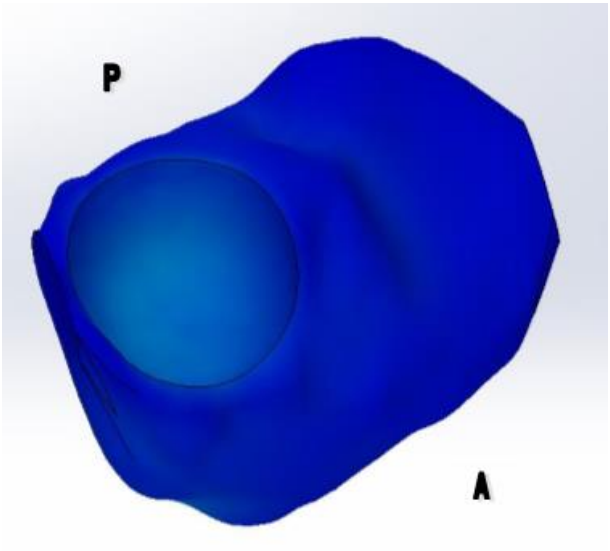

Figure 9.1-15: Superior View of R15 Profile
This figure is from the von Mises plot of the R15 under axial condition.

9.3.6 R15

9.3.6.1 Axial

The yellow and greens colours are no longer present at the base of the sphere, instead the cut surface is a light blue colour, seen in the superior view in figure 9.1-15. The stress is directed again along the longitude axis in figure 9.1-13 from a larger area of the sphere's base and the stress distribution is less in concentration. The dark zone is almost the entire proximal surface of the tibia.

9.3.6.2 Shear

The yellow and green colours in figure 9.1-14 are darker shade in the same locations as R10 under axial conditions. The stress distribution is similar to the R10 stress distributions: along the longitude axis from the anterior and posterior face of the spherical cut then filling up the middle of the lateral side of the tibia. Again, the proximal surface of the tibia is plotted in dark blue in the von Mises plot.

9.3.6.3 Discussion

The lack of stress concentration under axial loading is a good sign, though it requires a large volume of cancellous bone removal. The reduced stress concentration is most likely caused by the increase in surface area.

Because the stress is distributed through the cancellous bone, this causes the surface of the tibia to have low concentration stress that is indicated by the dark blue area, this might not be ideal.

The stress concentration appears to be better in this loading condition than the axial loading condition. Also the stress distribution because the stress is covering more volume in the tibia but it is still transferring down the middle of the tibia, through the cancellous bone.

The stress concentration in this profile is better than the smaller R10 sphere in both conditions. The distribution was also slightly improved by the bigger size. Both of these conditions are good but it does require more cancellous tissue removal yet reduces the cortical bone removal.

There is still the problem with the lateral cortical bone lacking stress concentration.

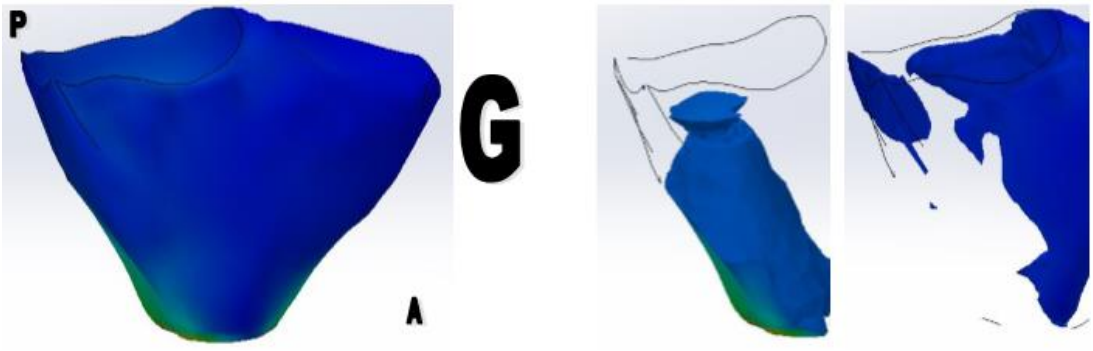

Figure 9.1-16: Von Mises plots of the R20 Profile under Axial Loading

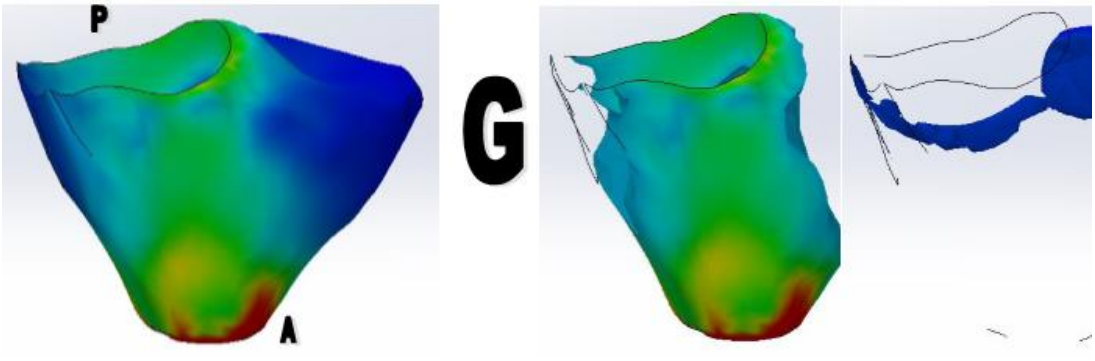

Figure 9.1-17: Von Mises plots of theR20 Profile under Shear Loading

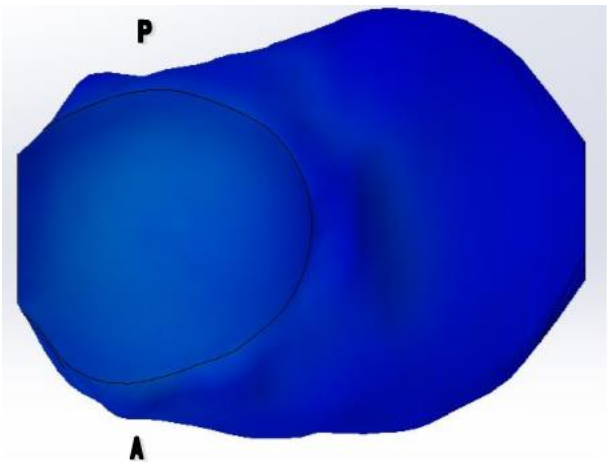

Figure 9.1-18: Superior View of R20 Profile
This figure is from the von Mises plot of the R20 under axial condition.

9.3.7 R20

9.3.7.1 Axial

Under axial loading conditions, there did not appear to be any 'hot' colours on the proximal surface of the tibia, seen in the superior view in figure 9.1-18. The stress distribution is like the other spherical profiles (figure 9.1-17), distributed along the longitude axis from under the base of the sphere. The dark blue area is now only located around the proximal posterior and proximal lateral side of the tibia.

9.3.7.2 Shear

The shear condition has green 'hot' colour in figure 9.1-17 is similar place to the other spherical profiles: across the anterior, medial and posterior side of the tibia. The stress is distributed along the longitude axis from the mentioned stress concentration on the cut spherical surface. The dark blue is in a line along the transverse axis from the lateral surface to the middle of the tibia, tangential to the base of the cut sphere.

9.3.7.3 Discussion

The larger and mostly flat surface of the bigger sphere appears to be better at reducing stress concentrations. Though it still leaves the proximal surfaces of the tibia to be in low von Mises stress.

The bigger surface area means the stress distribution is closer to the outer surface area. The low stress in the middle of the tibia head under the sphere conditions may reduce the bone density and lead to aseptic loosening.

The combination of the loading may counteract the negative effects of the stress characteristics. The stress transmitted into the middle of the tibial head under axial loading may not be enough stress to prevent the reduction of bone density. On top of that, the volume of bone tissue needed to remove is more than desired.

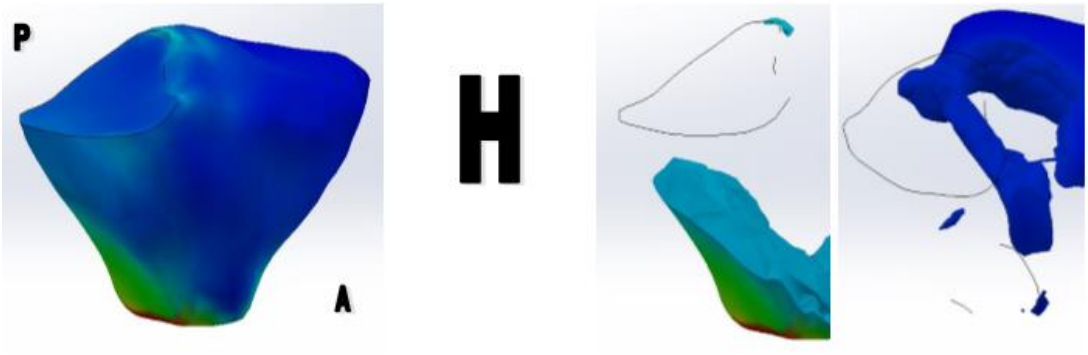

Figure 9.1-19: Von Mises plots of the Rod 55 Profile under Axial Loading

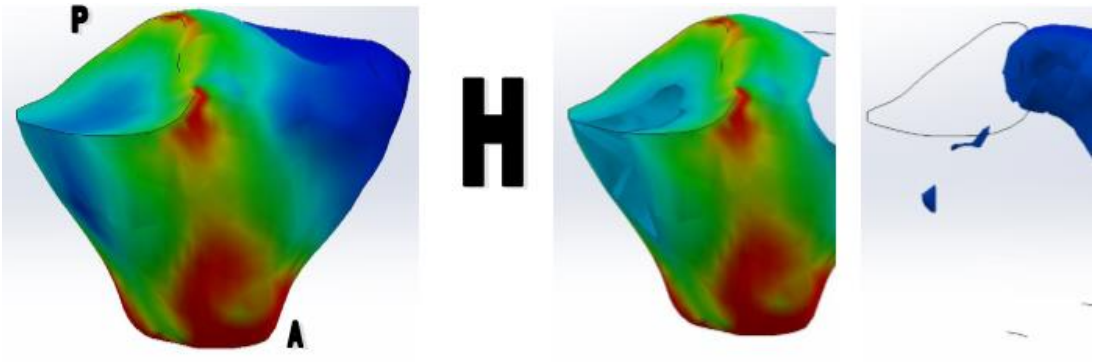

Figure 9.1-20: Von Mises plots of the Rod55 Profile under Shear Loading

9.3.8 Rod 55

9.3.8.1 Axial

The proximal rim of the cut rod surface is a light blue colour, other than that there is no other observed 'hot' colours under axial loading. Directly distal to the light blue is the location of area of little von Mises stress. It appears the main stress distribution is next to the lateral side of the tibia; the lesser stress distribution is across the proximal surface and down on both anterior and posterior surfaces of the tibia.

9.3.8.2 Shear

The shearing loading has more stress concentrated areas; the red zones are located on the proximal rim from the rod cut surface, and on the anterior and posterior surface of the tibia. The area between the loop these zones make has a range of 'hot' colours. In the middle of this loop, in the lateral side of the tibia, is the small low von Mises stress zone. The stress is distributed inwards to the dark blue zone in the lateral side of the tibia.

9.3.8.3 Discussion

This stress distribution is a closer to the desired situation of directing it to the surface of the tibia. The stress shielding is minimal, a little more than the flat profile but when the shear loading condition is applied there is almost no stress shielded areas.

The stress distribution seems to follow the desired route of primarily going down the tibial surface, where *in vivo* the stress will be carried by the cortical bone.

The two low stress zones created by the two loading conditions do not overlap which is a good sign that if the tibia is experiencing a combinations of these conditions then there might not be a risk of zones of low stress that will result in reduced bone density. Therefore, it seems that this profile is a promising one for stress patterns considered desirable.

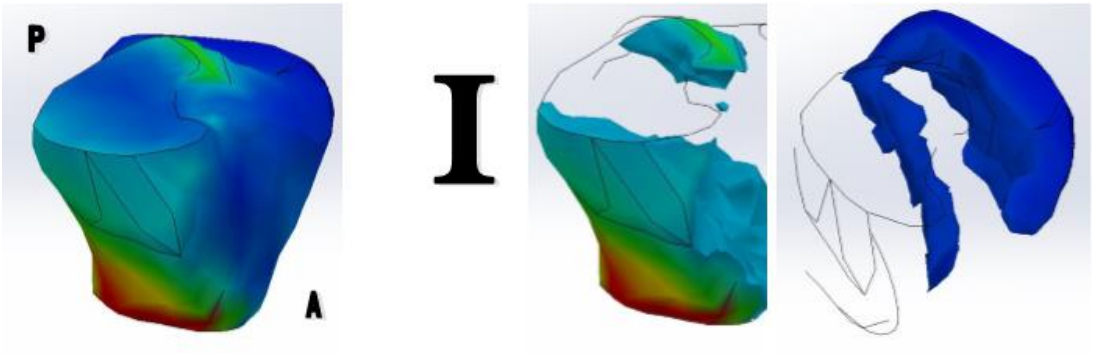

Figure 9.1-21: Von Mises plots of the Rod 200 Profile under Axial Loading

Figure 9.1-22: Von Mises plots of the Rod200 Profile under Shear Loading

9.3.9 Rod 200

9.3.9.1 Axial

The 'hot' green can be seen in the at the proximal ridge of the tibia, and light blue colours around the lateral cut edge of the tibia; this is similar to the rod55 profile under axial loading condition but with the colours less 'hot'. The stress distribution is the same as rod55 profile. The dark blue zone is through the middle of the lateral side of the tibia in parallel to the sagittal axis.

9.3.9.2 Shear

With the shear loading condition, the tibia experiences the same stress concentration and distribution as the rod55 profile but with 'hotter' colours. There appears to be no dark blue areas present in the lateral half of the tibia under these conditions.

9.3.9.3 Discussion

The axial loading condition has predicted stresses to be greater than the rod55 profile but the hottest is only green in colour therefore it is of concern of failing. The stress distribution is similar to rod55 profile, thus is considered desirable as it directs most towards the surface of the tibia. Plus the low von Mises stress location and size is the same as rod55 profile.

On the other hand, the von Mises stresses under shear loading condition is very concerning because most of the tibia is shaded in red which is greater than all

the other models. The stress distribution and stress shielding is similar as rod55 profile.

The axial condition is better than the shear condition. The knee will experience shearing forces and this larger radius might not be ideal for the implant because of the less desirable stress patterns.

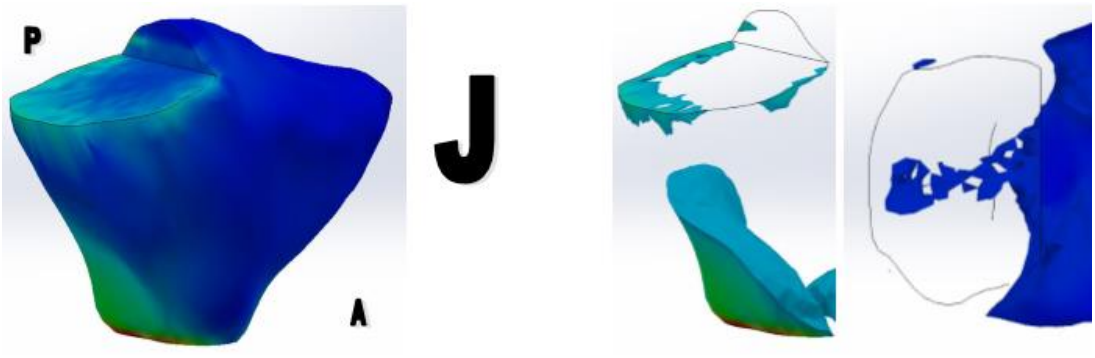

Figure 9.1-23: Von Mises plots of the Slant 10 L Profile under Axial Loading

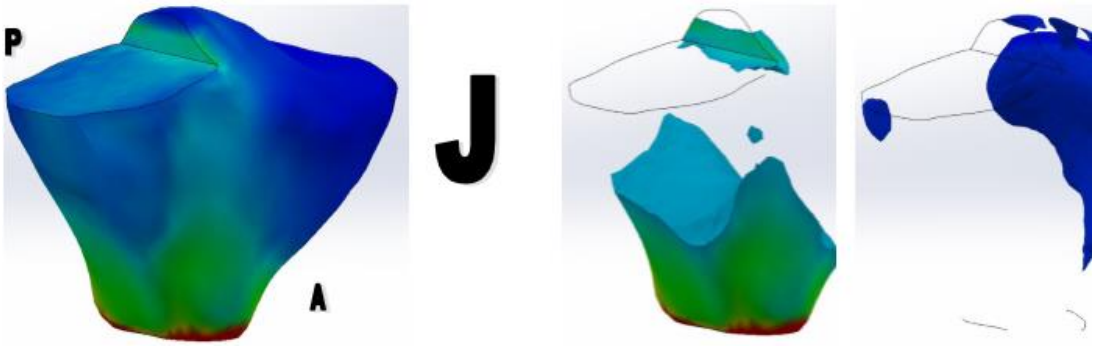

Figure 9.1-24: Von Mises plots of the Slant 10 L Profile under Shear Loading

9.3.10 Slant 10 L

9.3.10.1 Axial

The 'hottest' colour under the axial on the proximal half of the tibia is a light blue to light green located around the cut edge of the tibia. The dark blue area is on the coral plane, just under the surface of the cut tibia slant. The stress is distributed through the lateral side of the tibial head adjacent to the posterior lateral side of the tibia.

9.3.10.2 Shear

The stress is concentrated on the cut wall of the tibia with a light green colour. The dark blue zone is one the posterior bony landmark. The stress distribution is almost uniform in the transverse plane though it stress is higher near the anterior and posterior surface of the tibia.

9.3.10.3 Discussion

The stress distribution under axial loading is a mix of the desired and the flat profile pattern; this potentially means more of the stresses will go through cortical bone of the tibia. The stress distribution under shear loading conditions is half ideal because it won't create stress concentration in the tibial head but it does not direct the stress to the stronger outside surface of the tibia.

The spotted nature of the dark blue area for the axial loading condition means it is just in the von Mises stress cut off. Under shear loading condition, the

dark blue area is in not an ideal location because it could mean a breakdown of the cortical bone but it is less likely to cause aseptic loosening of a prosthesis; yet the knee will experience a combination of shear and axial loading thus the lateral side of the tibia may not be as strong as other profiles but won't be of concern.

Overall this shape suggests good stress concentration and fairly good stress distribution. The stress shielding is most likely not going to happen because the knee will experience combination of the loading conditions and since they don't overlap, all the bone should experience stress. One concern that isn't addressed in the objective is the possibility of migration, this implant is relying on good attachment to the bone and if it doesn't there are no physical features to prevent the prosthesis from slipping off the knee due to the slant.

Figure 9.1-25: Von Mises plots of the Slant 10 M Profile under Axial Loading

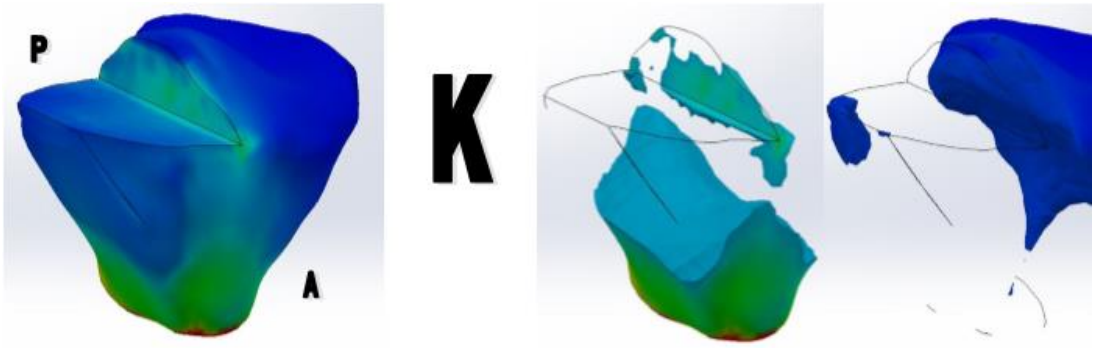

Figure 9.1-26: Von Mises plots of the Slant 10 M Profile under Shear Loading

9.3.11 Slant 10 M

9.3.11.1 Axial

Under axial conditions the hot colours are located on the anterior and posterior cut edge of the tibia. The stress is distributed through the lateral side of tibial head, predominantly from the posterior wall corner down the posterior surface of the tibia. There are two dark blue zones:- on the posterior bone landmark and on the lateral surface of the tibia.

9.3.11.2 Shear

The shear condition has the 'hot' von Mises colours on the anterior wall corner area and the dark blue von Mises stress is on the posterior bony landmark. The stress is distributed predominantly on the anterior and posterior surface from the wall corners. Then it radiates inwards head before distributing to the latera side of the tibia, uniformly in the sagittal plane.

9.3.11.3 Discussion

The stress is distributed in both cases across the tibial surface in the middle but not at the lateral surface of the tibia; this leaves the lateral side with low von Mises stress as shown in figure 7.1-9K.

The tibial wall will prevent the migration of the prosthesis on the transverse axis but at the cost of transferring the stresses through the middle of the tibial head.

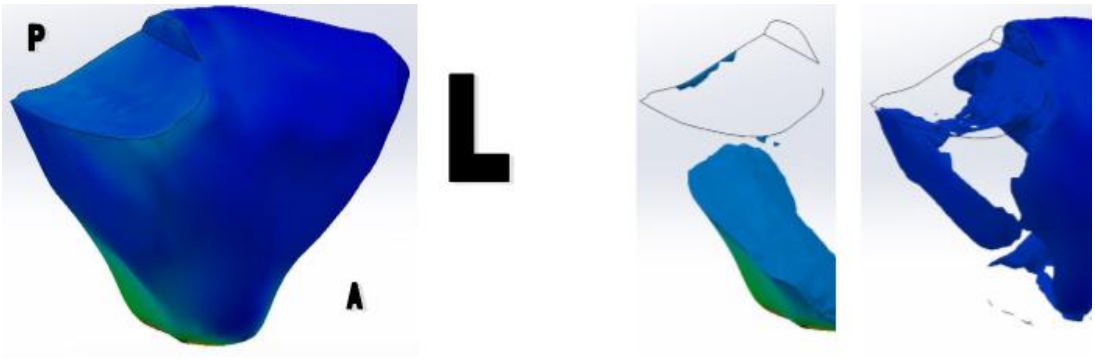

Figure 9.1-27: Von Mises plots of the Cone Profile under Axial Loading

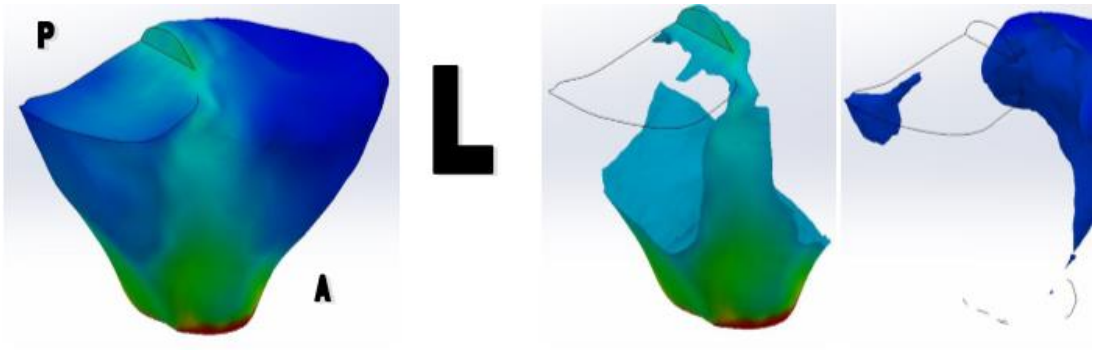

Figure 9.1-28: Von Mises plots of the Cone Profile under Shear Loading

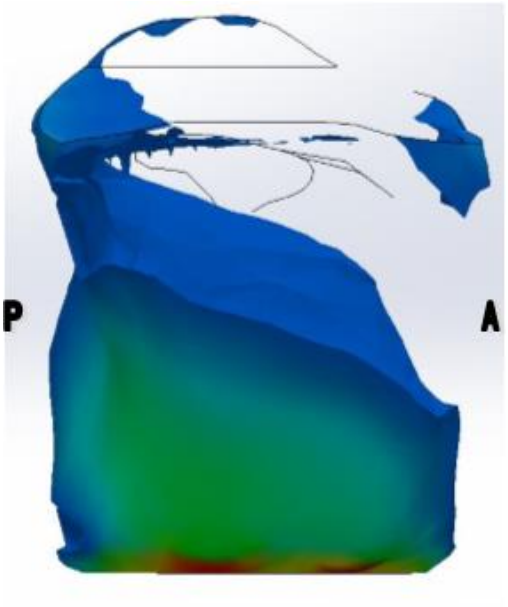

Figure 9.1-29: Iso Clipping of Cone
This figure is from the von Mises plot of the Cone under axial condition.

9.3.12 Cone

9.3.12.1 Axial

The cone does not have any hot colours under axial loading conditions but it has light blue areas at on the cut curve surface, in particular near the anterior and posterior edge. The dark blue zone appears to be almost continuous. It from the proximal lateral surface of the tibia, the blue zone wraps around the tibia surface to anterior and posterior of the tibia in a distal direction. Also from the proximal lateral surface, the dark blue lies just under the surface in the middle of the cut curve surface in the coronal plane. The stress is distributed from the posterior apex of the rod figure 9.1-29.

9.3.12.2 Shear

There are 'hot' colours under shear loading conditions, they are located on the tibia wall, and on the posterior and anterior surfaces of the tibia. The stress is distributed from the mentioned high stressed areas, into the tibial head on the sagittal before dispersing out to the lateral side of the tibia. The dark blue zone is on the surface just under the posterior rim, including the posterior bony landmark.

9.3.12.3 Discussion

The slant 10 L and the rod profiles all have the potential of migrating because of they slope outwards from the tibia without any physical impedance.

The stress distribution under axial loading condition is through the tibial head near the rod's apex, in this case next to the lateral surface of the tibia. The stress distribution is less favourable than in the shear loading because it is going through the middle of the tibial head but it does have the highest stresses go down the anterior and posterior tibial surface.

The two areas of low von Mises stress are very small and their location on the lateral surface is likely to reduce density of the cortical bone. This is desirable to preserve for any future surgeries and if the cortical is weaken then there is increase potential that the lateral side of the tibia could break off that could the prosthesis to migrate.

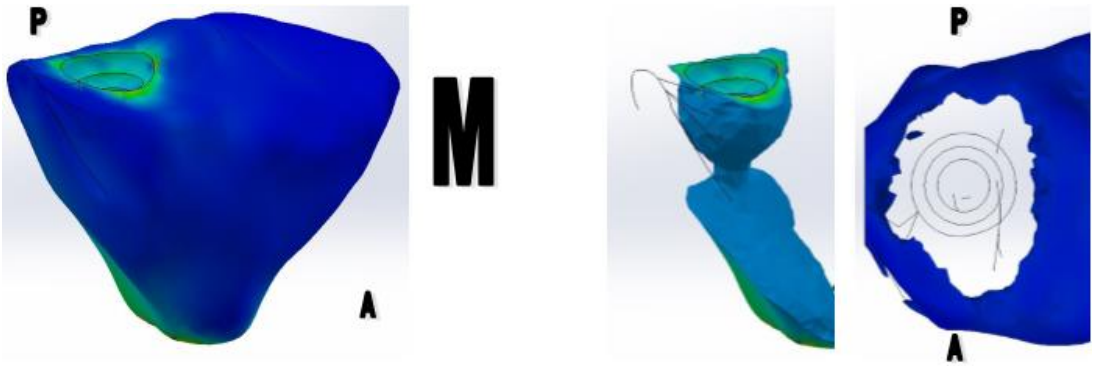

Figure 9.1-30: Von Mises plots of the Dip Profile under Axial Loading

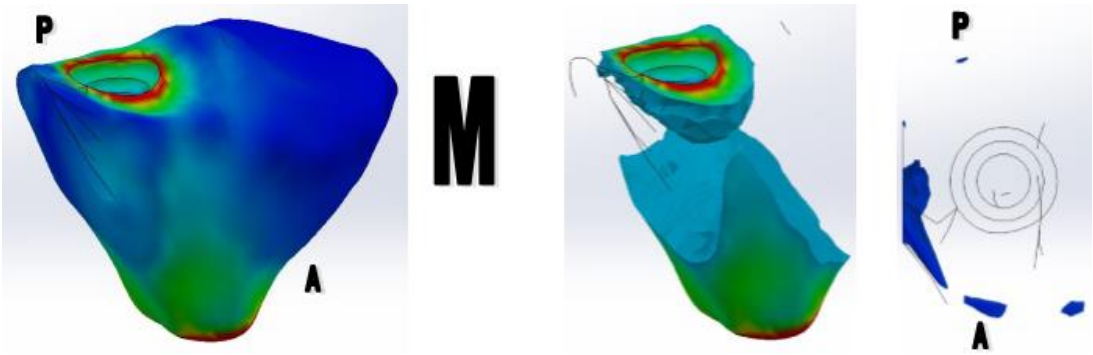

Figure 9.1-31: Von Mises plots of the Dip Profile under Shear Loading

9.3.13 Dip

9.3.13.1 Axial

Under the axial loading condition, the hot colours are mainly a mix of green and light blue on and around the cut for the dip profile, the highest location of stress is on the proximal rim on the medial of the tibia. The stress is distributed along the longitude axis from the cut surface through the tibial head. The area of little von Mises stress (dark blue) is on the uncut, proximal surface of the tibia.

9.3.13.2 Shear

Under the shear loading condition, the proximal rim of the dip's cut was shaded in red and the colours of the cut surface get 'colder' distally from the rim. The dark blue zone is located on the outer surface of the tibia at the proximal anterior lateral position. The stress is distributed down the surface the anterior and posterior of the tibia and down from the base of the dip shape.

9.3.13.3 Discussion

This result is very similar to the R10 shape but it has a more even distribution of stress across the surface and through the middle of the lateral side of the tibial head.

The stress distribution under shear loading conditions, again, goes down the middle of the lateral side of the tibial head but it has more stress being transfer across the outer proximal surface of the tibia and down the anterior and posterior

surfaces. On the downside, this stress distribution leaves the lateral side of the tibia with a low von Mises stress.

This is better than the R10 profile because it spreads more of the stresses across the cut surfaces. Plus, in the shear load it transfers more of the stresses across the surface of the tibia which will be the cortical bone under *in vitro* conditions. However, there is still the disadvantage, particularly if this is an inlay type prosthesis, that there is large volume of stress shielded because is almost all the stresses are by passed the proximal surface.

Figure 9.1-32: Von Mises plots of the Inlay Profile under Axial Loading

Figure 9.1-33: Von Mises plots of the Inlay Profile under Shear Loading

9.3.14 Inlay

9.3.14.1 Axial

There are 'hottest' colour on the tibia was a light blue under axial loading condition, while the dark blue area of the tibia is almost the whole area of the uncut proximal surface. The stress is distributed from the middle of the cut recess of the inlay through the longitude axis of the tibia.

9.3.14.2 Shear

The walls of the inlay are shaded in green to light blue under shear loading conditions, particularly the anterior medial edge and the posterior medial edge. From the mentioned edges, the stress is distributed along the longitude axis through the tibia; some of the stress is distributed across the proximal surface of the tibia and down the anterior and posterior surfaces of the tibia. The dark blue zone is located on the lateral surface and the posterior bony landmark of the tibia.

9.3.14.3 Discussion

The stress distribution under axial loading condition is very similar to the flat profile but with the downfall of the surfaces above the cut base of the inlay experience low von Mises stress that may weaken the knee over time.

The stress distribution under shear loading is better because it has stresses transferred across the proximal surface where the cortical bone will be present. However, even with the mix of loading conditions, the axial load is far from ideal, then this might not be the best route for inlay design.

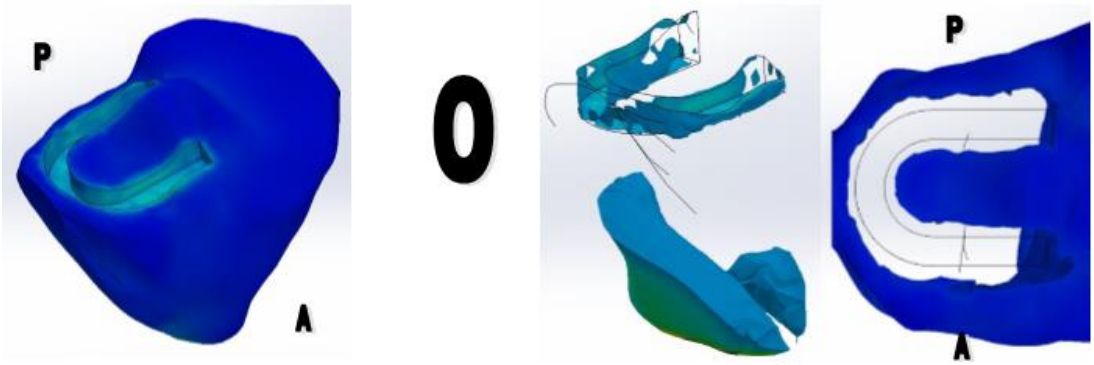

Figure 9.1-34: Von Mises plots of the Channel Profile under Axial Loading

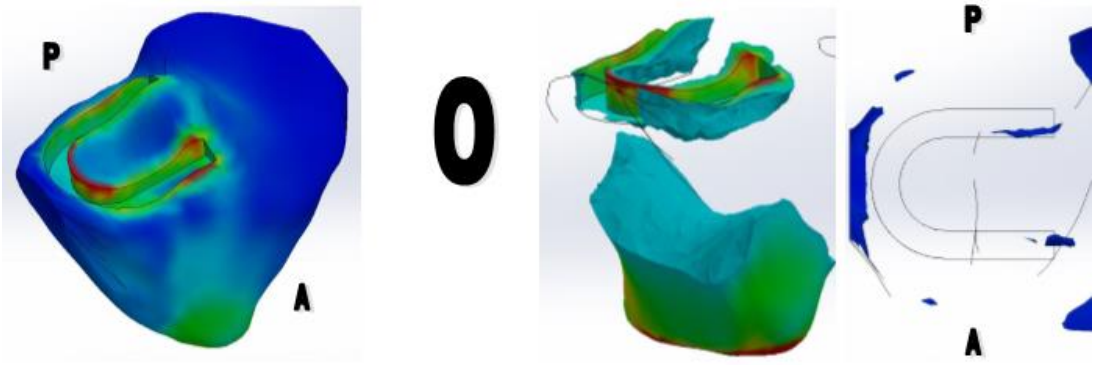

Figure 9.1-35: Von Mises plots of the Channel Profile under Shear Loading

9.3.15 Channel

9.3.15.1 Axial

With the axial loading condition, there is no colour on the primal half of the tibia that is 'hotter' than light blue. The dark blue zone is spread across the uncut proximal surface of the tibia. The main stress distribution is underneath the apex of the channel and halfway down the tibial head it meets the lateral side of the tibial surface. The areas underneath the channel legs had the stress distributed towards the apex stresses.

9.3.15.2 Shear

The 'hot' colours are located on the channel's apex inner walls and on the a-leg walls. The dark blue zone is on the lateral tibial surface. The stress is distributed through the posterior and anterior surfaces then inwards in the sagittal plane.

9.3.15.3 Discussion

The stress distribution is different in the two modelled conditions. The axial condition has the stress going through the tibial head, not ideal, but becomes ideal when the tibia narrows and the stress is distributed close to the wall. Though this isn't not even and could cause stress concentrated sections in the tibial head. Yet, in shear loading condition, the stress distribution is better as most of it is across the surface of the tibia where cortical is expected to be present to carry the load.

This design is a little better with load transference than the inlay type but there are many areas of the tibia unloaded that could lead to component loosening.

Figure 9.1-36: Von Mises plots of the Channel Dip Profile under Axial Loading

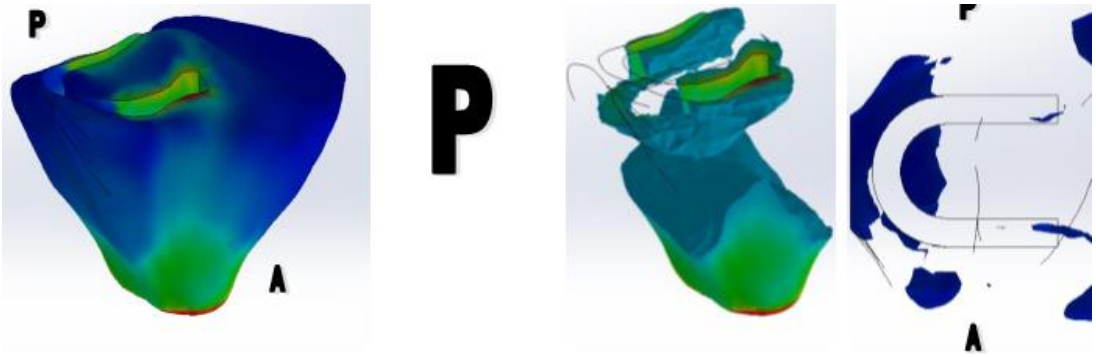

Figure 9.1-37: Von Mises plots of the Channel Dip Profile under Shear Loading

9.3.16 Channel Dip

9.3.16.1 Axial

There was no 'hot' colours present in the tibia under axial loading conditions, while the dark blue zone was quite extensive, covering all the uncut proximal surface of the tibia. The stress distributed mainly underneath the apex of the channel and halfway down the tibial head it meets the lateral side of the tibial surface. The areas underneath the legs had the stress distributed towards the distribution at the apex stress.

9.3.16.2 Shear

The 'hot' colours are located anterior and posterior walls of the channel dip's a-leg. There are two dark blue zones, next to each other; the locations are on the lateral proximal outer surface of the tibia and on the lateral outer surfaces of the kernel. The stress is distributed along the longitude axis from under the legs of the channel dip through the tibia and down the anterior or posterior tibia.

9.3.16.3 Discussion

Both condition have similar stress distribution as the channel profile. Under the axial loading condition, the stress appears to be more directed towards the lateral surface of the tibial. But this could be leaving the very middle of the tibia without experiencing stress and thus potential lose strength through resorption.

The inclusion of the dip feature to the channel profile would require larger volume of bone removal without much gain of a good stress pattern.

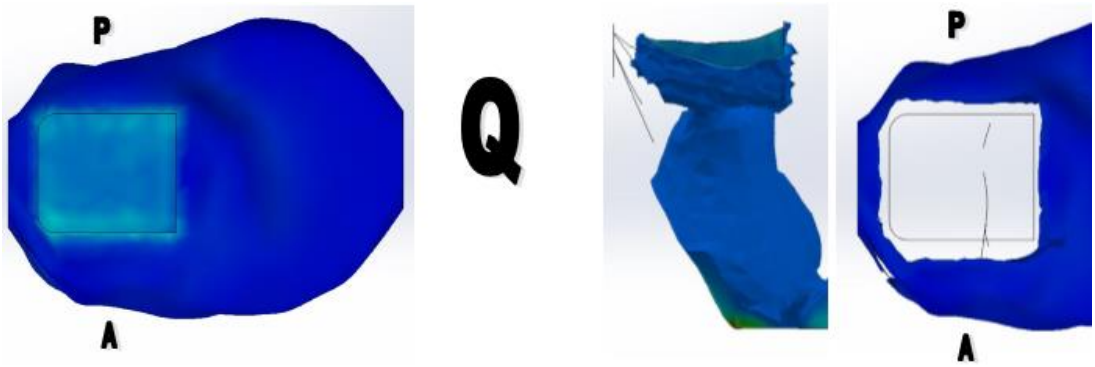

Figure 7.1-14: Von Mises plots of the Slant 10 I Profile under Axial Loading

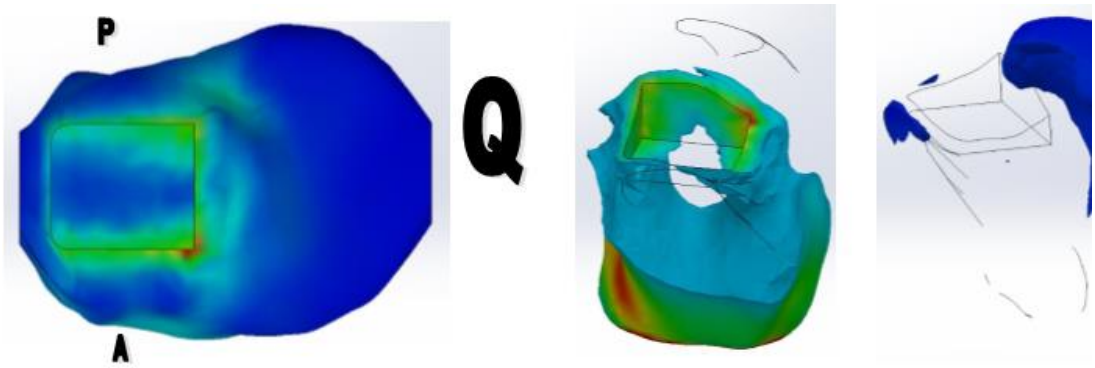

Figure 7.1-15: Von Mises plots of the Slant 10 I Profile under Shear Loading

9.3.17 Slant 10 I

9.3.17.1 Axial

Under axial loading condition, there are no 'hot' colours present; while the dark blue colour covers the uncut proximal surface and the anterior surface of the tibia. The stress is distributed from the medial side of the slant travels distally down the middle of the lateral side of the tibial head.

9.3.17.2 Shear

The shear loading condition has 'hot' colours located anterior medial edge of the inlay, and lesser on the posterior medial edge. The stress is distributed from these two points down the tibia and filling in the middle of the lateral of the tibial head last; there is also some stress distributed across the proximal surface of the tibia then down the anterior and posterior surface of the tibia. The dark blue zone is located on the lateral top point of the tibia.

9.3.17.3 Discussion

The results are similar to the inlay profile but the stress distribution a little more to the medial side of the tibia because of the slope. There is also a greater stress concentration on the medial walls for the inlay cut.

Therefore, the slant doesn't appear to improve the stress patterns of the inlay profile.

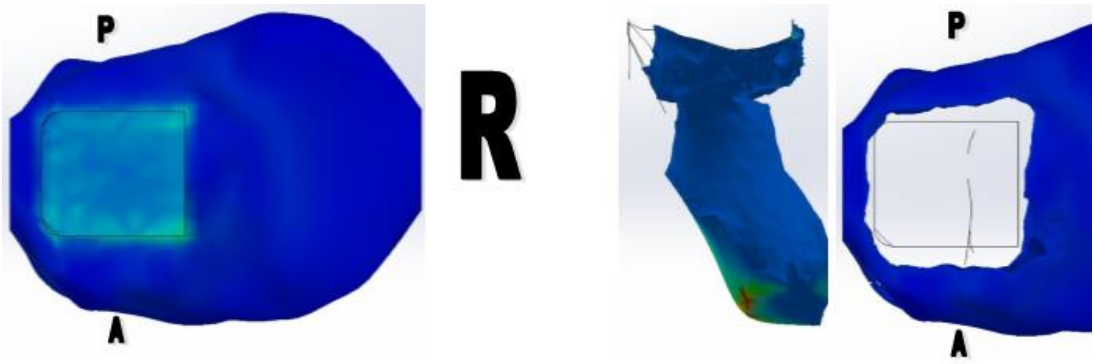

Figure 9.1-40: Von Mises plots of the Slant 10 J Profile under Axial Loading

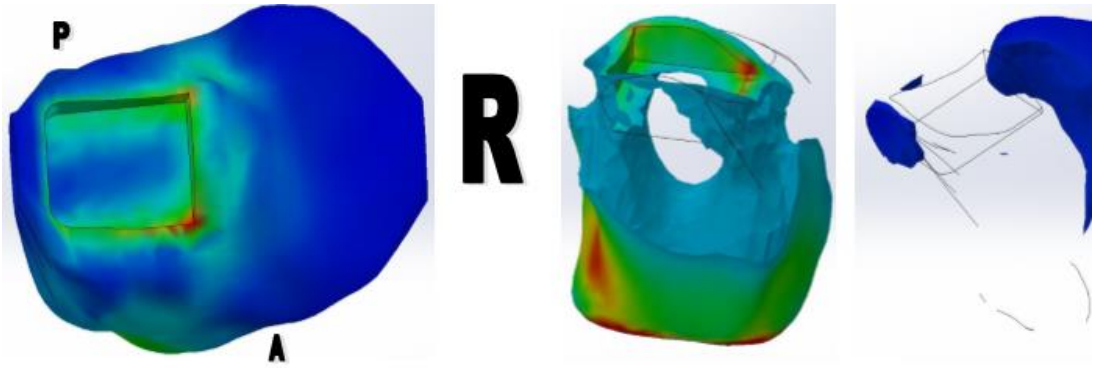

Figure 9.1-41: Von Mises plots of the Slant 10 J Profile under Shear Loading

9.3.18 Slant 10 J

9.3.18.1 Axial

There was no 'hot' colours under axial loading conditions but an extensive dark blue area that covers all the uncut proximal surface of the tibia and the anterior surface of the tibia. The stress is distributed from the lateral side of the slant and through the tibial hand along the longitude axis.

9.3.18.2 Shear

The two main zones of 'hot' colours under axial condition were located on the anterior medial cut edge and lesser so on the posterior medial cut edge. From these two locations the stress is distributed towards the nearest tibia surface; in addition there is some stress distributed across the proximal surface of the tibia then down the anterior and posterior surfaces of the tibia.

9.3.18.3 Discussion

Likewise, the results are similar to the inlay profile but the stress distribution through the tibia is perceived to be near the lateral side of the tibia.

Again, the slant, even in the opposite direction, doesn't appear to improve the stress patterns.

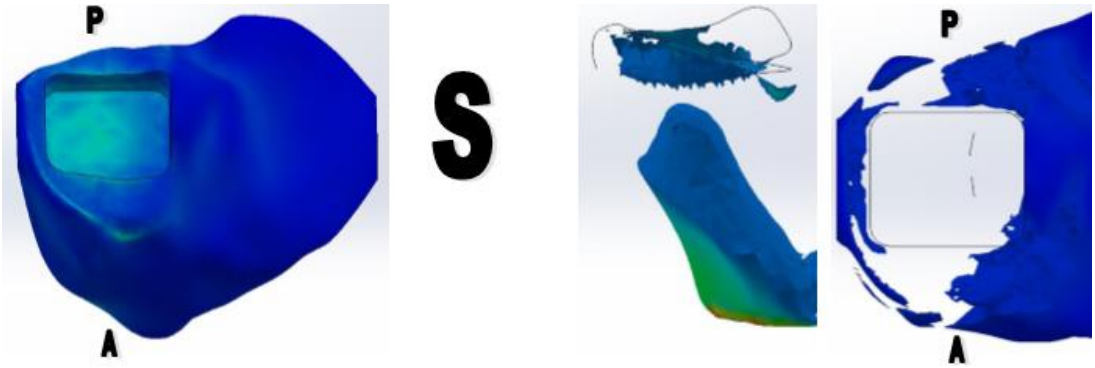

Figure 9.1-42: Von Mises plots of the Arch Profile under Axial Loading

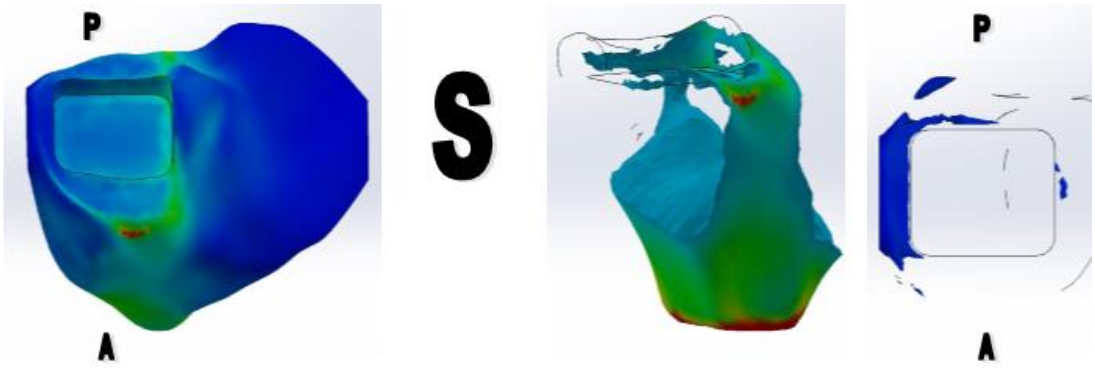

Figure 9.1-43: Von Mises plots of the Arch Profile under Shear Loading

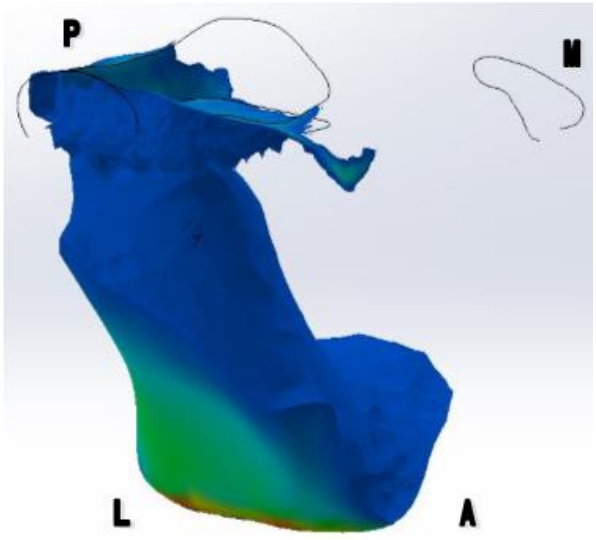

Figure 9.1-44: Iso Clipping of Inlay Arch
This figure is from the von Mises plot of the Inlay Arch profile under axial condition.

9.3.19 Arch

9.3.19.1 Axial

Under axial loading condition there was a small green spot on the anterior point of the tibial plateau and light blue zone across the base of the cut. The dark blue zones are located on the surface of the tibia, mainly on the lateral- and anterior side. The stress is distributed through the longitude axis from the lateral side of the recess. The stresses also distributed along the tibial surfaces.

9.3.19.2 Shear

Under shear loading conditions, there is green colour spread across the proximal surface in line with the medial cut wall that is also shaded in green. There is a red spot on the anterior point of the tibial plateau. The stress is distributed from the green zones of the tibia down the anterior and posterior surfaces of the tibia; in the lateral side of the tibia, the stress is distributed fairly uniform transverse plane. The dark blue zone is located on the upper lateral side of the tibia, and on the lateral uncut proximal surface of the tibia.

9.3.19.3 Discussion

The stress distribution under axial loading condition is improved as more of the stress was carried through the outer surface of the tibia but there was still some of the loading transfer straight through the middle of the lateral side tibia head. The profile covers the whole tibial plateau, then the stress is going to be distributed across the surface of the tibia and at lower stress because of the increased area.

The stress distribution also means that there is less stress shielding on the proximal tibial surfaces as seen in the results.

Though there is still shielding on the lateral side of the tibia in both conditions.

Figure 9.1-45: Von Mises plots of the Arch with Hole Profile under Axial Loading

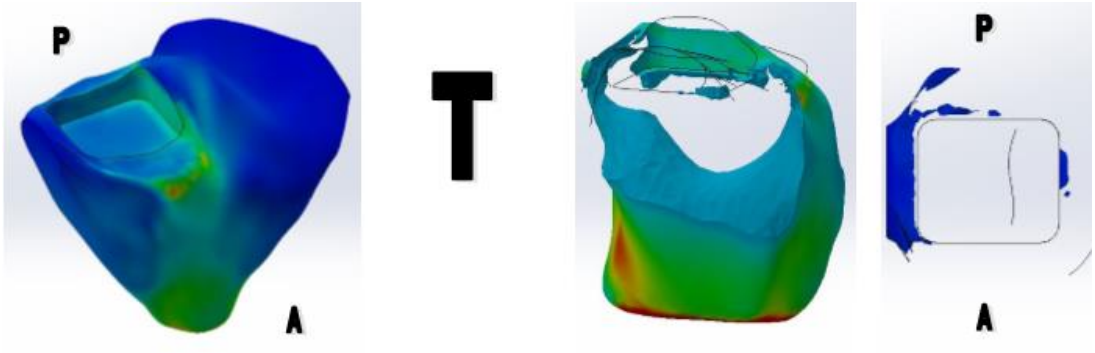

Figure 9.1-46: Von Mises plots of the Arch with Hole Profile under Shear Loading

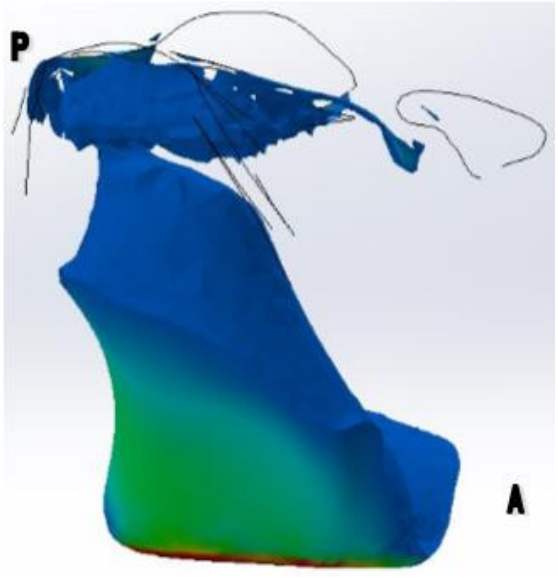

Figure 9.1-47: Iso Clipping of Inlay Arch with Hole
This figure is from the von Mises plot of the Inlay Arch with hole profile under axial condition.

9.3.20 Arch Hole

9.3.20.1 Axial

Under axial loading condition there was a small green spot on the anterior point of the tibial plateau and light blue zone across the base of the cut. The dark blue zones are located on the surface of the tibia, mainly on the lateral- and anterior side. The stress is distributed through the longitude axis from the lateral side of the recess. The stresses also distributed along the tibial surfaces, see figure 9.1-47.

9.3.20.2 Shear

Under shear loading conditions, there is green colour spread across the proximal surface in line with the medial cut wall that is also shaded in green. There is a red spot on the anterior point of the tibial plateau. The stress is distributed from the green zones of the tibia down the anterior and posterior surfaces of the tibia; in the lateral side of the tibia, the stress is distributed fairly uniform transverse plane. The dark blue zone is located on the upper lateral side of the tibia, and on the lateral uncut proximal surface of the tibia.

The volume and von Mises colour is lesser than the inlay arch without a hole, see figure 9.1-47.

9.3.20.3 Discussion

The hole in the arch is meant to distribute the stress to the outer surface of the tibia and less through the middle of the tibia and inlay. From the results it appears that it does to a small degree. It is possible if the hole in the arch is altered it could direct more of the stress to the outer surface of the tibia.

The stress iso clipping from the arch with and without the hole, figures 9.1-42 and 9.1-45, show demonstrates the idea of putting a hole in the profile can help direct the stresses.

9.4 Discussion

The loading of the models was a limitation on these models because it was simplistic, i.e. it had a uniform load applied to the top surface of the titanium. In some models there was a bit of an overhang on three sides of the cut tibial plateau (lateral, anterior, and posterior sides), which means that the edges will carry a little more load due to material bending. However, this analysis was not to fully mimic knee kinematics, it was to observe stress patterns and it kept in mind that the edges of the tibia were a limitation in some models. The advantage of using qualitative modelling is that input in does not have to be the exact values and model outputs are scaled and 'in the region' versions of the exact values if they are within the elastic region of the material. This type of modelling saves resources, doing a quantitative model would have required resources unavailable to the investigation – main two were computer processing, time for modelling all 20 models. Since the input values are estimation of the *in vivo* condition then the values out are also estimations (with errors in simplifications), thus the analysis of the data relies on interpreting the visual information. The patterns the investigation was looking for was areas of stress concentration/build-up and stress shielding. The stress concentration the areas are most likely to fail first when loading exceeds the yield limit, this could be the areas the prosthesis subsides into if there isn't substantial bone density. The areas with the least stress values, stress shielded areas, will have the bone density reduced due to the living nature of bone remodelling in response to reduced force stimulus.

The material properties of the modelled tibia were a simplified version because an actual tibia will have cortical bone with fluctuating thickness surrounding cancellous bone that has anisotropic material properties. This could be modelled in one of two way: using the imported mesh to create a surface and offsetting/shrinking the surface by a couple of millimetres to give an estimation of the cortical-cancellous bone transition (this method was tried but SolidWorks was unable to perform this function); or by creating a filleted cylinder that fits inside the imported tibial mesh which would represent the cancellous bone within the tibia. Additionally, every tibia would be slightly different because biological make-up, mechanical stimuli, and/or bone related diseases (like osteopenia/osteoporosis etc). Nonetheless, this simplified version was enough to judge the stress patterns the profiles geometry might produce in the tibia. The stress pattern this investigation hypothesises to be desired is one that directs the stress toward the outer surface of the tibia as this is the location of the stronger cortical bone. Yet, this feature is comparable to stress concentration and could potentially overload the cortical bone thus increase mechanical failure of the bone. A good balance must be struck to have the stress directed to the cortical bone without overloading the tissue, while still observing the limitations to the FEA model. Furthermore, the areas of low von Mises stress plotted for the inlay style profiles are similar to the images of the MAKO's inlay prosthesis presented in Conditt's commercial paper[5], adding confidence to the analysis.

Another limitation of this investigation is that the load applied to the knee is in an unrealistic scenario where all the body weight is going through one compartment of one knee. For example, a person standing will spread their weight across both knees, and if they were standing on one leg (still or in stance phase gait) then it is expected the weight is spread (not necessarily equal) between the two knee compartments. The knee is a hard-working joint that has forces that cab be many times the person's body weight cause by impact forces and moment force, for example walking alone can put as much as 4 times body weight on the joint[253].

The fixed geometry at the distal part of the tibia (boundary condition) created high stress artefacts; it was assumed that the effect of the fixed geometry boundary condition was limited due the distance away from the knee joint, and was constant in all models. Lastly the contact between the parts was set as an ideal bond, i.e. perfect tie, but this does not match reality. It was assumed that the loading under real and virtual conditions were not sufficient to cause the bonds of the surfaces to dislocate. With the addition, there was no large displacements in the models then the ideal bond condition was acceptable for the investigation to observe the general patterns of stress distributions on the tibial head.

The flat profile was set as the control for the other profiles to be compare to, plus it mimics the typical undercarriage profile of prostheses found in the market minus the anchoring features such as pegs. The flat profile does not appear to show any stress concentration on the on proximal half of the tibia. The flat profile has some areas of stress shielding, indicated by low von Mises stresses, in the axial load

but under the shear loading the stress shielding was just in the bony landmark. The rim and curve profiles perform very similar to the flat surface. The profile is not ideal because it removes more of the cortical bone than needed. Most of the inlay style profiles (R10, R15, dip, channel, channel dip, slant I, slant J, arch, and arch with hole) do not perform well compared to the flat profile as the stress distributed goes through the middle leaving more of the proximal half of the tibia. The arch, with and without the hole, perform better than the other inlay types because it distributes more of the stress across the proximal surface of the tibia. This could be an option when designing an inlay prosthesis – have some of the prosthesis protruding to cover the proximal surface of the tibia to aid distribute the stress over the cortical bone.

The profiles that incline towards the lateral side of the tibia (R20, Rod 55, Rod 200, and Slant 10 L) have a better stress distribution than the flat profile because more of the stresses seem to be directed to the outer surfaces of the tibia, the region where cortical bone exists. It is assumed that if the stress is directed naturally to the outer surface of the tibia then there is a higher chance that the stresses are directed through the strong cortical bone present at this area. In spite of these profile's having lesser volume of stress shielding indicated by low von Mises stress zones, they have an increased chance of slipping off the cut tibia surface. The cone profile is an attempt to prevent slipping because there is a slight lip at the lateral side of the tibia yet this seem to cause the stresses to be directed down under the apex through the middle of the tibial condyle before going down

the lateral surface of the tibia. The undercut profile also prevents the prosthesis from slipping and it direct stress towards the lateral side surfaced but it leaves a large volume of stress shielding in the lateral side of the tibia.

From this, it is concluded that any features on the undercarriage of a prosthesis will have the tendency to be the location where the stresses will distribute from, sometimes they can create a larger volume of stress concentration like the dip profile compared to the R10 profile. Inlay designs show poor results because of the stress is distributed from the recess leaving much of the proximal part of the tibia free from von Mises stress and further work needs to be looked at to see the possibility of an inlay with a cover.

9.5 Conclusion

The flat profile was shown to have an even distribution of the von Mises stress with no indication of stress concentration and low volume of stress shielding. When features were added to the flat profile, they naturally became points of stress concentration where the stress is distributed from; it also created stress shielding within the condyle of the tibia. The names profiles had a stress distribution that directed some of the stress, without overloading the tissue, towards the outer surface of the tibia which has been hypothesis to be advantageous as the bone located on the surface of the tibia is slightly stronger than the bone within the tibial head.

9.6 Key Messages

The results and discussion from the experiments in the previous chapter will provide evidence to rationalise design choices in the next chapter, *10 Concept Selection*. The key results were:

- A pre-drilled hole discrepancy in size will improve fixation as well as increasing peg size.
- Pressure during cementing is a key factor in increasing the cement adhesion strength.
- If pressure is applied during cementing, the surface texture does not seem to alter the bone cement adhesion when applied to a non-porous material.
- It appears that a rougher surface texture does not improve bone cement adhesion in porous surfaces.
- Partial cement is a possible route to take for inlay prosthesis.
- The results of the partial cement indicated that cemented prosthesis pull-off strength can be increased with the use of features, such as ribs.

The results and discussion from the FEA experiments in this chapter will provide evidence to rationalise design choices in the next chapter, *10 Concept Selection*. The key results were:

- The flat profile was one of the most uniform stress distributions through the tibial condyle in the distal direction.

- Profiles R20, Rod 55, Rod 200, and Slant 10 L seem to distribute more of the stresses towards the surface of the tibia; while profiles slant M and slant J seem to distribute the stresses towards the middle of the tibial head.
- Features to the undercarriage profile tended to be points of stress concentration.

Chapter 10

Concept Selection

This chapter covers the concept selection process which forms the iterative loop of stage 4 in the project design process. It is an important stage in any design process as it determines which of the many generated concepts of the project will proceed to the final stages. This process will require reference to information gathered in the exploration stage and the results from the experimentation stage of the project design process in order to complete with full confidence and rational thinking.

This chapter will rely on exercises used in previous established design processes, such as Pugh's Total Design, they are used strategically in the selection process. The subsequent iterations of the thought process through the evaluation, elimination, and concept generation are described with the rationale.

10.1 The Initial Unicondylar Implant Concepts Selection Process

10.1.1 Introduction

The process for concept solution is covered in great detail in Pugh's Total Design and it is a valuable process as it continues the development of the ideas into

concepts. The selection process can be seen as an upside-down fir tree due to the number of concepts converging and diverging, as illustrated in figure 10.1-1. Pugh calls it a control conversion, as using logical reasoning with the help of exercises concepts are kept, rejected, or adjusted. The project design process employs two design matrices, seen in figure 10.1-1

Concept / Criteria	1	2	3	4	5	6	7	8	9	10	11
A	+	–	+	–	+	–	D	–	+	+	+
B	+	S	+	S	–	–		+	–	+	–
C	–	+	–	–	S	S	A	+	S	–	–
D	–	+	+	–	S	+		S	–	–	S
E	+	–	+	–	S	+	T	S	+	+	+
F	–	–	S	+	+	–		+	–	+	S
Σ+	3	2	4	1	2	2	U	3	2	4	2
Σ–	3	3	1	4	1	3		1	3	2	2
ΣS	0	1	1	1	3	1	M		1	0	2

Criteria / Concept		1	2	3	4
		0-5	0-5	0-5	0-5
A	2	1 / 2	2 / 4	3 / 6	3 / 6
B	1	5 / 5	2 / 2	5 / 5	4 / 4
C	2	2 / 4	0 / 0	5 / 10	2 / 4
SUM		11	6	21	14

Figure 10.1-1 Design and Evaluation Matrices
Left is an example of a design matrix suggested by Pugh[227], right is a weighted and rated design matrix.

The design matrix is a tool and it is only as useful as the person(s) using it. It can be used just as an eliminator or for the retention of concepts, yet it can do more than that. First off, it is a good evaluator because it gets the user(s) to envision the concept and analyse it in each specification. Therefore, it is valuable to keep notes of significant features, or possible alternatives to bad features so they can be brought in the divergence stage. When the matrix is complete, it can highlight strong or weak contending concepts, or features within concepts that are a solution to a difficult specification etc.

10.1.2 Iterations

The goal at this stage is to review the list brought forward from the concept generation chapter to assess if it will fulfil the PDS. It was then decided that most of the ideas concentrated on the tibial component. This area also has a lot of focus in the literature – as a result of this, the PDS that the project will follow was filtered to focus on tibial component designs. Using the above methodology as guidance, the concept selection process is as follows drawing in any information acquired from the experiments, literature, and further exploration. The concept selection seemed to go through a 2-step iteration starting with evaluating the concepts with the use of a design matrix, this commenced rational thought processes of discarding and creating new concepts. All concept family, identification, and descriptions can be found in appendix 15, and all the matrices can be found in appendix 16.

10.1.2.1Matrix 1

The ideas generated from the initial concept generation stage that were relevant to the PDS were further developed generating 57 concepts.

The first design matrix (pages A87-88) was based on the one suggested by Pugh's, the datum was the industry standard of a cemented flat base with two pegs. The whole PDS wasn't included in the matrix as it was determined it will be beneficially efficient to have only 7 important criteria chosen from the PDS, see table 10.2-1.

Table 10.1-1: The Selected Characteristics from the PDS		
Characteristic	**criteria in the matrix**	**Description**
Mechanical Function	Load Transfer	This is the projected potential path(s) the loading will take from the concept to the tibia and through the tibial head.
	Stress Concentration/Shielding	This is the projected potential of area that may have a build-up of stress or lack of stress.
	Stability	This is the perceived stability the implant will have in the three possible degrees of freedom: torsional, anterior to posterior, and medial to lateral.
Tooling	No Tool change	If the implant requires a change to a different size then it is not ideal design because the current standard prosthesis does not require a change in burr size.
Burring	Simple to cut	This is the perceived difficulty of burring the shape thus designs with difficult undercuts, thin structures and/or sharp edges.
	Bone Loss	This is the excepted volume of bone tissue removal for the implant.
	Accuracy it needs to have	This is the accuracy that may be needed for burring the bone and the placement of the prosthesis. The less accuracy that is required may increase the prosthesis survival and/or reduced the time for implantation.

The first matrix had 57 concepts; a lot of the concepts shared an idea and/or feature so they were considered a ‘family’. After evaluating them, 44 of them were discarded either due to not performing as well as other concepts within their perceived ‘family’ or they were replaced with an adjusted version. The creative space that commenced used the three different generation approaches allowed for 26 concepts to be generated.

The following table 10.2-2, has the notes that were taken during the first cycle of the concept selection process.

Table 10.1-2: Notes from Matrix 1 Concept Selection

Concept or family	**Notes**
Waves	The load transfer could be improved if the overall shape is altered.
Circle	A new concept: have the concentric circles be non-continuous bumps.
Inlay	Make the shape be full sphere.
Curved ones	Have the main point of attachment of the prosthesis at the top and outer cortical points of the cut tibia.
Dome	Put the edge closer to the outer cortical edge.
Lines	Make the line jaggy, like toblerone peaks.
New group	Combining the two wave groups together to have the under surface be perpendicular interfering waves.
New group	A inlay dome group.
Standard Group	Seems to be really good in some aspects but worse in others, yet it doesn't normally lay in the middle.
Improvements:	
Pi	Combine with the table idea.
Pi	Shorten the peg structure.
Pi	Combine the above two ideas.
D1	Shorten the peg structure.
D2	Shorten the peg structure.
L1 and Q	Remove the fin, the fin only affects torsion stability which can be achieved by other methods.
Waves and V waves	These have been improved by changing the structure of the thus all apart from the 6mm ones are removed.
Concentric circles	Most require a change of the burr. There would be a change to a smaller burr size for the concepts with the higher number and smaller diameter of concentric circles; because of the burr chance, these ones were removed.
C1	Have the circle have at a slight angle to improve stability.
Toblerone	New ideas are generated based on reduced the complicatedness of the peaks and to increase their number.

S2	The main feature does not seem to add much and if it is turned into an inlay then its shape maybe be beneficial and reduced the volume of bone tissue.
S3	Does not seem to be beneficial and requires excess bone loss. If it is combined with the S1 and S4 the benefits and reduced bone tissue removal could be improved.
I1 and I2	The flanges can be turned into curves or angles to create new concepts.
Dip	Make the bone loss more minimal.
Dip	Combine it with the table types as inlay and onlay designs.
Inverted Dome	These concepts don't seem to advantageous to the non-inverted ones but if they were made into inlays then it could have some benefit.
Slants	Don't have the best load transfer so it was changed to the other way around.
K4	A line bump was added to the lower part of the slant to improve the stability.
H1 and 3	They required unnecessary tool change, thus they were removed.

10.1.2.2 Matrix 2

As the result of the convergence and divergence phase above, 39 concepts were evaluated in the second matrix (page A89-90) which was again Pugh's method with the industry standard as the datum. The methodology used in Pugh's design matrix reached its limitations in reducing the number of concepts in the convergence phase but it did produce 14 additional ideas in the divergence phase, see table 10.2-3. This resulted in 53 concepts to be evaluated in matrix 3.

Table 10.1-3: Notes from Matrix 2 Concept Selection	
Concept or family	**Notes**
S2.2	Have the edges of the cortical bone hold up the prosthesis, based on the arch theory.
Dip	Have the concentric circles go down the towards the outside edge of the cut surface.
K4	Add a small undercut.
Pi	To reduce the difficulty of creating an undercut, the legs are shortened.
D2.2	Is almost impossible to do, thus the dovetail feature in the cross is removed,
A1	Make the angle cuts the same size as the burr.
	Undercuts were added to prevent lift, it is possible to do but isn't easy.
	Try to add a curve to the flat concepts to improve the load transfer.
L2 and Q2	Add two undercuts to the line.
C6, S3.2, and S1	These concepts are almost the same except from the position of the bumps.
G7	Was combined with A1, L2, Q2, W2, and V2.
	The knee already has a concave curve on the tibial plateaux.

10.1.2.3Matrix 3

Reluctance to discard concepts from matrix two was a problem because if concepts couldn't be eliminated then the concept selection process would not narrow down to a small number of promising concepts. Ideas from discarded concepts could be revisited, implemented differently and potentially lead to a plausible solution. All concepts and ideas were recorded in the log book which could be looked back on for inspiration. To aid in this process, it was decided that further

evaluation was needed to be done on 53 remaining concepts. The exercise used to do this was the weighting and rating matrix as it seemed it might be beneficial even though it requires a considerable length of time to complete with large number of concepts. The rating and weighting matrix was also combined with Pugh's matrix to help with the evaluation process. Matrix 3 can be found in Appendix 16, pages A105-111.

In the composite matrix, each cell contains the rating score, the multiplication of the rating score with the weighting factor, and a sign (+, -, or s) and this was used in matrices from the 3rd matrix onwards. The stability was split into the 4 possible degrees of freedoms criteria: torsional, anterior to posterior, medial to lateral, and lift off. The criteria in the matrix was assigned a value between 1 to 3 – with 3 being the factor that was important for the prosthesis to have, and 1 being the least important factor. Table 10.2-4 displaces the assigned scale number for the criteria. The scale for how compliant the concept is to the criteria is 0-5.

Table 10.1-4: The Value Assigned to the Assess Characteristics	
Criteria	**Scale**
Load Transfer	3
Stress Concentration/Shield	3
Stability Anterior to Posterior	3
Stability Medial to Lateral	2
Stability in Torsion	2
Stability from Lift Off	1
Tool Change?	2
Large burr or minimal removal	1
Simple to Cut	3
Bone Loss	1
Accuracy Required	2

The process for matrix 3 was, as predicted, a bit lengthy but it did help with only keeping the promising concepts as the number of concepts went down to 12. When all the concepts were evaluated in the matrix 3, the so called families were kept together (Appendix 15); the families are concepts that have similar traits or are variations of a feature, for example the circle family (C) all have one or more features that are circles. From each family, the concepts were evaluated to give strong contenders, table 10.2-5, that were brought forward to be compared with the other families. These concepts were compared using the same evaluative matrix but just concerning the 24 highlighted contenders.

Table 10.1-5: The Strongest Concepts from Each 'Family' With the Perceived Thoughts	
Contenders	**Notes**
π1.4 π1.8 U4 U5.2	Undercuts are difficult and could create potential stress concentration and shielding but give the prosthesis stability.
T 4 T6.2	Basically lines that hold the prosthesis in position.
D1.2	Strong but only as strong as the bone and can't be easily shaped.
S2.3	Dip gives stability.
C1 C5 C6	Overall stable in anterior-posterior and medial-lateral directions but not axial/torisional.
I1.2 I2.2	Simple and useful stability in 1 direction.
M6 M7	Good for stability but there is excess bone loss.
G9	Is a fundamental idea. The curve helps transfer load but could be disadvantageous.
L2.3	Line are strong stableness in only in one direction.
Q2.3 Q3	Much stronger with the 2 angle lines.
H4	Minimal bone loss and easy to shape. Can be used to transfer load to cortical
A	Has no strong contender(s) – the idea is used in other concepts as but is good at preventing lift off but difficult to create.
W2.3 V2.3	They are like the features that use lines and thus are are only good in one direction yet it is less likely to creature stress concentration.
B 1 B1.2	These are like the bumps concepts but with less potential of creating stress concentration.

During the creative divergent phase, 16 new concepts were generated. It was decided that certain families (L, A, G, W, V, and B) had one core fundamental idea each but were not strong on their own and thus these ideas were combined with each other to generate new concepts, see table 10.2-6. The creative process then proposed 4 fresh concepts, see table 10.2-6, but only one was put into forward because the other three had fundamental ideas that had already been established to be unbeneficial to the concept's performance; for example, the concept generated (ID H5) was using the previous H2 design but with an undercut – undercuts have been rejected by both user dairy and simple FEA simulation because they are difficult to produce and cause a stress concentration (respectfully). All the remaining and additional concepts (29 in total) are put into matrix 4.

Table 10.1-6: Concepts Generated from Combing 'Families'	
New concepts	**Notes**
W1.2	The waves (W1) are combined with table feature (H3).
W1.3	The waves (W1) are combined with bumps (S2.3).
B1.3	The interfering waves (B1) are combined with bumps (S2.3).
G8.1	It combines the G8 idea with an undercut on the medial side of the tibia.
G8.2	The G8 idea is combined with the interfering wave feature as the surface between the upper and lower parts of the prosthesis.
G8.3	Combines G8.1 with a line (L) from anterior to posterior in the middle of the plateau.
H3.2	The getting deeper crescent from concept M6 was applied to the crescent in H3.
H4.2	The getting deeper crescent from concept M6 was applied to the crescent in H4.
V1.2	The waves (V1) are combined with table feature (H3).
C8	Has the curved shape of G7 and has a circle added to it (C1).
K4.2	Combines K4 design with waves (W).
Pi1.9	
C5.2	The circle in C5 is made into a square/rectangle and keeps the angled undercut.
S3.3	The circle is made asymmetrical to improve bone loss.
G8	The upper and lower part of the prosthesis is place on a flat surface to reduce migration.
F3	G with a 'S' shaped line.
F1 (rejected)	Combine G with L and have a line on the posterior side.
F2 (rejected)	Combine G with W, V, and B with a line on the posterior side.
H5 (rejected)	Has an undercut.

10.1.2.4Matrix 4

The fourth matrix (page A98) used the same composite matrix as in the third matrix and the same datum but the matrix only evaluated based on the mechanical function criteria and surgeon compliance, see table 10.2-7. There were two reasons why the criteria were reduced, the first was to evaluate a smaller number of criteria to process was faster and slightly easier to complete. The second reason it felt as if some of the criteria were not as important as others and that made it hard to choose because there were concepts contradicting criteria.

Table 10.1-7: List of the Evaluated Characteristics and the Assigned Value

Criteria	**Scale**
Load Transfer	3
Compliance	1
Stability Anterior to Posterior	2
Stability Medial to Lateral	2

When evaluating the concepts, it was noted that when some concepts were very similar, one of them was weaker and the other was stronger. It was concluded that only the stronger concept would be the one to be taken to the next matrix. The ones brought forward are not necessary the ones with the highest weighted and rated scale but also the concepts which had the most positives. Eleven concepts were selected from the 29.

10.1.2.5Matrix 5

The concept evaluation used a composite matrix for the fourth matrix, concept B1.2 was the datum concept.

The eleven concepts selected for matrix 5 were thought to represent the most potentially promising concepts. However, to ensure the best were selected both matrices 4 and 5 (pages A98 and A99, respectively) were used to eliminate and generate ideas. As a result, it allowed the 11 concepts that were picked to be compared with a different datums/data, which turns out to be constructive as the results changed slightly. This allowed a rational thought to proceed that allowed new concepts to be generated along with confident elimination of 18 concepts. The new concepts had 7 fresh generated concept (only 4 were considered to have potential for matrix 6) and 3 concepts there were adjusted.

Table 10.1-8: New Concepts Generated from Matrix 5

New Concepts	**Notes**
R1 (not included)	Have a MAKO like fin on the medial wall to help with stability of the prosthesis.
R2 (not included)	Have burred lines on the medial wall to help with stability of the prosthesis.
R3	Have a structure in the medial wall that is like a dental implant to create mechanical tie.
R4	Have a screw with spokes to create a mechanical tie to the wall of the tibia.
R4.2	Have a screw with bars, similarly to create a mechanical tie to the wall of the tibia.
R5	Have a curved medial wall to help with the stability and load transference of the prosthesis.
R6 (not included)	Combine ideas R5 and R4/R4.2.

10.1.2.6Matrix 6

Matrix 6 (page A100), the final matrix, 17 concepts were evaluated using the composite matrix with concept H4 as the datum. The strong contending concepts were T6.2, Q 2.3, and B1.2. One final alteration of concepts Q2.3 and B1.2 this was to join them together to make concept BQ.

Table 10.1-9: Notes from Matrix 6

New Concepts	**Notes**
R4, 4.2, and 5	They were considered to be add on ideas, they can be
B1.3	The concept is a strong one but it was considered not to be reproducible
G8.4	The concept seems strong but not as beneficial as once thought

The concept T6.2, figure 10.1-2, is changing the standard fixation method for an easier to produce 'T' that is less likely to produce unfavourable stress patterns. The BQ1.2 concept, figure 10.1-3, is like a shallow conical bowl that has an undulating surface and uses two flanges in a 'V' formation to assist fixation.

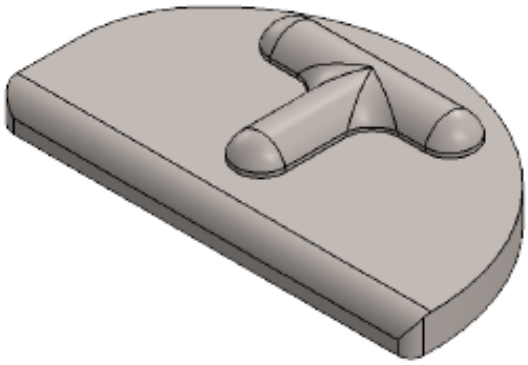

Figure 10.1-2: T6.2 Prototype
This is one of the final two with an undercarriage profile from concept T6.2

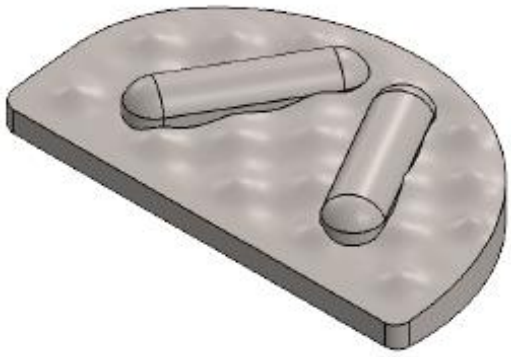

Figure 10.1-3: BQ1.2 Prototype
This is one of the final two with an undercarriage profile from concept BQ1.2. also referred to as just BQ

10.1.3 Discussion and Conclusion

This process aim was to narrow down to two strong potential concepts that can be compared with the standard UKR prosthesis; these two concepts are T6.2 and BQ, seen figures 10.1-2 and 10.1-3. Rational elimination down to just two concepts for prototyping is very limiting and potential ideas may have been lost in the process. The cost of prototyping and testing is often a limiting factor, amongst other resources; this is being one of the reasons why only two concepts were chosen. Just because only two concepts were brought forward for prototyping does not mean all the ideas from this exercise should be forgotten about. Some ideas may still have potential, such as R3, R4, and R4.2 they all have a feature that can be implemented to the two final concepts and the standard UKR prosthesis. The main reason why they were not bolted on to any of the designs was the manufacturing of them: it will not be an easy task to create these features for the prosthesis primarily due to the mechanics of implementing them. Other good potential concepts were: have a modular design that only removes unhealthy tissue sparing the healthy tissue, this would have been tricky to manufacture and it might have the same issue that faces the inlay designs; replace the traditional PMMA cement with an alternative, this would change the goal and direction of the investigation; there was the arching inlay designs, they seem to show potential in the FEA analysis of stress concentration, shielding and distribution but this design approach did not focus on project design brief.

Inlay designs were initially considered but were slowly filtered out near the beginning of the concept selection process. This was because of the loading transference because the inlays had the tendency to transfer the load to the cancellous bone and not to direct it to the stronger cortical bone. The last matrix had two inlay designs to be compared with the onlay designs. They performed theoretically better than the others. They weren't chosen to be prototypes because the final experiment would not allow fair comparison with the standard onlay UKR prosthesis. In addition to this the design has a potential for not being compatible with the knee mechanics because of the material extending on to the tibia plateau. Therefore, these inlay designs in matrix 6 will need further investigation for refining the concept to a feasible inlay prosthesis.

Design matrices can only get designers so far because it is a theoretical thought process. If the user(s) thinks a feature will behave in a certain way, based on their knowledge and experience, then its results will reflect that but in reality, it could act differently from the user's theory. This is when experiments are necessary to be conducted to provide evidence for the reasoning. The experiments can test a theorised feature of a concept to establish if it will work and can be done without having to test the whole concept; or it can test the concept as a whole – the latter is often called prototyping. Most design processes will produce at least one prototype of sorts which normally happens in later stages of selection as this tends to cost more than the feature testing. The experiments and prototypes can be lab/mechanical based testing and/or can be done in simulations such as finite

element analysis (FEA); the decision depended on many factors and down to the tester(s) to use discretion which approach their budget allowed for in order to yield results.

10.2 Interview about the Final Two Designs

The consultant from the previous interview, chapter *3 Personal Experience Exploration*, was asked a series of questions based on the final two concepts. The final two concepts were presented to the consultant as technical drawings, seen in figures 7.1-4 and 7.1-5. The dialogue with the consultant was very positive; the consultant was able to see that the presented prostheses were adapted to and take advantage of the robotic orthopaedic tools that are becoming available to more and more surgeons.

The BQ design was enthusiastically well received by the consultant: it has the potential of bone preservation by minimal removal especially by the removal of deep cuts for the pegs which makes revision easier. The straight shallow troughs were thought to be a promising method of anchoring the prosthesis but there was concern that the ‘v’ is too close together that the bony strut between them would be too narrow that it might break. Two solutions to this is either join the ‘v’ together or separate them further apart. The surgeon also suggested that if it curved in the other direction so it is like a bowl it can preserve more of the cortical bone. These two suggestions were taken on board before the prototypes were created.

The T6.2 was also well received due to the removal of the pegs thus making revision procedures easier. There was concern that curved shape of the 'T' wouldn't be easy to re-create on the bone. The discussion of this particular concept (and to a lesser extent the BQ concept), concluded that if the prosthesis is cemented then, along with the bigger cuts, this would allow a larger margin of error for cutting bone during surgery.

With the inlay design, he was a little confused but he liked the idea that it was like filling in a pot hole.

Conclusion

The interview was encouraging as it confirmed the rationale that had gone into the concept selection process. The initial interview with the consultant was an open dialogue of possibilities for improvement; this successive interview showed the consultant two concept directions that can improve prosthesis design with enthusiastically promising feedback. This demonstrates that the concepts have homed into concept improvement without compromising the inherent strengths of the original prosthesis.

The interview with the orthopaedic surgeon was positive, and gave insight as to the thoughts of an important stakeholder group. However, this is was xyr opinion and will not represent the views of all orthopaedic surgeons, thus evidence must be treated circumspectly.

Lastly, the consultant suggested altering the flanges in the BQ concept to prevent bone fractures; increasing the gap between flanges was one solution to solve the problem and thus changed before the prototype was manufactured.

10.3 Key Message

This process took a while to complete because of the detailed evaluation into every iteration of the concept selection process. The final two concepts appear to be the strong potential designs from the 200+ concepts that were generated through this investigation. Along the way there were other potential ideas that should not be entirely forgotten and could be also investigated for use in future designs. However, these designs were eliminated as not being as strong potential as T6.2 and BQ, see figures 10.1-2 and 10.1-3. These concepts were then tested in chapter *11 Prototyping* to compare their performances to each other and to the conventional UKR design in the market today.

Chapter 11

Prototyping

The previous chapter (C*oncept Selection)* selected 2 concepts under the guidance of the designs matrices that utilised the PDS and the results from the experiments in chapters 8 and 9. These selected concepts were manufactured into prototypes, together with the standard market design that is characterised with a flat base with one to three pegs that are usually angled off from the vertical. The MAKO prosthesis fits this bill; the base is flat and has two pegs angled inwards. The experiments turned a size 6 MAKO trial prosthesis into a prototype to represent the standard market design.

The aim of this chapter is to investigate and compare the performances of the three prototyped designs. The prototypes adhesion strength and stress analysis were the investigated by laboratory and virtual experiments (respectively).

11.1 Prototype Experiment

Prototypes of the final 2 deigns (BQ, and T6.2), and the model of the MAKO were produced from 3D printing in aluminium. They were cemented to a foam block and put under combined shear and axial loading to determine the mechanical behaviour of each prototype in situ. The reason for shear loading is that the

prostheses will most likely to displace due to shear rather than in tension *in vivo* conditions. This is because when the condyles rotate, it causes anterior-posterior forces which result in pushing the prosthesis in this direction; this in turn will cause a shearing action on the interfaces of the tibia component.

11.1.1 Aims

The aim of this experiment was to determine mechanically which of the 2 concepts provide a stronger attachment to the foam block (representing cancellous bone) and how they compare to the standard prosthesis strength.

11.1.2 Results

The graph of the results from all the prototypes can be found in figures 11.1-1 and 11.1-12 – green lines is the original design, blue lines is the BQ design, and red lines is the T6.2 design. From these two figures, it is clear to see that the BQ design has the highest force to go the same displacement in the foam. For displacement up to 1.5mm, the original design performs better than the T6.2 design but it is unclear if this is the case for displacements up to 5mm where the T6.2 design just out performs the original design but there is only one result for this model. The maximum forces and the estimated stiffness's are found in table 11.1-1 and in table 11.1-2 are the statistical results.

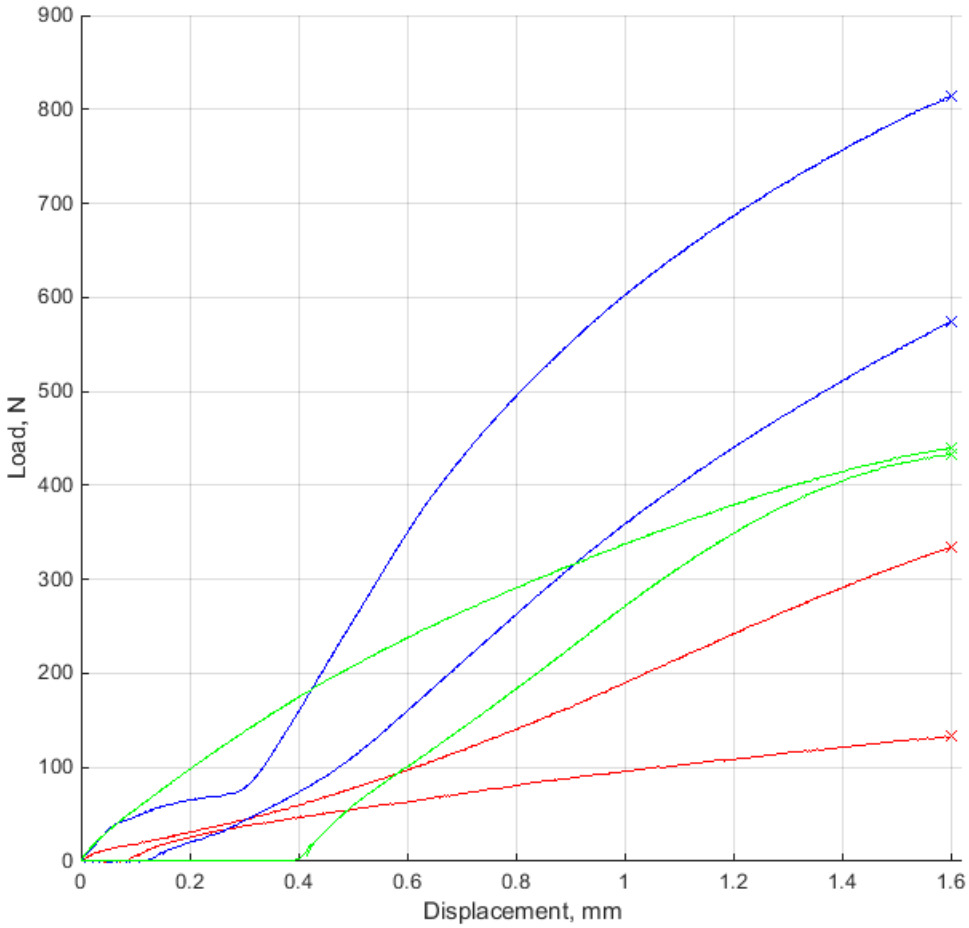

Figure 11.1-1: Force Vs Displacement Graph of the Prototypes under 1.5mm
Green lines are the original design, blue lines are the BQ design, and red lines are the T6.2 design.

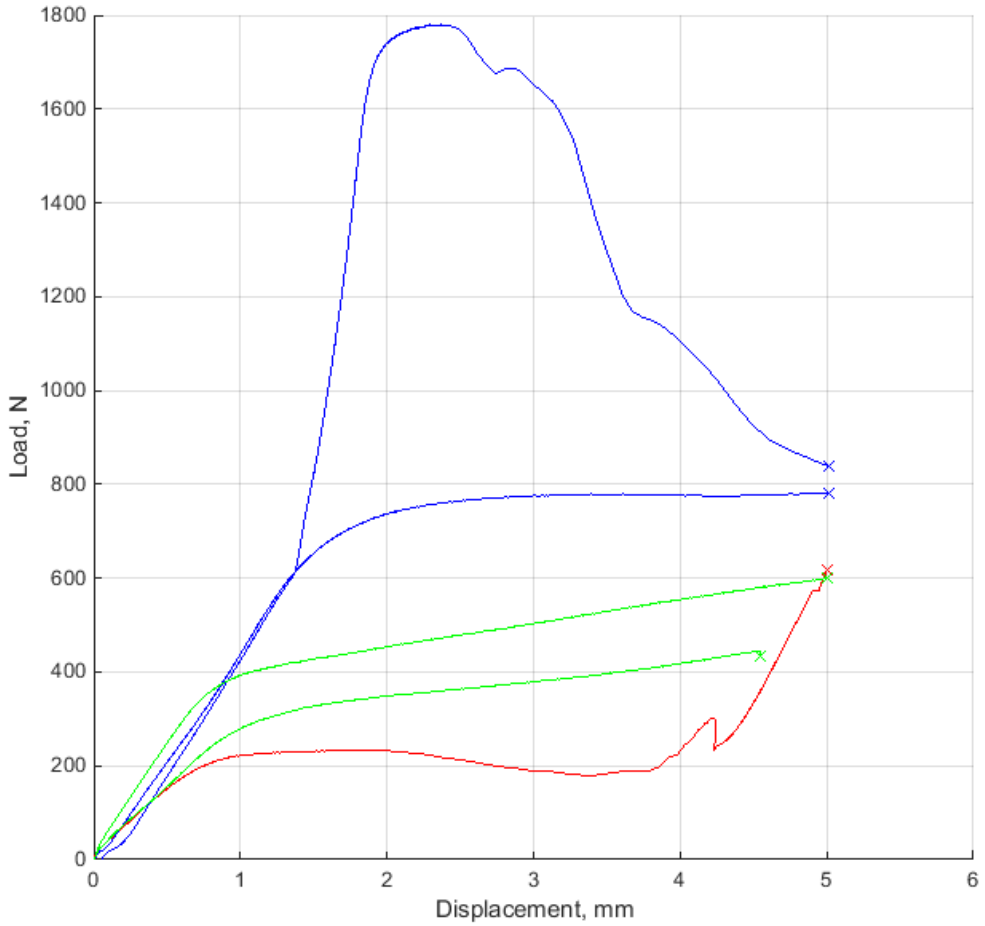

Figure 11.1-2: Force Vs Displacement Graph of the Prototypes under 5mm. *Green lines are the original design, blue lines are the BQ design, and red lines are the T6.2 design.*

Table 11.1-1: Prototype Experimental Results

	Original		**BQ**		**T6.2**	
	Max Stress (N)	*Stiffness (N/mm)*	*Max Stress (N)*	*Stiffness (N/mm)*	*Max Stress (N)*	*Stiffness (N/mm)*
1.5	440	275	814	509	133	83.1
1.5	433	270	575	359	334	209
5	435	95.5	781	156	-	-
5	599	120	1,780	167	617	123

Table 11.1-2: Statistics of the Prototype Results.						
	Original		**BQ**		**T6.2**	
	Max Stress	*Stiffness*	*Max Stress*	*Stiffness*	*Max Stress*	*Stiffness*
@1.5mm						
Mean	436 N	273 N/mm	694 N	434 N/mm	234 N	146 N/mm
SD	5.49	3.40	169	106	142	88.8
SD error	1.37	0.849	42.3	26.4	35.5	22.2
CV	1.26%	1.25%	24.4%	24.4%	60.9%	60.9%
@5.0mm						
Mean	517 N	108 N/mm	1,280 N	161 N/mm	(617) N	(123) N/mm
SD	116	17.1	707	8.01	-	-
SD error	29.1	4.28	177	2.00	-	-
CV	22.5%	15.9%	55.2%	4.96%	-	-

For all the samples, the cement was still strongly attached to the foam and implant after 1.5mm and 5mm even if the foam has subsided and the edges of the prototype were lifted off the foam, as seen in photos in figure 11.1-3. The level of penetration of the bone cement into the foam is roughly comparable to the penetration into the bovine cancellous bone experiments, comparison in figure 11.1-4.

For the T6.2 prototype, figure 11.1-5, the displacement of the implant was noticeable on the foam above the pushing of the prototype. When the prototypes were pulled off the foam blocks, the cement stayed as a whole entity attached to the prototypes and it revealed that the prototypes for both batches were not aligned to the intended grooves in the foams. The first batch was misaligned

estimated to be 5mm out and the second batch around 3mm. The 'T' shape flange in the foam for the first batch did not have clear signs of subsidence, this could be due to the prototype being misaligned and ended up not having a full force within the flange. Whereas the second time less misaligned as the first batch and there was distortion in the foam block's 'T' shape.

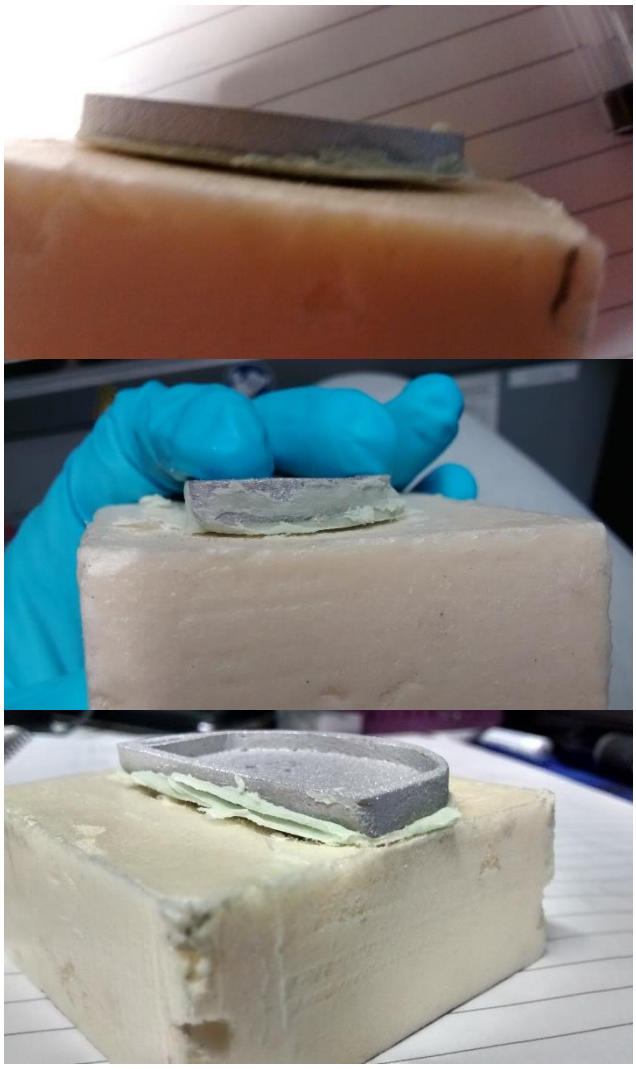

Figure 11.1-3: Photos of the Original Prototype Samples Post Testing
The top photo is batch one original prototype;
Middle photo is batch one BQ prototype;
Bottom photo batch one of the T62.2 prototype.

Figure 11.1-4: Photo of the Foam Stuck to the Original Prototype
On the left is the original prototype peg with foam integrated with the cement. On the right is bone cement with a little bone integration.

Figure 11.1-5: Photos of the T6.2 Prototype Samples Post Testing
To the left are the photos from batch one, and to the right are the photos of batch 2 samples.

Figure 11.1-6: Photos of the BQ Prototype Samples Post Testing
To the left are the photos from batch one, and to the right are the photos of batch 2 samples.

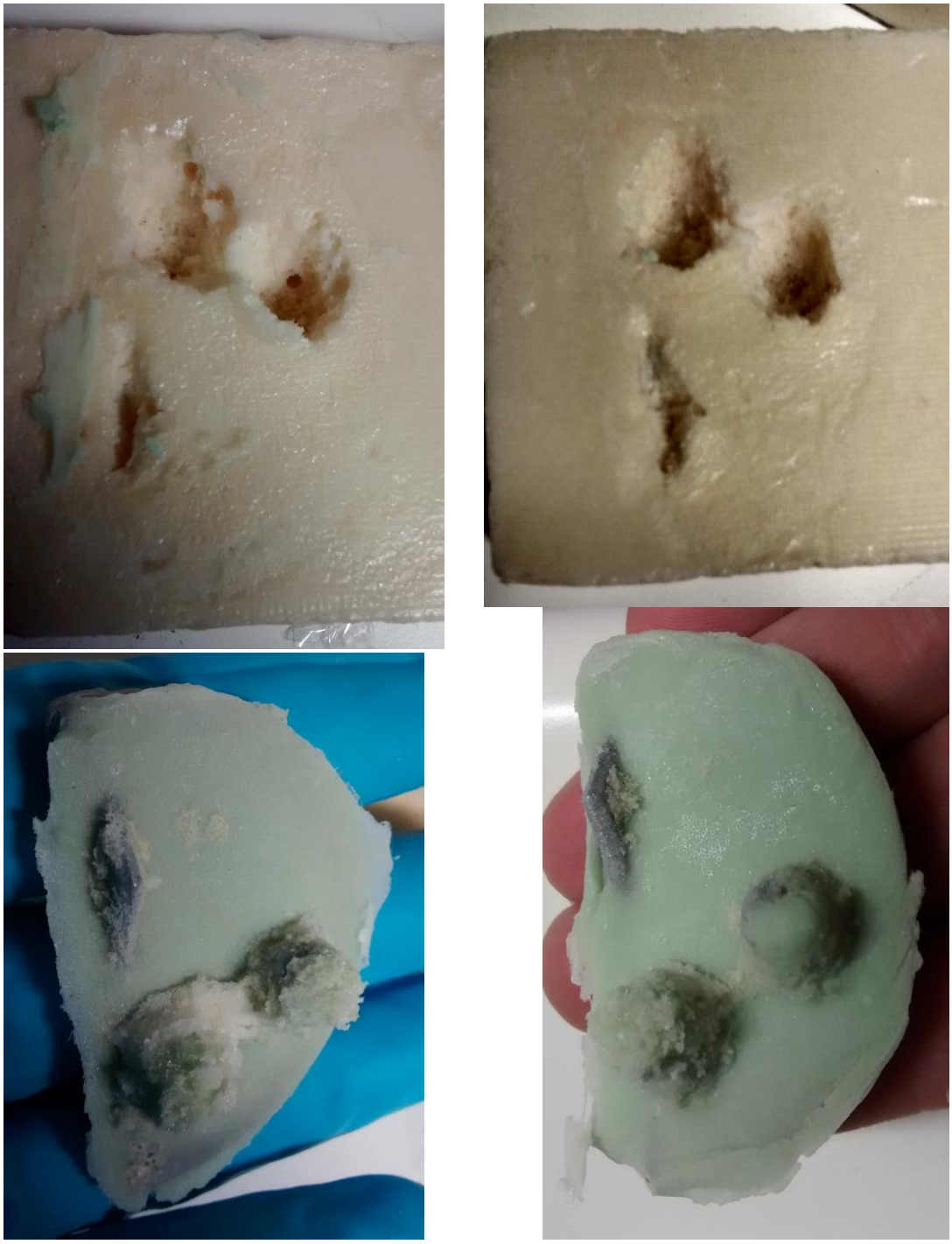

Figure 11.1-7: Photos of the Original Prototype Samples Post Testing
To the left are the photos from batch one, and to the right are the photos of batch 2 samples.

When the BQ prototype (figure 11.1-6) was pulled off, the cement remained on the prototype and took with it almost an even thin layer of foam, with some

areas having more foam present than others – around the furthest (posterior) away flange from the applied shear load and in the furrows of the rippled surface. The alignment of the prototype was unclear due to most of the flange shape being distorted by the shear loading and the removal of some foam – it was considered to be mostly aligned to the patterned in the foam. The foam was crushed on the posterior side of the foam block and the posterior walls of the flanges were crushed.

The figure 11.1-6 are the original prototype; the foam did not appear to have distortion due to the prototype's displacement at first, but a closer looked suggested that the prototype underwent rotational displacement as well as translational displacement. The hole left by the fin shape was not straight, it had a little triangle shape in the top half of the line, using this information it was then noted that there might be some distortion in the upper left of the pegs. In the first batch it seemed if the prototype was additionally aligned off axis. The cement took some foam off when the prototype was removed – the first batch was cleaner but had a bit of foam around the base of the pegs and fin. In the second batch the foam was in the acute angle of the peg and round the base of the peg.

11.1.3 Discussion

The graphs and the table show that design BQ required a larger force to displace the implant suggesting that this design performs better than the other two because it has a higher maximum force and higher stiffness. The original

prototype's maximum force for the 1.5mm displacement does not increase when 5.0mm is applied unlike the other two prototypes; this suggests that the original prototype reaches the maximum resistance at a lower displacement and the interface is experiencing a plastic deformation. Even if there is an displacement offset, as suggested by figure 11.1-, this is unlikely to affect the maximum force which the prosthesis can handle. The T6.2 prototype from the qualitative data suggests that both prototypes were not position correctly when cementing. The second batch of the T6.2 prototype had better alignment compared to the first batch and as such had a higher maximum force – this could explain the 60% CV value; extrapolating this, if the T6.2 prototype was aligned as intended then it might be have a higher maximum load than the original. However, it might not be the case and since it did not line up in both batches, it might not be an ideal fixation if misalignment during cementing can happen.

The CV values for the samples are acceptably low, taking into account the cement variation from batch to batch and given that only two samples were tested. The exceptions are for the T6.2 prototype stiffness and maximum load, and the BQ prototype's maximum load. As mentioned, the T6.2 difference is possibly due to misalignment when cementing, because second batch had a better alignment and a higher maximum load. This might be the case for the BQ prototype because it was not fully known if the samples were aligned with the BQ prototypes. Though, the variation of the BQ prototype stiffness was not affected like with the T6.2

prototype, the cause of the variation in the BQ prototype may not be due to misalignment as the stiffness would also be assumed to be affected.

The foam substance used did not seem to be as porous as cleaned cancellous bone and the surface of the foam is less porous than main body of the foam due to the close cell nature of the material. The foam was meant to be cut by the burr and this would have exposed the porous surface, instead a negative mould was used to create the shape and this meant the prototype would be cemented onto the less porous surface of the foam block. However, this was not the case, when the mould was pulled off the foam block after setting it evenly removed the top surface of the foam that meant the cementing surface was almost as porous as the main body. The penetration of the cement into the foam was approximately the same depth as the bovine cemented samples. Even though the foam does not fully match cancellous bone physical material properties, it is a reasonable and repeatable representation of the prosthesis-cement-tibia system. The other limitation of this experiment was the small sample size, but with the sample size of 2, the standard deviations and the coefficient of variance are low enough to draw preliminary conclusions from.

Knee kinematics are more complicated than the shear and tensile condition represented in this experiment. To assess the *in vivo* performance would be very difficult because of the loading patterns for walking is different from running, crouching, going up and stairs, and just standing. In addition to the different load patterns for movement, everyone has a slight variation which will cause different

combination of forces. On top of that average loading pattern is complicated to replicate and be able to produce meaningful results. Not to say it can't be done because NYU has created a testing apparatus that they call a crouching machine. Their machine can manipulate cadaveric knees to replicate a crouching motion[254]–[256]. This could be next step in assessing the performance of the prototypes.

The qualitative data suggests that the BQ prototype was consistently aligned with both batches; this could be due to the convex under surface of the prototype innately centres into in the concave surface of the foam. The original prototype also seem to be misaligned but this less affect the quantitative lesser than the misaligned T6.2 prototypes. This suggests that the pegs and MAKO fin are forgiving fixation methods than the T6.2 prototype. However, it seems that if the original prototype is misaligned then there are rotational forces being applied to the interfaces, and from the literature this is not ideal.

Due to the high maximum force and stiffness along with the potentially high alignment, the BQ prototype is a strong candidate in adhesion performance in comparison to the other two prototypes.

11.2 FEA Representing Prototypes Experiment

Modelling and analysing with FEA is great way to try out many new designs and concepts to investigate how well they perform under different conditions but it does have the downfall that the results might not be represent reality. Therefore, to gain qualitative validation of the FEA analysis, this virtual model represented the above prototype experiment in order to compare the results.

11.2.1 Aims

The aim was to validate the FEA models to the laboratory work done in the previous section of this chapter. An FEA model that represented the laboratorial prototype adhesion experiment was modelled, meshed, and analysed. The FEA results compared the stress concentrations and deformation to the experimental results to see if these corresponding areas behaviours are equivalent to each other.

11.2.2 Results

The maximum von Mises and strain equivalent experienced by each foam block was entered into the table 11.2-1 below. The von Mises values of the foam block with the original prototype experienced was approximately 3 times greater than the other two prototypes. The strain equivalent values were less dramatic: the original prototype was only approximately a third more than the other two prototypes. The von Mises and strain equivalent values increased proportionally in a linear manner in accordance with the increase in shear displacement conditions from 0.1mm to 1.5mm to 5mm. This means that the strain equivalent values in 5mm displacement condition are high (up to 165%) this due to the large displacement factor which reduces the reliability of the FEA numerical values but these results are meant to be for comparison of the three prototypes.

Table 11.2-1: The Maximum von Mises and Strain Equivalent Values Experienced in the Foam

	Original		**BQ**		**T6.2**	
	Von Mises (MPa)	*Strain Equivalent*	*Von Mises (MPa)*	*Strain Equivalent*	*Von Mises (MPa)*	*Strain Equivalent*
0.1mm	5.002	0.03305	1.705	0.02428	1.826	0.02551
1.5mm	89.68	0.4946	25.62	0.3587	27.15	0.3885
5.0mm	302.1	1.648	85.42	1.195	90.47	1.296

The peak von Mises location for the original prototype was on the apical point of the fin; BQ peak von Mises was the area under the apical point of the prototype; and T6.2 was under tail point of the prototype. The images in figure 11.2-1 show the location of the peak von Mises at each prototype.

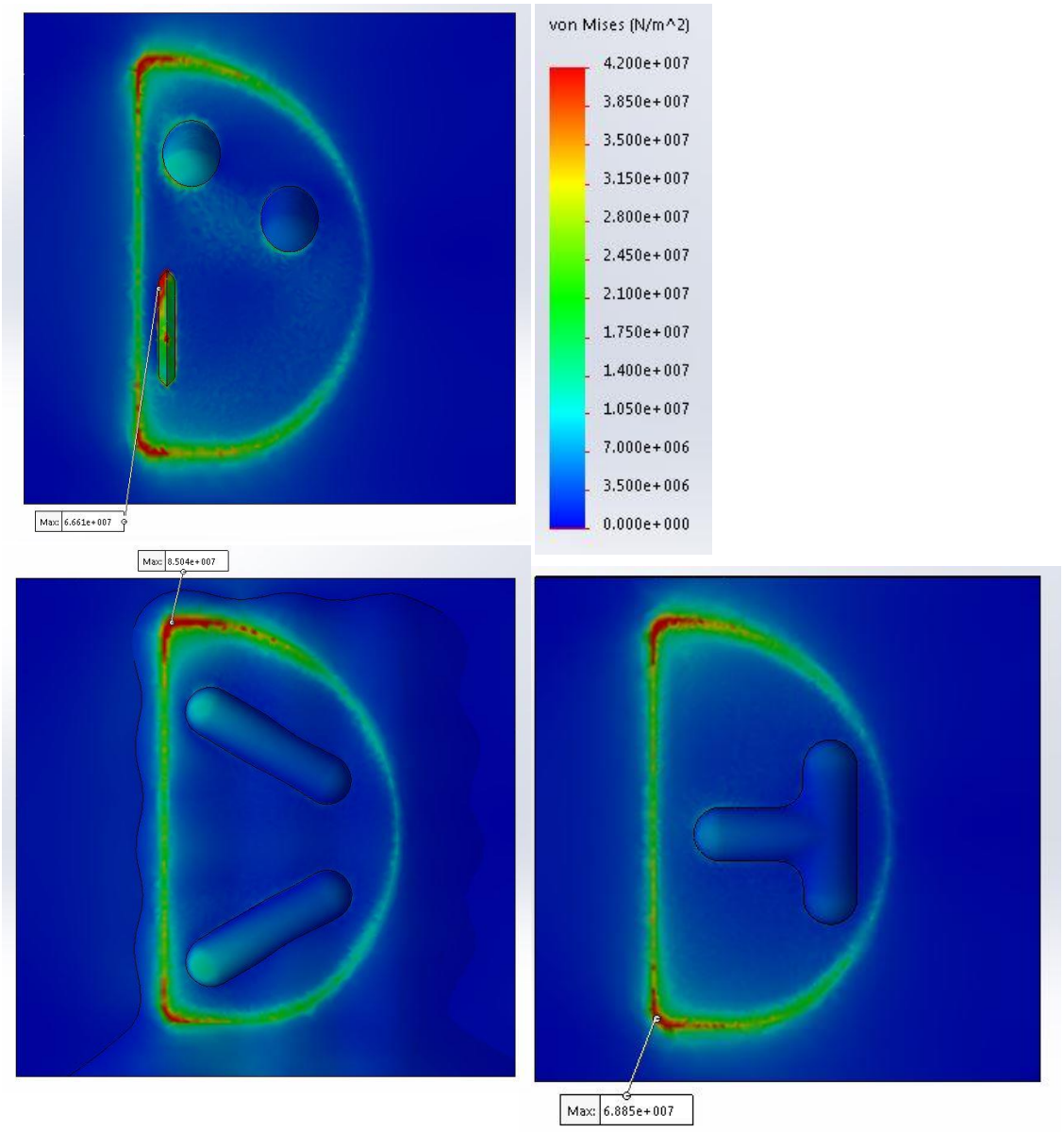

Figure 11.2-1: Von Mises Results under 1.5mm
Top left is the original prototype, bottom left is the BQ prototype, bottom right is T6.2 prototype, and top right is the von Mises Scale

Though were the plot highlights the maximum von Mises stress value, they were at least one more location with high stress concentration. The original model, seen in the iso-clipping in figure 11.2-2, has a small area directly under the apical and tail points of the prototype, and on the tip of the fin. The BQ and T6.2 models

have a stress concentration on the surface opposite the peak von Mises stress, see figures 11.2-2. In all cases, it seems the stress concentrations occur on the elements near the surface and they don't penetrate into the foam.

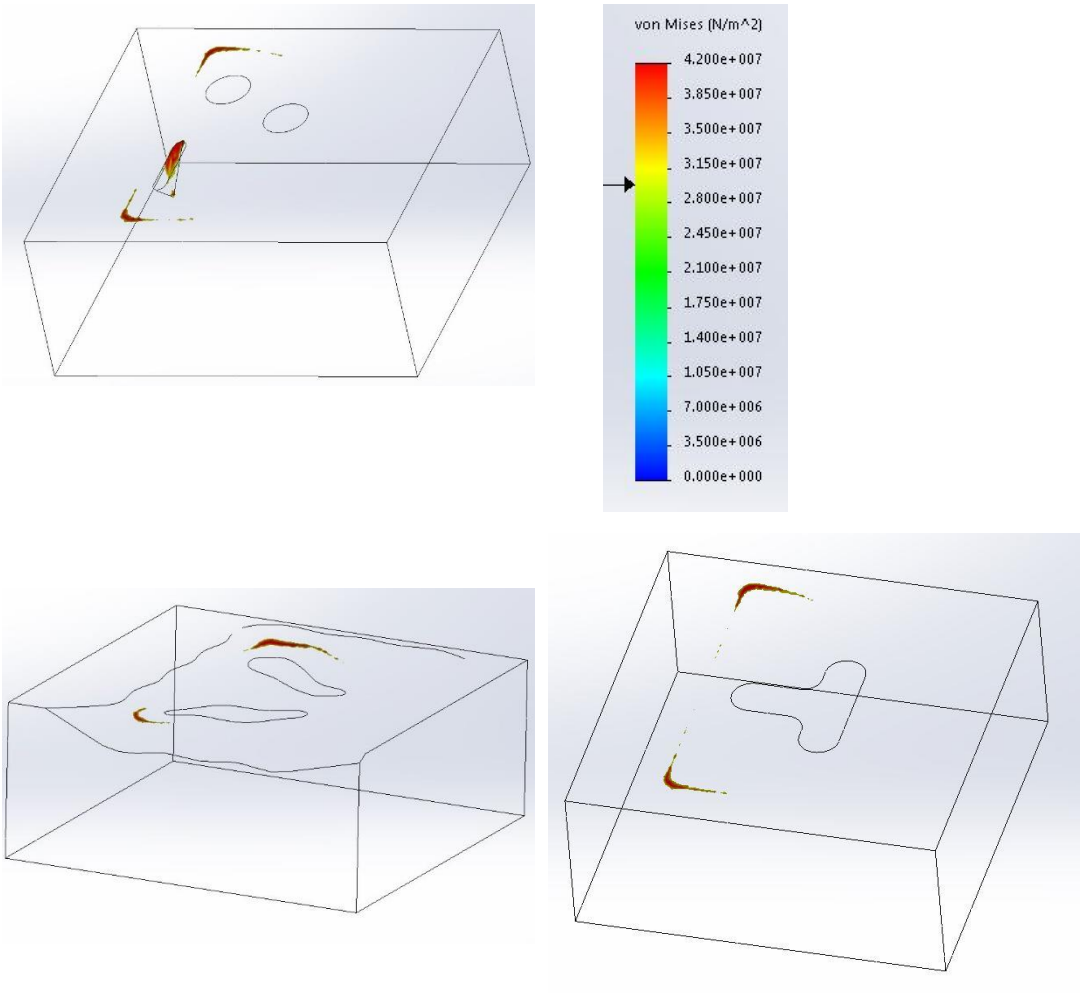

Figure 11.2-2: Von Mises Iso Clipping Results under 1.5mm Condition
Top left is the original prototype, bottom left is the BQ prototype, bottom right is T6.2 prototype, and top right is the von Mises Scale with arrow indicating the arrow.

The distribution of the stress can be seen in the iso-clippings in figure 11.2-3. In the original model, the stresses were distributed down leading from the base of the pegs and the area under the straightedge of the prototype. The stress distribution of the T6.2 and BQ models initially spreads across the surface starting at

the straight edge around the apical and tail, before going down the foam almost uniformly.

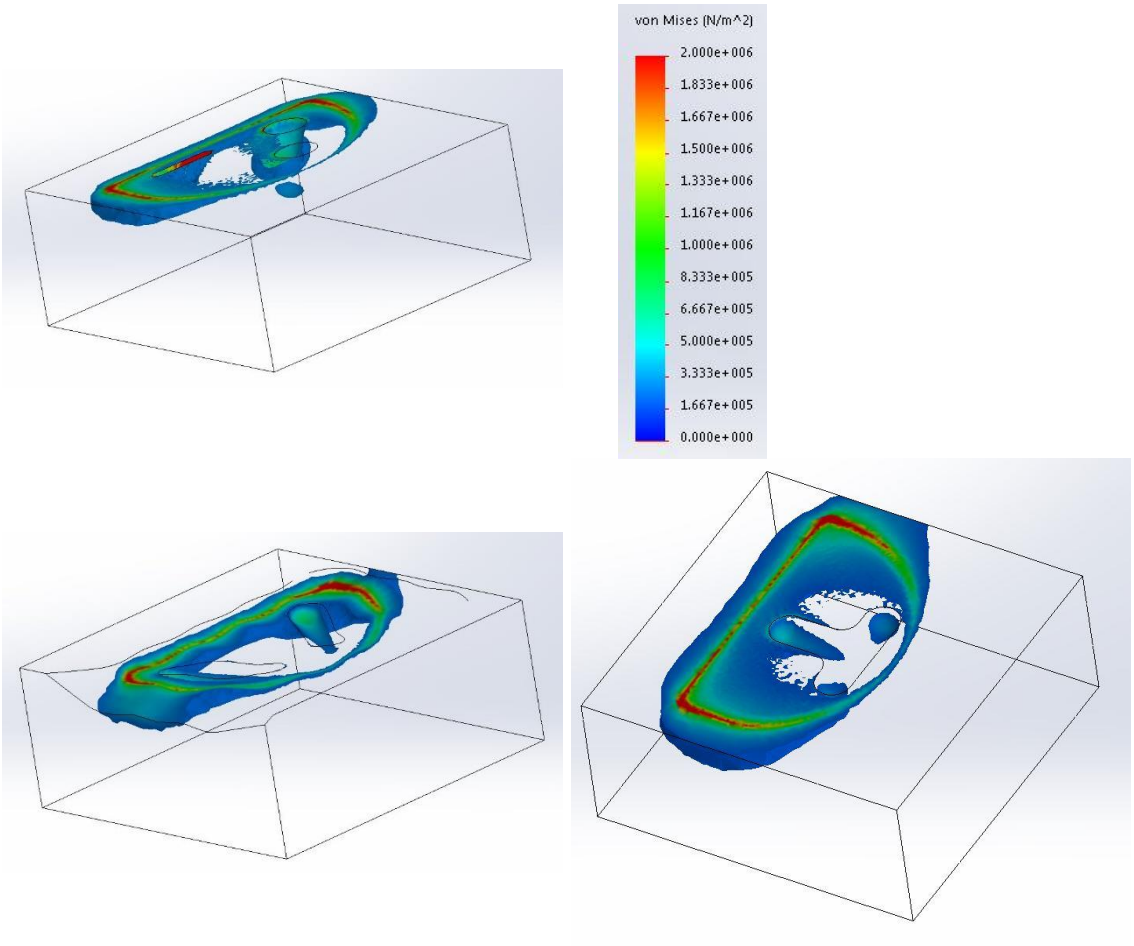

Figure 11.2-3: Von Mises Iso Clipping Results under 0.1mm Condition
Top left is the original prototype, bottom left is the BQ prototype, bottom right is T6.2 prototype, and top right is the von Mises Scale with arrow indicating the arrow.

Looking into the shear stress on the XY plane, i.e. in the apical-tail direction, the pole shear peaks were located under the apical and tail points of the prototype for all three designs, the values all being roughly in the same ball park. The original prototype also experiences ca. 0.6MPa and 30MPa shear on the MAKO fin and -0.6MPa and -30MPa shear on the apical peg (0.1mm and 5mm displacement values

respectfully). The BQ design has just about noticeable shear stress of ±0.3MPa and ±16MPa on the inside curves of the flanges.

From the triaxial plot, the axial stresses in the apical part of the foam were generally under tensile conditions, while the tail part of the foam was the polar opposite i.e. compression. The foam surface under all three of the prototypes has the apical section of the crescent part under tension, and the tail section of the crescent under compression; the opposite is true for the straightedge, can be seen in figure 11.2-4. Additionally the tension from the apical point extends up to the apical wall, likewise for the opposite side, this can been seen in figure 11.2-4. The peak tension (3.07MPa) in the original prototype is on the rim of the apical peg, the rim on the tail peg is around half the stress value. The peak compression (-3.82MPa) was on apical side of the fin. At the base of the pegs had compression of approximately 0.4MPa and 0.2MPa (apical and tail respectively) but on the back of the peg (wall nearest the apical) is in tension. The T6.2 prototype had compression on the apical edge of the leg of the 'T', but this was just on the surface where the elements underneath were experiencing tensile conditions. This also observed at the tail edge with experiencing tension at the surface. The peak tension and compression stresses are almost complete opposites (in position and value), the peak tension is located at the apical tip of the prototype with a value of 3.42MPa and the compressive peak it at the tail tip with a stress of 3.12MPa. The compressive peak of the foam under BQ model is 2.13MPa at the tail tip, the tensile peak stress is at the apical tip at 3.44MPa. The elements on the tail walls of the

flanges experiences compressive stress, the stresses concentrated on the apical flange next to the straightedge, stress approximately 0.6MPa. The opposite is true for the apical wall of the flanges, the peak tension force is on the apical flange next to the straightedge (0.4MPa); both of these can be seen in figure 11.2-4.

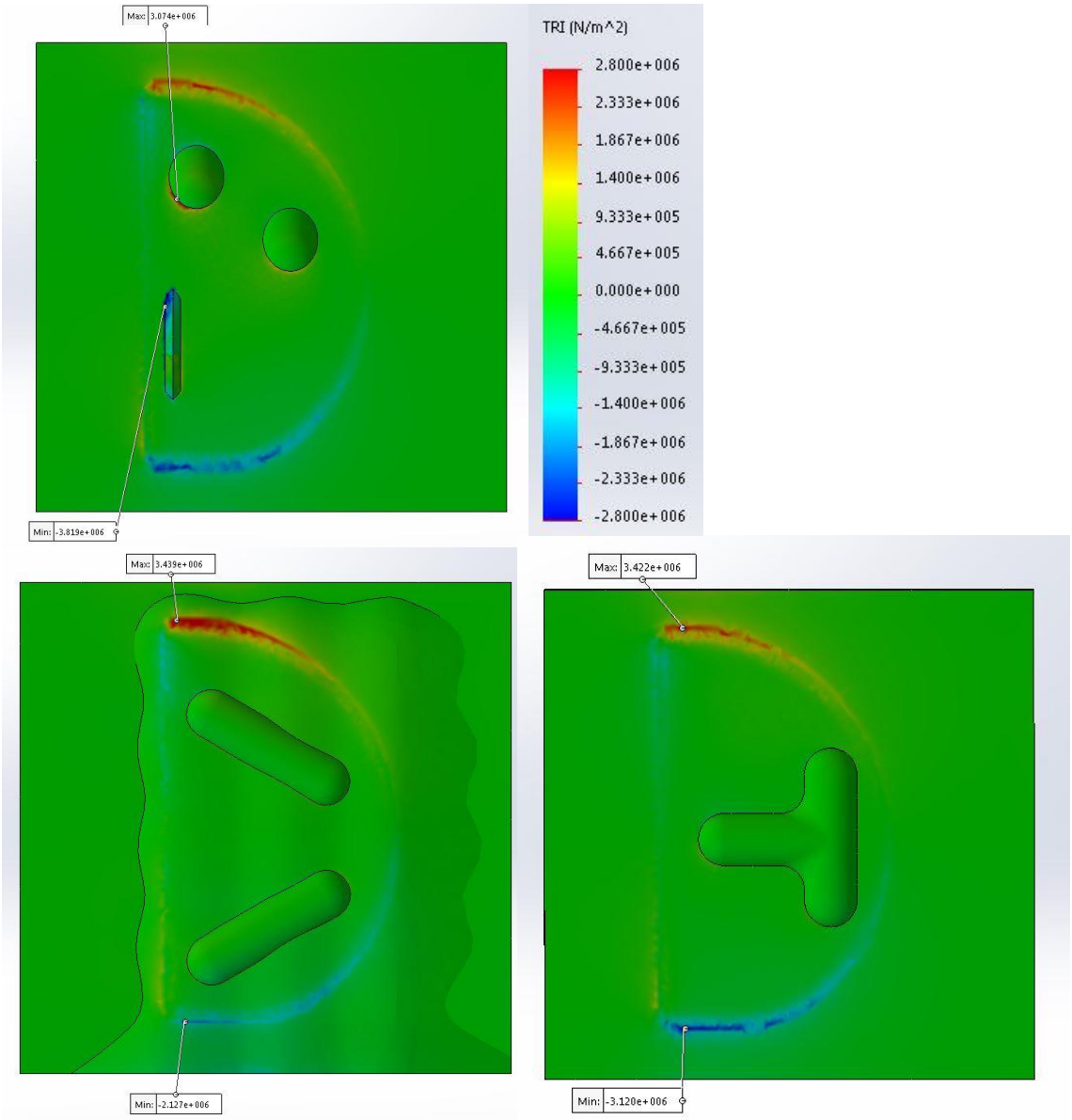

Figure 11.2-4: Triaxial Results under 0.1mm
Top left is the original prototype, bottom left is the BQ prototype, bottom right is T6.2 prototype, and top right is the triaxial Scale

11.2.3 Discussion

Using the results above and the results from the experimental prototypes, the simulated models were compared with the experimental models. The zones most likely to fail would be the ones with the highest von Mises. Though von Mises is expressed always as a positive integer, as a result it is unreliable to predict if the failure will be due to tensile, compression, or shear. The knowledge from the iso-clipping suggests that the stress concentrations lie on the surface, and the shear plots in the apical-tail direction strongly suggest that the main mode of failure is of shearing. With the triaxial plot, the stress concentrations on the apical side were possibly experiencing tension; compression in the tail posterior side.

Experimentally, the cement pulled away from the apical surfaces. This suggests that the apical half of prototype was experiencing tension until the cement broke off from the foam. The tail portions of the foam were crushed in the laboratory experiment, suggesting that the foam was under compression. This is similar to the triaxial plot information in the FEA results. The triaxial results from the original prototype had the rim around the pegs that were expected to be under compression were instead expressing tensile values; likewise, the base of the pegs were expected to experience a high level of compression stress, but the tri-axial plot displayed it mostly without stress, with some elements in tension and some in compression. The inspection of the original's foam blocks does not clearly indicate this FEA stress observation. On the physical foam sample, the rim around the peg did not seem to have been compressed, though a number of the pegs on the tail

side had foam stuck to the cement. This could have happened because of compression on the walls of the peg – this skews the interpret results. In the FEA boundary conditions and the laboratory set-up, the axial force is pushing the pegs into the foam, which could be causing the base to be slightly compressive and pull on the rim of the peg, while the shear force pushes the tail wall of the peg into the foam causing compression (and tension on the other side of the peg).

The FEA results had the original prototype with the greatest peak von Mises stress with several stress concentrations. If it is assumed that having a higher localised peak concentration will result in material failure, and each site increases the rate of material failure; then the force required for failure of the system can be assumed to be reduced. With this assumption, the FEA results suggest that the force required to displace the original prototype to be smaller than the other two prototypes; this agrees with the experimental results at 5mm.

The FEA model has its limitations, as a consequence to its simplicity it doesn't fully represent the experimental conditions. The bond between the assembled parts is a known as a perfect bond, i.e. the surfaces interfaces are permanently attached and as a result, if one of the surfaces is deformed the other surface is also deformed. This isn't true representation to reality under the majority of circumstances but it removed the guess work needed to assimilate the factors that influence interface (such as friction – static and dynamic). For small displacements, the perfect bond feature is unlikely to influence the analysis as both virtual and physical bond in reality should perform in the same manor till just before

bond failure. When there is failure of the interface bonds, other factors become bigger influences at the interface; thus, making the perfect bond assumption unrealistic when big displacements are being examined. The shear displacement conditions increases by 15 times and then 3.33 times; the von Mises and strain equivalent values also increase in the same manor. Therefore, the simulation remained in a linear fashion for all three conditions, which means the increase displacement 'amplified' the loading patterns linearly, so the results from any displacement could be used to predict the initial potential failures. From the results in the experimental supports the FEA analysis, thus suggesting that the FEA can be relied to represent potential areas of initial failure.

11.3 FEA Modelling of Prototypes Attached to a Tibia

The advantage of finite elements is it that it can provide localised stress and strain values. The previous experimental work qualitative data of potential areas of stress concentrations; FEA can give this information in a numerical fashion. Areas where there is stress concentration are areas that are likely to fail and could be the site of initiating system failure. As bone regenerates, it remodels its structure depending on the stress experienced. If there are areas of low to no stress then the bone is going to remodel that area by reducing the density.

11.3.1 Aims

The aim is to compare the prototypes to the standard design to determine the optimal design in terms of stress concentration and stress distribution. The

approach was an FEA on a proximal half of a tibial under two conditions: a person standing (axial load of 750N) and conditions similar to the experimental prototypes (axial load of 33.79N and shear displacement of 0.1mm). Then the stresses and strains of the models were analysed in terms of stress concentration, low stress concentration, maximum stresses, and stress distribution.

11.3.2 Results

The first part of the results is comparing all the results, then the section is broken into 8 for the different boundary conditions to express and discuss the stress observations in the tibia.

Regarding at the tibia component only, as this is the area of interest, the maximum von Mises and strain equivalent that were experienced are presented in tables 11.3-4 and 11.3-5 below. The A and B denotes conditions A and B respectively; the L and M denotes the lateral and medial plateau of the tibia the prototype was positioned on – please refer to table 11.3.2.

Table 11.3-1: The Maximum Von Mises Stress Values Experienced in the Tibia

σ (MPa)		**Original**		**BQ**		**T6.2**	
		Non Cement	*Cement*	*Non Cement*	*Cement*	*Non Cement*	*Cement*
A	**L**	470	11.6	11.4	17.3	17.9	25.6
B		17.6	3.88	0.731	2.36	0.944	5.00
A	**M**	130	17.1	18.5	40.2	24.7	22.3
B		5.64	10.1	1.83	20.2	1.48	19.7

Table 11.3-2: The Maximum Strain Equivalent Values Experienced in the Tibia							
ε		**Original**		**BQ**		**T6.2**	
		Non Cement	*Cement*	*Non Cement*	*Cement*	*Non Cement*	*Cement*
A	**L**	1.90	0.0759	0.0749	0.0912	0.134	0.0700
B		0.0694	0.00635	0.00517	0.00684	0.00605	0.00491
A	**M**	0.748	0.129	0.114	0.139	0.130	0.128
B		0.0327	0.00691	0.00776	0.00649	0.000455	0.000543

The two loading conditions, A and B, appears to have an effect on the maximum von Mises stress, A had a higher axial load applied and had a higher peak von Mises stress. For condition A (axial loading), the original design on the lateral tibial plateau had the highest von Mises stress in all 24 simulations and was located on the rim of the anterior peg on the tibia. The second highest von Mises again was the original prototype in condition A on the medial plateau. BQ has the lowest peak von Mises in condition B on the lateral plateau, closely followed by T6.2 design of the same parameters.

The cementless original prototype had the highest peak von Mises values; whilst the original prototype with cement had lower peak von Mises stress values than the other two cemented prototypes – expect for lateral BQ under condition B (axial and shear loading) that was lower than the original. In 3 out of 4, the original prototype had at least 4 times greater peak von Mises stress than the cementless group. The opposite is true for the other two prototypes, they had the cement models expresses at least 50% more von Mises stress (in 7 out of 8) than the

cementless group. In condition A, there was little difference in peak von Mises stress values between the BQ and T6.2 prototypes on the medial and lateral plateau; but in condition B the peak von Mises stress in the lateral plateau was considerably lower than the medial plateau.

As expected the strain values follow similar pattern to the von Mises stresses above, the two highest strains were in the original cementless prototypes. The strain values were greater in condition A than in condition B and condition A on the medial plateau was often greater than the lateral plateau.

From the visual von Mises plots, the following general observations were noted. Under condition A, the presence of cement seems to dampen the level of stresses transferred to the bone and it also changed how the stresses distributed through the head of the tibia. For the models with cement, the cement carries a lot of stress and strain along the upper most part of the cement; this is also the thinnest part of the cement. Medial condyle had lesser value of stress concentrations and the load distribution in the tibia head is directed more to the outer surface of the tibia. The features tended to be the location of the stress and strain concentrations: for the fin it was the tip and the sharp corners with the stress concentrations; the pegs the concentration is around the tray base and not so much at the ends; the 'T' shape it was the curves and the right angle at the base that had the stress concentrations; and the two grooves in BQ the lateral curves had the stress concentration. It is also these features that transfers stresses almost straight down the tibia and it is from the base the stresses build up the side of the tibia.

Under condition B, the cement prototypes had less stress transfer onto the tibia from the prototype. The stress concentration on the tibia wall also occurred on the models with cement; the plot suggests it is greater in condition B. The following subsections express the observed stress features in modelled prototype in the 8 conditions.

The simulations in presented here are simplistic analysis, the numerical values presented provides the strength in comparing the prototypes. Therefore, each simulation will be presented and discussed in the following subsections. The results are displayed using colour as an indicator to the level of stress within the elements of the model; red indicates elements that likely to fail first due to experiencing high stress while darkest blue areas are elements not experiencing stress.

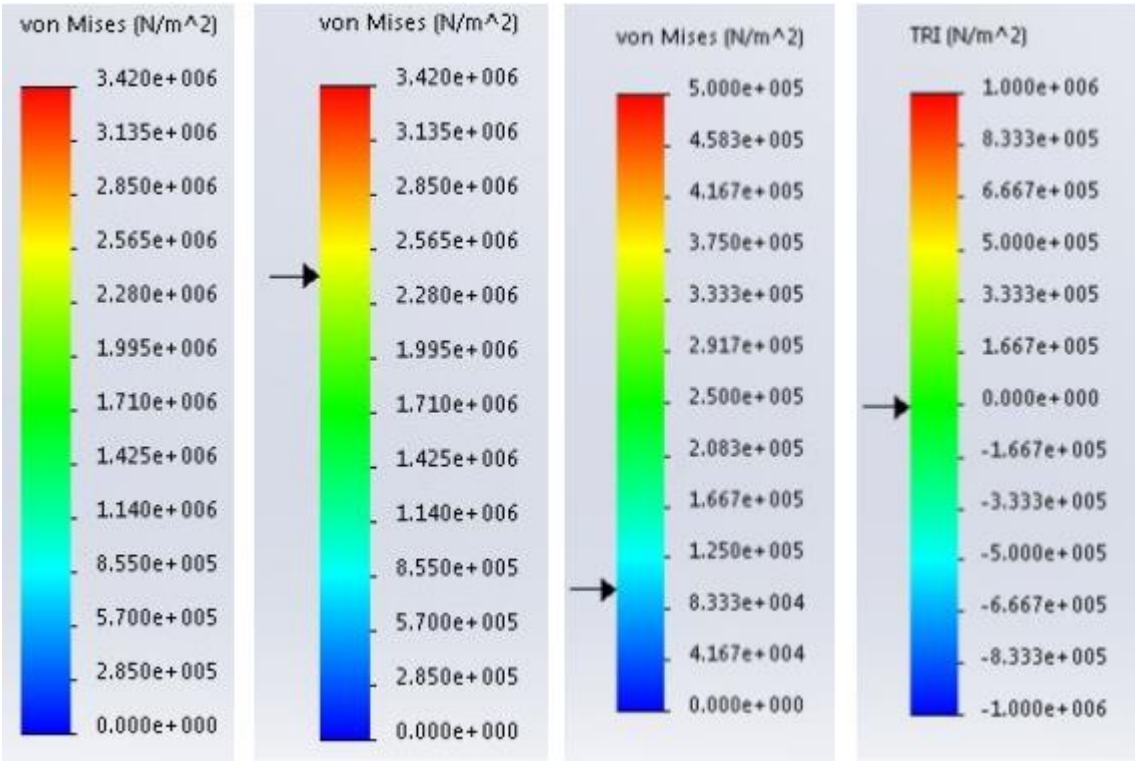

Figure 11.3-1: The Four Scales

On the left is the von Mises scale from 0MPa to 3.42MPa. In the middle left is the same Von Mises scale but has an arrow that indicates the level the ISO clipping taken from. The middle right is the von Mises scale used for the ISO clipping of the models under condition B; this was due to the smaller magnitude of stresses. The right image is the triaxial scale with the arrow indicating the zero stress colour.

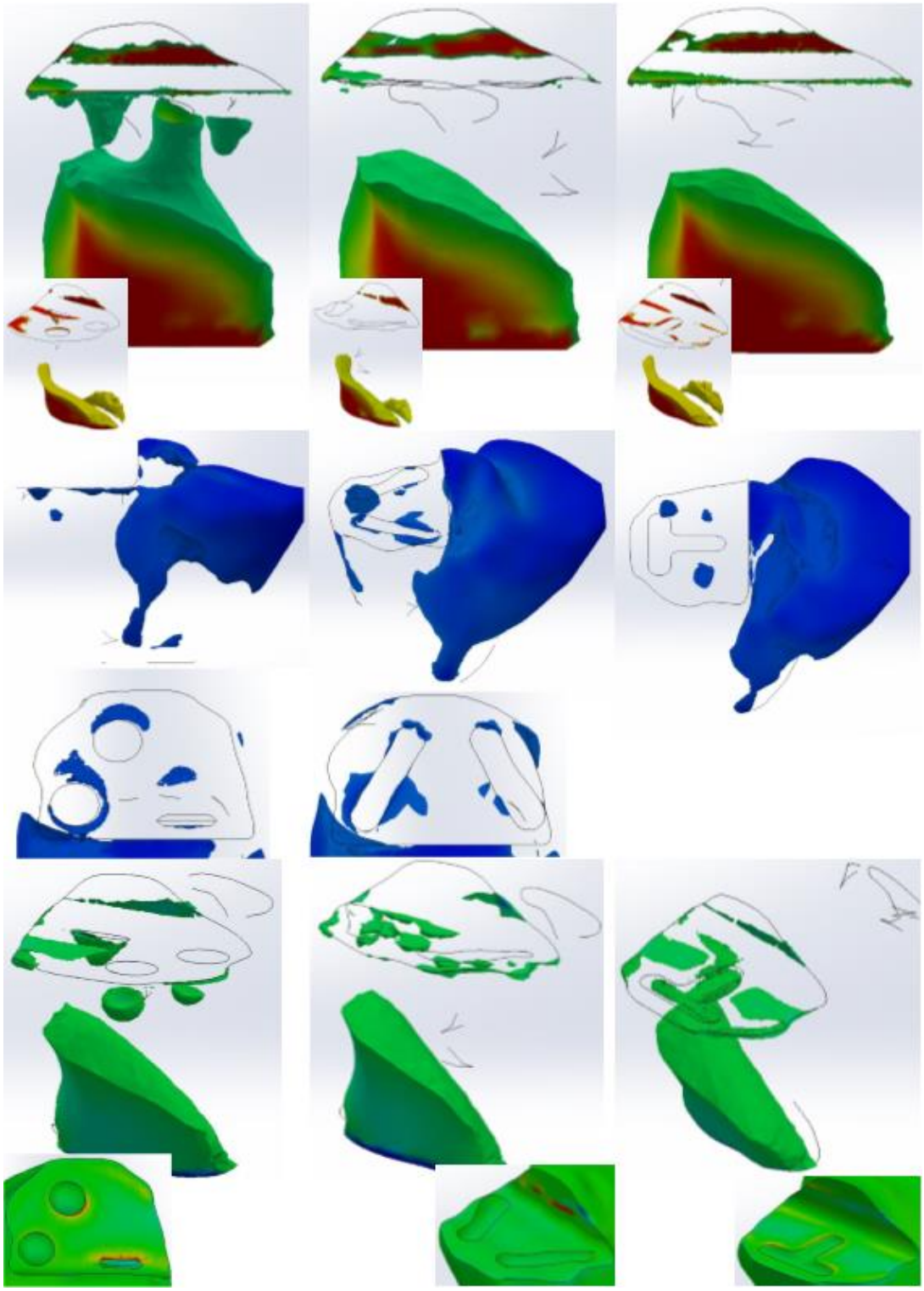

Figure 11.3-2: Results from ALC Condition
This figure shows the three prototypes: original, BQ, and T6.2 in respective column; and the three numerical analysis.
Top row shows the locations of high stress from the von Mises criterion.
Middle row shows the locations of no-to low stress from the von Mises criterion.
The bottom row shows the element tension in the longitudinal axis – Triaxial.

11.3.2.1ALC Analysis

11.3.2.1.1 Results

The von Mises plot, in figure 11.3-2, has red zones on the original prototype around the MAKO fin, the tail peg, the posterior of the cut surface, on the cut wall and on the surface distal to the tibia. This is similar to the T6.2 prototype, most of the cut surface has red zones: running next to the fillet and around the medial surfaces of the 'T' flange; as well as red zones on the wall and surface distal tibia. The BQ prototype has only the latter two red zones – the cut all wall and surface distal to the tibia.

The von Mises iso-clipping, in figure 11.3-2: the zones on the cut surfaces are superficial while the stresses in the distal tibia were takes up around a third of the small distal stock. Utilising the iso-clipping interactive feature, the bone under the pegs and the fin on the original prototype has von Mises stress around 1.5MPa. From these features the stress radiates longitude down the tibia before radiating to the outer surfaces. The T6.2 prototype has von Mises stress approximately 1MPa at the base of the 'T'. The von Mises stresses in T6.2 favours the posterior side of the tibia. The BQ prototype is slightly different, the tail flange has .8MPa stress across the base, and the apical flange is approximately 0.5MPa. The stress is little less uniform across the transverse plane, it favours the posterior side of the tibia.

The von Mises shows no elements experiencing zero stress, in middle row of figure 11.3-2, but there are zones of interest that demonstrates von Mises stress less than 0.2MPa. On the original prototype, the areas of low von Mises stresses are

around the top the pegs and in the middle of the cut surface. The posterior bony landmark, around the edges of the apical flange, and the crescent tip of the tail flange experiences low von Mises stress in the BQ prototype. Prototype T6.2 has areas of low von Mises stress on the bony landmark and in the middle of the cut surface.

The triaxial plot, bottom row in figure 11.3-2, shows that the cut surfaces on the prototypes don't experience high levels of axial loads in any direction. Though the original prototype and T6.2 prototype have areas that were red in the von Mises plot have tensile stress ranging from 5MPa to at least 10MPa. The T6.2 prototype has an area of compressive axial stress, ca. 2.2MPa, in the middle of the cut surface, parallel to the fillet. The bases of the BQ flanges appear to be in compressive axial force approximately 1MPa.

The triaxial iso clipping of the BQ and T6.2 prototypes suggest that the whole lateral side of the knee is under compressive stresses, except for small zones around the 'T' and angle flanges, seen in the bottom right of figure 11.3-2. The original prototype also suggests the same but the cut tibia surface around the fin and the pegs are in tension, see in top two rows of figure 11.3-2.

11.3.2.1.2 Discussion

The von Mises and the iso-clippings of the prototypes indicate that the original and T6.2 prototypes do not produce an even distribution of the stress across the surface and through the head of the tibia. This has created zones on the

cut surface that potentially could fail due to yield of the bone material. In addition, all the stresses go through the middle of the lateral tibial head.

The areas of low stress suggest that the presence of features cause not only stress concentration but also zone of stress shielding. The BQ prototype does not seem to have any stress concentration present in the lateral (interested) side of the tibia.

The triaxial plot of the original prototype reveals some of the unexpected stress patterns observed in the von Mises plot. It was expected that the red zones in the von Mises plot to have the stress pattern from them but iso clipping just has the stress on the surface and not into the tibia; these red zones match the red zones in the triaxial plot that suggest that the elements are in tensile. While tensile stress patterns show up in the von Mises plot, the tensile forces would be playing a smaller role than the compressive and shear forces.

From both the von Mises and triaxial plots suggest, this condition, the BQ prototype produces the least stress concentration, the least stress shielding, and the only tension experiences is from the wall cut which is produced by the ideal contact condition of the prototype (to cement) to bone.

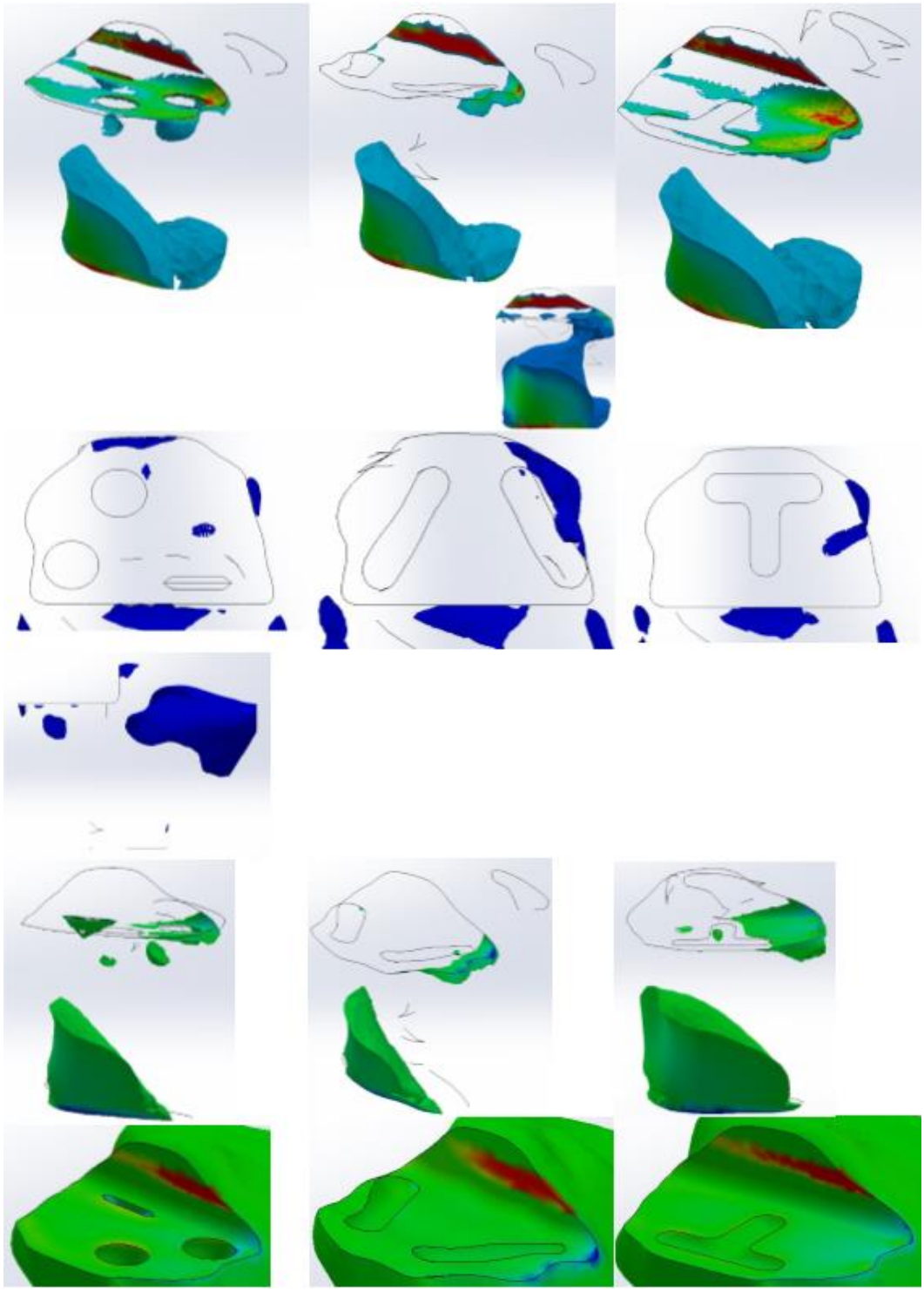

Figure 11.3-3: Results from BLC Condition
This figure shows the three prototypes: original, BQ, and T6.2 in respective column; and the three numerical analysis.
Top row shows the locations of high stress from the von Mises criterion.
Middle row shows the locations of no-to low stress from the von Mises criterion.
The bottom row shows the element tension in the longitudinal axis – Triaxial.

11.3.2.2 BLC Analysis

11.3.2.2.1 Results

All three prototypes have red zones on the cut wall, figure 11.3-3. The original prototype has areas of the light blue around the pegs, under the apical of the prototype, the rim of the fin, and in the fin. The other two designs also have light blue area under the apical of the prototype but have dark blue around their features.

The iso clippings, figure 11.3-3, show that the high stresses are located on the cut tibial surfaces and the distal of the tibia. Interacting with the iso-clipping, the original prototype has the base of the apical peg around 0.2MPa, and the bases of the tail peg and the fin around 0.1MPa. The stress radiates down the tibia primarily by the apical peg stress concentration, followed by the tail peg and then by the fin. The stresses fill out the middle of the tibia before radiating out to the other surfaces. The T6.2 prototype, has the anterior area experiencing von Mises stresses approximately 0.1MPa and this then radiates down the tibia anterior surface before almost in 45° plane to the transverse and coronal plane of uniform stress distribution. The base of the 'T' has von Mises stress approximately 0.05MPa. The BQ prototype also had the stress concentration at the anterior point, at the very tip it is approximately 0.4MPa and the bulk of the stress in the anterior point is approximately 0.1MPa. The anterior point of the apical flange has stress of ca. 0.1MPa; this joins with the radiating stress of the anterior surface, when this occurs the stress distribution travels diagonally towards the posterior side of the tibia.

According to the von Mises plots, middle row in figure 11.3-3, there are no areas of zero stress in the three prototypes. Taking 0.1MPa as the cut off, the three prototypes have dots of areas of low von Mises stress in the bony landmark along with other dark blue areas.

The triaxial plots suggest there is no stress on the cut tibia surface except from: around the pegs and fin of the original prototype; and under the apical point on the BQ and T6.2 prototypes.

The axial stresses in tibia of the T6.2 and BQ prototypes have very low compressive stresses, below 0.8MPa – figure 11.3-3. The bulk of the tibia with the original prototype has lower compressive stress, 0.3MPa, and has a zone in the middle that is 0.4MPa compressive. The BQ and T6.2 have almost the whole lateral side of the tibia in compression apart from small surface zones. The original prototype has an estimate third of the cut surface in tension; around the areas of the peg and fin the tension has approximate peaks of 0.5MPa. There is tension on the some of the wall of each peg and the triangle sides of the fin, ca. 0.2MPa.

11.3.2.2.2 Discussion

All three prototypes have red zones on the cut wall. The original prototype has more of the light blue areas, these are located around the pegs, and around and in the fin.

The von Mises iso-clipping suggest the pegs of the original prototype generate a higher stress concentration at their base. This then transfers the stress down through the tibia. This has been suggested in the PDS not the best mode of

stress transfer as ideally, as the stress should be carried on the outside of the tibia where the cortical bone is located which is better adapted to transfer of load. The other two prototypes do not transfer the load to the outside of the tibia but it doesn't have the stress concentration pattern the original prototype has.

The prototypes in this condition do not seem to affect the areas of low von Mises stress on the posterior surface. The original has an additional area of low von Mises stress, that is on the proximal lateral surface of the tibia.

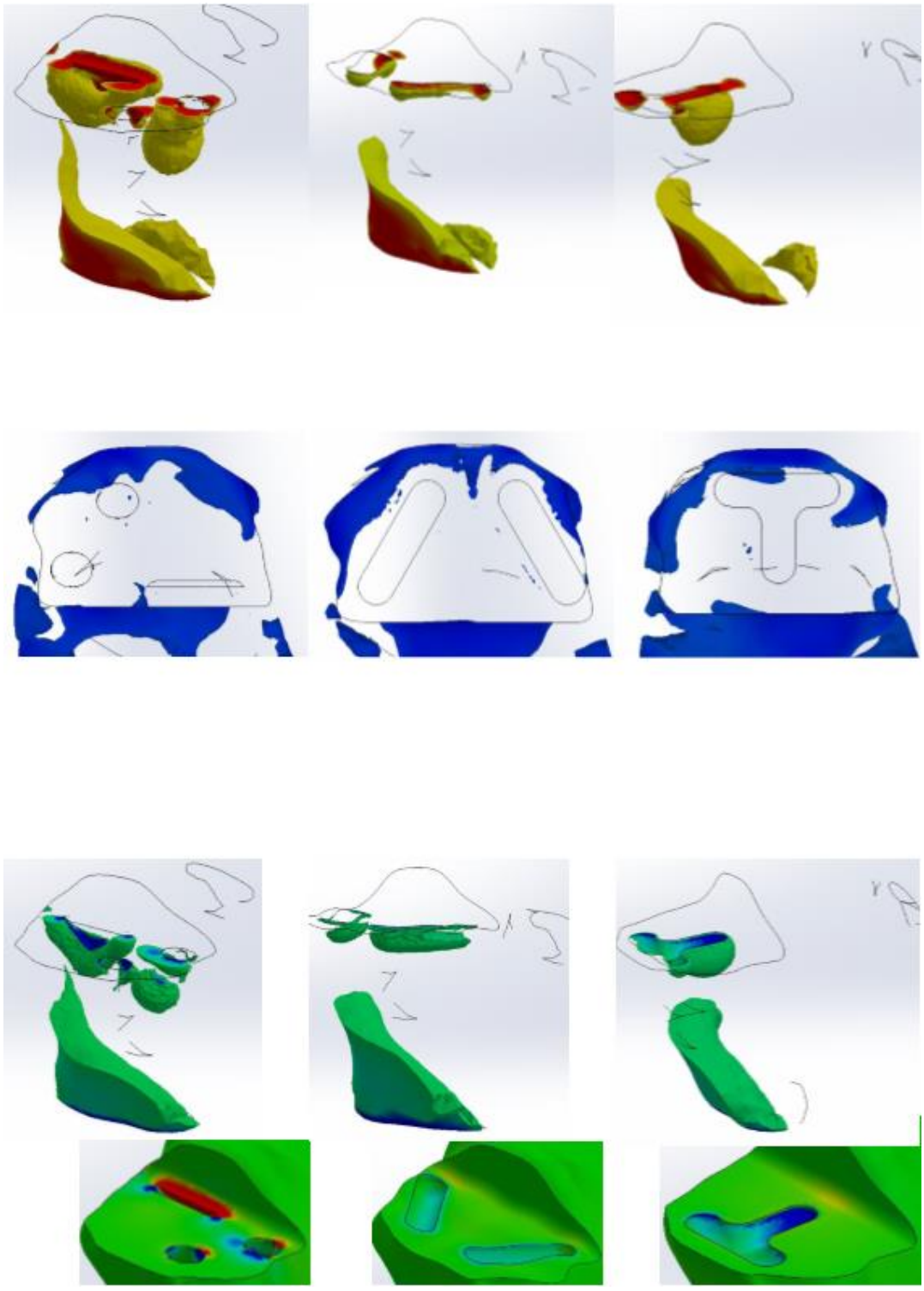

Figure 11.3-4: Results from ALN Condition
This figure shows the three prototypes: original, BQ, and T6.2 in respective column; and the three numerical analysis.
Top row shows the locations of high stress from the von Mises criterion.
Middle row shows the locations of no-to low stress from the von Mises criterion.
The bottom row shows the element tension in the longitudinal axis – Triaxial.

11.3.2.3ALN Analysis

11.3.2.3.1 Results

All von Mises plots, in figure 11.3-4, display large areas of red across the cut surfaces and the distal lateral side of the tibia. The original prototype has red plotted around the rim of the pegs, the base of the apical peg, almost all the cut surface in the fin, and around 5 out of 6 sides of the fin's rim. The T6.2 prototype has red covering almost all the leg of the 'T', half of each tip of the arms of the 'T', and the cut surface from the leg of the 'T' to the fillet. On the BQ prototype the red is around walls of the flanges and small spot on the fillet.

The iso-clipping, in figure 11.3-4, showed that all three prototypes had large von Mises stresses not just present on the surface elements. The original prototype has large red and yellow plotted zones around the base of the apical peg, and all around the fin. The T6.2 prototype has a large 'hot' zone around the 'T' leg, and two smaller zones on the 'T' arms. The BQ prototype has the least volume of red zones, each located at the ends of the flanges.

In the original prototype, the stress is distributed downwards from the above mentioned red zones, then towards to the outer surface of the tibia. Similarly, the T6.2 prototype distribution of stress extends downwards from the leg of the 'T', followed by the 'T' arms before distributing the stress to the outer surface of the tibia. The BQ prototype has the stress distributing across the tail flange surface before extending downwards, likewise for the apical flange but at lower von

Mises stress; the stress distribution then goes both out to the outer surface and inwards of the tibia.

All three prototypes experience zones of low von Mises stress around the cut surface outer rim, as seen in figure 11.3-4.

The triaxial stress plot, in figure 11.3-4, shows all three prototypes experience both compressive and tensile stresses on the cut surface. Prototype BQ has compressive stress of approximately 4MPa on the base of the flanges and the rims; BQ also has tensile stress (ca. 4MPa) on the fillet next to the tail flange and the majority of the rest of the cut surface has a lower tensile stress of 2MPa. The T6.2 prototype has compressive stress around the leg and arms of the 'T', approximately 6MPa; and the tensile stress (ca. 2MPa) covers most of the cut surface with a peak on the fillet next the 'T' leg. The original prototype has compressive and tensile stresses right next to each other, both at the same magnitude. The compressive stresses are on the rim of the pegs, on the base of the apical peg, lateral tail edge of the fin, the lateral apical edge of the fin, and most surfaces of the fin. The tensile stresses are located on the rim of the pegs, the wall of the apical peg, the medial side of the fin, and the part of the fin's tip. The majority of the cut surface of the original prototype is under tensile forces of approximately 0.2MPa as well as the base of the posterior peg.

11.3.2.3.2 Discussion

The red zones in the von Mises plots indicate that these zones are likely to fail first due to high stress.

The stress distribution does not seem very favourable in all three models as most of the distribution is through the middle of the lateral condyle. As a result, all three of them have stress shielding present in the lateral rim of the cut surface.

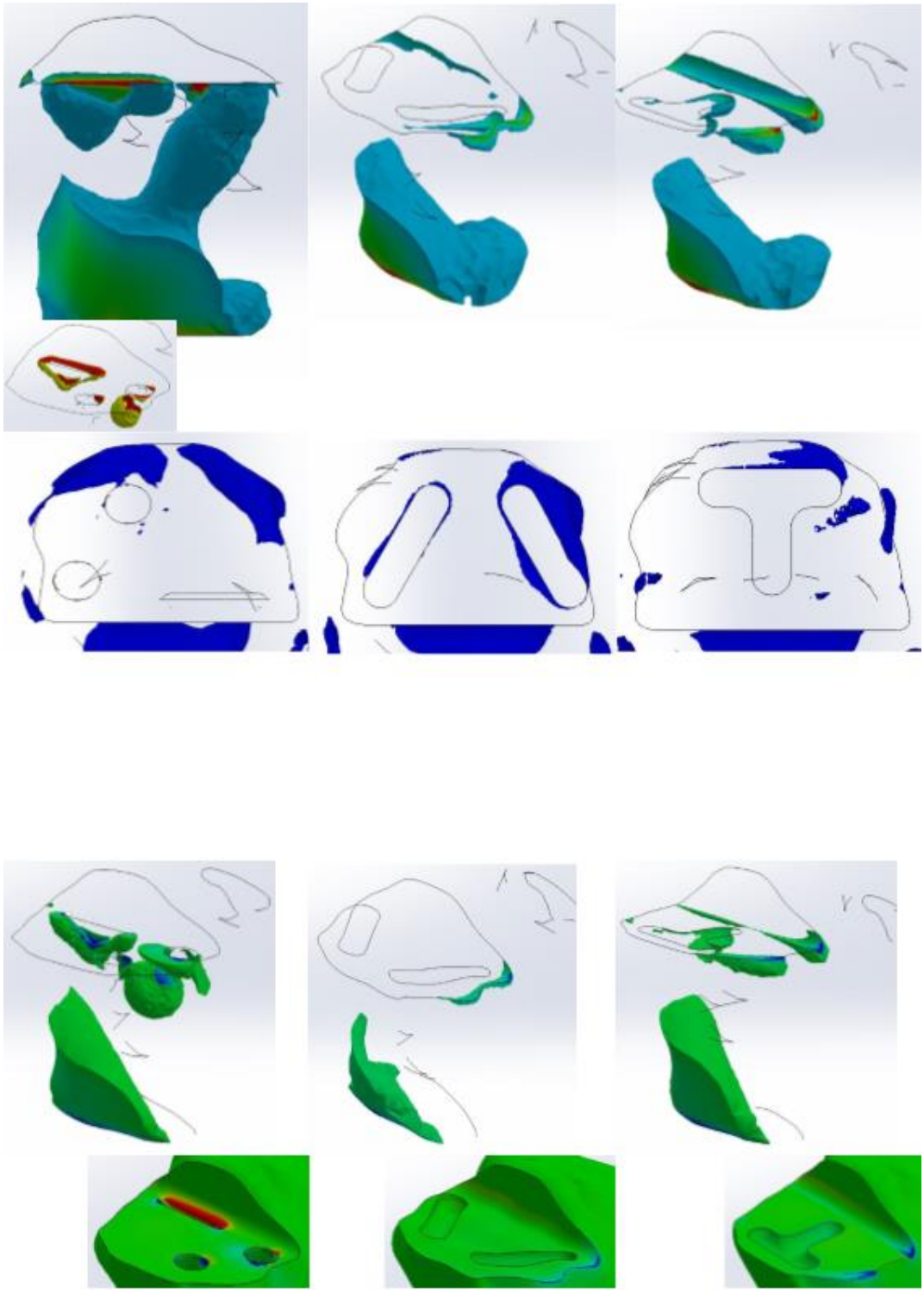

Figure11.3-5: Results from BLN Condition
This figure shows the three prototypes: original, BQ, and T6.2 in respective column; and the three numerical analysis.
Top row shows the locations of high stress from the von Mises criterion.
Middle row shows the locations of no-to low stress from the von Mises criterion.
The bottom row shows the element tension in the longitudinal axis – Triaxial.

11.3.2.4BLN Analysis

11.3.2.4.1 Results

The von Mises plots, in figure 11.3-5, on the BQ prototype and T6.2 prototype have a light blue colouring anterior point under the apical part of the prototype; while the original prototype has red surface spots on the apical peg, the apical point of the fin, and the fin's tip. Plus, on the original prototype, there is a mix of yellow and green at the base of the apical peg, around the straightedge side of the fin's rim, and the tail wall of the fin.

The interactive iso-clipping, in figure 11.3-5, for the von Mises of the original prototype shows the stress concentrations around the apical peg's base and the tip of the fin; these radiates downwards before expanding out to the tibia's surface. The T6.2 prototype distributes the stress downwards from the leg of the 'T', the apical arm of the 'T', and the lateral anterior edge of the cut surface; it then distributes the stress to the outer tibial surface. Similarly, the BQ prototype has the same stress distribution as the T6.2 prototypes from the concentration zones located at the base of the apical flange and the anterior edge of the cut surface.

The area of low von Mises stress are again, generally located on the lateral edge of the cut surface and on the bony landmark, in figure 11.3-5. For the T6.2 prototype the main area is the tail crescent edge of the 'T' and the medial wall of the 'T'. The BQ prototype the areas of low von Mises are around the flanges, more predominantly on the tail flange. The original prototype had low von Mises laterally to the tail peg and on the lateral posterior edge of the cut surface.

The triaxial stress, in figure 11.3-5, plots show that the original prototype experiencing majority of tensile stress across the flat cut surface. The original prototype has compressive and tensile stresses right next to each other, both at the same magnitude. The compressive stresses are on the rim of the pegs, on the base of the apical peg, lateral tail edge of the fin, the lateral apical edge of the fin, and most surfaces of the fin. The tensile stresses of the original prototype are located on the rim of the pegs, the wall of the apical peg, the medial side of the fin, and the part of the fin's tip. Most the cut surface of the original prototype is under tensile forces of approximately 0.01MPa, this is the same approximation stress at the base of the tail peg. Prototype BQ has compressive stress of approximately 1MPa on the anterior edge, under the apical point of the prototype; BQ also has tensile stress (ca. 0.01MPa) on posterior tip. The T6.2 prototype has compressive stress around the anterior tip (~1MPa), the anterior lateral tip (~1MPa), and the apical arm of the 'T' (0.1MPa); and the tensile stress (ca. 0.1MPa) covers most of the cut surface and the apical wall the 'T' leg.

11.3.2.4.2 Discussion

The BQ and T6.2 prototype have stress concentration, low in volume and magnitude while the original prototype has large volume of stress concentration that are closer to the yielding value of cancellous bone.

The stress distribution in T6.2 prototype arises from under the flange and through the middle of the lateral tibial condyle; is not as favourable as the original prototype that have the angled pegs distribute the stress evenly towards the

posterior tibial surface. To have the stress go through the middle of the tibia means the stress is carried on the cancellous bone instead of the stronger cortical bone.

The original prototype seems to have a greater volume of low von Mises stress than the other two; the low stresses are located on the surfaces. The BQ prototype has low stress around the flanges which is not ideal as it will weaken the bone in accordance to wolf's law.

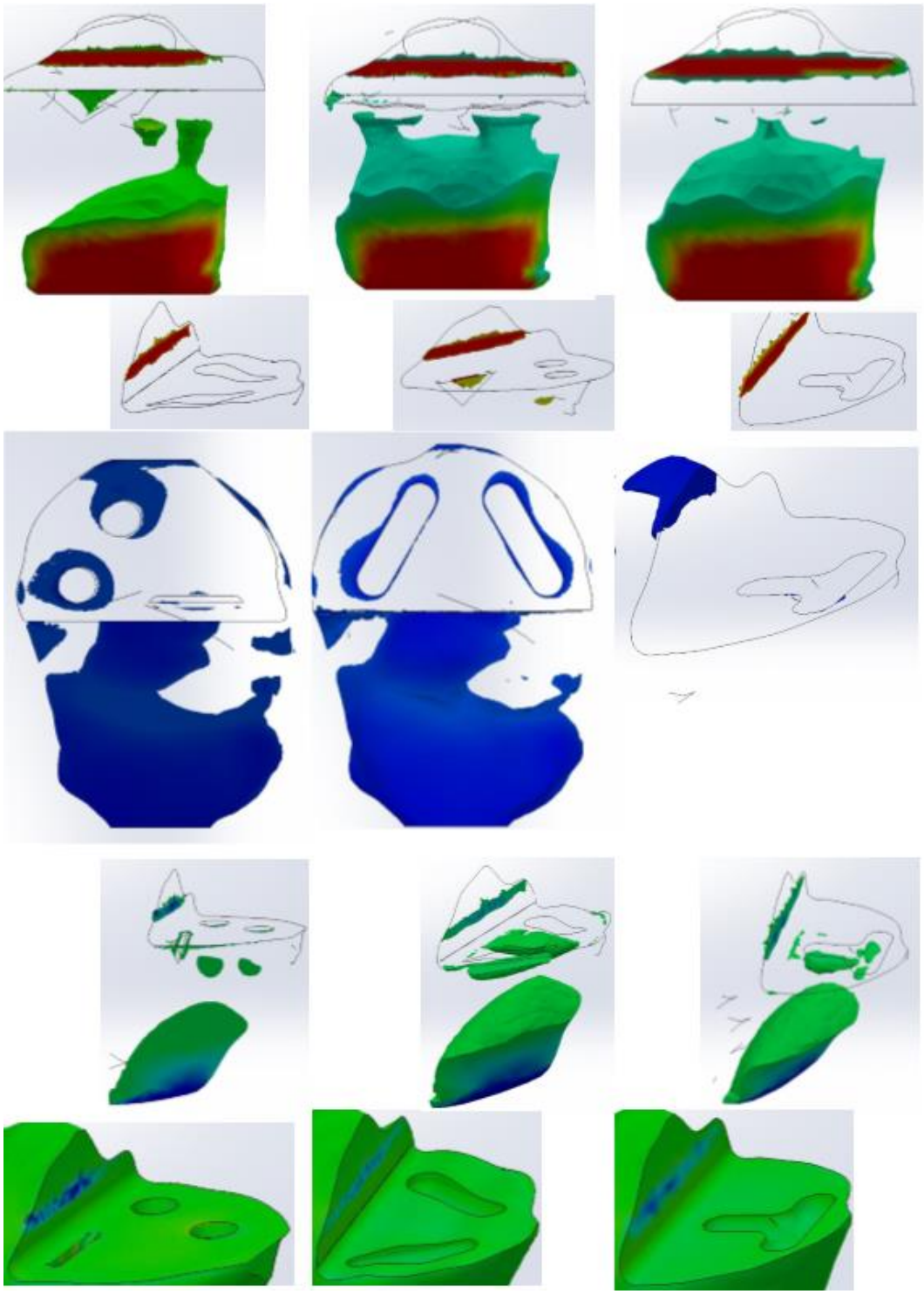

Figure 11.3-6: Results from AMC Condition
This figure shows the three prototypes: original, BQ, and T6.2 in respective column; and the three numerical analysis.
Top row shows the locations of high stress from the von Mises criterion.
Middle row shows the locations of no-to low stress from the von Mises criterion.
The bottom row shows the element tension in the longitudinal axis – Triaxial.

11.3.2.5AMC Analysis

11.3.2.5.1 Results

The original prototype has red von Mises plot stress zones on the on the sides of the MAKO fin, the tail peg, on the cut wall, and on the surface distal to the tibia. The T6.2 and BQ prototypes have only the latter two red zones – the cut all wall and surface distal to the tibia. These can been seen in figure 11.3-6.

From the von Mises iso-clippings in figure 11.3-6, the T6.2 prototype has von Mises stress approximately 1MPa at the base of the 'T' and the stress uniform across the transverse plane, decreasing in stress nearer the cut surface. The BQ prototype has von Mises stress approximately 1MPa at the base of the flanges, the stress distributes evenly out around the flanges and up to the cut surface. The original prototype apical peg has von Mises stress around 2.5MPa; the stress radiates from the apical peg diagonally down the tibia, see figure 11.3-6. The tail peg has von Mises stress approximately 2MPa and this also direct stresses diagonally down and to the centre of the tibia.

All three models, middle row in figure 11.3-6, have areas of low von Mises stress on the medial side of the tibia, the smallest quantity is the T6.2 prototype where the low von Mises stress zone is around the top of the 'T', and on the lateral wall of the 'T'. The BQ prototype has low von Mises stress around the rim and walls of both flanges, and spots on the outer edge of the tibia. The original prototype has low von Mises stress around the walls of the pegs and on the outer surface of the tibia.

The triaxial plot, in figure 11.3-6, shows that the cut surfaces on the prototypes don't experience high levels of axial loads in either compressive or tensile. Though the original prototype has small areas that were red in the von Mises plot have tensile stress ranging approximately 3MPa. The bases of the BQ flanges, the base of 'T' flange, and the base of the pegs appear to be in compressive axial force approximately 2MPa, 5MPa, and 3MPa (respectfully). The centre of the BQ prototype has compressive stresses around 1.5MPa.

From the triaxial iso-clippings, the majority of the BQ and T6.2 prototype have only small zones of tensile axial forces on the medial half of the tibia. This is also mostly true for the original prototype, but it has tensile axial forces of approximately 1MPa across most the cut surface.

11.3.2.5.2 Discussion

The von Mises and the iso-clippings of the prototypes indicate that the original prototype does not produce an even distribution of the stress across the surface and through the head of the tibia. This has created zones on the cut surface that are likely to fail first.

The BQ and T6.2 have distribution of the stresses arises from the features, i.e. area below the flanges have higher concentration of stress than the flat areas the T6.2 prototype is more evenly spread across the tibia than the BQ prototype. This seems to be a very good stress distribution especially compared to the original prototype.

The BQ prototype has a large zone of stress shielding around the edge of the flanges which is not ideal, as it has potential reduce bone growth that can lead to loosening of the prosthesis. Also the original prototype has stress shielding around the top pegs, the volume seem deeper than the BQ prototype. The T6.2 has a little stress across the crescent side of the 'T' flange.

In this both T6.2 performs well as the T6.2 has better distribution and less stress shielding. The BQ seems to perform better than the original prototype because the volume of stress shielding is less and distribution of stress is more even across the tibial surface.

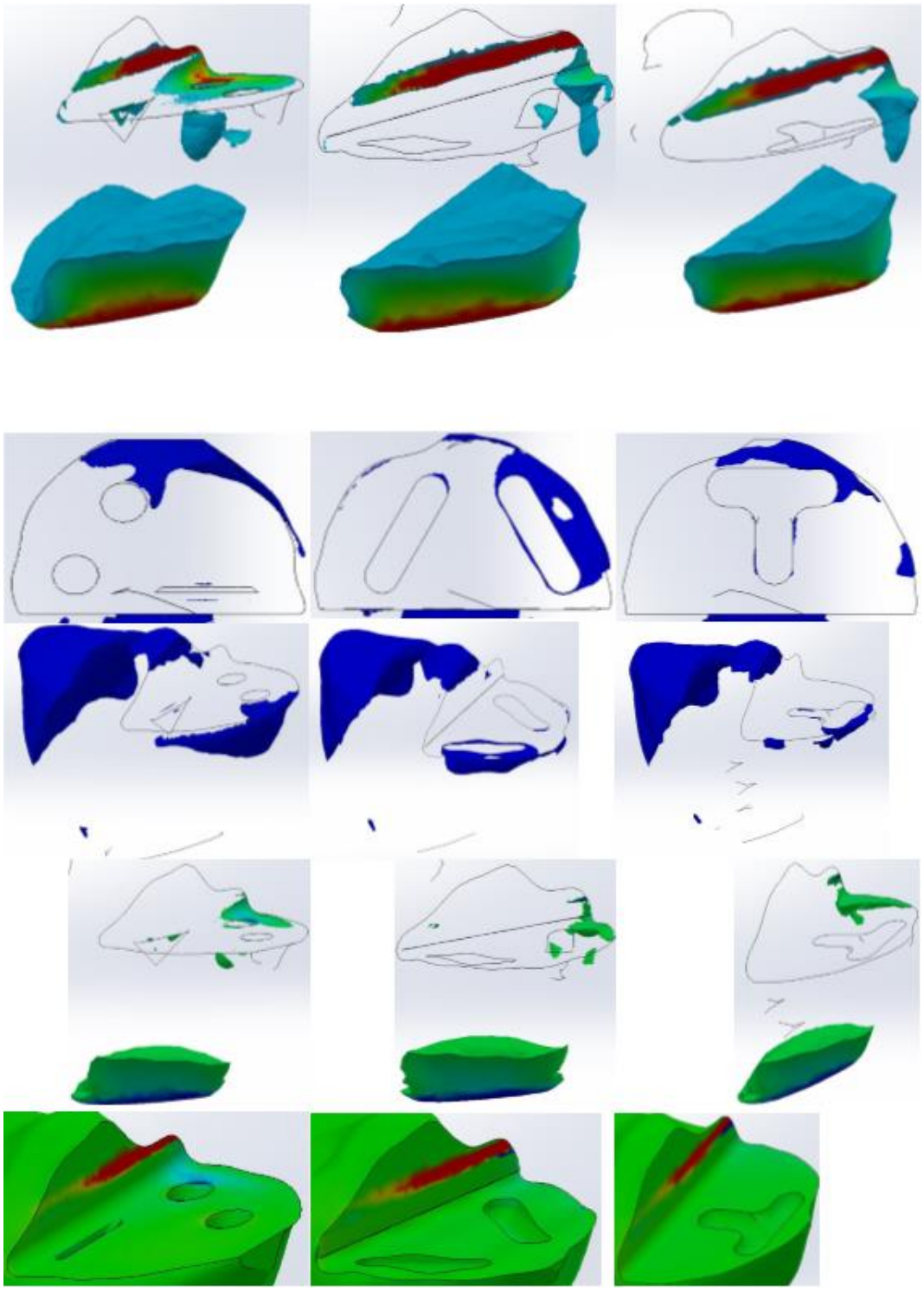

Figure 11.3-7: Results from BMC Condition
This figure shows the three prototypes: original, BQ, and T6.2 in respective column; and the three numerical analysis.
Top row shows the locations of high stress from the von Mises criterion.
Middle row shows the locations of no-to low stress from the von Mises criterion.
The bottom row shows the element tension in the longitudinal axis – Triaxial.

11.3.2.6 BMC Analysis

11.3.2.6.1 Results

All three prototypes have red zones on the cut wall in figure 11.3-7. The original prototype has light blue areas around the anterior point and anterior peg, seen in top left of figure 11.3-7. For the other two prototypes the cut surface is dark blue in colour.

The von Mises iso-clippings, in figure 11.3-7, showed stresses on the area under the apical point on all three prototypes, most notable on the original prototype. Interacting with the iso-clipping, the base of the apical peg in the original prototype experiences von Mises stress ca. 0.2MPa and the tail peg ca. 0.1MPa. The stress distributes from the apical peg base downwards at the angle of the peg, followed by the tail peg. The apical point transfer the stress along the outside of the tibia and the cut surface progressing through the tibia posteriorly. The T6.2 prototype cut surface stress at the apical point is distributed down the outer posterior side of the tibia and the spreads across the tibia in a 45° plane to the transverse and coronal planes to the anterior side. The base at the bottom of the 'T' experiences approximately 0.7MPa von Mises stress. The BQ prototype distributes the stress in the same fashion as the T6.2 prototype with downward stress radiation from the ends of each flange, and the base of the apical flange experiences approximately 1MPa von Mises stress.

All three prototypes, middle row in figure 11.3-7, have a low stress von Mises area at the posterior outer edge of the cut surface. It covered the whole

perimeter of the tail flange in the BQ prototype. The original prototype has the coverage across the outer surface of the tibia and into the anterior side of the tail peg. Similarly, the low von Mises stress in the T6.2 prototype is across the outer surface of the tibia and to the tail arm the 'T'.

The triaxial plot suggests there are not high axial stresses on the surface of the prototypes with the expectation of the apical point in the original prototype which experiences compressive stresses, greatest is at the rim of the apical peg, ca. 1MPa.

Figure 11.3-7 are the triaxial iso-clippings, the majority of the BQ and T6.2 prototype have only small zones of tensile axial forces on the medial half of the tibia. The original prototype has a layer of tensile axial stresses forces of approximately 0.005MPa across most the cut surface, greatest stress next to the tail peg of 0.3MPa.

11.3.2.6.2 Discussion

The stress distribution is as expected as the overall force experienced by the system would be in the downward posterior direction.

The low von Mises stress on all three prototypes maybe suggested by the direction of the overall force of condition B, it could be suggested if the shear displacement went the opposite direction, the opposite side of the tibia would experience the low von Mises stresses. Therefore, it is not of big concern as the shear force is assumed to act in both directions with just the same magnitude.

Though it is concerning the anterior area on the tail peg experiencing low von Mises stresses because the design is not mirrored in the coronal plane, as this area might not experience high stress when the shear displace is in the opposite direction.

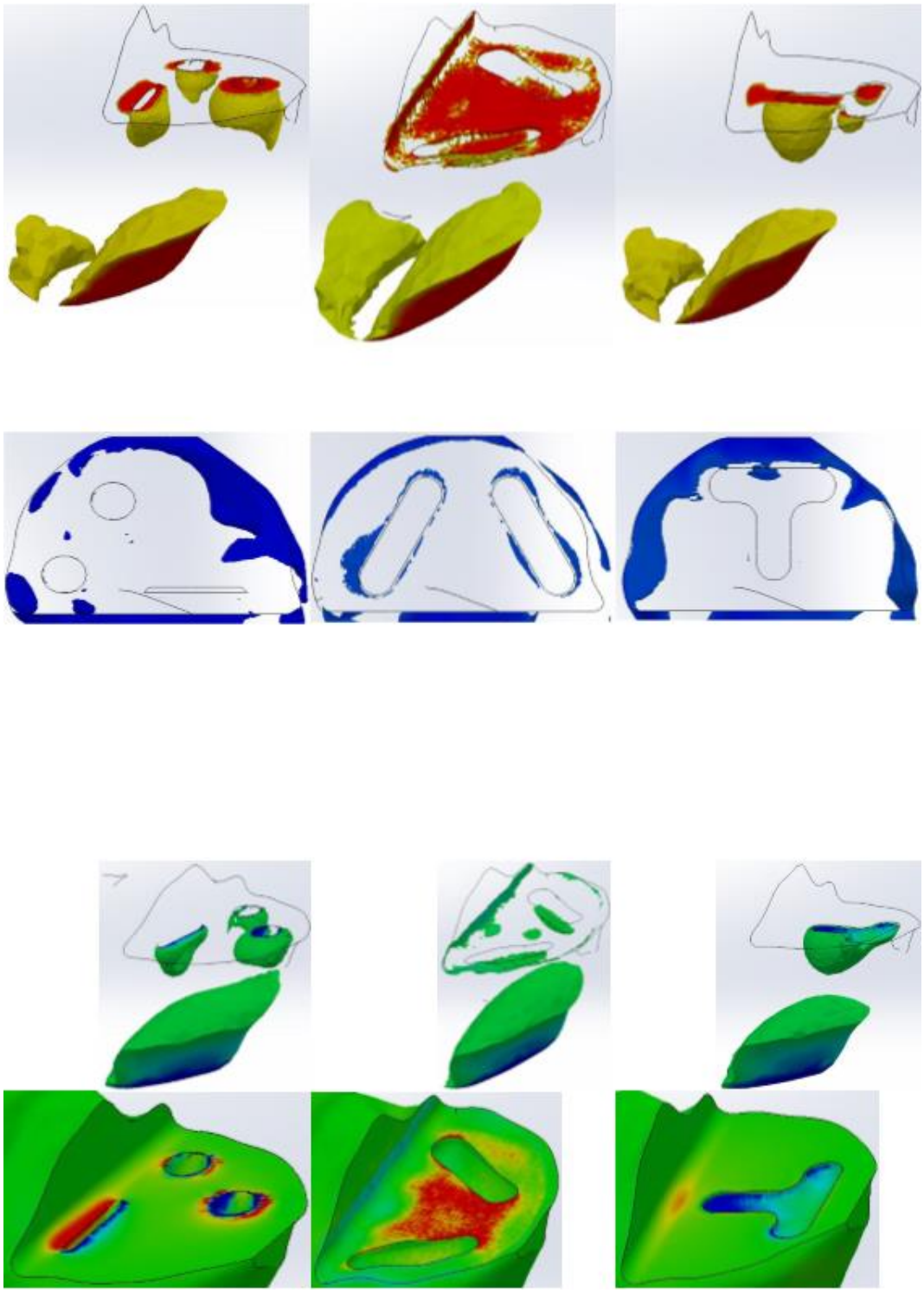

Figure 11.3-8: Results from AMN Condition
This figure shows the three prototypes: original, BQ, and T6.2 in respective column; and the three numerical analysis.
Top row shows the locations of high stress from the von Mises criterion.
Middle row shows the locations of no-to low stress from the von Mises criterion.
The bottom row shows the element tension in the longitudinal axis – Triaxial.

11.3.2.7AMN Analysis

11.3.2.7.1 Results

All prototype's von Mises plots, in figure 11.3-8, display large areas of red that spread across the cut surfaces and the distal medial side of the tibia. The original prototype has red plotted around the rim of the pegs, the walls of the pegs, almost all the cut surface in the fin, and all around the fin's rim. The T6.2 prototype has red covering almost all the leg of the 'T', half of each tip of the arms of 'T', and the cut flat surface from the leg of the 'T' to the fillet. On the BQ prototype, the red is on the base of the flanges, most of the surface between the two flanges, and most of the fillet.

Interacting with the iso-clipping, top row in figure 11.3-8, von Mises of 3.42MPa and greater, are not just solely represent on the surface elements for the original and T6.2 prototypes. The original has large red plotted zones around the wall of the tail peg, and all around the tip of the fin. The T6.2 prototype has a large red zone around the bottom of the 'T' leg, and two smaller zones on the 'T' arms. The BQ prototype has the biggest surface area coved by red but it is only on the cut surface.

In the original prototype, the stress is distributed outwards from the tail peg, transferring some of the load down the tibial surface; the fin transmits the stress down the tibia. Then the stress is distributed towards to the outer surface of the tibia before spreading up to the cut surface. The T6.2 prototype distribution of stress extends downwards from the leg of the 'T', followed by the 'T' arms before

distributing the stress to the outer surface of the tibia. The BQ prototype has the stress distributing across the surfaces of the flanges before extending downwards from each flange; the stress distribution then goes both out to the outer surface and inwards of the tibia.

All three prototypes experience zones of low von Mises stress around the cut surface outer rim, seen in figure 11.3-8. The BQ prototype also had the rim of the flanges as areas of low von Mises stress.

The triaxial stress, in figure 11.3-8, plot has all three prototypes experience both compressive and tensile stresses on the cut surface. Prototype BQ has compressive stress of approximately 1MPa on the base of the flanges and the cut surface edges; BQ also has tensile stress (ca. 4MPa) on the surface between the flanges. The T6.2 prototype has compressive stress around the leg and arms of the 'T', approximately 10MPa; and the tensile stress (ca. 0.6MPa) covers most of the cut surface with a peak on the fillet next the 'T' leg of approximately 6MPa. The original prototype has compressive and tensile stresses right next to each other, both at the same magnitude. The compressive stresses are on the rim and walls of the pegs, medial edge of the fin, and most surfaces of the fin. The tensile stresses are located on the rim of the pegs, the lateral side of the fin, and the part of the fin's tip. The majority of the cut surface of the original prototype is under tensile forces of approximately 0.4MPa as well as the base of the pegs and the medial wall of the fin.

11.3.2.7.2 Discussion

All the prototypes have high potential of failure due to the high stress concentration on the cut surface as observed by the red shaded elements in the simulations.

The stress distribution for all three prototypes are primarily down the middle of the medial tibial condyle. As a result, the stress shielding occurs in all three prototype designs with a similarly on the medial side of the cut rim.

The T6.2 has the worst distribution as the majority goes through the tibial condyle in the longitude axis under the 'T' leg. This is followed by the original prototype with three points of stress transferring along longitudinal axis.

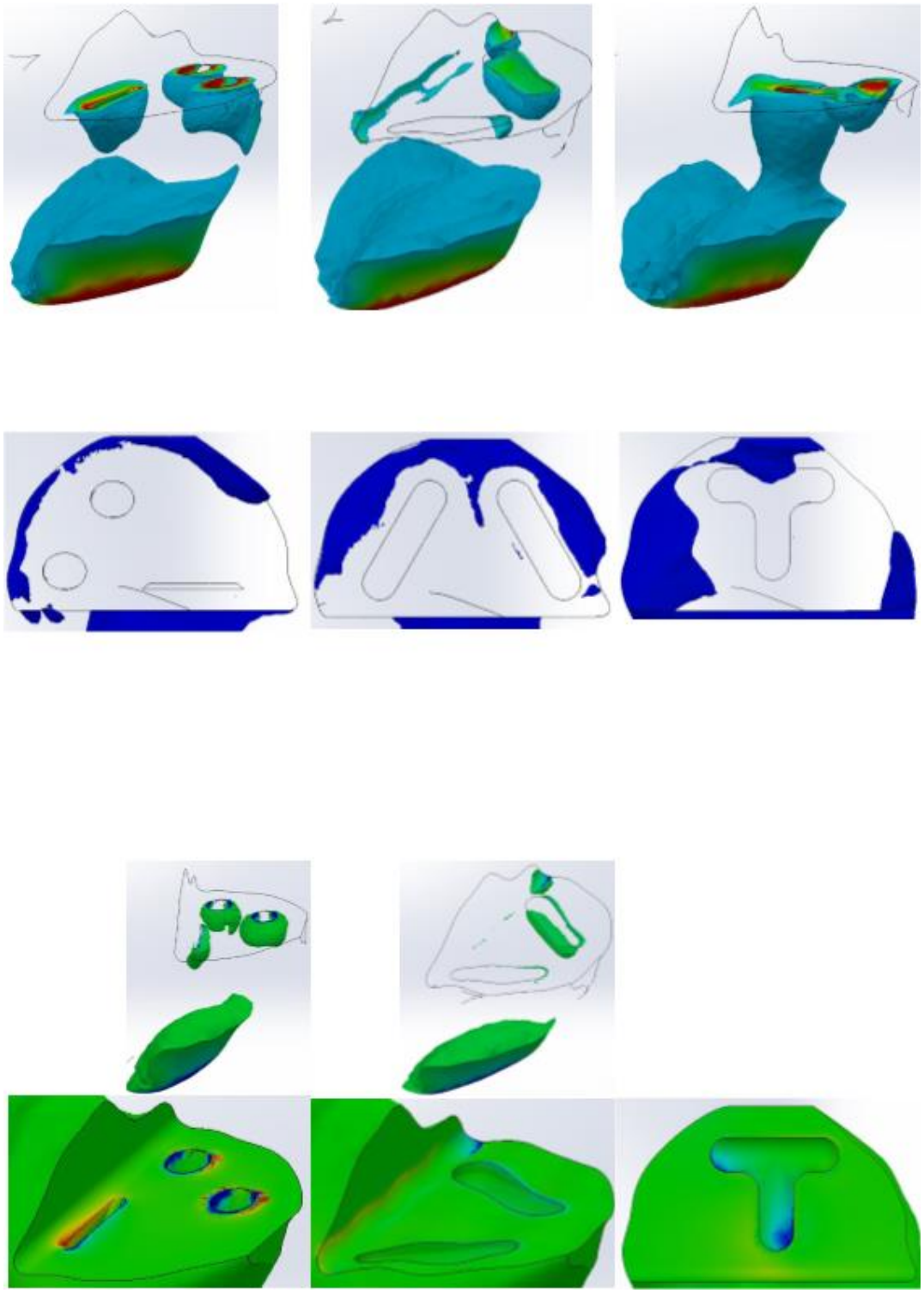

Figure 11.3-9: Results from BMN Condition
This figure shows the three prototypes: original, BQ, and T6.2 in respective column; and the three numerical analysis.
Top row shows the locations of high stress from the von Mises criterion.
Middle row shows the locations of no-to low stress from the von Mises criterion.
The bottom row shows the element tension in the longitudinal axis – Triaxial.

11.3.2.8BMN Analysis

11.3.2.8.1 Results

The von Mises plots on the BQ prototype show a stressed area of approximately 1.8MPa on the cut surface at edge under the prototype's apical point. T6.2 prototype has a stressed area of approximately 1.5MPa on the bottom of the 'T' leg. While the original prototype has two red spots on the tail peg's rim and yellow surface spots on the apical peg, around the rim of the fin, and the fin's tip. It also on the original prototype stress on the base of the apical peg, around the lateral rim of the fin, and the posterior wall of the fin.

The interactive iso-clipping, in figure 11.3-9, for the von Mises of the original prototype the stress concentration around rims and walls of the tail peg and lesser on the apical peg, and around the fin; the peg's stress concentrations radiates outwards to the tibia surfaces before expanding downwards and the fin's stress concentration radiates downward before out to the tibia's surface. The T6.2 prototype distributed the stress downwards from the leg of the 'T', and the apical arm of the 'T'; it then distributes the stress to the outer tibial surface. Similarly, the BQ prototype does the same from its concentration zones at the base of the apical flange and the posterior edge of the cut surface.

The area of low von Mises stress are again, generally located on the lateral edge of the cut surface, seen in figure 11.3-9. For the T6.2 prototype the main areas are the posterior surface and the medial edge of the 'T' with the lateral facing wall in the 'T'. The BQ prototype the areas of low von Mises stress are around the tail

flange, and the medial edge of cut surface of the tibia. The original prototype had low von Mises along the edge of the cut surface, from the posterior side to the medial side.

The triaxial stress plot has all three prototypes experience both compressive and tensile stresses on the cut surface, as observed bottom row in figure 11.3-9. The original prototype has compressive and tensile stresses right next to each other, both at the same magnitude. The compressive stresses are located on the rim of the pegs, partly down the walls of the pegs, medial edge of the fin, and most half of the fin's tip. The tensile stresses are located on the medial rim of the pegs, the lateral side of the fin, and the other half of the fin's tip. The majority of the cut surface of the original prototype is under tensile forces of approximately 0.02MPa as well as the base of the pegs (~0.1MPa). Prototype BQ has compressive stress of approximately 1MPa on the area under the apical tip and has tensile stress (ca. 0.05MPa) on tail end; BQ also has compressive stress (ca. 0.2MPa) on the base of the apical flange. The T6.2 prototype has compressive stress around the base of the 'T' leg and of the apical 'T' arm (~1MPa); and the tensile stress (ca. 0.1MPa) covers most of the cut surface with a peak of approximately 0.2MPa on the fillet next the 'T' leg.

11.3.2.8.2 Discussion

Only the BQ prototype has a stress concentration of little concern. The T6.2 prototype has a stress concentration that isn't ideal but not as concerning as the original prototype.

The T6.2 prototype features carry the stress distribution unfavourably under the flange down through the middle of the lateral tibia condyle. The original pegs and fin actually help to evenly distribute across the tibial head and even direct some on to the posterior tibial surface.

The lack of stress on the edge of the cut surface is not good either because it can weaken the bone, in accordance to wolf's law.

11.3.3 FEA Discussion

In general, the non-cement (medial and lateral) plots are similar to each other, and the same maybe said for the cement (medial and lateral). As already mentioned in *6.4.5 Discussion*, the boundary condition set up for this analysis results in the distal part of the tibia to experience high stress concentration. This is logical because the cross-sectional area decreased in the distal direction thus the stress increase because the force is constant.

As much as stress concentrations are important to avoid, stress shielding is also equally needing to be avoided. The von Mises iso-clipping of the zones with the least value of stress (appears as dark blue) are shown in figures 11.3-2 to 99. From these plots, the cementless prototypes have very little stress over at the outer lateral rim of the cut tibial surface in both conditions. The cemented models low von Mises stress areas were less generalised, typically for all three prototypes the cut surface area free from pegs and flanges had low stress and along rim of the

tibial cut surface. The stress is shielded especially so on the original prototype, as the majority of the flat cut surface is under low von Mises stress.

For the axial loading, none of the prototypes seemed to transfer the stress onto the surface of the tibia but the BQ prototype had a consistent even load distribution, across the 4 different scenarios. The prototypes did not evenly distribute the load particularly well in the non-cemented cases, this often displayed areas that plotted in red that would indicate possible failure of the bone material.

The cement seems to play a key role in stress distribution; from the previous FEA experimental data in chapter 9 and from the non-cemented prototypes, features on the undercarriage, such as the pegs and flanges, were the sources of stress concentrations. With the presence of cement in the prototype models, it seems to lower the stress concentrations from these features and creates a more uniform stress distribution plane located at 45 degrees between the coronal and transverse planes.

The FEA models produced were simple models to get preliminary indications as to the stress patterns underloading. This means the models do not need to replicate knee mechanics exactly. However, the whole point of this simulation was to get an insight into the stress concentration, stress shielding, and stress distribution of the three prototypes to compare with each other. This is also not the first investigation that utilised FEA analysis for comparing and simulating prosthesis designs. Hopkins *et al.*[257] simulated gait kinematic of a healthy knee, damaged knee, and a knee with the oxford UKR prosthesis; Walker *et al.*[258] used a CAD

package to help re-design the articulating surfaces of a UKR to help stability of the knee in the absence of the cruciate ligaments; Taylor *et al.*[259] modelled the proximal tibia with the tibial TKR component under investigation to compare three different parameters. There are many more examples of papers utilising FEA, they are similar to this investigation's modelling but the difference lies in the question they are asking. Therefore, only relevant information is included in simulations; for example the simulation presented here did not include the femoral condyle pressing on the tibial plateau because the question was focused on the tibial components whereas Hopkins *et al.*[257] included the femoral condyle as they their question was "to investigate the biomechanical response of the natural knee to the implantation of a Unicompartmental device".

The FEA models were to observe the stress patterns in the tibia with different loading conditions but as already mention they were not meant to be a full imitation of the knee. One example, the tibial bone had no differentiation between cortical and cancellous tissue which have different mechanical properties to each other.

It would have been preferable to model the proximal tibia more realistically, incorporating a cortical shell surround cancellous bone; yet, due to the limitation of the imported mesh of a standard knee and the software. In the interest of optimising resources it was concluded that since the FE analysis was to observe stress patterns within the immediate cancellous bone, then the presence of cortical shell was not necessary in this experiment. Though the cancellous bone could have

been modelled isotropically similar to the structure within the body. In general, bone tissue in a cancellous matrix around the proximal tibia would be aligned so as to withstand high stresses in the longitudinal axis. The other two axes would have lesser mechanical strength. Had it been modelled this way, the laboratory prototype experiment's foam material would not match the model and thus the confidence in the FEA model would have been reduced. One possible way around this would be to do an additional mesh convergence analysis. This was not performed as all the models had the same mesh geometry input and the results were pattern based and not reliant on numerical values. The model was also validated by changing the material properties to those of cortical bone. The observed patterns were very similar to those seen with cancellous bone material properties. This was expected as the material properties alter the forces experienced by the elements, though if a parameter like the poisson's value was changed or if the material is orthotropic, then not just the magnitudes are change but also the stress pattern. As the prosthesis would be positioned on cancellous bone, only these results were reported.

In addition, the *in vivo* properties of the tissue are viscoelastic[106] these properties may affect the stress patterns with stress relaxing with time. Future work would be to model the tibia with the viscoelastic so a clearer picture of the stress relaxation can be obtained.

The other limitation of the FEA models is the perfect bond at interface. The interface between the tibia and cement in vivo will not be a perfect bond and it may

have interdigitation zone that isn't modelled in the FEA. This could alter the stress patterns as seen with the high stress zones on the cut wall, especially on the cemented side models.

Overall the BQ prototype seems to consistently perform well in all the scenarios, this is closely followed with the T6.2 prototype. The original prototype on a couple of conditions outperformed the other two prototypes; but in the other conditions it created stress concentration areas and areas of stress shielding that were of concern.

11.4 Key Message

The three experiments here showed that BQ prototype performed well compared to the other two prototypes. The laboratory work was the initial testing of the final two design concepts to compare them with a standard UKR designed. The laboratory experiments was used to verify the results of the FEA analysis by comparing the observed damaged done to the foam block with the von Mises predicted stress. This allowed an FEA analysis approach to have a clearer picture of the stress patterns inside the tibial head.

It is recommended that the BQ design should be taken forward and analysed with more complicated models, as it shows potential to outperform the existing designs.

Chapter 12

Discussion and Conclusion

The project's ultimate aim was to develop concepts for novel UKR tibial components into prototypes for testing. Along the way, concepts were developed and were eliminated from the process; the concept selection rationale eliminated them for justified reasons while retaining positive characteristic in the final design; for example, the partial cement rib design samples were used as flanges in the final prototypes. Nevertheless, the eliminated concepts might still hold potential for development and/or developing into other concepts that may work as well as the final concepts in this investigation. Therefore, the discussion is split into two sections: the first section is the discussion of the tested prototypes and the second section discusses all the designs that were eliminated.

12.1 Prototyping Discussion

The end product of this investigation was to produce two physical prototypes to test and compare with a standard prosthesis. Within the concept selection process was the evaluation process that made it possible to develop and select two final concepts that had the greatest potential of performing well in accordance to the brief and PDS of the investigation.

The prototypes that were produced and modelled had their strengths in different attributes. Taking the information acquired from the experiments, it was concluded that the BQ prototype, having two flanges and an undulating curved undercarriage profile, consistently performed better than the other two prototypes. The original prototype that represents the market standard seemed to perform well under cement conditions but worse when there wasn't cement; this is to be expected because this prosthesis was designed to be used with cement, yet the aspects of original prototype is not far off all the current market prostheses designed for cement and cementless. From this, it seems that the biggest improvement could be with cementless prosthesis because the prototypes investigated in the experiments seem to have a better stress pattern than the market standard design under cementless conditions.

The experiments were limited in replicating the *in vivo* conditions. The data from the prototype experiments is useful comparatively, whereby samples were tested as closely to the in vivo condition that resources permitted. The simulations had all the same input qualities (forces, meshing, boundary conditions, software version, material etc.) with the only differences being the undercarriage profiles. The results from the computer simulations were validated by comparing them to the laboratory experiment that had the same displacement and force conditions applied to the samples. Nevertheless, validation was difficult and a qualitative comparison was managed.

Before the prototypes are ready for medical use, further experiments (such as investigating wear and fatigue mechanisms) are necessary to address other important requirements for a successful prosthesis.

12.2 Discussion of Possible Novel Prosthesis Routes and Future Works

The end product of this investigation was to develop and produce two physical prototypes to compare to the standard prosthesis; along the design process additional novel designs were developed. The ideas produced in the investigation ranged from sensible -to not much of a change -to surreal. Frequently, the ideas produced followed a theme, the common ones being: using different type of cement or no cement at all; 3D printed/milled before or during surgery to produce patient specific prostheses; pattern matching/interlocking of the tibia and prosthesis; and curves. No matter how simple or abstract the ideas were, they all aided concept development because each idea promoted creativity and increased the chance for developing a suitable solution. The ideas that were not developed into concepts, but nonetheless still had potential were: in-op 3D printed/milled or modified prosthesis; stems cells; altering to the robotic system; alternative/bio-mimic material and cement alternatives. The 3D printing/milling ideas could be explored in future work as producing 3D models is becoming much more economical as interest grows within this field; for example, 3D milling of dental crowns is practiced in some dental surgeries. Therefore, coupling this with the adaptableness of the system and burr drill could dramatically change the way knee surgeries are done. Alternative materials, particularly injectable/mouldable

material, can also be integrated with burring systems because they can be versatile to work with the burring systems.

In the experimental chapter, section *8.3 Effect of Surface Texture Experiment,* showed that the texture created by burring does not effect the adhesion strength of the bone cement. There is capability to use the burring method to design inlay and onlay prostheses with a geometry that complements an ideal stress pattern and with adequate fixation. This was investigated in the following chapter, *9 Virtual Experiments of Concept Ideas*, to help in the concept evaluation. In addition, the prosthesis designs could include the benefits from both cement and cementless by having a partial cement design.

There are further experiments that could benefit future designs. Additional experiments on the effect of surface texture on cement adhesion would produce more statistically robust results. Furthermore, the affect the burr texture has on cementless prosthesis is another area to be considered: for example, is 'burring compatible with osseointegration?'. Additionally, further research into the potential of partial cementing needs to be examined to test the theory and to see if it can provide the best of both worlds. To the knowledge of the author this novel type of prosthesis attachment has not been reported on before.

The limitation of the concept generation and concept selection process is the absence of surgical medical knowledge. To limit the lack of surgical training, surgeons were called upon to bridge gaps in the knowledge. This proved very useful, yet, if the investigation team was expanded to include a surgeon in the

design process, their input would be continuous thus the concepts developed would be slightly different. Withal, the final concepts would be more practical based and the impractical concepts most likely would have been rejected near the beginning of the process; this different dynamic could be advantageous in the sense the concept will have a strong foundation of theory but it would have a limiting effect on creativity. This investigation really wanted to generate novel concepts and processes as a way to get UKR procedures thinking differently about prostheses, as a result not being constantly tied down to practical implementation was beneficial to the investigation. Considering the eliminated ideas, there might have been some that could be developed if there were orthopaedic experts included in the team. Therefore, it could be very beneficial in prosthesis development to go through these ideas/concepts with a team of experts through a concept selection process to pick out any missed ideas.

Overall, this investigation accomplished the goal of producing novel concepts for UKR prostheses. A few ideas were tested, the prospective of future work is ample as this investigation had limited resources and thus was not able to test all ideas generated. Some of the potential promising future work has been mentioned but there is possibility of additional future work arising from the ideas and concepts. Plus, if this investigation is developed in the future with industrial experts then there is the possibility of more research questions that can aid the future development of UKR prostheses.

12.3 Final Notes

There were a number of experiments that could have been conducted within the scope of the thesis, but only the important experiments expected to relate to concept development and prototyping were prioritised. The other experiments that were considered were put to one side for various reasons: the results may not contribute to the concept evaluation and selection process, or that they were impractical to perform while providing meaningful results. This includes the desire to conduct a final user diary of the prototypes using a previous student's augmented reality (AR) system. Code was generated to input into the AR system but limited access to the system meant that this approach had to be discarded for a future investigation. Another experiment that was also discussed and scoped which utilised surface properties to take advantage of proteins present in the knee joint. Pilot data was gained but did not look promising in the timescale available.

This thesis has delivered on the objectives set out in chapter 5, *Project Aim and Specification*. The primary goal in the brief, and thus the project aim, was to recommend a novel prosthesis concept for use with robotic orthopaedic tools in UKR procedures. The recommend concept was BQ and it had an enthusiastic reaction from the interviewed consultant and was had the better results across the board in the experiments. A secondary goal discussed in the brief was to initiate creativity in UKR design in order to encourage UKR prosthesis designers to fully utilise the becoming available technology. The outline design process and the subsequent documented notes regarding the ideas and concepts could ignite a new generation of UKR prostheses with improved performance over the current

standard UKR. There is lots of potential scope that can be drawn from this project, as mentioned in the above section, *10.1 Discussion of Possible Novel Prosthesis Routes and Future Work.*

To have the BQ prototype ready for use will require further investigation. For all potential novel prosthesis designs, there is still considerable volume of work to do, this investigation has only provided preliminary ground work. To the knowledge of the author, this is a unique approach to prosthesis development with the potential to initiate advancements in novel prosthesis design. There have been investigations into design processes to generate new prosthesis design, such as Walker's 2012 paper[258] that pursues a TKR solution to maintain stability in the absence of the cruciate ligaments. These papers build upon the existing prototypes structure, whilst this investigation approaches the UKR prosthesis from a different direction. The investigation has succeeded in creating the foundation for taking UKR prosthesis designs into a new direction.

References

.

[1] S. E. Lamb *et al.*, “Factors that modify the association between knee pain and mobility limitation in older women: the Women’s Health and Aging Study.,” *Ann. Rheum. Dis.*, vol. 59, no. 5, pp. 331–7, May 2000.

[2] D. Bhatia, T. Bejarano, and M. Novo, “Current interventions in the management of knee osteoarthritis.,” *J. Pharm. Bioallied Sci.*, vol. 5, no. 1, pp. 30–8, Jan. 2013.

[3] P. Jüni, S. Reichenbach, and P. Dieppe, “Osteoarthritis: rational approach to treating the individual.,” *Best Pract. Res. Clin. Rheumatol.*, vol. 20, no. 4, pp. 721–40, Aug. 2006.

[4] G. Yildirim, I. Fernandez-Madrid, R. Schwarzkopf, P. Walker, and R. Karia, “Comparison of Robot Surgery Modular and Total Knee Arthroplasty Kinematics,” *J. Knee Surg.*, vol. 27, no. 2, pp. 157–164, 2013.

[5] M. Conditt, S. Horowitz, and J. Jones, “Annual Summary of Clinical and Economic Research MAKO Surgical Corp . - 2010,” 2010.

[6] J. H. Newman, C. E. Ackroyd, and N. A. Shah, “Unicompartmental or total knee replacement ?,” pp. 862–865, 1998.

[7] B. T. Rougraff, D. A. Heck, and A. E. Gibson, “A comparison of tricompartmental and unicompartmental arthroplasty for the treatment of gonarthrosis.,” *Clin. Orthop. Relat. Res.*, no. 273, pp. 157–64, Dec. 1991.

[8] A. E. Weale, D. W. Murray, J. H. Newman, and C. E. Ackroyd, “The length of the patellar tendon after unicompartmental and total knee replacement,” *J Bone Jt. Surg Br*, vol. 81–B, no. 5, pp. 790–795, Sep. 1999.

[9] T. J. Gioe *et al.*, “Analysis of unicompartmental knee arthroplasty in a community-based implant registry.,” *Clin. Orthop. Relat. Res.*, no. 416, pp. 111–9, Dec. 2003.

[10] S. Patil, C. W. J. Colwell, K. A. Ezzet, and D. D. D’Lima, “Can Normal Knee Kinematics Be Restored with Unicompartmental Knee Replacement?,” 2014.

[11] O. Furnes, B. Espehaug, S. a Lie, S. E. Vollset, L. B. Engesaeter, and L. I. Havelin, “Failure mechanisms after unicompartmental and tricompartmental primary knee replacement with cement.,” *J. Bone Joint Surg. Am.*, vol. 89, no. 3, pp. 519–25, Mar. 2007.

[12] M. S. Noticewala, J. a Geller, J. H. Lee, and W. Macaulay, “Unicompartmental knee arthroplasty relieves pain and improves function more than total knee arthroplasty.,” *J. Arthroplasty*, vol. 27, no. 8 Suppl, pp. 99–105, Sep. 2012.

[13] A. V Lombardi, K. R. Berend, C. a Walter, J. Aziz-Jacobo, and N. a Cheney, “Is

recovery faster for mobile-bearing unicompartmental than total knee arthroplasty?," *Clin. Orthop. Relat. Res.*, vol. 467, no. 6, pp. 1450–7, Jun. 2009.

[14] E. Felts, S. Parratte, V. Pauly, J.-M. Aubaniac, and J.-N. Argenson, "Function and quality of life following medial unicompartmental knee arthroplasty in patients 60 years of age or younger.," *Orthop. Traumatol. Surg. Res.*, vol. 96, no. 8, pp. 861–7, Dec. 2010.

[15] R. H. Emerson and W. C. Head, "Failure mechanisms of unicompartmental knee replacement: the impact of changes in operative technique and component design.," *Seminars in arthroplasty*, vol. 2, no. 1. pp. 23–8, Jan-1991.

[16] P. N. Baker *et al.*, "Comparison of patient-reported outcome measures following total and unicondylar knee replacement.," *J. Bone Joint Surg. Br.*, vol. 94, no. 7, pp. 919–27, Jul. 2012.

[17] C. T. Laurencin, S. B. Zelicof, R. D. Scott, and F. C. Ewald, "Unicompartmental Versus Total Knee Arthroplasty in the Same Patient," *Clin. Orthop. Relat. Res.*, vol. NA;, no. 273, pp. 151–156, Dec. 1991.

[18] D. A. Fisher, M. Watts, and K. E. Davis, "Implant position in knee surgery," *J. Arthroplasty*, vol. 18, pp. 2–8, Oct. 2003.

[19] N. Confalonieri and A. Manzotti, "Mini-invasive computer assisted bi-unicompartimental knee replacement," *Int. J. Med. Robot. Comput. Assist.*

Surg., vol. 1, no. 4, pp. 45–50, Dec. 2005.

[20] A. Gulati *et al.*, "The incidence of physiological radiolucency following Oxford unicompartmental knee replacement and its relationship to outcome.," *J. Bone Joint Surg. Br.*, vol. 91, no. 7, pp. 896–902, Jul. 2009.

[21] J. K. Seon, E. K. Song, S. J. Park, T. R. Yoon, K. B. Lee, and S. T. Jung, "Comparison of minimally invasive unicompartmental knee arthroplasty with or without a navigation system.," *J. Arthroplasty*, vol. 24, no. 3, pp. 351–7, Apr. 2009.

[22] M. Citak *et al.*, "Unicompartmental knee arthroplasty: is robotic technology more accurate than conventional technique?," *Knee*, vol. 20, no. 4, pp. 268–71, Aug. 2013.

[23] R. K. Sinha, "Outcomes of robotic arm-assisted unicompartmental knee arthroplasty.," *Am. J. Orthop. (Belle Mead. NJ).*, vol. 38, no. 2 Suppl, pp. 20–2, Feb. 2009.

[24] A. D. Pearle, P. F. O'Loughlin, and D. O. Kendoff, "Robot-assisted unicompartmental knee arthroplasty.," *J. Arthroplasty*, vol. 25, no. 2, pp. 230–7, Feb. 2010.

[25] M. Roche, P. F. O'Loughlin, D. Kendoff, V. Musahl, and A. D. Pearle, "Robotic arm-assisted unicompartmental knee arthroplasty: preoperative planning and surgical technique.," *Am. J. Orthop. (Belle Mead. NJ).*, vol. 38, no. 2 Suppl, pp. 10–5, Feb. 2009.

[26] V. B. Kasodekar, S. J. Yeo, and S. Othman, “Clinical outcome of unicompartmental knee arthroplasty and influence of alignment on prosthesis survival rate.,” *Singapore Med. J.*, vol. 47, no. 9, pp. 796–802, Sep. 2006.

[27] R. Becker and M. Hirschmann, “The pertinent question in treatment of unicompartmental osteoarthritis of the knee: high tibial osteotomy or unicondylar knee arthroplasty or total knee arthroplasty,” *Knee Surgery, Sport. Traumatol. Arthrosc.*, vol. 25, no. 3, pp. 637–638, Mar. 2017.

[28] L. Marmor, “Unicompartmental Knee Arthroplasty: Ten- to 13-Year Follow-up Study,” *Clinical orthopaedics and related research*, Jan-1988. [Online]. Available: http://journals.lww.com/corr/abstract/1988/01000/unicompartmental_knee_arthroplasty__ten__to.4.aspx. [Accessed: 24-Sep-2014].

[29] J.-N. A. Argenson, Y. Chevrol-Benkeddache, and J.-M. Aubaniac, “Modern unicompartmental knee arthroplasty with cement: a three to ten-year follow-up study.,” *J. Bone Joint Surg. Am.*, vol. 84–A, no. 12, pp. 2235–2239, 2002.

[30] S. Arno, D. Maffei, P. S. Walker, R. Schwarzkopf, P. Desai, and G. C. Steiner, “Retrospective analysis of total knee arthroplasty cases for visual, histological, and clinical eligibility of unicompartmental knee arthroplasties.,” *J. Arthroplasty*, vol. 26, no. 8, pp. 1396–403, Dec. 2011.

[31] A. J. Price and U. Svard, “A second decade lifetable survival analysis of the

Oxford unicompartmental knee arthroplasty.," *Clin. Orthop. Relat. Res.*, vol. 469, no. 1, pp. 174–9, Jan. 2011.

[32] A. Miniaci, N. P. Cohen, and F. J. Rodriguez, "Arthroscopically Assisted, Meniscal Sparing Tibiofemoral Knee Resurfacing."

[33] C. E. Ackroyd, "Medial Compartment Arthroplasty of the Knee," *J. Bone Jt. Surg.*, vol. 85, no. 7, pp. 937–942, 2003.

[34] J. G. Martin, D. A. Wallace, A. J. Carr, and D. W. Murray, "Revision of unicondylar knee replacements to total knee replacement." .

[35] G. Chakrabarty, J. H. Newman, and C. E. Ackroyd, "Revision of Unicompartmental Arthoplasty of the Knee," vol. 13, no. 2, 1998.

[36] M. J. Halawi and W. K. Barsoum, "Unicondylar knee arthroplasty: Key concepts," *J. Clin. Orthop. Trauma*, vol. 8, no. 1, pp. 11–13, Jan. 2017.

[37] A. J. Pearse, G. J. Hooper, A. Rothwell, and C. Frampton, "Survival and functional outcome after revision of a unicompartmental to a total knee replacement: THE NEW ZEALAND NATIONAL JOINT REGISTRY," *J. Bone Jt. Surg. - Br. Vol.*, vol. 92–B, no. 4, pp. 508–512, 2010.

[38] H. Wynn Jones, W. Chan, T. Harrison, T. O. Smith, P. Masonda, and N. P. Walton, "Revision of medial Oxford unicompartmental knee replacement to a total knee replacement: Similar to a primary?," *Knee*, vol. 19, no. 4, pp. 339–343, 2012.

[39] T. J. Aleto, M. E. Berend, M. A. Ritter, P. M. Faris, and R. M. Meneghini, "Early

Failure of Unicompartmental Knee Arthroplasty Leading to Revision," *J. Arthroplasty*, vol. 23, no. 2, pp. 159–163, Feb. 2008.

[40] T. Niinimäki, A. Eskelinen, K. Mäkelä, P. Ohtonen, A.-P. Puhto, and V. Remes, "Unicompartmental Knee Arthroplasty Survivorship is Lower Than TKA Survivorship: A 27-year Finnish Registry Study," *Clin. Orthop. Relat. Res.*, vol. 472, no. 5, pp. 1496–1501, May 2014.

[41] G. Peersman, W. Jak, T. Vandenlangenbergh, C. Jans, P. Cartier, and P. Fennema, "Cost-effectiveness of unicondylar versus total knee arthroplasty: a Markov model analysis," *Knee*, vol. 21, pp. S37–S42, 2014.

[42] A. D. Liddle *et al.*, "Cementless fixation in Oxford unicompartmental knee replacement: a multicentre study of 1000 knees.," *Bone Joint J.*, vol. 95–B, no. 2, pp. 181–7, Feb. 2013.

[43] A. V. Lombardi, K. R. Berend, R. E. Howell, and N. J. Turnbull, "Unicompartmental knee arthroplasty," *Curr. Orthop. Pract.*, vol. 26, no. 3, pp. 243–246, 2015.

[44] V. Kulshrestha, B. Datta, S. Kumar, and G. Mittal, "Outcome of Unicondylar Knee Arthroplasty vs Total Knee Arthroplasty for Early Medial Compartment Arthritis: A Randomized Study," *J. Arthroplasty*, Dec. 2016.

[45] M. W. Squire, J. J. Callaghan, D. D. Goetz, P. M. Sullivan, and R. C. Johnston, "Unicompartmental knee replacement. A minimum 15 year followup study.," *Clin. Orthop. Relat. Res.*, no. 367, pp. 61–72, Oct. 1999.

[46] J. P. Van der List, L. S. McDonald, and A. D. Pearle, “Systematic review of medial versus lateral survivorship in unicompartmental knee arthroplasty,” *Knee*, vol. 22, no. 6, pp. 454–460, Dec. 2015.

[47] M. Badawy, B. Espehaug, K. Indrekvam, L. I. Havelin, and O. Furnes, “Higher revision risk for unicompartmental knee arthroplasty in low-volume hospitals,” *Acta Orthop.*, vol. 85, no. 4, pp. 342–347, Aug. 2014.

[48] K. T. Kim, S. Lee, H. S. Park, K. H. Cho, and K. S. Kim, “Unicompartmental versus Total Knee Arthroplasty in the Same Patient,” *J. Korean Orthop. Assoc.*, vol. 43, no. 4, p. 451, 2008.

[49] D. A. Crawford, K. R. Berend, and A. V. Lombardi, “Same-Day Unicondylar Knee Arthroplasty,” in *Minimally Invasive Surgery in Orthopedics*, Cham: Springer International Publishing, 2016, pp. 13–21.

[50] N. Bradbury, D. Borton, G. Spoo, and M. J. Cross, “Participation in sports after total knee replacement.,” *Am. J. Sports Med.*, vol. 26, no. 4, pp. 530–5.

[51] N. Fisher, M. Agarwal, S. F. Reuben, D. S. Johnson, and P. G. Turner, “Sporting and physical activity following Oxford medial unicompartmental knee arthroplasty,” *Knee*, vol. 13, no. 4, pp. 296–300, Aug. 2006.

[52] R. Clifford, “Mosaicplasty and Cartilage Transplants for Chondral Injuries of the Knee,” 2012. [Online]. Available: http://www.wheelessonline.com/ortho/mosaicplasty_and_cartilage_transplants_for_chondral_injuries_of_the_knee. [Accessed: 09-Jul-2014].

[53] NICE, “Mosaicplasty for knee Cartilage Defects,” 2006. [Online]. Available: http://www.nice.org.uk/guidance/ipg162/resources/ipg162-mosaicplasty-for-knee-cartilage-defects-information-for-the-public2.

[54] NICE, “Mosaicplasty for knee cartilage defects | Guidance and guidelines | NICE,” 2006. [Online]. Available: http://www.nice.org.uk/Guidance/IPG162. [Accessed: 09-Jul-2014].

[55] H. Robert, “Chondral repair of the knee joint using mosaicplasty.,” *Orthop. Traumatol. Surg. Res.*, vol. 97, no. 4, pp. 418–29, Jun. 2011.

[56] L. Hangody, P. Feczkó, L. Bartha, G. Bodó, and G. Kish, “Mosaicplasty for the treatment of articular defects of the knee and ankle.,” *Clinical orthopaedics and related research*, no. 391 Suppl. pp. S328-36, Oct-2001.

[57] “Mosaicplasty for the treatment of articular cartilage defects.” .

[58] G. Bentley *et al.*, “A prospective, randomised comparison of autologous chondrocyte implantation versus mosaicplasty for osteochondral defects in the knee.,” *J. Bone Joint Surg. Br.*, vol. 85, no. 2, pp. 223–30, Mar. 2003.

[59] S. Derrett, E. a Stokes, M. James, W. Bartlett, and G. Bentley, “Cost and health status analysis after autologous chondrocyte implantation and mosaicplasty: a retrospective comparison.,” *Int. J. Technol. Assess. Health Care*, vol. 21, no. 3, pp. 359–67, Jan. 2005.

[60] J. L. Koh, A. Kowalski, and E. Lautenschlager, “The effect of angled osteochondral grafting on contact pressure: a biomechanical study.,” *Am. J.*

Sports Med., vol. 34, no. 1, pp. 116–9, Jan. 2006.

[61] L. Hangody *et al.*, "Autologous osteochondral grafting--technique and long-term results.," *Injury*, vol. 39 Suppl 1, pp. S32-9, Apr. 2008.

[62] B. R. Snyder, A. M. Chiu, D. J. Prockop, and A. W. S. Chan, "Human multipotent stromal cells (MSCs) increase neurogenesis and decrease atrophy of the striatum in a transgenic mouse model for Huntington's disease.," *PLoS One*, vol. 5, no. 2, p. e9347, Jan. 2010.

[63] T. I. Zarembinski, W. P. Tew, and S. K. Atzet, "The Use of a Hydrogel Matrix as a Cellular Delivery Vehicle in Future Cell-Based Therapies : Biological and Non-Biological Considerations," 2010.

[64] M. Bohner, "Bone Substitute Materials," in *Reference Module in Biomedical Sciences*, 2014.

[65] "IMAGE TO COME Zimmer ® NexGen ® LPS Fixed Knee."

[66] "Laser triangulation of the femoral head for total knee arthroplasty alignment instruments and surgical method," Sep. 2003.

[67] G. Yildirim, R. Davignon, L. Scholl, G. Schmidig, K. M. Carroll, and A. D. Pearle, "Advantages of a Cementless Unicompartmental Knee Arthroplasty Approach," *Oper. Tech. Orthop.*, vol. 25, no. 2, pp. 150–154, Jun. 2015.

[68] W. E. Moschetti, J. F. Konopka, H. E. Rubash, and J. W. Genuario, "Can Robot-Assisted Unicompartmental Knee Arthroplasty Be Cost-Effective? A Markov Decision Analysis," *J. Arthroplasty*, vol. 31, no. 4, pp. 759–765, Apr. 2016.

[69] F. Picard *et al.*, “Handheld Robot-Assisted Unicondylar Knee Arthroplasty: A Clinical Review,” *Bone & Jt. J. Orthop. Proc. Suppl.*, vol. 96–B, no. SUPP 16, p. 25 LP-25, Oct. 2014.

[70] H. Mizu-uchi, S. Matsuda, H. Miura, K. Okazaki, Y. Akasaki, and Y. Iwamoto, “The evaluation of post-operative alignment in total knee replacement using a CT-based navigation system,” vol. 90, no. 8, pp. 21–26, 2008.

[71] M. Roche and M. Conditt, “Robotic Arm-Assisted Unicompartmental Knee Arthroplasty: Preoperative Planning and Surgical Technique,” in *Intraoperative Imaging and Image-Guided Therapy*, New York, NY: Springer New York, 2014, pp. 677–683.

[72] P. Weber *et al.*, “Improved accuracy in computer-assisted unicondylar knee arthroplasty: a meta-analysis,” *Knee Surgery, Sport. Traumatol. Arthrosc.*, vol. 21, no. 11, pp. 2453–2461, Nov. 2013.

[73] A. Manzotti, P. Cerveri, C. Pullen, and N. Confalonieri, “Computer-assisted unicompartmental knee arthroplasty using dedicated software versus a conventional technique,” *Int. Orthop.*, vol. 38, no. 2, pp. 457–463, Feb. 2014.

[74] J. H. Lonner, J. R. Smith, F. Picard, B. Hamlin, P. J. Rowe, and P. E. Riches, “High Degree of Accuracy of a Novel Image-free Handheld Robot for Unicondylar Knee Arthroplasty in a Cadaveric Study,” *Clin. Orthop. Relat. Res.*, vol. 473, no. 1, pp. 206–212, Jan. 2015.

[75] S. G. Kini and S. S. Sathappan, “Robot-Assisted Unicondylar Knee

Arthroplasty: A Critical Review," *Orthopaedics*, vol. 1, no. 1, p. 4, 2013.

[76] S. Khamaisy, B. P. Gladnick, D. Nam, K. R. Reinhardt, T. J. Heyse, and A. D. Pearle, "Lower limb alignment control: Is it more challenging in lateral compared to medial unicondylar knee arthroplasty?," *Knee*, vol. 22, no. 4, pp. 347–350, Sep. 2015.

[77] Z. Jaffry *et al.*, "Unicompartmental knee arthroplasties: Robot vs. patient specific instrumentation," *Knee*, vol. 21, no. 2, pp. 428–434, Mar. 2014.

[78] G. F. Tawy, P. J. Rowe, and P. E. Riches, "Thermal Damage Done to Bone by Burring and Sawing With and Without Irrigation in Knee Arthroplasty.," *J. Arthroplasty*, Nov. 2015.

[79] S. Saha and S. Pal, "Mechanical properties of bone cement: a review.," *J. Biomed. Mater. Res.*, vol. 18, no. 4, pp. 435–62, Apr. 1984.

[80] R. Vaishya, M. Chauhan, and A. Vaish, "Bone cement.," *J. Clin. Orthop. trauma*, vol. 4, no. 4, pp. 157–63, Dec. 2013.

[81] Heraeus, "High viscosity, radiopaque bone cement." .

[82] W. MacDonald, E. Swarts, and R. Beaver, "Penetration and shear strength of cement-bone interfaces in vivo," *Clin Orthop Relat Res*, no. 286, pp. 283–288, 1993.

[83] Y. H. Chang, C. L. Tai, H. Y. Hsu, P. H. Hsieh, M. S. Lee, and S. W. N. Ueng, "Liquid antibiotics in bone cement: an effective way to improve the efficiency of antibiotic release in antibiotic loaded bone cement.," *Bone Joint Res.*, vol.

3, no. 8, pp. 246–51, Aug. 2014.

[84] P. C. Noble and E. Swarts, “Penetration of Acrylic Bone Cements into Cancellous Bone,” *Acta Orthop.*, vol. 54, no. 4, pp. 566–573, 1983.

[85] M. Halawa, A. J. C. Lee, R. S. M. Ling, and S. S. Vangala, “The shear strength of trabecular bone from the femur, and some factors affecting the shear strength of the cement-bone interface,” *Arch. Orthop. Trauma. Surg.*, vol. 92, no. 1, pp. 19–30, 1978.

[86] D. Waanders, D. Janssen, K. A. Mann, and N. Verdonschot, “The mechanical effects of different levels of cement penetration at the cement-bone interface,” *J. Biomech.*, vol. 43, no. 6, pp. 1167–1175, 2010.

[87] K. A. Mann, F. W. Werner, and D. C. Ayers, “Mechanical strength of the cement–bone interface is greater in shear than in tension,” *J. Biomech.*, vol. 32, no. 11, pp. 1251–1254, Nov. 1999.

[88] N. J. Dunne and J. F. Orr, “Thermal characteristics of curing acrylic bone cement,” *ITBM-RBM*, vol. 22, no. 2, pp. 88–97, Apr. 2001.

[89] G. Lewis, “Properties of acrylic bone cement: state of the art review.,” *J. Biomed. Mater. Res.*, vol. 38, no. 2, pp. 155–82, Jan. 1997.

[90] J. Wang and S. J. Breusch, “Mixing : Choice of Mixing System,” pp. 4–9.

[91] H. Mau, K. Schelling, C. Heisel, J.-S. Wang, and S. J. Breusch, “Comparison of various vacuum mixing systems and bone cements as regards reliability, porosity and bending strength.,” *Acta Orthop. Scand.*, vol. 75, no. 2, pp. 160–

72, Apr. 2004.

[92] L. Lidgren, B. Bodelind, and J. Möller, “Bone cement improved by vacuum mixing and chilling,” *Acta Orthop. Scand.*, vol. 58, no. 1, pp. 27–32, Jan. 1987.

[93] T. W. Bauer and J. Schils, “The pathology of total joint arthroplasty Part I. Mechanisms of Implant Fixation,” *Skeletal Radiol.*, vol. 28, no. 8, pp. 423–432, Sep. 1999.

[94] N. A. Ramaniraka, L. R. Rakotomanana, and P. F. Leyvraz, “The fixation of the cemented femoral component. Effects of stem stiffness, cement thickness and roughness of the cement-bone surface.,” *J. Bone Joint Surg. Br.*, vol. 82, no. 2, pp. 297–303, Mar. 2000.

[95] W. R. Krause, W. Krug, and J. Miller, “Strength of the cement-bone interface.,” *Clin. Orthop. Relat. Res.*, no. 163, pp. 290–9, Mar. 1982.

[96] M. Thompson, M. Conditt, and M. Redish, “The Importance of Cement Penetration with an All-Poly Inlay UKA The Importance of Cement Penetration with an All-Poly.”

[97] R. S. Majkowski, A. W. Miles, G. C. Bannister, J. Perkins, and G. J. Taylor, “Bone surface preparation in cemented joint replacement.,” *J. Bone Joint Surg. Br.*, vol. 75, no. 3, pp. 459–63, May 1993.

[98] C. Scheele *et al.*, “Effect of lavage and brush preparation on cement penetration and primary stability in tibial unicompartmental total knee arthroplasty: An experimental cadaver study,” *Knee*, vol. 24, no. 2, pp. 402–

408, Mar. 2017.

[99] Q.-H. Zhang, G. Tozzi, and J. Tong, “Micro-mechanical damage of trabecular bone-cement interface under selected loading conditions: a finite element study.,” *Comput. Methods Biomech. Biomed. Engin.*, vol. 17, no. 3, pp. 230–8, 2014.

[100] R. Skripitz and P. Aspenberg, “Attachment of PMMA cement to bone: force measurements in rats,” *Biomaterials*, vol. 20, no. 4, pp. 351–356, Feb. 1999.

[101] L. L. Hench and J. Wilson, *An Introduction to Bioceramics*. WORLD SCIENTIFIC, 1993.

[102] O. Clarkin, D. Boyd, and M. R. Towler, “Comparison of failure mechanisms for cements used in skeletal luting applications,” *J. Mater. Sci. Mater. Med.*, vol. 20, no. 8, pp. 1585–1594, 2009.

[103] K. A. Mann, D. C. Ayers, F. W. Werner, R. J. Nicoletta, and M. D. Fortino, “Tensile strength of the cement-bone interface depends on the amount of bone interdigitated with PMMA cement,” *J. Biomech.*, vol. 30, no. 4, pp. 339–346, Apr. 1997.

[104] D. D. Arola, D. T. Yang, and K. A. Stoffel, “The apparent volume of interdigitation: a new parameter for evaluating the influence of surface topography on mechanical interlock.,” *J. Biomed. Mater. Res.*, vol. 58, no. 5, pp. 519–24, Jan. 2001.

[105] D. Janssen, K. A. Mann, and N. Verdonschot, “Micro-mechanical modeling of

the cement-bone interface: The effect of friction, morphology and material properties on the micromechanical response," *J. Biomech.*, vol. 41, no. 15, pp. 3158–3163, 2008.

[106] R. Y. Hori and J. L. Lewis, "Mechanical properties of the fibrous tissue found at the bone-cement interface following total joint replacement.," *J. Biomed. Mater. Res.*, vol. 16, no. 6, pp. 911–27, Nov. 1982.

[107] M. E. Forsythe, R. E. Englund, and R. K. Leighton, "Unicondylar knee arthroplasty: a cementless perspective.," *Can. J. Surg.*, vol. 43, no. 6, pp. 417–24, Dec. 2000.

[108] J. P. Davies and W. H. Harris, "Tensile Bonding Strength of the Cement-Prosthesis Interface," *Orthopedics*, vol. 17, no. 2, pp. 171–173, 1994.

[109] R. D. Crowninshield, J. D. Jennings, M. L. Laurent, and W. J. Maloney, "Cemented femoral component surface finish mechanics.," *Clin. Orthop. Relat. Res.*, no. 355, pp. 90–102, Oct. 1998.

[110] A. B. Lennon, B. A. O. McCormack, and P. J. Prendergast, "The relationship between cement fatigue damage and implant surface finish in proximal femoral prostheses," *Med. Eng. Phys.*, vol. 25, no. 10, pp. 833–841, 2003.

[111] N. Verdonschot and R. Huiskes, "Surface roughness of debonded straight-tapered stems in cemented THA reduces subsidence but not cement damage," *Biomaterials*, vol. 19, no. 19, pp. 1773–1779, 1998.

[112] R. S. Majkowski, G. C. Bannister, and A. W. Miles, "The effect of bleeding on

the cement-bone interface. An experimental study.," *Clin. Orthop. Relat. Res.*, no. 299, pp. 293–7, Feb. 1994.

[113] M. Conditt and D. Augustin, "An Assessment of Onlay Unicompartmental An Assessment of Onlay Unicompartmental."

[114] "The Importance of Good Cement Mantle With an All-Poly Inlay UKA." [Online]. Available: http://www.ors.org/Transactions/56/2121.pdf. [Accessed: 21-Jul-2014].

[115] T. M. Coon, "Minimally Invasive Unicompartmental Knee Arthroplasty Using the QuadSparing Instruments," *Oper. Tech. Orthop.*, vol. 16, no. 3, pp. 195–206, Jul. 2006.

[116] B. P. Gladnick, D. Nam, S. Khamaisy, S. Paul, and A. D. Pearle, "Onlay Tibial Implants Appear to Provide Superior Clinical Results in Robotic Unicompartmental Knee Arthroplasty," *HSS J. ®*, vol. 11, no. 1, pp. 43–49, Feb. 2015.

[117] H. Zuiderbaan *et al.*, "Predictors of Outcome Following Robot-Assisted Unicompartmental Knee Arthroplasty," *Bone & Jt. J. Orthop. Proc. Suppl.*, vol. 98–B, no. SUPP 4, p. 153 LP-153, Jan. 2016.

[118] P. S. Walker, D. S. Parakh, M. E. Chaudhary, and C.-S. Wei, "Comparison of Interface Stresses and Strains for Onlay and Inlay Unicompartmental Tibial Components," in *ASME 2011 Summer Bioengineering Conference, Parts A and B*, 2011, p. 379.

[119] E. M. Suero, M. Citak, I. U. Njoku, and A. D. Pearle, “Does the type of tibial component affect mechanical alignment in unicompartmental knee replacement? - Technology and Health Care - Volume 21, Number 1 / 2013 - IOS Press,” *Technology and health care : official journal of the European Society for Engineering and Medicine*, Jan-2013. [Online]. Available: http://iospress.metapress.com/content/t5287313182k7k8r/. [Accessed: 29-May-2014].

[120] B. Gladnick, D. Nam, S. Khamaisy, S. Paul, and A. Pearle, “Inlay Versus Onlay Tibial Implants in Robotic Unicondylar Knee Arthroplasty,” *Bone Jt. J. Orthop. Proc. Suppl.*, vol. 95–B, no. SUPP 34, p. 66, Dec. 2013.

[121] R. E. Gleeson, R. Evans, C. E. Ackroyd, J. Webb, and J. H. Newman, “Fixed or mobile bearing unicompartmental knee replacement? A comparative cohort study.,” *Knee*, vol. 11, no. 5, pp. 379–84, Oct. 2004.

[122] J. F. Plate *et al.*, “Obesity has no effect on outcomes following unicompartmental knee arthroplasty,” *Knee Surgery, Sport. Traumatol. Arthrosc.*, vol. 25, no. 3, pp. 645–651, Mar. 2017.

[123] M. E. Chaudhary and P. S. Walker, “Analysis of an early intervention tibial component for medial osteoarthritis.,” *J. Biomech. Eng.*, vol. 136, no. 6, p. 61008, May 2014.

[124] “Mobile bearing knees superior to fixed bearing.” [Online]. Available: www.smith-nephew.com.

[125] C.-H. Huang, J.-J. Liau, and C.-K. Cheng, “Fixed or mobile-bearing total knee arthroplasty.,” *J. Orthop. Surg. Res.*, vol. 2, p. 1, Jan. 2007.

[126] T. Watanabe, T. Tomita, M. Fujii, J. Hashimoto, K. Sugamoto, and H. Yoshikawa, “Comparison between mobile-bearing and fixed-bearing knees in bilateral total knee replacements.,” *Int. Orthop.*, vol. 29, no. 3, pp. 179–81, Jun. 2005.

[127] Z. D. Post, W. Y. Matar, T. van de Leur, E. L. Grossman, and M. S. Austin, “Mobile-bearing total knee arthroplasty: better than a fixed-bearing?,” *J. Arthroplasty*, vol. 25, no. 6, pp. 998–1003, Sep. 2010.

[128] Y.-H. Kim, J.-S. Kim, J.-W. Choe, and H.-J. Kim, “Long-term comparison of fixed-bearing and mobile-bearing total knee replacements in patients younger than fifty-one years of age with osteoarthritis.,” *J. Bone Joint Surg. Am.*, vol. 94, no. 10, pp. 866–73, May 2012.

[129] C.-H. Huang *et al.*, “Particle size and morphology of UHMWPE wear debris in failed total knee arthroplasties--a comparison between mobile bearing and fixed bearing knees.,” *J. Orthop. Res.*, vol. 20, no. 5, pp. 1038–41, Sep. 2002.

[130] S. A. Atwood, J. H. Currier, M. B. Mayor, J. P. Collier, D. W. Van Citters, and F. E. Kennedy, “Clinical wear measurement on low contact stress rotating platform knee bearings.,” *J. Arthroplasty*, vol. 23, no. 3, pp. 431–40, Apr. 2008.

[131] S. P. Zysk *et al.*, “Particles of All Sizes Provoke Inflammatory Responses In

Vivo," *Clin. Orthop. Relat. Res.*, vol. NA;, no. 433, pp. 258–264, Apr. 2005.

[132] T. R. Green, J. Fisher, M. Stone, B. M. Wroblewski, and E. Ingham, "Polyethylene particles of a 'critical size' are necessary for the induction of cytokines by macrophages in vitro," *Biomaterials*, vol. 19, no. 24, pp. 2297–2302, Dec. 1998.

[133] K. Evensen, A. I. Spitzer, P. Goodmanson, and K. Suthers, "Mobile Bearing TKA Does Not Reduce the Need for Lateral Release," *J. Bone Jt. Surgery, Br. Vol.*, vol. 87–B, no. SUPP III, p. 389, Sep. 2005.

[134] "Rotating Platform Knees Did Not Improve Patellar Tracking: A Prospective, Randomized Study of 240 Primary Total Knee Arthroplasties." [Online]. Available: http://journals.lww.com/corr/Abstract/2004/11000/Rotating_Platform_Knees_Did_Not_Improve_Patellar.35.aspx. [Accessed: 18-Sep-2014].

[135] R. H. Emerson, "Unicompartmental mobile-bearing knee arthroplasty.," *Instr. Course Lect.*, vol. 54, pp. 221–4, Jan. 2005.

[136] M. G. Li, F. Yao, B. Joss, J. Ioppolo, B. Nivbrant, and D. Wood, "Mobile vs. fixed bearing unicondylar knee arthroplasty: A randomized study on short term clinical outcomes and knee kinematics.," *Knee*, vol. 13, no. 5, pp. 365–70, Oct. 2006.

[137] A. J. Price *et al.*, "Ten-year in vivo wear measurement of a fully congruent mobile bearing unicompartmental knee arthroplasty.," *J. Bone Joint Surg. Br.*,

vol. 87, no. 11, pp. 1493–7, Nov. 2005.

[138] M. Deng, R. A. Latour, A. A. Ogale, and S. W. Shalaby, “Study of creep behavior of ultra-high-molecular-weight polyethylene systems.,” *J. Biomed. Mater. Res.*, vol. 40, no. 2, pp. 214–23, May 1998.

[139] T. Ashraf, J. H. Newman, V. V Desai, D. Beard, and J. E. Nevelos, “Polyethylene wear in a non-congruous unicompartmental knee replacement: a retrieval analysis.,” *Knee*, vol. 11, no. 3, pp. 177–81, Jun. 2004.

[140] V. Psychoyios, R. W. Crawford, J. J. O’Connor, D. W. Murray, and J. J. O’Connor, “Wear of congruent meniscal bearings in unicompartmental knee arthroplasty: A Retrieval Study of 16 Specimens,” *J. Bone Jt. Surg.*, vol. 80, no. 6, pp. 976–982, Nov. 1998.

[141] M. H. Arastu, J. Vijayaraghavan, H. Chissell, J. B. Hull, J. H. Newman, and J. R. Robinson, “Early failure of a mobile-bearing unicompartmental knee replacement.,” *Knee Surg. Sports Traumatol. Arthrosc.*, vol. 17, no. 10, pp. 1178–83, Oct. 2009.

[142] J. H. Lonner, “Robotic Arm–Assisted Unicompartmental Arthroplasty,” *Semin. Arthroplasty*, vol. 20, no. 1, pp. 15–22, Mar. 2009.

[143] P. A. Keblish and J. L. Briard, “Mobile-bearing unicompartmental knee arthroplasty,” *J. Arthroplasty*, vol. 19, no. 7, pp. 87–94, Oct. 2004.

[144] R. H. Emerson, T. Hansborough, R. D. Reitman, W. Rosenfeldt, and L. L. Higgins, “Comparison of a mobile with a fixed-bearing unicompartmental

knee implant.," *Clinical orthopaedics and related research*, no. 404. pp. 62–70, Nov-2002.

[145] N. Confalonieri, A. Manzotti, and C. Pullen, "Comparison of a mobile with a fixed tibial bearing unicompartimental knee prosthesis: a prospective randomized trial using a dedicated outcome score.," *Knee*, vol. 11, no. 5, pp. 357–62, Oct. 2004.

[146] T. Loidolt and B. Curtin, "Unicompartmental Knee Arthroplasty in the Young Patient," in *Management of Knee Osteoarthritis in the Younger, Active Patient*, Berlin, Heidelberg: Springer Berlin Heidelberg, 2016, pp. 115–132.

[147] M. Ettinger *et al.*, "In vitro kinematics of fixed versus mobile bearing in unicondylar knee arthroplasty," *Arch. Orthop. Trauma Surg.*, vol. 135, no. 6, pp. 871–877, Jun. 2015.

[148] K. R. Berend, N. J. Turnbull, R. E. Howell, and A. V. Lombardi, "The Current Trends for Lateral Unicondylar Knee Arthroplasty," *Orthop. Clin. North Am.*, vol. 46, no. 2, pp. 177–184, Apr. 2015.

[149] J. R. A. Smith *et al.*, "Fixed bearing lateral unicompartmental knee arthroplasty—Short to midterm survivorship and knee scores for 101 prostheses," *Knee*, vol. 21, no. 4, pp. 843–847, Aug. 2014.

[150] M. Ollivier, M. P. Abdel, S. Parratte, and J.-N. Argenson, "Lateral unicondylar knee arthroplasty (UKA): Contemporary indications, surgical technique, and results," *Int. Orthop.*, vol. 38, no. 2, pp. 449–455, Feb. 2014.

[151] S. H. Palmer, P. J. Morrison, and A. C. Ross, “Early catastrophic tibial component wear after unicompartmental knee arthroplasty.,” *Clin. Orthop. Relat. Res.*, no. 350, pp. 143–8, May 1998.

[152] J. E. Stoddard, D. J. Deehan, A. M. J. Bull, A. W. McCaskie, and A. a Amis, “The kinematics and stability of single-radius versus multi-radius femoral components related to mid-range instability after TKA.,” *J. Orthop. Res.*, vol. 31, no. 1, pp. 53–8, Jan. 2013.

[153] E. Gómez-Barrena, C. Fernandez-García, A. Fernandez-Bravo, R. Cutillas-Ruiz, and G. Bermejo-Fernandez, “Functional performance with a single-radius femoral design total knee arthroplasty.,” *Clin. Orthop. Relat. Res.*, vol. 468, no. 5, pp. 1214–20, May 2010.

[154] M. Molt, P. Ljung, and S. Toksvig-Larsen, “Does a new knee design perform as well as the design it replaces?,” *Bone Joint Res.*, vol. 1, no. 12, pp. 315–23, Dec. 2012.

[155] V. Pinskerova, H. Iwaki, and M. A. R. Freeman, “The shapes and relative movements of the femur and tibia at the knee,” *Orthopade*, vol. 29, no. S1, pp. S3–S5, Jun. 2000.

[156] S. Ostermeier and C. Stukenborg-Colsman, “Quadriceps force after TKA with femoral single radius.,” *Acta Orthop.*, vol. 82, no. 3, pp. 339–43, Jun. 2011.

[157] J. Hall, S. N. Copp, W. S. Adelson, D. D. D’Lima, and C. W. Colwell, “Extensor mechanism function in single-radius vs multiradius femoral components for

total knee arthroplasty.," *J. Arthroplasty*, vol. 23, no. 2, pp. 216–9, Feb. 2008.

[158] H. Wang, K. J. Simpson, M. S. Ferrara, S. Chamnongkich, T. Kinsey, and O. M. Mahoney, "Biomechanical differences exhibited during sit-to-stand between total knee arthroplasty designs of varying radii.," *J. Arthroplasty*, vol. 21, no. 8, pp. 1193–9, Dec. 2006.

[159] M. Freeman, G. Bradley, and P. Revell, "Observations upon the interface between bone and polymethylmethacrylate cement," *J Bone Jt. Surg Br*, vol. 64–B, no. 4, pp. 489–493, Aug. 1982.

[160] N. J. Giori, L. Ryd, and D. R. Carter, "Mechanical influences on tissue differentiation at bone-cement interfaces.," *J. Arthroplasty*, vol. 10, no. 4, pp. 514–22, Aug. 1995.

[161] R. D. Komistek, D. A. Dennis, J. A. Mabe, and S. A. Walker, "An in vivo determination of patellofemoral contact positions.," *Clin. Biomech. (Bristol, Avon)*, vol. 15, no. 1, pp. 29–36, Jan. 2000.

[162] L. Linder, "Reaction of bone to the acute chemical trauma of bone cement.," *J. Bone Joint Surg. Am.*, vol. 59, no. 1, pp. 82–7, Jan. 1977.

[163] K. A. Mann, M. A. Miller, C. L. Pray, N. Verdonschot, and D. Janssen, "A New Approach to Quantify Trabecular Resorption Adjacent to Cemented Knee Arthroplasty.," *J. Biomech.*, vol. 45, no. 4, pp. 711–5, Feb. 2012.

[164] D. R. Carter, P. R. Blenman, and G. S. Beaupré, "Correlations between mechanical stress history and tissue differentiation in initial fracture healing,"

J. Orthop. Res., vol. 6, no. 5, pp. 736–748, Sep. 1988.

[165] H. Oonishi, "Mechanical and chemical bonding of Artificial joints," *Clin. Mater.*, vol. 5, no. 2–4, pp. 217–233, Jan. 1990.

[166] S. Campi, H. G. Pandit, C. A. F. Dodd, and D. W. Murray, "Cementless fixation in medial unicompartmental knee arthroplasty: a systematic review," *Knee Surgery, Sport. Traumatol. Arthrosc.*, vol. 25, no. 3, pp. 736–745, Mar. 2017.

[167] C. J. Sutherland, A. H. Wilde, L. S. Borden, and K. E. Marks, "A ten-year follow-up of one hundred consecutive Müller curved-stem total hip-replacement arthroplasties.," *J. Bone Joint Surg. Am.*, vol. 64, no. 7, pp. 970–82, Sep. 1982.

[168] M. E. Torchia, R. A. Klassen, and A. J. Bianco, "Total hip arthroplasty with cement in patients less than twenty years old. Long-term results.," *J. Bone Joint Surg. Am.*, vol. 78, no. 7, pp. 995–1003, Jul. 1996.

[169] H. Malchau, P. Herberts, and L. Ahnfelt, "Prognosis of total hip replacement in Sweden: Follow-up of 92,675 operations performed 1978–1990," *Acta Orthop. Scand.*, vol. 64, no. 5, pp. 497–506, Jan. 1993.

[170] London Hospital, "Observations Upon the Interface and Between," vol. 64, no. 4, 1982.

[171] H. Pandit *et al.*, "Cementless Oxford unicompartmental knee replacement shows reduced radiolucency at one year.," *J. Bone Joint Surg. Br.*, vol. 91, no. 2, pp. 185–9, Feb. 2009.

[172] J. Charnley, "Cement-Bone Interface," in *Low Friction Arthroplasty of the Hip*,

Berlin, Heidelberg: Springer Berlin Heidelberg, 1979, pp. 25–40.

[173] S. Lustig *et al.*, “5- to 16-Year Follow-Up of 54 Consecutive Lateral Unicondylar Knee Arthroplasties With a Fixed-All Polyethylene Bearing,” *J. Arthroplasty*, vol. 26, no. 8, pp. 1318–1325, 2011.

[174] T. E. McAlindon, S. Snow, C. Cooper, and P. A. Dieppe, “Radiographic patterns of osteoarthritis of the knee joint in the community: the importance of the patellofemoral joint.,” *Ann. Rheum. Dis.*, vol. 51, no. 7, pp. 844–9, Jul. 1992.

[175] T. D. Brown and D. T. Shaw, “In vitro contact stress distribution on the femoral condyles,” *J. Orthop. Res.*, vol. 2, no. 2, pp. 190–199, Jan. 1984.

[176] E. M. Mariani, M. H. Bourne, R. T. Jackson, S. T. Jackson, and P. Jones, “Early Failure of Unicompartmental Knee Arthroplasty,” *J. Arthroplasty*, vol. 22, no. 6, pp. 81–84, Sep. 2007.

[177] R. D. Scott and R. F. Santore, “Unicondylar unicompartmental replacement for osteoarthritis of the knee.,” *J. Bone Joint Surg. Am.*, vol. 63, no. 4, pp. 536–44, Apr. 1981.

[178] H. U. Cameron, G. A. Hunter, R. P. Welsh, and W. H. Bailey, “Unicompartmental knee replacement.,” *Clin. Orthop. Relat. Res.*, no. 160, pp. 109–13, Oct. 1981.

[179] J. Insall and P. Aglietti, “A five to seven-year follow-up of unicondylar arthroplasty.,” *J. Bone Joint Surg. Am.*, vol. 62, no. 8, pp. 1329–37, Dec. 1980.

[180] R. S. Laskin, “Unicompartmental tibiofemoral resurfacing arthroplasty.,” *J.*

Bone Joint Surg. Am., vol. 60, no. 2, pp. 182–5, Mar. 1978.

[181] B. Tibrewal and A. Grant, “The radiolucent of,” vol. 66, no. 4, 1984.

[182] B. J. L. Kendrick *et al.*, “Histology of the bone-cement interface in retrieved Oxford unicompartmental knee replacements.,” *Knee*, vol. 19, no. 6, pp. 918–22, Dec. 2012.

[183] M. T. Vestermark, J. E. Bechtold, P. Swider, and K. Søballe, “Mechanical interface conditions affect morphology and cellular activity of sclerotic bone rims forming around experimental loaded implants.,” *J. Orthop. Res.*, vol. 22, no. 3, pp. 647–52, May 2004.

[184] E. L. Radin *et al.*, “Changes in the bone-cement interface after total hip replacement. An in vivo animal study.,” *J. Bone Joint Surg. Am.*, vol. 64, no. 8, pp. 1188–200, Oct. 1982.

[185] D. J. Simpson, A. J. Price, A. Gulati, D. W. Murray, and H. S. Gill, “Elevated proximal tibial strains following unicompartmental knee replacement--a possible cause of pain.,” *Med. Eng. Phys.*, vol. 31, no. 7, pp. 752–7, Sep. 2009.

[186] S. Kalra, T. O. Smith, B. Berko, and N. P. Walton, “Assessment of radiolucent lines around the Oxford unicompartmental knee replacement: sensitivity and specificity for loosening,” *J Bone Jt. Surg*, vol. 93, 2011.

[187] A. Gulati, R. Chau, D. J. Simpson, C. A. F. Dodd, H. S. Gill, and D. W. Murray, “Influence of component alignment on outcome for unicompartmental knee replacement,” *Knee*, vol. 16, no. 3, pp. 196–9, Jun. 2009.

[188] D. J. Simpson, B. J. L. Kendrick, C. a. F. Dodd, A. J. Price, H. S. Gill, and D. W. Murray, “Load transfer in the proximal tibia following implantation with a unicompartmental knee replacement: a static snapshot,” *Proc. Inst. Mech. Eng. Part H J. Eng. Med.*, vol. 225, no. 5, pp. 521–529, Apr. 2011.

[189] D. W. Murray and N. Rushton, “Macrophages Stimulate Bone Resorption When They Phagocytose Particles,” *J. Bone Jt. Surg.*, vol. British Vo, no. 6, pp. 988–992, 1990.

[190] D. W. Murray, T. Rae, and N. Rushton, “The Influence of the Surface Energy and Roughness of Implants on Bone Resorption,” *Br. Editor. Soc. Bone Jt. Surg.*, vol. 71, no. 4, pp. 632–637, 1989.

[191] A. Rich and A. K. Harris, “Anomalous preferences of cultured macrophages for hydrophobic and roughened substrata.,” *J. Cell Sci.*, vol. 50, pp. 1–7, Aug. 1981.

[192] J. E. Bechtold, O. Mouzin, and L. Kidder, “Part II . Implementation with loaded titanium implants and bone graft,” vol. 72, no. 6, pp. 650–656, 2001.

[193] P. Swider, A. Pedrono, O. Mouzin, K. Søballe, and J. E. Bechtold, “Biomechanical analysis of the shear behaviour adjacent to an axially loaded implant.,” *J. Biomech.*, vol. 39, no. 10, pp. 1873–82, Jan. 2006.

[194] J. J. Callaghan, M. R. O’Rourke, and K. J. Saleh, “Why knees fail,” *J. Arthroplasty*, vol. 19, no. 4, pp. 31–34, Jun. 2004.

[195] K. G. Vince, “Why knees fail.,” *J. Arthroplasty*, vol. 18, no. 3 Suppl 1, pp. 39–

44, 2003.

[196] T. W. Bauer and J. Schils, “The pathology of total joint arthroplasty.II. Mechanisms of implant failure.,” *Skeletal Radiol.*, vol. 28, no. 9, pp. 483–97, Sep. 1999.

[197] M. E. Portillo *et al.*, “Prosthesis failure within 2 years of implantation is highly predictive of infection.,” *Clin. Orthop. Relat. Res.*, vol. 471, no. 11, pp. 3672–8, Nov. 2013.

[198] S. D. Ulrich *et al.*, “Total hip arthroplasties: what are the reasons for revision?,” *Int. Orthop.*, vol. 32, no. 5, pp. 597–604, Oct. 2008.

[199] R. P. Grelsamer and P. Cartier, “A unicompartmental knee replacement is not ‘half a total knee’: five major differences.,” *Orthop. Rev.*, vol. 21, no. 11, pp. 1350–6, Nov. 1992.

[200] A. D. Skyrme, M. M. Mencia, and P. W. Skinner, “Early failure of the porous-coated anatomic cemented unicompartmental knee arthroplasty,” *J. Arthroplasty*, vol. 17, no. 2, pp. 201–205, Feb. 2002.

[201] C. L. Saenz, M. S. McGrath, D. R. Marker, T. M. Seyler, M. A. Mont, and P. M. Bonutti, “Early failure of a unicompartmental knee arthroplasty design with an all-polyethylene tibial component.,” *Knee*, vol. 17, no. 1, pp. 53–6, Jan. 2010.

[202] J. M. Bert, “Unicompartmental Knee Replacement,” vol. 36, pp. 513–522, 2005.

[203] R. E. Bartley, S. D. Stulberg, W. J. Robb, and H. J. Sweeney, “Polyethylene wear in unicompartmental knee arthroplasty.,” *Clin. Orthop. Relat. Res.*, no. 299, pp. 18–24, Feb. 1994.

[204] S. Akizuki, J. K. P. Mueller, H. Horiuchi, D. Matsunaga, A. Shibakawa, and R. D. Komistek, “In vivo determination of kinematics for subjects having a Zimmer Unicompartmental High Flex Knee System.,” *J. Arthroplasty*, vol. 24, no. 6, pp. 963–71, Sep. 2009.

[205] T. P. Schmalzried, D. L. Scott, and C. Zahiri, “Variables affecting wear in vivo: analysis of 1080 hips with computer-assisted technique,” in *24 th Annual Meeting of the Society for Biomaterials*, 1998, p. 1998.

[206] W. P. Barrett and R. D. Scott, *Revision of failed unicondylar unicompartmental knee arthroplasty.*, vol. 69, no. 9. 1987, pp. 1328–35.

[207] W. T. Jones, R. S. Bryan, L. F. Peterson, and D. M. Ilstrup, “Unicompartmental knee arthroplasty using polycentric and geometric hemicomponents.,” *J. Bone Joint Surg. Am.*, vol. 63, no. 6, pp. 946–54, Jul. 1981.

[208] J. R. Moreland, “Mechanisms of failure in total knee arthroplasty.,” *Clin. Orthop. Relat. Res.*, no. 226, pp. 49–64, Jan. 1988.

[209] D. W. Murray *et al.*, “The use of the Oxford hip and knee scores.,” *J. Bone Joint Surg. Br.*, vol. 89, no. 8, pp. 1010–4, Aug. 2007.

[210] S. Tilley and N. Thomas, “What knee scoring system?,” *J Bone Jt. Surg*, vol. Focus on, 2010.

[211] J. R. Lieberman *et al.*, “Differences between patients’ and physicians’ evaluations of outcome after total hip arthroplasty.,” *J. Bone Joint Surg. Am.*, vol. 78, no. 6, pp. 835–8, Jun. 1996.

[212] J. N. Insall *et al.*, “A Comparison of Four Models of Total Knee-Replacement Prostheses,” *Clin. Orthop. Relat. Res.*, vol. 367, 1979.

[213] M. J. Dunbar, “Subjective outcomes after knee arthroplasty,” *Acta Orthop. Scand.*, vol. 72, no. 3, pp. 1–63, Jan. 2001.

[214] A. T. Bremner-Smith, P. Ewings, and A. E. Weale, “Knee scores in a ‘normal’ elderly population.,” *Knee*, vol. 11, no. 4, pp. 279–82, Aug. 2004.

[215] R. Becker, C. Döring, A. Denecke, and M. Brosz, “Expectation, satisfaction and clinical outcome of patients after total knee arthroplasty,” *Knee Surgery, Sport. Traumatol. Arthrosc.*, vol. 19, no. 9, pp. 1433–1441, Sep. 2011.

[216] P. S. Walker and M. J. Erkman, “The role of the menisci in force transmission across the knee.,” *Clinical orthopaedics and related research*, vol. 109, no. 109. pp. 184–92, Jan-1975.

[217] P. S. Walker, S. Arno, C. Bell, G. Salvadore, I. Borukhov, and C. Oh, “Function of the medial meniscus in force transmission and stability,” *J. Biomech.*, vol. 48, no. 8, pp. 1383–1388, 2015.

[218] S. Arno *et al.*, “Relation between cartilage volume and meniscal contact in medial osteoarthritis of the knee.,” *Knee*, vol. 19, no. 6, pp. 896–901, Dec. 2012.

[219] S. Arno *et al.*, “Relationship between meniscal integrity and risk factors for cartilage degeneration,” *Knee*, vol. 23, no. 4, pp. 686–691, 2016.

[220] P. S. Walker and J. V Hajek, “The load-bearing area in the knee joint.,” *J. Biomech.*, vol. 5, no. 6, pp. 581–9, Nov. 1972.

[221] P. S. Walker, G. Yildirim, J. Sussman-Fort, and G. R. Klein, “Relative positions of the contacts on the cartilage surfaces of the knee joint.,” *Knee*, vol. 13, no. 5, pp. 382–8, Oct. 2006.

[222] G. Yildirim, P. S. Walker, J. Sussman-Fort, G. Aggarwal, B. White, and G. R. Klein, “The contact locations in the knee during high flexion.,” *Knee*, vol. 14, no. 5, pp. 379–84, Oct. 2007.

[223] I. Summers and D. E. White, “Creativity Techniques: Toward Improvement of the Decision Process.,” *Acad. Manag. Rev.*, vol. 1, no. 2, pp. 99–108, Apr. 1976.

[224] J. R. Evans, “Creativity in MS/OR: Improving Problem Solving through Creative Thinking,” *Interfaces (Providence).*, vol. 22, no. 2, pp. 87–91, Apr. 1992.

[225] A. Davlin, “Building An ‘About Us’ Page That Reels Readers In – Tips and Examples - Hongkiat.” [Online]. Available: http://www.hongkiat.com/blog/building-about-us-page/. [Accessed: 01-Jun-2017].

[226] Design Council, “A Study of the Design Process,” *Des. Counc.*, vol. 44, no. 0, pp. 1–144, 2005.

[227] S. Pugh, *Total design : integrated methods for successful product engineering*. Wokingham, England: Wokingham, England : Addison-Wesley, 1990.

[228] K. Alexander and P. J. Clarkson, “Good design practice for medical devices and equipment, Part I: a Review of Current Literature,” *Jou rnal Med. En gineerin g Tech n ology*, pp. 5–13, 2000.

[229] K. Alexander and P. J. Clarkson, “Good design practice for medical devices and equipment, Part II: design for validation,” *J. Med. Eng. Technol.*, vol. 24, no. 2, pp. 53–62, 2000.

[230] FDA, “Design Control Guidance for Medical Device Manufacturers,” 1997.

[231] M. A. Orloff, *Inventive thinking through TRIZ: a practical guide*, 2nd ed. . Berlin: Berlin, 2006.

[232] M. A. Orloff, *Triz 123*. .

[233] K. Rantanen, *Simplified TRIZ : new problem-solving applications for engineers and manufacturing professionals*. Boca Raton: Boca Raton : St. Lucie Press, 2002.

[234] SolidCreativity, “TRIZ Matrix / 40 principles / TRIZ contradictions table.” [Online]. Available: http://www.triz40.com/TRIZ_GB.php. [Accessed: 01-Jun-2017].

[235] K. T. Ulrich and S. D. Eppinger, *Product design and development*, 4th ed. . Boston: Boston : McGraw-Hill Higher Education, 2008.

[236] T. Rickards, “Designing for creativity: A state of the art review,” *Des. Stud.*, vol. 1, no. 5, pp. 262–272, Jul. 1980.

[237] A. Erdemir, “Open knee: open source modeling and simulation in knee biomechanics,” *J. Knee Surg.*, vol. 29, no. 2, pp. 107–116, 2016.

[238] A. Erdemir, “Open knee: a pathway to community driven modeling and simulation in joint biomechanics,” *J. Med. Device.*, vol. 7, no. 4, p. 40910, 2013.

[239] S. Sibole *et al.*, “Open knee: a 3D finite element representation of the knee joint,” in *34th annual meeting of the American Society of Biomechanics*, 2010, pp. 152–153.

[240] A. Erdemir and S. Sibole, “Open knee: a three-dimensional finite element representation of the knee joint,” *User’s Guid. version*, vol. 1, no. 0, 2010.

[241] S. C. Cowin, *Bone mechanics*. CRC press Boca Raton, FL, 1989.

[242] C. E. H. Scott and L. C. Biant, “The role of the design of tibial components and stems in knee replacement,” *Bone Joint J.*, vol. 94–B, no. 8, 2012.

[243] C. L. Brockett, L. M. Jennings, and J. Fisher, “The wear of fixed and mobile bearing unicompartmental knee replacements,” *Proc. Inst. Mech. Eng. Part H J. Eng. Med.*, vol. 225, no. 5, pp. 511–519, May 2011.

[244] M. Poukalova *et al.*, “Pullout strength of suture anchors: Effect of mechanical properties of trabecular bone,” *J. Biomech.*, vol. 43, no. 6, pp. 1138–1145, 2010.

[245] A. Gracco, C. Giagnorio, S. Incerti Parenti, G. Alessandri Bonetti, and G. Siciliani, “Effects of thread shape on the pullout strength of miniscrews,” *Am. J. Orthod. Dentofac. Orthop.*, vol. 142, no. 2, pp. 186–190, 2012.

[246] J. W. Savage, W. Limthongkul, H.-S. Park, L.-Q. Zhang, and E. E. Karaikovic, “A comparison of biomechanical stability and pullout strength of two C1–C2 fixation constructs,” *Spine J.*, vol. 11, no. 7, pp. 654–658, 2011.

[247] L. A. Degernes, S. C. Roe, and C. F. Abrams, “Holding Power of Different Pin Designs and Pin Insertion Methods in Avian Cortical Bone,” *Vet. Surg.*, vol. 27, no. 4, pp. 301–306, Jul. 1998.

[248] T. Albrektesson, P.-I. Branemark, H.-A. Hansson, and J. Lindstrom, “Osseointegrated Titanium Implants,” *Acta orthop. scand*, pp. 155–170, 1981.

[249] N. Moritz, J. J. Alm, P. Lankinen, T. J. Mäkinen, K. Mattila, and H. T. Aro, “Quality of intertrochanteric cancellous bone as predictor of femoral stem RSA migration in cementless total hip arthroplasty.,” *J. Biomech.*, vol. 44, no. 2, pp. 221–7, Jan. 2011.

[250] K. A. Mann, M. A. Miller, R. J. Cleary, D. Janssen, and N. Verdonschot, “Experimental micromechanics of the cement-bone interface,” *J. Orthop. Res.*, vol. 26, no. 6, pp. 872–879, 2008.

[251] M. Donkerwolcke, F. Burny, and D. Muster, “Tissues and bone adhesives—historical aspects,” *Biomaterials*, vol. 19, no. 16, pp. 1461–1466, Aug. 1998.

[252] E. J. Harper and W. Bonfield, “Tensile characteristics of ten commercial

acrylic bone cements.," *J. Biomed. Mater. Res.*, vol. 53, no. 5, pp. 605–16, Sep. 2000.

[253] J. B. Morrison, "The mechanics of the knee joint in relation to normal walking," *J. Biomech.*, vol. 3, no. 1, pp. 51–61, Jan. 1970.

[254] G. Yildirim, P. S. Walker, and J. Boyer, "Total knees designed for normal kinematics evaluated in an up-and-down crouching machine," *J. Orthop. Res.*, vol. 27, no. 8, pp. 1022–1027, 2009.

[255] P. S. Walker, S. M. Glauber, and H. Wang, "Laboratory Evaluation Method for the Functional Performance of Total Knee Replacements," *J. ASTM Int.*, vol. 9, no. 4, p. 103444, Apr. 2012.

[256] P. S. Walker, S. Arno, I. Borukhoy, and C. P. Bell, "Characterising knee motion and laxity in a testing machine for application to total knee evaluation," *J. Biomech.*, vol. 48, no. 13, pp. 3551–3558, 2015.

[257] A. R. Hopkins, A. M. New, F. Rodriguez-y-Baena, and M. Taylor, "Finite element analysis of unicompartmental knee arthroplasty," *Med. Eng. Phys.*, vol. 32, no. 1, pp. 14–21, 2010.

[258] P. S. Walker, "Application of a novel design method for knee replacements to achieve normal mechanics," *Knee*, vol. 21, no. 2, pp. 353–358, 2014.

[259] M. Taylor, K. E. Tanner, and M. A. R. Freeman, "Finite element analysis of the implanted proximal tibia," *J. Biomech.*, vol. 31, no. 4, pp. 303–310, Apr. 1998.

[260] H. S. Center, "Unicompartmental Knee Arthroplasty." [Online]. Available:

https://en.wikipedia.org/wiki/File:Pkrvstotalknee.jpg. [Accessed: 28-Aug-2017].

[261] V. Powell, “A Surgical Operation: Total Knee Replacement,” 1997. [Online]. Available: https://commons.wikimedia.org/wiki/File:A_surgical_operation;_total_knee_replacement._Drawing_by_Vir_Wellcome_L0028360.jpg. [Accessed: 28-Aug-2017].

[262] V. Y. Ng, J. H. DeClaire, K. R. Berend, B. C. Gulick, and A. V. Lombardi, “Improved Accuracy of Alignment With Patient-specific Positioning Guides Compared With Manual Instrumentation in TKA,” *Clin. Orthop. Relat. Res.*, vol. 470, no. 1, pp. 99–107, Jan. 2012.

[263] M. Carroll, R. Obert, and P. Stemniski, “Method For Forming A Patient Specific Surgical Guide Mount,” 26-Aug-2010.

[264] “10-K form of MAKO Surgical Corp.,” Washington, 2012.